One night with Venus, a lifetime with Mercury: Understanding syphilis and mercury treatment at St. Gertrude's infirmary (1382 - ca. 1611) in Kampen, the Netherlands

Nagelhout, Lotte

One night with Venus, a lifetime with Mercury

Understanding syphilis and mercury treatment at St. Gertrude's infirmary (1382 - ca. 1611) in Kampen, the Netherlands.

Lotte Nagelhout

Cover figure: "The Martyrdom of Mercury", depicting treatments with mercury. By J. Sintelaer, 1709. From G. Harris et al., London, 1709, via https://wellcomecollection.org/works/zhhau7uz

One night with Venus, a lifetime with Mercury

Understanding syphilis and mercury treatment at St. Gertrude's infirmary (1382 - ca. 1611) in Kampen, the Netherlands.

Author: Lotte Nagelhout (s2000350)

Course and course code: RMSC Thesis Archaeology, 1086VTRSY

Supervisors: Dr. A.G. Henry, Dr. R. Schats, and Dr. D.J.G. Braekmans.

Leiden University, Faculty of Archaeology.

Delft

19-10-2023

Final version

Acknowledgements

As this thesis is the result of more than two years of collective effort, I would like to express my deepest appreciation to my (co-)supervisors Dr. Amanda Henry, Dr. Rachel Schats, and Dr. Dennis Braekmans. I would like to thank Amanda for taking me under her wing and keeping me on track through weekly meetings, thorough discussions, and constructive feedback. This helped me enormously in making sense of this multifaceted project and how to go from idea to research to actual words on paper. I also owe many thanks to Rachel, whose continuous support was not only present during many aspects of this thesis process, but already since my first Osteology lectures during my Bachelor program. Her unwavering and enthusiastic guidance throughout my academic studies have greatly influenced my passion for human osteoarchaeological research, as well as my broader academic and personal goals. I want to thank Dennis for his willingness to contribute greatly to this project after it had already started. He formed an integral part in the practicalities of the research presented here, most importantly through introducing me to the intricacies of pXRF analyses (including a few necessary sessions of troubleshooting…), but also by discussing the evaluation and interpretation of the other trace elemental analyses.

Additionally, I would like to thank the other professionals and organizations that took part in various aspects of the research for this thesis. Firstly, I want to thank Dr. Ineke Joosten and her colleagues at the Dutch Cultural Heritage Agency, who both performed and reported the SEM-EDX analyses. Stichting Nederlands Museum voor Antropologie en Praehistorie (SNMAP) I would like to thank for graciously provided funding for the ICP-MS analyses, which were conducted by Measurlabs in Finland. In this line, I would also like to thank the staff at Stadsarchief Kampen, who provided access to centuries-old archival materials.

Another thank you goes out to the many peers or lecturers who have had to endure discussions on ideas, quick reviews of my writing, giving feedback on my first academic poster and presentation, or who participated in any other way, no matter how small.

Lastly, this thesis could not have been written without the support of my friends and family, who provided the necessary peptalks (or words of reason…), gaming sessions, and movie nights that helped mitigate my stress levels, especially during the writing process. Most importantly, my gratitude goes out to Boudewijn, who has formed my backbone in every step of this journey by endlessly encouraging me, brewing me fresh cups of coffee, and sometimes forcing me to take a day off. I could not have done this without him.

Table of Contents

List of Figures

List of Tables

List of Appendices

Please note that Appendix 4 is only available through a supplementary .pdf file

1. Introduction

Syphilis first became epidemic in Europe during the late 15th century, and has been a debilitating and life-threatening disease ever since. This chronic disease is one of four treponemal diseases and is caused by an infection with *Treponema pallidum* bacteria (Tampa et al., 2014, p. 4). In syphilis, this bacteria can be transmitted sexually or in utero from mother to the unborn child (Wicher & Wicher, 2001, p. 354). The former results in *venereal* syphilis and the latter in *congenital* syphilis (Waldron, 2009, p. 102). If left untreated, venereal syphilis can manifest itself through three major stages with distinctive symptoms. The primary and secondary stages can last from a few weeks up to several months after initial infection and are characterized by a wide variety of symptoms, often starting with small genital ulcers, or chancres, that can lead to the development of wide-spread skin rashes accompanied by flu-like symptoms, among others. The tertiary stage, only reached in approximately one-third of cases, can result in more debilitating syndromes, such as cardiovascular syphilis and neurosyphilis (Sparling et al., 2008, pp. 662–665). It is during this phase that the skeleton may be permanently affected as well and display signs of systemic infection with necrotic, gummatous lesions, commonly found in the skull and long bones (Hackett, 1975).

As infection rates rose rapidly during the 15th and 16th centuries, medieval physicians sought many, but not always effective, ways of treating the disease (Tampa et al., 2014, p. 8; Zuckerman, 2016, p. 42). These included remedies made from plants, arsenic, or bismuth. However, the most popular treatment for syphilis throughout Europe incorporated mercury (Hg) (Zuckerman, 2016, p. 43). At the time, the use of mercury in syphilis treatment was paradoxically based on the symptoms caused by the toxic nature of mercury itself (Waldron, 2009, p. 102). Mercury induced extreme salivation and urination, which was believed to rid the body of syphilitic particles. The practice stayed in use well into the 19th century, despite the fact that mercury poisoning was a common occurrence due to the high dosages administered (O'Shea, 1990, pp. 392–393). The uncomfortable nature of the treatment has been expressed in various historical imageries and sayings, such as "for a night with Venus, a lifetime with Mercury" or "for a pleasure, a thousand pains" (Figure 1.1) (Tampa et al., 2014; Waldron, 2009, p. 102).

Mercury could be administered to patients in various ways, mostly depending on the symptoms experienced by the affected patients. It could be applied topically as an ointment, ingested orally or administered by injection. Another prevalent treatment method was that of fumigation or inhalation of mercuric vapours, in which patients were repeatedly enclosed in heated spaces (Figure 1.1) (O'Shea, 1990, p. 393; Zuckerman, 2016, p. 44). Particularly during the 16th century, when the syphilis outbreak in Europe was at its peak, high doses and prolonged treatments served as a desperate attempt to keep the number of fatalities low (Tampa et al., 2014; Zuckerman, 2016, p. 45).

Figure 1.1: Woodcut engraving by Jacques Laniet, Paris (1659), depicting an individual undergoing fumigation treatment in a stove. The description reads the proverb "For one pleasure, a thousand pains". (Tampa et al., 2014).

1.1 Research problem

Even though historical knowledge about syphilis is quite extensive (McGough, 2005), the origin of the disease is still heavily debated, as the beginning of the European epidemic closely aligns with Columbus' travel to and from the New World (Waldron, 2009, p. 104). Already since its first outbreak in the late 14th century, ample discussion regarding the disease's origin has taken place among many academics from various scientific fields. Proponents of the Columbian hypothesis (e.g., Baker & Armelagos, 1988; Crosby, 1969) propose that syphilis originated in the New World and, when transported to Europe by returning sailors, rapidly spread through the vulnerable European population (Harper et al., 2011, p. 100). It is hypothesized that this spread was exacerbated by a continental-wide unstable political environment, accompanied by extensive warfare and large scale movements of people (McGough, 2005, p. 574). In contrast, proponents of the pre-Columbian hypothesis (e.g., Hackett, 1963; Holcomb, 1934) suggest that syphilis existed in Europe prior to Columbus' return, albeit not in the same virulent form (Baker & Armelagos, 1988; Waldron, 2009). While other origin theories exist, these two opposing hypotheses form the backbone of the academic discourse (Harper et al., 2011). Recently, DNA research appears to be tipping the scale in favor of the pre-Columbian hypothesis (Majander et al., 2020), but more research is needed before definite conclusions can be drawn.

In addition to questions about the origin of the disease, a more holistic understanding of infected individuals and their treatment in late medieval Europe is still lacking. Historical records were often

influenced by sociocultural stigmas of shame and immorality connected to syphilis (McGough, 2005, p. 574; Tampa et al., 2014). While archaeological analysis could minimize the influence of such stigma, osteoarchaeological study of syphilis and its treatment is challenging due to limited skeletal visibility of the infection. Syphilis has been referred to as "the Great Imitator" (Kent & Romanelli, 2008, p. 226; Radolf, 1996), emphasizing this difficulty in identifying the infection in skeletal remains due to the wide variety of lesion types, most of which are non-diagnostic (Hackett, 1976; Waldron, 2009). Skeletal tissues are most commonly and permanently affected by syphilis during the tertiary stage (Waldron, 2009, p. 105). However, in roughly 60 to 85% of the affected individuals, infection is overcome or otherwise avoided before the disease reaches this phase (Singh & Romanowski, 1999, p. 191). Even so, not all patients affected by tertiary stage syphilis experience osseous changes, limiting the archaeological detectability of the disease even further (Kent & Romanelli, 2008, p. 229).

Thus, gaining a holistic understanding of affected individuals during the beginning of the European epidemic requires a broader analytical scope and as such, this thesis applies a multidisciplinary approach to study the disease from an archaeological perspective. While some regions, like the UK, have received many in-depth studies, syphilis in the Netherlands has remained an understudied topic with scarce evidence of the impact of the disease (Baker et al., 2020, p. 23). Therefore, using skeletal remains from a late medieval and early modern infirmary site in Kampen, the Netherlands, this study aims to gain a better understanding of syphilis and its treatment in the Netherlands during this period.

Building on previous analysis and reporting by Schats, Hoogland, et al. (2017) and Schats and Klomp (2019), one of the aims of this study is to re-examine the osteoarchaeological remains with a more in-depth focus on treponemal lesions, to further establish the paleopathological evidence for treponemal disease at the site. In addition, archival research was conducted with the aim to gain historical insight into the presence of disease at the infirmary as well as the treatments that were available.

In order to go beyond the historical and osteoarchaeological research, this thesis aims to identify possible treatment with mercury in the skeletal remains from Kampen by conducting various trace elemental analyses. While recent bioarchaeological studies have experimented with various techniques to establish mercury levels in skeletal remains, such methods are often difficult to compare or evaluate. As such, other researchers have emphasized the importance of establishing a best practice by verifying the reliability and comparability of different analytical techniques (Baker et al., 2020, p. 17). Therefore, this thesis not only aims to combine the osteoarchaeological and historical knowledge of the site with trace elemental analyses to investigate the use of mercury treatments on the one hand, but also aims to evaluate the efficacy of three different analytical techniques (pXRF, SEM-EDX and ICP-MS) to identify elemental mercury in archaeological human remains.

1.2 Research questions

The main research question for this thesis is:

To what extent can the presence of syphilis and its treatment with mercury be identified in the human skeletal remains from the late medieval and early modern St. Gertrude's infirmary in Kampen, the Netherlands?

In order to answer the main research question and gain a more comprehensive and multifocal understanding of the subject, the following sub-questions are investigated:

How can treponemal disease be identified in skeletal remains and what is the prevalence of treponemal disease in the skeletal remains from the late medieval and early modern St. Gertrude's infirmary in Kampen?

Can evidence of syphilis infections and treatment with mercury be found in archival records from late medieval and early modern Kampen?

Can elemental mercury be detected in human skeletal remains from late medieval and early modern Kampen through portable X-Ray Fluorescence Spectrometry (pXRF) and what does this say about the use of mercury treatments at St. Gertrude's infirmary?

Can elemental mercury be detected in human skeletal remains from late medieval and early modern Kampen through Inductively Coupled Plasma Mass Spectrometry (ICP-MS) and what does this say about the use of mercury treatments at St. Gertrude's infirmary?

Can elemental mercury be detected in human dental calculus from late medieval and early modern Kampen through Scanning Electron Microscopy with Energy Dispersive X-rays Spectroscopy (SEM-EDX) and what does this say about the use of mercury treatments at St. Gertrude's infirmary?

1.3 Approach

In order to study skeletal syphilis and to investigate the presence and detectability of mercury treatments, the Dutch medieval site of Saint Gertrude's infirmary, or *Sint Geertruidengasthuis,* in Kampen was used. The site's primary function was that of a late medieval infirmary, but it also provided general care and residency for the poor or travellers (Jager, 2015, p. 352). The St. Gertrude's infirmary complex is likely to have been used from 1382 onwards and while the infirmary remained active until its destruction in 1897 (Klomp, 2017b, p. 95; van der Sligte-de Jong, 1993), burials in the adjacent cemetery are believed to have terminated around 1611 (Schats & Klomp, 2019, p. 107).

Excavations in 2014 unearthed the remains of 89 primary burials and subsequent osteoarchaeological analysis revealed two individuals who were likely affected by syphilis, as well as one case of possible

infection (Schats, Hoogland, et al., 2017, p. 247). Together, these three individuals have previously been dated through ^{14}C dating, resulting in possible pre-Columbian origins of the disease and coinciding with the first severe syphilis outbreak in Europe (Schats & Klomp, 2019, p. 114). Due to the nature of the infirmary, they may have been treated with mercury prior to their death. Further confirmation of the presence of treponemal disease in late medieval Kampen was established through DNA of the *Treponema* bacteria in a single tibia with periosteal lesions, retrieved from a bone pit at the site (Majander et al., 2020). Additionally, the collection contained many individuals with bilateral and diffuse periosteal new bone formation, a sign of potential systemic infection (Schats & Klomp, 2019, pp. 112–113). The setting and timing of this site provides a unique opportunity to study both syphilis and its treatment in the medieval Netherlands.

Human skeletal remains from St. Gertrude's infirmary were previously analyzed to assess completeness, age-at-death and biological sex, as well as the presence of pathological conditions. With this osteological analysis as foundation, the skeletal collection from Kampen was re-examined with an in-depth focus on lesions consistent with, suggestive of, or diagnostic for treponemal infection. Following Harper et al. (2011), individuals were given a score that reflects the likelihood of an accurate treponemal diagnosis.

To investigate the role of mercury treatment for syphilis in the late medieval Netherlands, trace elemental analyses were conducted to establish mercury levels in human skeletal remains and to assess the applicability of these techniques. As a best practice method remains unidentified and as mercury may accumulate in the skeletal tissues in different ways related to its administration to the patient, this study adopted multiple biomolecular and analytical methods to detect mercury.

Firstly, portable X-Ray Fluorescence Spectrometry (pXRF) was conducted on the femora, humeri, ribs, and/or specific lesions of individuals from the skeletal collection of St. Gertrude's infirmary. This approach may detect late medieval treatments that involved applying mercury topically as ointment or inhaling mercuric fumes, which may have resulted in the incorporation of mercury into the bone matrix over time.

Secondly, a selection of bone samples from syphilitic and control individuals as well as soil samples were subjected to Inductively Coupled Plasma Mass Spectrometry (ICP-MS) to determine their precise mercury levels.

Lastly, a number of teeth with mineralized dental plaque (calculus) were analyzed for mercury using Scanning Electron Microscopy with Energy Dispersive X-rays Spectroscopy (SEM-EDX). This study may reflect treatment methods that aimed to cure syphilis through ingestion of mercury-enriched foods and possibly fumigation, which could allow for the metal to be incorporated in dental calculus on teeth.

In addition to the molecular and osteoarchaeological analyses, this study also conducted historic archival research at the *Stadsarchief Kampen* (municipal and city archives), in order to gather more information about the patients and inhabitants of St. Gertrude's infirmary, but also about the methods of treatment that were practiced in the region at the time.

1.4 Thesis outline

This thesis continues with an introductory chapter that discusses the cause and clinical symptoms of syphilis, with a particular focus on how it can affect the skeletal system, as this thesis studies past cases of possible syphilis in archaeological bone. The third chapter takes a more historical approach to the disease and describes the numerous hypotheses on how syphilis became epidemic in late 15th century Europe. In addition, this chapter takes a look at the history of syphilis treatment as a whole as well as the local history of syphilis and its treatment in the Netherlands during the late medieval and early modern period. The fourth chapter discusses the historical and archaeological context of the skeletal remains used in this study. In doing so, it will first set the stage for the historical development of the Dutch city of Kampen and its healthcare facilities during the late medieval and early modern period, after which St. Gertrude's infirmary, the excavation of the cemetery, and the materials used in this study will receive more attention. Following this, the various methods adopted in this thesis are addressed in chapter five. These include the osteoarchaeological analysis and historic archival study, as well as the different types of trace elemental analyses, namely pXRF, ICP-MS, and SEM-EDX analyses, conducted for this research. The sixth chapter discusses the results of the different analyses, after which chapter 7 contains a contextual and extensive interpretative discussion of these results, as well as the study's considerations and limitations. Taking this into account, the final chapter answers each of the research questions separately and draws an overall conclusion by bringing the different perspectives together.

2. Syphilis From A Clinical Perspective

As this research focusses on venereal syphilis and its treatment, it is essential to understand the background of this chronic affliction. This chapter discusses syphilis from a clinical perspective to provide a better understanding of its natural history and the ways in which it can affect its patients.

2.1 Treponematoses

When discussing syphilis, it is pertinent to differentiate the venereal and congenital variant from other infectious diseases caused by the same bacterial genus, which are collectively referred to as treponemal diseases or treponematoses. For humans, treponematoses include four infectious diseases caused by four subspecies of the bacterial genus *Treponema,* a spiral-shaped spirochete (Figure 2.1) (Edmondson & Norris, 2021, p. 1; Radolf, 1996). The species *Treponema pallidum* is the causative agent for venereal syphilis (subspecies *pallidum*), bejel or endemic syphilis (subsp. *endemicum*), and yaws, (subsp. *pertenue*), whereas *Treponema carateum* is responsible for pinta (Norris et al., 2001, p. 38). Of these, only venereal syphilis is transmitted sexually or congenitally, whereas the others are mainly transmitted by skin-to-skin contact, with children being most commonly affected (Hackett, 1963, p. 8).

Although pathogenetic analysis has recently experienced major breakthroughs (Edmondson et al., 2018; Romeis et al., 2021), thoroughly mapping the treponematoses has remained challenging due to the morphological, biochemical, serological and immunological similarity between the subspecies of *T. pallidum* (Baker et al., 2020, p. 8; Kawahata et al., 2019, p. 1581; Rothschild & Rothschild, 1995, p. 1402). As a result, various efforts to distinguish the treponematoses have been undertaken. While pinta does not leave any osseous markers, some studies have indicated that the other three treponematoses can be identified based on their expression within the skeleton (Rothschild, 2005, p. 1460). Yet, most researchers agree that, while venereal syphilis is generally acknowledged as leaving the most destructive changes (de Melo et al., 2010, p. 2), skeletal changes in the later stages of treponemal infections are mostly identical, making differentiation difficult (Harper et al., 2011, p. 101).

Figure 2.1: Treponema pallidum *bacteria. SEM image showcasing the spiral structure of the bacteria situated on top of cultured rabbit epithelial tissue. (Rehm, 2018).*

Additionally, differentiation between yaws, bejel, and venereal syphilis is often based on the distinct geographical and climatic areas in which they operate. Yaws is mainly found in regions with high temperatures and humidity, such as the tropics in the Americas and Africa, whereas bejel is present in arid and hot or temperate climates, such as regions of the Middle East (de Melo et al., 2010, p. 2; Livingstone, 1991, p. 588; Waldron, 2009, p. 103). Taking these geographical and climatic factors into consideration, European cases of treponemal disease are most likely attributable to syphilis, which is present worldwide (Hackett, 1963, p. 8; von Hunnius et al., 2006, p. 563; Waldron, 2009, pp. 102–103).

However, it should be noted that recent studies have emphasized that the genetic differences between the treponemal subspecies are negligible and that their clinical and pathological symptoms may be indistinguishable (Baker et al., 2020, pp. 7–8). For example, Kawahata et al. (2019) and Mikalová et al. (2017) reported recent cases in which clinical manifestations commonly attributed to venereal syphilis were actually caused by *T. pallidum* subsp. *endemicum*, the causative agent for bejel. This goes to show that even in the face of modern medical knowledge, distinguishing the diseases from each other is an intricate matter. This thesis will follow the conclusions by Baker et al. (2020), who articulate that, at least from a pathophysiological perspective, syphilis, bejel and yaws are the result from the same bacterial species (*T. pallidum)* and are thus different expressions of the same disease (p. 28). In order to accurately reflect this distinction and to acknowledge that venereal syphilis cannot be diagnosed in archaeological remains without aDNA research (see section 3.2.1), this thesis will refer to treponemal disease in the case of unknown aetiology, for example when discussing the paleopathological study of skeletal remains, whereas syphilis will be used to refer to the disease in historical and clinical context.

2.2 Clinical manifestations

Being a systemic and chronic disease, untreated syphilis progresses through three active stages – the primary, secondary, and tertiary stages – as well as an asymptomatic or latent period. The various symptoms displayed throughout these stages are thought to be expressions of the host's inflammatory or immune responses and may not directly reflect cytotoxic effects of the bacteria (Lukehart, 2008, pp. 651–653). If left untreated, syphilis' mortality is believed to be 8 to 14% (Peeling & Hook, 2006, p. 227).

2.2.1 Primary syphilis

The primary stage begins with direct exposure to an infectious lesion, usually during sexual contact, after which bacteria penetrate the skin or mucous membrane and are disseminated throughout their new host via the lymphatic system (Lukehart, 2008, p. 651; Roberts & Buikstra, 2019, p. 381). An ulcerated but painless lesion, called a chancre, develops at the site of infection after 3-90 days and can grow to be 0,3-3 cm in diameter (Singh & Romanowski, 1999, p. 192). These chancres generally heal

independent from treatment over a span of 3 to 6 weeks, but an untreated patient can remain infectious up until two years after initial infection (Sparling et al., 2008, pp. 662–663).

2.2.2 Secondary syphilis

Over the course of a few weeks or months, further spread of *T. pallidum* throughout the body allows for the onset of the secondary stage (Sparling et al., 2008, p. 664). This stage is characterized by a wide variety of symptoms, which can range in severity, making diagnosis difficult (Baker et al., 2020, p. 7; Chapel, 1980, p. 164). Typically, skin rashes develop on the extremities, specifically the hand palms and foot soles, and torso, although the intensity and type of rash can differ between individuals. Other symptoms include itchiness, a sore throat, malaise, headache, fever, muscle aches, enlarged lymph nodes, weight and hair loss, ulcerated mucous surfaces, and in rare cases syphilitic meningitis (Chapel, 1980, p. 162; Kent & Romanelli, 2008, p. 229; Sparling et al., 2008, p. 664).

Usually, secondary syphilis resolves naturally and the patient enters a period of latency, characterized by the absence of clinical symptoms. Latent syphilis can last from one year up to two decades and is often divided into early and late periods that may be separated by a reoccurrence of secondary syphilis (Kent & Romanelli, 2008, p. 228; Sparling et al., 2008, p. 665). While patients suffering from the active secondary stage or the early latent stage of syphilis are still regarded as infectious, the disease's communicability ceases from the late latent stage onwards (Singh & Romanowski, 1999, p. 193).

2.2.3 Tertiary syphilis

Following this latent stage, the infection can develop into tertiary syphilis, although the majority of patients remain unaffected. Due to modern medicine, the natural history of untreated infection is understudied and the prevalence of tertiary syphilis can only be approximated. In three pre-antibiotic studies, which have been heavily criticized for various reasons, the tertiary stage developed in roughly 15-40% of untreated patients (Singh & Romanowski, 1999, p. 191), reported by other studies as one-third or 30% (Kent & Romanelli, 2008, p. 230; Lukehart, 2008, p. 651; Waldron, 2009, p. 103). Clinical manifestations of tertiary syphilis are grossly categorized as cardiovascular syphilis, neurosyphilis, and late benign or gummatous syphilis, each of which is differentiated by the location of bacterial presence and characterized by a specific set of symptoms and incubation period, which are described below (Sparling et al., 2008, p. 665). The occurrence rate of these three syndromes differs between the three pre-antibiotic studies, with one indicating that gummatous syphilis may have been most prevalent and neurosyphilis being the least prevalent (Clark & Danbolt, 1955, p. 342), whereas another indicates that cardiovascular syphilis was significantly more prevalent (Rosahn, 1947, as cited in Peeling & Hook, 2006, p. 227).

Neurosyphilis occurs if the cerebrospinal fluid and central nervous system are infected by *Treponema* bacteria, which can already occur during the early stages of syphilis (Daey Ouwens, 2019, p. 18). If so, it remains asymptomatic or, in a small number of cases, progresses to syphilitic meningitis (Kent & Romanelli, 2008, pp. 228–229). In this form of tertiary syphilis, the infected central nervous system displays a variety of clinical syndromes, depending on the affected area and related symptoms. These include meningovascular syphilis (4-7 years after infection), general paresis[1] (15-20 years after infection), and tabes dorsalis[2] (5-25 years after infection). Each can cause numerous clinical manifestations, ranging from psychiatric to neurological disorders. Symptoms include personality changes, vertigo, memory loss, depression, paranoia, delusions, lightning pains, sensory impairment and many others (Kent & Romanelli, 2008, p. 228; Singh & Romanowski, 1999, pp. 193–194; Sparling et al., 2008, pp. 668–669).

Cardiovascular syphilis is a form of tertiary syphilis that typically develops 10 to 30 years after initial infection, with symptoms including aortitis, aortic regurgitation, coronary artery disease, or aortic aneurysms (Singh & Romanowski, 1999, p. 193). Its similarity with other cardiac diseases complicates diagnosis based on clinical symptoms alone (Sparling et al., 2008, p. 672). Together with neurosyphilis, it is responsible for the majority of direct mortality by syphilis (Peeling & Hook, 2006, p. 225).

Gummatous or late benign syphilis can appear as late as 46 years after the secondary stage has resolved and can reoccur throughout time, with a majority of instances occurring around the 15 year mark (Clark & Danbolt, 1955, pp. 330, 342). It is characterized by the formation of so-called gummas or gummata, which can affect bone, skin, and internal organs (Singh & Romanowski, 1999, p. 194). Gummas are localized, tumour-like nodules with soft necrotic tissue at the centre, and are the result of progressive granulomatous inflammation. In the skin, the lesions appear as solitary gummas or multiple nodular and nudolo-ulcerative gummas, differentiated by their depth and severity (Sparling et al., 2008, pp. 674–675). Nudolar and nodulo-ulcerative lesions are pink-reddish papules and while localized healing often occurs, the phenomenon spreads to other areas of the body in the absence of treatment. Solitary gummas develop subcutaneously (i.e. underneath the skin), with subsequent ulceration, leaving a "punched out" lesion that can penetrate as deep as bone tissue (Crissey & Denenholz, 1984, p. 109). Gumma formation can also take place in the mouth and throat region and in some cases results in destruction of the cartilage and bones of the palate and nose (Crissey & Denenholz, 1984, pp. 112–114).

[1] General paresis is a form of dementia that progressively worsens and can ultimately lead to a broad and diverse range of psychotic symptoms (Singh & Romanowski, 1999, p. 194).

[2] Tabes dorsalis refers to the degeneration of the spinal cord, which results in a suite of neurological problems, often sensory-related (Sparling et al., 2008, pp. 670-671).

Besides this, bones can also be affected by gummatous growths themselves, which can leave localized destruction, surrounded by sclerotic (i.e. hardened and dense) bone growths (Aufderheide & Rodriguez-Martin, 1998, p. 160), or instigate various inflammatory reactions in the bone itself or involving the periosteal membrane that covers the bone surfaces (Sparling et al., 2008, p. 675). The prevalence of bone involvement in syphilitic patients without access to treatment varies widely per account, from as little as 1% up to 20% (Roberts & Buikstra, 2019, pp. 381–382). More specific skeletal lesions attributable to syphilis and their paleopathological significance are discussed in-depth in the section 2.3.

2.2.4 Congenital syphilis

In addition to venereal transfer, syphilis can also be transmitted from mother to unborn child. This transplacental infection appears to be unique to syphilis, as congenital cases are rare in yaws and unreported for bejel (Roberts & Buikstra, 2019, p. 402). Early stage congenital syphilis refers to the infection before the age of two years, whereas the late stage occurs from the age of two onwards (Rasool & Govender, 1989, p. 752).

Most clinically recognizable symptoms only develop later, and some deformities may even persist into adulthood. Early stage symptoms often include anaemia, liver and spleen enlargement, rhinitis, fever, skin rashes, pseudoparalysis, and occasionally bone involvement. Late stage symptoms include keratitis (i.e. inflammation of the cornea), blindness, deafness, nerve degeneration, dental defects, synovial joint inflammation, and further bone involvement, which is described in more depth in section 2.3.3 (Hillson et al., 1998, p. 26; Ioannou et al., 2016; Rasool & Govender, 1989, p. 752; Singh & Romanowski, 1999, p. 194).

2.3 Skeletal manifestations

As this thesis aims to investigate syphilis in the skeletal remains, it is important to understand how the infection can affect the skeleton. While the most significant changes occur in the tertiary phase, local inflammation of the periosteum, potentially resulting in diffuse new bone formation, can already happen during the secondary stage, but this is usually overcome with complete healing and bone remodelling (Harper et al., 2011, p. 101; Roberts & Buikstra, 2019, p. 381).

During the tertiary stage, a variety of permanent skeletal changes can be produced by the formation of gummas, but occasionally also by non-gummatous processes. Generally, these modifications are present bilaterally and in multiple bones throughout the body, although the skull and long bones are generally deemed to be the most commonly affected elements (Crissey & Denenholz, 1984, p. 114; Roberts & Buikstra, 2019, p. 382).

2.3.1 Non-gummatous skeletal lesions

Non-gummatous lesions indicative of syphilis include the formation of periosteal new bone (PNB), osteitis, and osteomyelitis as a result of inflammatory processes (Harper et al., 2011, p. 101). Together, these inflammations can present in skeletal remains as nodes and expansions of localised thickening of the bone, with various morphological changes in the cortical surface, ranging from fine striations to extensive and rugose growths (Hackett, 1976, pp. 79–90; Roberts & Buikstra, 2019, p. 388). PNB is prevalent on bones that sit close to the skin. This is especially common in the shin bones or tibiae, where excessive new bone deposits on the anterior shaft can thicken and completely alter the shape of the bone, a phenomenon commonly referred to as sabre-shin (Figure 2.2) (Waldron, 2009, p. 105). A word of caution is necessary here, as osteitis, osteomyelitis, and PNB in particular can have many other causes, both specific (related to certain diseases) and non-specific. As such, these skeletal changes cannot be used as reliable diagnostic indicators for syphilis (Weston, 2008), and only provide tentative support of a diagnosis if they co-occur with suggestive or diagnostic lesions.

Figure 2.2: Sabre-shin. The tibiae from Albrecht of Valdštejn, a late medieval Czech military leader, show extensive anterior deformation linked to treponemal infection. (Vargová et al., 2019, p. 528).

In addition to these non-gummatous lesions, the skeleton may display changes caused by other syphilitic processes. These include aortic aneurysms due to cardiovascular syphilis, and joint damage, such as Charcot's joints, due to sensory loss related to tabes dorsalis (Roberts & Buikstra, 2019, p. 391). Again, these changes could also have arisen from non-syphilitic afflictions, and can only be used as supportive indicators instead of a definite diagnosis.

2.3.2 Gummatous skeletal lesions

Osseous changes caused by the necrotizing effects of gummatous processes in soft tissue are characterized by destructive and lytic reactions (i.e. bone loss) that can result in focal cavitations and depressions of the cortex, also called gummas (Figure 2.3), that occasionally extend into the medullary cavity (Figure 2.4) (Hackett, 1976, p. 93; Roberts & Buikstra, 2019, pp. 382; 389). The necrotic centre of the gumma is generally well-defined by a surrounding rim of reactive and sclerotic or hardened and dense bone. If such areas of bone destruction coalesce, a chaotic and irregular bone surface of depressions and elevations may be the result (Aufderheide & Rodriguez-Martin, 1998, p. 160).

Figure 2.3: Tibia with gummatous lesions. This tibia, belonging to a young adult female from the late medieval monastic hospital of Skriðuklaustur, Iceland, shows extensive gummatous destruction around the midshaft and slight anterior bowing. (Walser et al., 2018, p. 57).

Figure 2.4: Gummatous lesion. This cavity is surrounded by a node of new bone with pitting and striations, and is found on the anterior femur of individual S4084 V1086 from Kampen. Adapted from Schats, Hoogland, et al. (2017, p. 248).

Post-cranially, gummas can develop within nodes or expansions and appear as superficial cavitation due to focal destruction. This description was introduced by Hackett (1976, pp. 93-97), who determined nodes or expansions with superficial cavitation to be a diagnostic indicator of syphilis if presented in the long bones. The skull and long bones are often affected by such changes, although frequent presence on the clavicle has also been reported (Crissey & Denenholz, 1984, pp. 114–115).

On the skull, these gummatous changes form a distinctive worm- or moth-eaten disfiguration known as caries sicca (Figure 2.5), which develops on the external surface, although complete perforation of the bone may occur (Turk, 1995, p. 148). Caries sicca is generally accepted as a diagnostic marker for syphilis (Hackett, 1976, p. 114; Waldron, 2009, p. 108), although its diagnostic value for paleopathological diagnosis depends on the precise developmental stage exhibited by a specimen. Hackett (1976) was the first to identify these various stages, schematized in Figure 2.6. The initial series of changes starts with the formation of localized clusters of small pits, which subsequently come together in confluent clustered

Figure 2.5: Caries sicca in a cranium excavated from the post-medieval site of Redcross Way, London. The frontal and parietal bones exhibit extensive lytic lesions with nodular, healed margins. (Tucker, 2007, p. 221).

pits. After these initial changes, the cranial lesions either stay focal and follow the discrete series of change, or expand peripherally over the cranial bones according to the contiguous series of change. The discrete series begins with the formation of focal superficial cavitation. Following this, focal cavitations can start to exhibit healing rims of new bone, a phenomenon known as circumvallate cavitation. If this healing remains uninterrupted, the cavitations will be completely remodelled into slight depressions with radial scars (Hackett, 1976, pp. 30-41).

If the confluent clustered pits of the initial series do extend over the cranial surface, the contiguous series is set off by the development of serpiginous cavitation, which is similar to focal superficial cavitation but affecting a larger area in a more complex pattern. This is followed by nodular cavitation, which, similar to circumvallate cavitation, centres around the healing process of the rims of the cavities, creating a pattern of bony nodules and cavities. The final stage shows the classic caries sicca, which is the healed and static result of complete nodulation across the cranial vault, with the new bone separated by small, depressed lines or spaces (Hackett, 1976, pp. 42-49). These various stages can co-

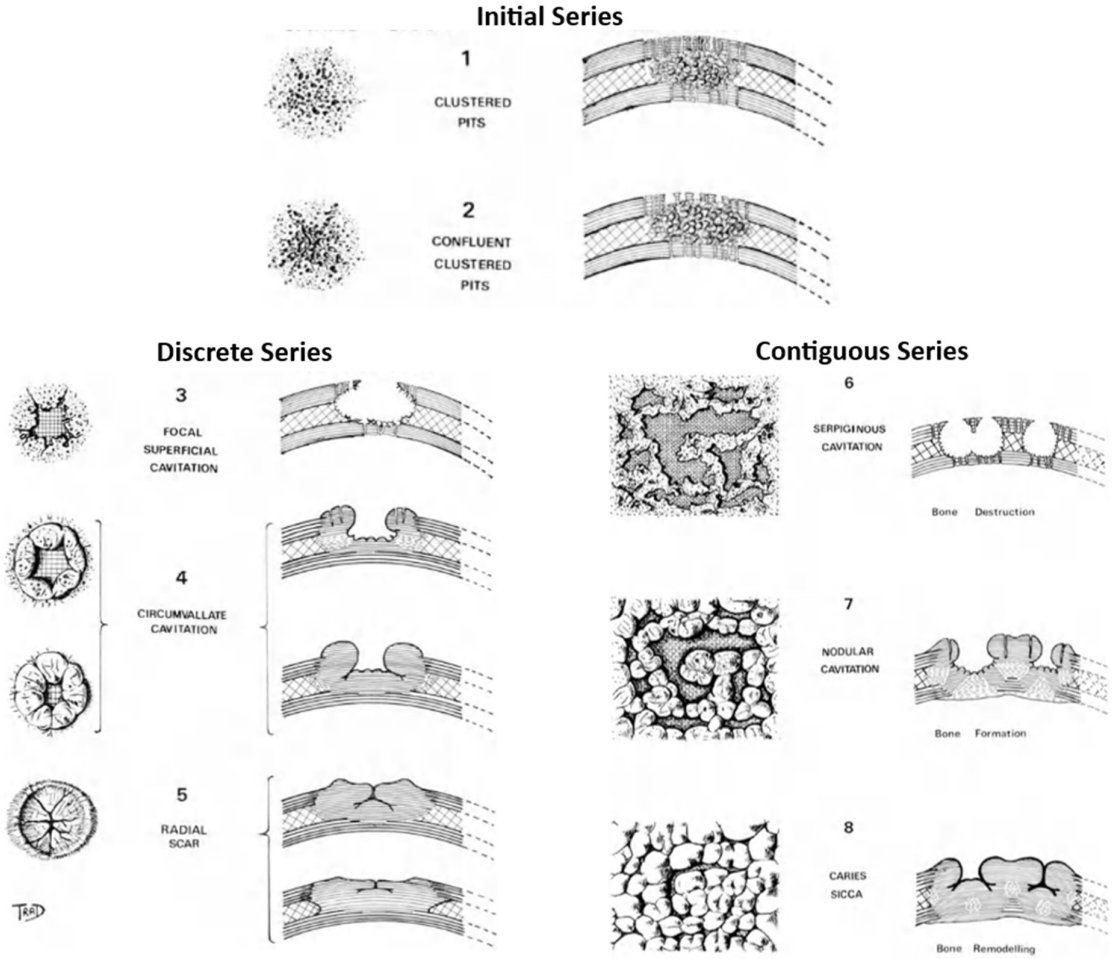

Figure 2.6: Hackett's caries sicca sequence. The diagram shows how the initial series can develop in either the discrete or contiguous series, with each series having various characteristic stages of bone destruction, bone formation and/or bone remodelling. Adapted from Hackett (1976, pp. 31-42).

occur in a single cranium, as caries sicca often progresses from one or multiple different centres and not in a linear manner simultaneously across the cranial vault (Hackett, 2976, p. 43).

Not all of these caries sicca stages are diagnostic for syphilis. Changes of the initial and discrete series can occur in other diseases, such as osteolytic metastatic cancer and tuberculosis. However, both of these diseases have relatively higher presence on the inner table of the cranium, whereas syphilis mostly affects the outer table (Hackett, 1976, p. 41; Roberts & Buikstra, 2019, p. 383). Hackett (1976) considers stage 4-8 to be diagnostic of syphilis infection (pp. 40-45).

Gummatous destruction can also result in perforation, destruction, or resorption of the nasal and palatine bones, leaving an empty nasal cavity with smooth, sclerotic margins (Roberts & Buikstra, 2019, pp. 385–386). Hackett (1976) regarded such destruction as a diagnostic lesion, but only if it is extensive (involving the complete nasal cavity, palatines and maxillary alveoli) and completely healed (pp. 63-65), which makes differential diagnosis a complex matter if these requirements are not fully met.

2.3.3 Congenital skeletal lesions

Congenital syphilis can involve the skeletal system already during the early stage with symptoms like periostitis, metaphyseal changes, osteitis, osteochondritis, and osteomyelitis, most often afflicting the long bones or the hand and feet (Rasool & Govender, 1989; Russo & Shryock, 1945).

Late stage congenital syphilis produces skeletal changes such as dental defects, frontal bossing (Parrot's sign), high arched palate, short maxillae, sabre-shins, and collapse of the nasal bridge, or a so-called "saddle nose", due to naso-palatine destruction (Figure 2.7), among many others (Ioannou & Henneberg, 2017, p. 451; Singh & Romanowski, 1999, p. 194). It is important to note that many of these lesions can also be the product of many other afflictions; a saddle nose, for example, can also be the result of leprosy (Schreiber et al., 2014).

Figure 2.7: Naso-palatine destruction (left) and the resulting "saddle nose" (right). The naso-palatine destruction has smooth, sclerotic margins typical of syphilis, which could lead to a saddle-nosed complexion. (Photo: Vargová et al., 2019, p. 525; drawing: Lexer, 1904 in Vargová et al., 2019, p. 525).

Instead, the most reliable markers for congenital syphilis are dental defects, which comprise of the notched Hutchinson's incisors, bud-shaped Moon's molars, and Fournier's mulberry molars (Figure 2.8) (Hillson et al., 1998). Of these, the first two are often deemed diagnostic, although their pathognomonic nature has been questioned (Harper et al., 2011, p. 103). Other dental defects used to identify congenital syphilis may also be attributable to historic treatment with mercury (further discussed in Chapter 3) that affected developing teeth in children. Such mercurial dental defects include enamel deficiencies that result in a discoloured "honeycombed" appearance of the teeth cusps (Ioannou et al., 2016). Post-cranially, a possible diagnostic, or at least strongly suggestive, indicator is the Higoumenakis' sign, which refers to thickening of the sternal end of the clavicle (Frangos et al., 2011).

Figure 2.8: Dental defects related to congenital syphilis. From left to right: a Hutchinson's incisor, a Moon's molar, and two Fournier's or mulberry molars. Adapted from Nissanka-Jayasuriya et al. (2016, p. 330).

2.3.4 Summary

Identifying these skeletal lesions in archaeological remains is especially important for tracing the history of the disease, but osteoarchaeological diagnosis of syphilis is impeded by the fact that the majority of syphilitic lesions have low specificity (occurrence in more than one disease) and/or low sensitivity (ratio of syphilitics that exhibit certain lesions) (Baker et al., 2020, pp. 19–20). As such, it requires a rigorous differential diagnosis if the diagnostic indicators are absent, especially for afflictions like leprosy, tuberculosis, non-specific periostitis, osteomyelitis and trauma (Roberts, 2019, p. 289; Vargová et al., 2019, p. 526). Due to this difficulty in diagnosing syphilis, the disease has received much attention in paleopathological and historical debates, most notably on its origin and further history.

3. Syphilis From A Historical Perspective

As this study aims to gain a better understanding of venereal syphilis and its treatment in the late medieval and early modern Netherlands, it is essential to understand the various historical and (paleo)pathological contexts of both the disease and the associated medical interventions. The history of syphilis is a rich field of study, so the goal for this chapter is to provide a contextual background for further discussion of this specific research. It will focus on the origin of syphilis, but will also discuss the various treatment methods developed over the past 500 years. The chapter finishes with a more historical focus on syphilis and its treatment in the late medieval and early modern Netherlands.

3.1 The European epidemic

Ever since the beginning of the first European outbreak during the 1490s, the origin of syphilis has been a topic of fierce debate, which initially flourished against the backdrop of warfare and turmoil throughout Europe (McGough, 2005, p. 574; Spates, 2011, p. 230). Although it is debated, syphilis likely made its first appearance during the French invasion of Naples in 1494 and 1495, an ideal cradle from which further dissemination could take place, as both the French and Italian army consisted of soldiers and mercenaries from countries across Europe (Meyer et al., 2002, p. 40). Following the war, they travelled back to their home countries, subsequently spreading the disease through modern-day France, Germany, and Switzerland before the end of 1495 (Figure 3.1). Syphilis reached further into Great-Britain, Scandinavia and south-eastern Europe, and by 1500 the entirety of Europe, as well as the Middle East and North Africa, had to deal with the ramifications of the infection (Frith, 2012, p. 50; Hays, 2009, p. 63).

During this time, the given name of the disease often symbolised unstable political relationships between countries by blaming neighbouring or rival nations for an occurring outbreak or by associating them with such an embarrassing affair (Hays, 2009, p. 64; Rothschild, 2005, p. 1457; Spates, 2011, p. 228).

Figure 3.1: A woodcut printing by Albrecht Dürer (1496). It depicts a mercenary with skin covered in syphilitic sores. https://commons.wikimedia.org/wiki/File:D%C3%BCrerSyphilis1496.jpg

As a result, syphilis was known under many names, such as the "French disease" or "*morbus Gallicus*" (according to the British, Germans, and Italians), the "Neapolitan disease" (according to the French), the "Polish disease" (according to the Russians), or the "German disease" (according to the Polish) (Hays, 2009, p. 64; Tampa et al., 2014, p. 4). The Dutch referred to it as the "Spanish sickness" (Rothschild, 2005, p. 1458), or locally as the "*Spaanse Pokken*" (Ladan, 2012, p. 48). More general denominations, often hinting at the venereal transmission of the affliction, were also common, such as "*lues venera*", "Venus disease", or the "Great Pox" (Blankaart, 1696; Meyer et al., 2002, pp. 40–41). The term "syphilis" was already coined in 1530 by Girolamo Fracastoro in his influential medical poem *Syphilis sive morbus Gallicus*, in which the main character Syphilus suffered from the disease, but would only gain popularity at the end of the 18th century (Plagens-Rotman et al., 2021, p. 552; Spates, 2011).

3.2 Hypotheses on the origin of syphilis

Within decades after the first epidemic, it was theorized that the onset and virulent spread of syphilis were related to the global explorations of the late 15th century (Spates, 2011, p. 238). The hypothesis that syphilis was transported from the New World, known as the *Columbian hypothesis*, remains one of the most prominent theories. Proponents argue that the disease was introduced to the European population after Columbus' return from the Americas in 1493 (Baker & Armelagos, 1988, p. 703). This hypothesis is supported by the apparent lack of unequivocal physical evidence of syphilis in Europe before 1493, whereas New World skeletal remains display plenty of lesions attributable to treponemal disease (Baker & Armelagos, 1988; Crosby, 1969, p. 220). Additionally, the severity of the first outbreak is indicative of a novel, virulent disease affecting a population with no previous exposure or herd-immunity (O'Shea, 1990, p. 392). This virulence was already recognized by contemporary writers like Ruiz Diaz de Isla and Gonsalvo Fernandez Oviedo y Valdez, whose elaborate descriptions serve as a historical backbone of the Columbian hypothesis (see for example Dennie, 1962; Holcomb, 1934).

In direct opposition to the Columbian hypothesis, proponents of the *pre-Columbian hypothesis* suppose that Europe was already familiar with a form of syphilis prior to 1493. This alternative theory was first proposed by Holcomb (1934; 1937) as he found that historical records did not align with the timeline of Columbus' travels. Instead, the initial epidemic may have been confused with other illnesses, like leprosy, that also severely affected the European population (Meyer et al., 2002). This hypothesis is supported by the growing number of Old World skeletal finds with lesions characteristic for treponemal infection (Figure 3.2) (e.g. Dawes & Magilton, 1980; Dutour et al., 1994; Gladykowska-Rzeczycka, 1994; Gladykowska-Rzeczycka et al., 2003; Henneberg & Henneberg, 1994; Lopez et al., 2017; Mays et al., 2003, 2012; Roberts, 1994; Stirland, 1991, 2009; von Hunnius et al., 2006). However, the interpretation and dating of such finds can be controversial (Armelagos et al., 2012) and is sometimes actually interpreted as support for the Columbian hypothesis (Harper et al., 2011, p. 123).

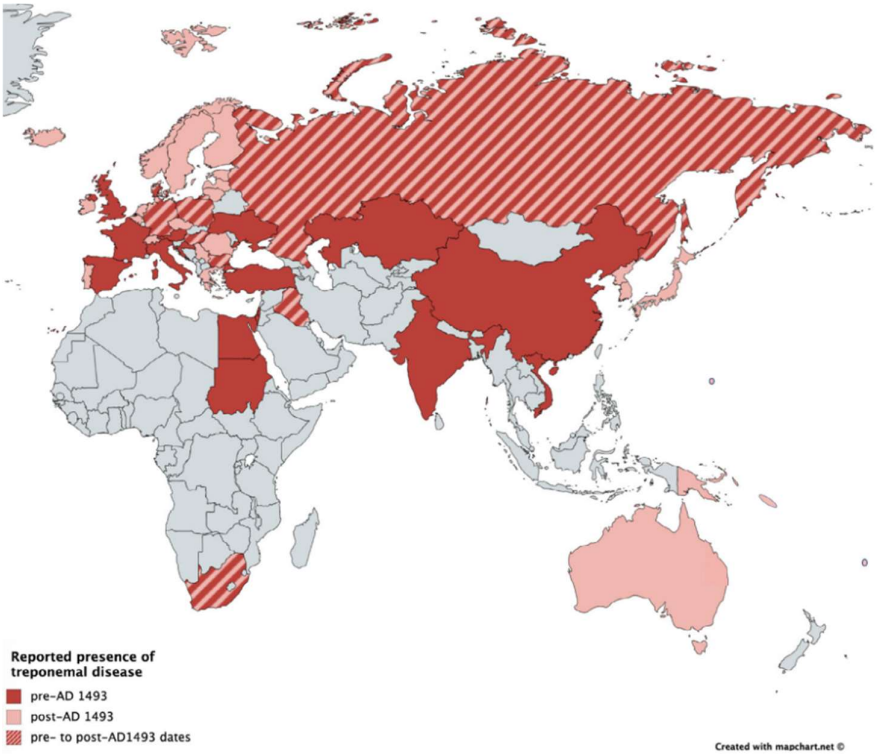

Figure 3.2: Overview of treponemal disease prevalence in the Old World. Data collected from paleopathological literature and mapped by Baker et al. (2020, p. 24).

While these two hypotheses are firmly established in the academic discourse, other theories have also been proposed, often focussing on the evolutionary rather than geographical origins. Building on the pre-Columbian hypothesis, Hackett (1963) proposed an evolutionary overview of the four treponematoses, sometimes referred to as the *Evolutionary hypothesis* (Baker et al., 2020). In this view, venereal syphilis originated from a mutation of bejel in southwestern Asia sometime around 3000 BC. This milder variant dispersed into Europe, after which its more virulent and destructive kind arose from another mutation around 1500 AD, causing the European epidemic (Hackett, 1963, p. 38).

The *Unitarian hypothesis* suggests that the treponematoses are actually evolutionary stages of the same disease, slightly differentiated through environmental pressures (Hudson, 1958; Powell & Cook, 2005). The various clinical manifestations are believed to be brought forth by localized adaptations to specific geographical regions, climatic conditions, and human behaviour (de Melo et al., 2010). The evolution of different versions of a single treponematosis was understood as a "biological gradient", with yaws considered as the primary treponematosis, evolving into bejel (Hudson, 1965, p. 885). With the rise of urban environments, bejel evolved into the venereal variant, under the assumption that city life would have improved personal hygiene, resulting in the bacteria developing an increased dependence on sexual transmission to survive (Giacani & Lukehart, 2014, p. 96; Hudson, 1963, 1965, p. 895). Recently, some scholars have deemed this hypothesis less relevant, as the different subspecies of *Treponema pallidum* have small, but distinct, genetic and molecular differences (Majander et al.,

2020, p. 3789). However, as noted in section 2.1, other research has given rise to the argument that genetic and clinical diversity between the four subspecies is too subtle (Baker et al., 2020, p. 28) and the Unitarian hypothesis thus cannot yet be completely disregarded (Giacani & Lukehart, 2014, pp. 97–99).

A fifth theory, although cited less often, is the *Alternative hypothesis*, proposed by Livingstone (1991). This theory supposes that while the European outbreak and the Columbian voyage do coincide, they do not correlate (Meyer et al., 2002, p. 42). Instead, a venereal adaptation to African treponemes could be a more likely cause for the European epidemic, as contact with African regions was established prior to contact with the Americas (Livingstone, 1991). This connection provides a broader timeline for venereal syphilis to arrive in Europe and subsequently infect its population (Meyer et al., 2002, p. 42). However, this hypothesis has ceased in popularity and has not been cited in more recent papers, which instead focus mostly on the Columbian, pre-Columbian and Unitarian hypotheses, with the occasional mention to Hackett's Evolutionary hypothesis (e.g. Baker et al., 2020; Harper et al., 2011).

3.2.1 Recent research on the origin of syphilis

While recent developments in ancient DNA (aDNA) and microbiological analyses have greatly improved research on the treponematoses, the historical debate on their origin has not yet been settled. aDNA research is especially challenging as the presence of *T. pallidum* in bone gradually decreases, and their detection in skeletal remains with tertiary lesions is often unsuccessful (Bouwman & Brown, 2005; von Hunnius et al., 2007). Instead, DNA can be successfully retrieved from remains with a higher pathogen load, as is the case in congenital or early stage venereal syphilis, both of which often go unrecognized during osteological analysis (Anastasiou & Mitchell, 2013, p. 36). As such, successful aDNA extraction requires a rigorous examination before conclusions can be justified (Bouwman & Brown, 2005).

Phylogenetic research on contemporary *T. pallidum* subspecies strains has indicated that there is a common ancestor in the 18th century, possibly supporting a post-Columbian hypothesis, but not rejecting the possible presence of pre-Columbian bacterial lineages that have since gone extinct (Arora et al., 2016, p. 3). Thus, recent studies have both emphasized and established the importance of ancient DNA research on historic samples to unravel the origin and evolutionary trajectory of treponemal disease (Majander et al., 2020; Schuenemann et al., 2018). Yet unknown *T. pallidum* lineages may have played a pivotal role in the spread of syphilis and its European epidemic, and some newly discovered lineages have tipped the scales in favour of a possible pre-Columbian origin (Majander et al., 2020, p. 3798). Despite these developments, definitive conclusions regarding the origin of venereal syphilis cannot yet be made, as the precise relations between the different *T. pallidum* subspecies remains insufficiently understood (Baker et al., 2020, pp. 8–9).

3.3 History of syphilis treatment

Following the European syphilis epidemic of the late 15th century, frantic attempts were made to control the spread of this feared disease. As its venereal nature was already recognised from the 1520's onwards, statutory regulations aimed to isolate communal spaces and individuals generally associated with unhygienic or sexual activities, such as bathhouses and brothels, as well as prostitutes and transient individuals (Dobson, 2015; Frith, 2012, pp. 51–52; Hays, 2009, p. 65). In addition, sufferers were isolated from the community, not only out of fear for contamination, but also to control those who fell victim to this 'divine punishment' (Plagens-Rotman et al., 2021, p. 552). To do so, some hospitals and infirmaries designed specialised rooms or institutions to cure syphilitics, not unlike the leprosaria that were used to isolate lepers from the general public. These institutions were likely to have been supported by nurses and other medical professionals that worked specifically with syphilis patients (Ladan, 2012, pp. 51–52).

Despite these attempts, sufferers of the disease remained desperate for treatment. In the absence of modern antibiotics, medieval physicians offered a variety of "cures", which were not only painful, but also mostly ineffective. One such treatment made use of hot irons to burn away the sores, but most treatment methods included the use of medicine, most commonly mercury (Sefton, 2001, p. 594).

3.3.1 Mercury treatment

Mercury, a toxic heavy metal also known as quicksilver or hydrargyrum (Hg), was already used in various regions across the world prior to the European syphilis epidemic, such as ancient Egypt, China, Tibet, Greece and the Roman Empire. In Europe, mercury was primarily mined in Almadén (Spain), Monte Amiata (Italy), and Idrija (now Slovenia), and was added to cosmetics and ointments (Kloprogge et al., 2020, pp. 786–787). In addition, it was used to treat various skin diseases, which was why the medicine rose to popularity to treat the syphilitic skin lesions as well (Karamanou et al., 2013, p. 317). This initial appeal was based on its apparent anti-inflammatory properties, as it resulted in permanent lightening of the skin and would seem to clear up any ulcers or rashes (Swiderski, 2008, pp. 98, 162–163; Tucker, 2007, p. 220). In addition, treatment may have appeared successful due to the nature of the disease itself (Ioannou & Henneberg, 2017, p. 450), as first and secondary stage symptoms usually heal spontaneously over time and the occurrence of latency may have been falsely interpreted as the syphilitic patient being cured. The use of mercury was implemented further by Phillipus von Hohenheim (1493-1541), also known as Paracelsus, who promoted the medicine as chemotherapy against syphilis in the early 16th century (O'Shea, 1990, p. 392). Following his writings, various treatments, all incorporating mercury in one form or another, would remain the primary cure for syphilis in Europe up until the early 1900s (Hays, 2009, p. 68; Tucker, 2007, p. 220).

Due to mercury's diuretic nature, it causes excessive urination, salivation, and sweating, which were believed to expel harmful syphilitic particles from the body (O'Shea, 1990, p. 392; Tampa et al., 2014, p. 9). In actuality, these reactions are indicative of acute mercury poisoning, which is likely to have been a common occurrence considering the exorbitant dosages administered (O'Shea, 1990, pp. 392–393). Side effects also included neuropathy, kidney failure, mouth and throat ulcers, tooth loss, tremors, gastrointestinal problems, and irritable or nervous tempers (Frith, 2012, p. 53; Tucker, 2007, p. 220). Chronic exposure to high levels of mercury can affect the central nervous system and result in erethism, which is also known as the mad hatter disease due to the exposure experienced by workers in the 18th to 20th century felt-hat industry that utilized mercury for hair removal from animal pelts. Common symptoms of this neurological disorder include amnesia, insomnia, and excitability, while the worst cases resulted in delirium or even coma (Aufderheide & Rodriguez-Martin, 1998, p. 320).

Although the exact dosing and intensity of the treatments varied extensively between regions and individual medical practitioners, it has been established that doses were especially high during the 16th century and gradually decreased in the following centuries to evade unpleasant side effects while maintaining mercury's therapeutic effects. In addition, treatment plans were frequently adjusted to the individual patients and as such a standardized regimen was not available (O'Shea, 1990, p. 393).

Mercury could be administered to patients through various forms and methods, mostly depending on the symptoms experienced by the affected patients. Ulcers, other skin lesions, and aching joints were covered with ointments made from a mixture of fat and mercuric chloride ($HgCl_2$), known as mercuric or corrosive sublimate due to its corrosive effects that could clear up the skin lesions (O'Shea, 1990, p. 393; Zuckerman, 2016, p. 44). Mercurous chloride (Hg_2Cl_2), colloquially named calomel or *mercurius dulcis* ("sweet mercury"), became more widely available during the late 16th and early 17th century and was supposedly less toxic than mercuric sublimate (O'Shea, 1990, p. 393; Urdang, 1948, p. 93). It could also be used as an ointment, but was otherwise administered to patients orally. During the 18th century, calomel could also be administered to patients by injection or by the consumption of a potion, which was known as "*Liquid Swietenii*" (Frith, 2012, p. 53; Koten, 2016, p. 5; O'Shea, 1990, p. 393). Besides these treatments, mercury could be added to other medicine, such as pills, which were often formulated with other ingredients to help clear the patient of the "acid" causing the disease (Blankaart, 1696, pp. 140–141; Heinsius, 1705, p. 40).

Another popular treatment, referred to as fumigation, centred around increased sweating and the inhalation of mercuric vapours derived from heating metallic mercury (Hg), mercuric chloride, or cinnabar (HgS) (Zuckerman, 2016, p. 22). Fumigation practices could last for weeks, during which patients were repeatedly enclosed in heated spaces such as tents, rooms, stoves (Figure 1.1), or special fumigation apparatuses that served to stimulate sweating (Figure 3.3 and Figure 3.4) (Zuckerman,

2016, p. 44). This treatment method, which was often combined or alternated with sweat therapies, was already adopted within a decade after the initial spread of the disease and would remain prominent until the early 1900s (O'Shea, 1990, p. 393). Nowadays, mercury's use in medicine has considerably declined due to its toxic nature, although the use of cinnabar is still prevalent in alternative or traditional medicine (see for example de Ruiter, 2021) (Kloprogge et al., 2020, p. 802).

Mercury's effectiveness against syphilitic infection has been the topic of considerable debate. Its anti-inflammatory, antimitotic, and bactericidal properties may have been able to aid in the abortion of the initial infection or in the healing of lesions in gummatous syphilis by inhibiting cell division and growth and reducing the amount of spirochetes, especially in skin lesions (O'Shea, 1990, p. 393). However, it remains difficult to assess the true effectiveness of mercury against syphilis as there are no *in vitro* studies and many other complicating factors, such as the natural progression of the infection, the numerous ways of administration of medicine, and the combination of mercury with other medicine or therapies (Ioannou & Henneberg, 2017, pp. 450–451).

Figure 3.3: Die Belägert und Entsetzte Venus. A German historical print from 1689 showcasing various treatment methods for syphilis, such as fumigation (forefront), sweat therapy (bed) and possibly ingestion (background). http://resource.nlm.nih.gov/101436361

Figure 3.4: De Spaanse Pokmeester. A Dutch historical print from 1691 showcasing a hospital with fumigation and sweating therapies and examinations for syphilis ("pokken"). Originally published in Lusart (1691), retrieved from http://resource.nlm.nih.gov/101435727

3.3.2 Guaiac and other remedies

From the early 16th century onwards, the use of toxic mercury was criticized. Most notably, Ulrich von Hutten (1488-1523) reported his negative experiences with mercury and instead promoted the use of guaiacum or guaiac (Karamanou et al., 2013, p. 317). Guaiac refers to wood derived from the guaiacum tree (*Guaiacum officinale*) (Figure 3.5), found in Central and South America as well as the West Indies. Its New World origins contributed to its popularity, as it was widely accepted that a disease should be curable with natural remedies from its region of origin (Biehler-Gomez et al., 2022, p. 502; Hays, 2009, p. 66). Guaiac's purgative nature caused excessive sweating, diarrhoea, and urination, not unlike the symptoms experienced during mercury treatments. The plant could be administered as a potion or ointment, sometimes combined with therapies that further promoted sweating (Karamanou et al., 2013, p. 317; Tampa et al., 2014, p. 8).

Figure 3.5: Watercolour painting of Guaiacum officinale *by Francis W. Horne (n.d.). https://sweetgum.nybg.org/science /world-flora/monographs-details/?irn=21739*

While mercury and guaiac formed the two most popular medicine for syphilis from 16th to the 18th century, other remedies were also in use. Sarsaparilla and sassafras, two other New World plants, were also imported as anti-syphilitic remedies due to their purgative effects (Forrai, 2011, pp. 46–48). During the 19th century, bismuth, iodine, and arsenic compounds were introduced as alternatives for mercury, as they were often less toxic and more effective in limiting spirochete presence (Forrai, 2011, p. 53; Karamanou et al., 2013, p. 318; O'Shea, 1990, p. 394). Despite these alternatives, mercury was still advocated for, but often administered in different ways or lower doses to prevent mercury poisoning and its associated symptoms (Forrai, 2011, pp. 55–56).

In the early 20th century, developments in the causes and diagnosis of syphilis paved the way for more effective management and treatment of the disease (Sefton, 2001, p. 594). In 1909, Paul Ehrlich and Sahachiro Hata developed the arsenic compound "606" and subsequently the medicine Salvarsan and Neosalvarsan, which acted as the first effective antibiotic cures for syphilis (Frith, 2012, p. 53; Tampa et al., 2014, p. 9). In 1917, Julus Wagner-Jauregg found that malaria could also be used as sweat therapy, due to its fever-inducing symptoms. Discovered by Alexander Fleming in 1928 and used against syphilis from 1943 onwards, penicillin fully replaced treatments with mercury, Neosalvarsan, and malaria, and remains the primary cure against syphilis today (Sefton, 2001, pp. 594–595; Tampa et al., 2014, p. 9).

3.4 Syphilis in the late medieval and early modern Netherlands

3.4.1 Historical evidence

Similar to the rest of Europe, the Low Countries could not evade the consequences of the late 15th century syphilis epidemic. The disease, locally referred to as *de Spaansche pokken* (the Spanish Pox), *de Venusziekte* (the Venus disease), or *de Sint Jobsziekte* (the Sint Jobs disease), is believed to have made its entry already in 1496 in Zeeland, and is likely to have been epidemic from 1498 onwards, when it first arrived in the northern provinces (Fokker, 1861, p. 452).

Historical records are often consulted to shine a light on the syphilis epidemic in the late medieval and early modern Netherlands. Several cities in the region of Holland have early records of a small number of syphilis patients in the first decades of the 15th century (Ladan, 2012, p. 50), but some records also reflect the experience of a more substantial syphilis epidemic, most notably in Middelburg (Fokker, 1861, p. 462). Additionally, these records show that medical treatment was provided within establishments specifically erected for and dedicated to syphilis treatment by specialised doctors known as *pokmeesters* ("pox masters"), which are also mentioned on Figure 3.4. These establishments were named *Pockhuysen* ("Pox houses"), and were often part of the already available infirmaries and other care institutions (Coronel, 1880, p. 384; Ladan, 2012, pp. 49–55). While the majority of professional medical care during this period was reserved for those who had sufficient financial means, syphilis treatment in these *Pockhuysen* was oftentimes readily accessible and free-of-charge for the poorest members of society (Fokker, 1861, p. 463), which is exemplary of the desperation with which all layers of society tried to rid themselves of the disease.

In general, early treatments primarily consisted of aggressive mercury therapies, but also made use of guaiac. However, 18th century medics became increasingly cautious with administering high doses of mercury (Van Voorst Vader, 2016, p. 25). Fokker (1861) describes the fluctuating medical preference during the 15th and 16th century between mercury and wood drinks, which could be made from guaiac and sarsaparilla. Around 1700, historic medical books, such as Blankaart (1696) and Heinsius (1704, 1705), were influential resources in describing and affirming the importance of mercury as a syphilis cure. They described how these mercury treatments were often combined with intensive and prolonged sweat therapy to further promote the excretion of the syphilitic particles. During these sweat therapies, flammable liquids, such as the widely available brandy, were burned in stoves and the produced steam was redirected towards the patient, often huddled in blankets or in bed to warm them up even more (Figure 3.3) (Blankaart, 1696). Other remedies included bloodletting, applying enemas, administering laxatives, and hot bathing, although these treatments were also likely promoted by quacks in an attempt to earn a buck from desperate sufferers (Coronel, 1880, pp. 380–

382). Besides medical treatment, the spread of syphilis was also limited by societal regulations, such as the closing of brothels and prosecution of prostitution in the late 16th century (Fokker, 1860).

3.4.1 Osteoarchaeological evidence

Osteoarchaeological evidence for the disease during this period is somewhat scarce. Skeletal remains with lesions suggestive of syphilis have been reported to be present in the towns of Breda (de Jonge & Baetsen, 2013, p. 242), Kampen (Schats, Hoogland, et al., 2017, pp. 247–248), Haarlem (Groot, 2013), Den Haag (Pavlović et al., 2021, p. 186), Hattem (Pavlović et al., 2021, p. 203), and Eindhoven (Arts, 2019, p. 60). However, considering the multitude of general historical records and medicine books, it is clear that the scarcity of the osteoarchaeological evidence for syphilis does not accurately reflect the true societal impact of the disease. This is especially striking in an example from Delft, which was renowned for its syphilitic salve containing cinnabar during the 16th century that was medically available in the *pokhuis* situated in the city's main infirmary complex (Fokker, 1861, pp. 463–464). Despite this history, osteological analysis on remains from this infirmary did not report any sign of syphilis infection (Onisto et al., 1998, pp. 17–20), although it should be noted that this original study did not use the same analytical methodology laid out in this thesis.

So, in order to more accurately study the impact of the disease in the Netherlands, a thorough examination is necessary and historical records or osteoarchaeological reports should not be employed in isolation. For this thesis, the site of St. Gertrude's infirmary in Kampen is re-examined with a more in-depth focus on syphilis, as well as its treatment. The next chapter discusses the historical context of the city of Kampen, its healthcare, and the infirmary site.

4. Materials

Before investigating syphilis and its treatment, it is pertinent to provide the historical context of the archaeological site and human skeletal remains studied in this thesis. This chapter briefly discusses the history of the city of Kampen during the late medieval and early modern period, as well as the development of local care institutions. As this thesis investigates the site of St. Gertrude's infirmary, the history and excavation of this institution will receive separate attention. Finally, as the skeletal assemblage recovered from this infirmary's cemetery and its previously conducted osteoarchaeological analysis will form the foundation of further study within this thesis, these findings will be discussed more extensively.

4.1 Kampen in the late medieval and early modern period

The city of Kampen has a rich and vibrant history that stretches back over 900 years. Its strategic position on the banks of the river IJssel allowed easy access to the *Zuiderzee* (now the IJsselmeer) and the North Sea beyond that. This location played a crucial role in the city's early development into one of the most prominent trading hubs of the Low Countries in the 13th and 14th century (Figure 4.1) (Speet, 1986, p. 7). The town is not mentioned in historical records prior to 1227, even though the settlement at that time already featured significant urban architecture, such as the St. Nicholas church. This scarcity of historical records, most notably the lack of any documents pertaining to the declaration of city rights, has allowed for much speculation, as of yet unresolved, on the town's early development and the origin of its first settlers (Kossmann-Putto & Kossmann, 1989, p. 1; Kreek, 2020, p. 66).

Nonetheless, historical and archaeological research focussed on the second half of the 13th century has shown that the city received multiple independent trading privileges and became increasingly engaged with Scandinavian trade. Following this, the city expanded it influences by participating in the Hanseatic League throughout the 14th and early 15th century, and its regular business contacts came to include the counties of Holland, Zeeland, and Flanders, as well as England, France, and several regions surrounding the Baltic and North Sea. In doing so, Kampen's citizens did not personally partake much in the trading business, but often filled a more intermediary role to handle and organize shipping between international merchants (Speet, 1986, pp. 7–8). This mediating role was extremely successful, which is for example visible by the number of seafaring ships the city controlled, which could be as many as 120, likely to have been more than the ships of the cities in the Northern Netherlands combined. Furthermore, the city's port functioned as a hub in transporting trading goods from and to the Dutch and German cities along the Rhine (Speet, 1986, p. 23). Its economic success did not go unnoticed, and due to subsequent population pressures the town grew and expanded multiple times during the 14th and 15th centuries, both within and outside the city walls (Kolman, 1990).

However, during the second half of the 16th century, this economic and population growth was challenged by the increasing competition from other Dutch trading cities, most notably in Holland and Zeeland. Additionally, Kampen's maritime trade became complicated as its waterways and connection with the Zuiderzee silted up, which ultimately inhibited larger ships from sailing through, despite numerous preventative efforts. Once key to its economic success, the city's primary but limited focus on international trade now added to its steady demise, as other industries, such as breweries or cloth productions, were relatively underdeveloped for an early modern city of its size (Speet, 1986, p. 23). This decline was exacerbated when the city was besieged and partially destroyed in 1572 and 1578 by various usurpers. Following a third siege in 1672 by the French, the city had to endure financial damages, a stark decrease in population, and a surge in poverty that persisted throughout the following centuries up until 1830. From that period onwards, Kampen saw some improvement in infrastructure, while lending itself to be a regional hub and developing small but successful tobacco and metal industries (Speet, 1986, pp. 25–26).

Figure 4.1: Historical map of the Netherlands by Zacharias Heyns (1598). The city of Kampen (indicated as Campen) is located on the far right. https://hdl.handle.net/1874/20413

4.1.1 Healthcare in late medieval and early modern Kampen

As life in a medieval city is not without the risk of disease or injuries, multiple institutions within Kampen provided social healthcare and more specialised medical care. Throughout the centuries, multiple institutions functioned as *gasthuizen*, which could be translated as "infirmary" or "hospice", although they often had more than one purpose. Practically, *gasthuizen* were frequently connected to religious institutions and served as a place to take in and care for travellers, the sick, the poor, and the old (van der Sligte-de Jong, 1993, p. 7). They housed three types of guests: the more affluent citizens, who could fully pay for their care and offered additional financial aid to the infirmary, the working residents, who received care in turn for physical labour, and the work-free residents, who paid a small sum but were not required to work (Don, 1966). Some infirmaries also offered permanent residency for *proveniers*, who suffered from old age, terminal illness, or debilitating injuries and paid for board and care for the remainder of their life, similar to modern-day retirement homes (van Zanten, 2017, pp. 33–34). Other infirmaries included a so-called *passantenhuis*, a place that could provide short-term residency to passers-by, such as travellers, merchants, or pilgrims (van der Sligte-de Jong, 1993, p. 9).

The infirmaries were managed by two church wardens, who were responsible for daily tasks such as organizing renovations or repairs, and, most importantly, managing the infirmary's finances. Besides overseeing expenses and leaseholds, this financial responsibility also included the supervision of assets of deceased residents, as these assets could be claimed by the infirmaries. In addition to the church wardens, daily healthcare was provided by the matron, a head nurse who also led the maids that performed general tasks such as baking, washing, and cleaning (van Zanten, 2017, pp. 31–33).

Founded at the end of the 13th century, the oldest infirmary in Kampen was known as the *Heilige Geestgasthuis* ("Holy Spirit infirmary"). It was comprised of two facilities, one dedicated to caring for the sick, and the other providing residency for *proveniers* or the poor (Jager, 2015, p. 351). In order to better provide for the poor, a second infirmary, called the *Melijs-* or *Melisgasthuis*, was established sometime prior to 1356. This infirmary is likely to have evolved into the *Sint Geertruidengasthuis*, or St. Gertrude's infirmary (van Zanten, 2017, pp. 28–29), which will be discussed separately in the next paragraph. In 1386, the city acquired a third infirmary: the *St. Catharina- en Maria Magdalena Gasthuis* or the *Melatengasthuis*, in reference to *melaatsheid* (leprosy) (Don, 1966). It was initially located outside of the city walls near a main road that led outside the city, which was also a designated place for beggars with leprosy, but only if they had obtained proof of the diagnosis. Besides facilities for lepers, the complex also featured a cemetery, chapel and houses for *proveniers* up until 1589, when the complex was merged with, and its patients transferred to, St. Gertrude's infirmary (Jager, 2015, pp. 352–354). The two institutions may have had to coalesce as a result of dwindling leprosy infections, making a specialised facility redundant (van der Sligte-de Jong, 1993, p. 25).

Besides these infirmaries, which provided more general care, a specialised *Pesthuis* (plague house) was established. To manage the repeated Black Death outbreaks of the 15th and 16th centuries, this institution was specifically designed to isolate and care for plague patients, and no other patients were allowed (Hallema, 1957, p. 204). However, it should be noted that many other afflictions may have been misdiagnosed as the plague and as such may have been treated in the *Pesthuis* after all (Jager, 2015, p. 351). Later, this facility would have abandoned its religious origins and hospice-like facilities, as it developed into the city's hospital (van der Sligte-de Jong, 1993, p. 24).

Even though each of the infirmaries' church wardens wrote up extensive financial records, there are no records that explicitly inform us about the medical care and treatment offered in this period. In this period, medicine were often prescribed by the *chirurgijn*, a barber surgeon that generally lacked the academic medical knowledge of the *doctor medicinae* (Ladan, 2012, pp. 15–16), and provided by the local pharmacy or the barber surgeon himself (Hallema, 1957, p. 211; van Vliet, 2013, p. 139). However, there is no known mention of a specialised *pokmeester* to cure syphilitic patients in Kampen.

4.2 Saint Gertrude's infirmary

St. Gertrude's infirmary likely originated from the *Melijsgasthuis*, although the precise timing of its establishment is unknown. The name of the infirmary is mentioned for the first time in 1382, although it is likely to have existed prior to this date (van Zanten, 2017, p. 30). It was situated within the historical centre of the city between the Boven Nieuwstraat and the Burgwal, also bordering the Brandsteeg that used to connect the two major streets (Figure 4.2) (Klomp, 2017a, p. 95). The complex was comprised of a sick ward, a chapel, and one or more altars, where religious sermons were held multiple times a week (van Zanten, 2017, p. 32), and the infirmary expanded multiple times throughout the centuries.

In the 14th century, the sick ward consisted of eight beds for sick individuals, whereas an undefined number of beds were reserved for the poor (van Zanten, 2017, p. 32). It was initially designed for taking in weary travellers and the sick or poor, but the second half of the 15th century saw the increased inclusion of *proveniers* (Jager, 2015, p. 352), who would later settle into the smaller houses that surrounded the courtyard. Additionally, a number of inhabitants are likely to have suffered from mental disabilities, pejoratively indicated as *onnoselen* in historical records. Later, in 1599, an isolated *dollhuys* (mental asylum) was created to house seriously disturbed patients (van Vliet, 2013, pp. 139–140). The complex expanded significantly in 1484, as it gained ownership of the courtyard and some of the buildings behind the infirmary and chapel. During this period, the number of beds available for the sick and poor rapidly increased and is likely to have doubled (van Zanten, 2017, pp. 33–34). In 1600, it was noted that the infirmary could house a maximum of 36 residents, although it is thought to be unlikely that this number of inhabitants was regularly achieved (van Vliet, 2013, p. 137).

Figure 4.2: Historical map of Kampen by Joan Blaeu (ca. 1650-1700). The added marker points to the location of St. Gertrude's infirmary, which is the building with the blue-grayish roof. Adapted from https://hdl.handle.net/1874/350230

In addition to the usual inhabitants of the infirmary, the complex functioned as a shelter in times of need. For example, Prince Maurice requested the city of Kampen twice to take in several soldiers at St. Gertrude's infirmary, as they were wounded during the Eighty Year's War in the 16th and 17th century (van Zanten, 2017, p. 34).

From the mid-16th century onwards, the courtyard may have featured a large stable to house 50 or more animals, like cows, pigs, and horses, during the winter. Combined with the small brewery and bakery, the infirmary was rather self-sufficient and only a select number of products needed to be purchased. Additionally, a variety of local tradesmen was employed to provide goods and services such as linen, furniture, renovations, repairs, and clothing or shoes for the residents (van Vliet, 2013). As described above, the infirmary merged with the *St. Catharinagasthuis* in 1598 and became known as the *Sint Geertruids- en Catharinagasthuis*, or colloquially as the *Bovengasthuis*. In 1611, the chapel on the complex was torn down and replaced by a gate, as shown in Figure 4.3 (Klomp, 2017a, p. 95). During the 19th century, the governance of Kampen's *gasthuizen* became increasingly tangled and ultimately resulted in the creation of the institute of *Vereenigde Kamper Gast- en Proveniershuizen*. St. Gertrude's infirmary stayed open as an individual facility until 1897 (van der Sligte-de Jong, 1993).

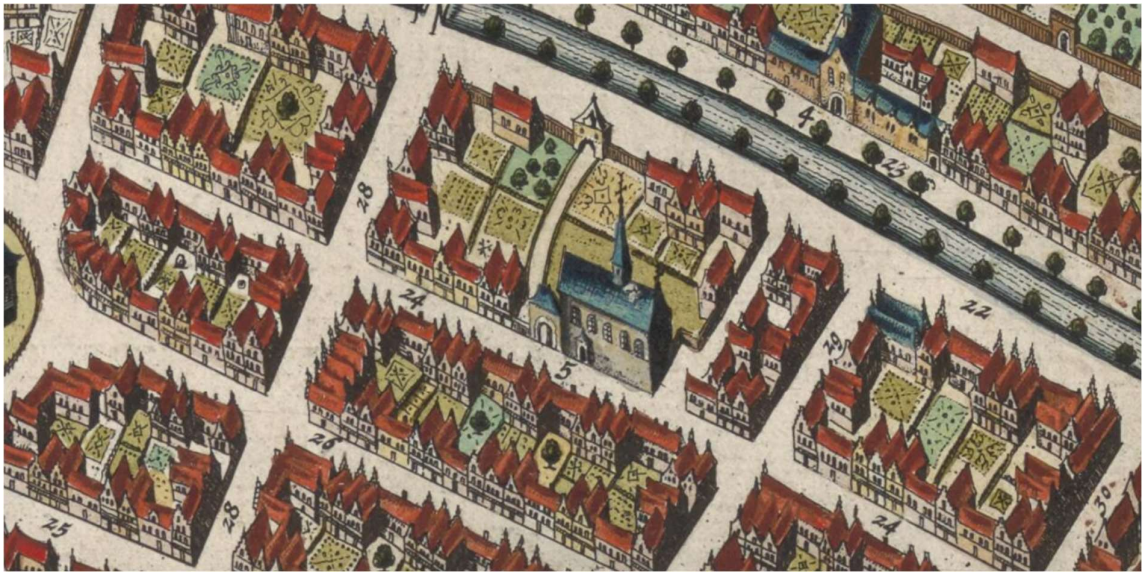

Figure 4.3: St. Gertrude's infirmary, indicated by no. 5 on this close-up of Joan Blaeu's map (ca. 1650-1700). The larger blue-roofed building is the sick ward, with the courtyard situated behind it.
Adapted from https://beeldbank.cultureelerfgoed.nl/zuiderzeemuseum/detail/9030273c-faa2-553d-8a0b-17cc2af512d7

Although it is known that the infirmary was in charge of burying deceased patients, a designated cemetery was not mentioned in historical records (van Vliet, 2013, pp. 140–141) and it remained unidentified until archaeological excavations in 2014 unearthed numerous human skeletal remains. It is believed that the destruction of the chapel in 1611 inhibited any burials on the grounds of the complex, and as such the timeline of the cemetery has been hypothesized to begin sometime during the 1380s, with 1382 being a definite date, and conclude around 1611 (Schats & Klomp, 2019, p. 107)

4.2.1 Excavation

In order to construct a new elderly care home, the site of St. Gertrude's infirmary, now known as the Margaretha and Myosotis grounds, was subjected to multiple large-scale excavations in 2011 and 2014. The trial trenches and subsequent excavation in 2011 focused on the northern part of the area and recovered a portion of St. Gertrude's sick ward, whereas the excavations in 2014 were located more to the south and unearthed more of the sick ward and chapel (Figure 4.4). Combined, these excavations recovered remnants of the chapel, sick ward, and cemetery, as well as stone and wooden foundations and intricate brick hearths of several late medieval houses. Additionally, two cellars were found behind the chapel, which were hypothesized to indicate the existence of a kitchen and privy (Klomp, 2017b). Other finds included a large number of remnants of earthenware, stoneware ceramics, leather, wood, animal bone, and various metal accessories, tools, or building materials, of which the majority has been dated to the 14th and, to a lesser extent, the 15th century (Klomp, 2017b, pp. 103–202). These findings received extensive further research, such as dendrochronological, entomological and parasitological analyses, which are discussed in detail in Klomp (2017b). Timber findings at the site are discussed extensively in Cremer (2018).

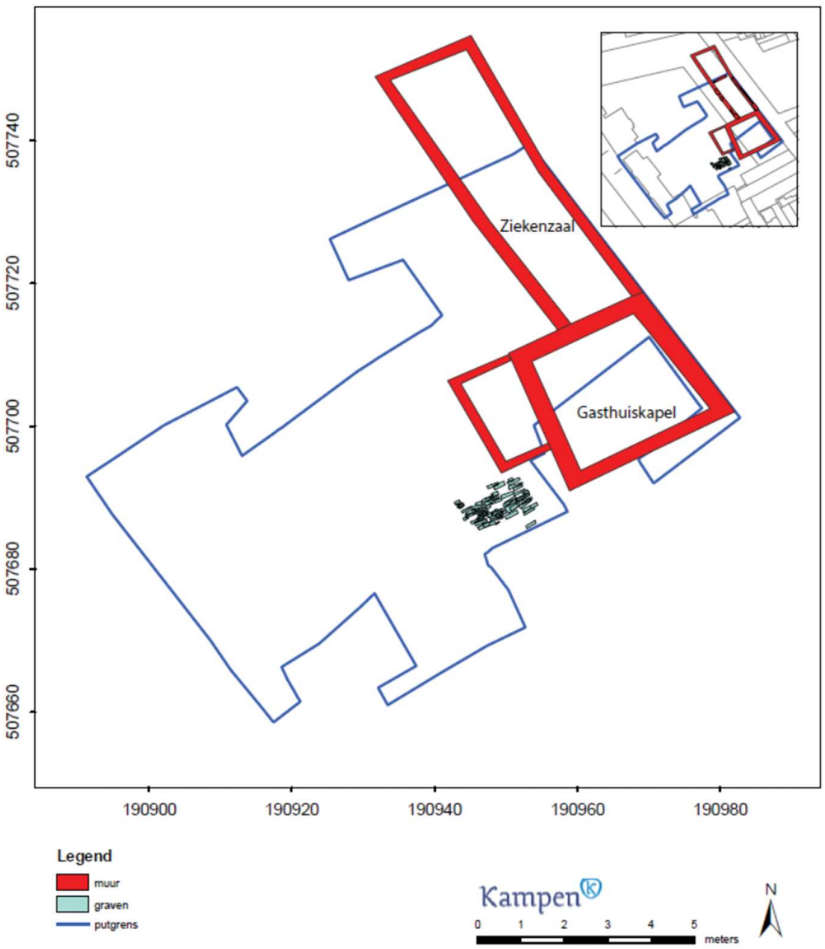

Figure 4.4: Map of the 2014 excavation. It showcases the reconstructed walls of the sick ward ("ziekenzaal") and chapel ("gasthuiskapel") in red, the outline of the excavation in blue and the burials in light blue. (Schats and Klomp, 2019, p. 107).

Note: the orientation of this map differs from the historical maps in Figure 4.2 and 4.3, which have a south-western orientation.

4.2.2 The cemetery

In the context of this thesis, the most significant finding is that of the cemetery, located to the southwest of the chapel and sick ward (Figure 4.4), and the human skeletal remains found therein. These were excavated in 2014 by students from the Faculty of Archaeology, Leiden University, with subsequent osteoarchaeological research conducted at the Laboratory for Human Osteoarchaeology, Leiden University, which was reported in Schats, Hoogland, et al. (2017). The excavation uncovered 89 individuals in primary burials and an unspecified number of secondary depositions, although the cemetery is believed to have been much larger with more inhumations. These can no longer be recovered due to earlier constructions in the 1970s (Schats & Klomp, 2019, p. 108).

Individuals were positioned with their head oriented to the southwest, which is, as noted by Schats and Klomp (2019), unlike most Christian burials (p. 108). All but one individual were laid to rest on their back, with their legs extended when present and their arms, if observable, in variable positions. As the

burial ground excavation retrieved almost no wood in comparison to other parts of the site, it is believed that wooden coffins were not used for the majority of the inhumations. This may also have allowed for more post-mortem movement of the skeletal remains and would explain the variety in positions of the upper extremities (Schats & Klomp, 2019, pp. 108–110). It is interesting to note that historical records from 1613 do suggest burials through mentioning the use of at least five coffins, as well as mortcloths (van Vliet, 2013, pp. 140–141), but as they do not specify a location of the burial and would have taken place after the destruction of the infirmary chapel, it is likely that these deceased individuals were buried elsewhere.

Following the excavation of St. Gertrude's infirmary in 2014, the skeletal remains were transported to and analysed by Leiden University. The 89 primary burials were subjected to an extensive physical anthropological analysis to gain insight into their demographic composition and pathological conditions. A biological profile was created for each individual, which includes skeletal preservation and completeness, estimations of biological sex, age-at-death, and stature, as well as any anatomical abnormalities and pathological observations. Skeletal preservation was categorized as either 'good', 'fair', or 'poor', and was deemed to be generally good, with only 3.4% of individuals categorized as poorly preserved. Skeletal completeness was categorized as percent ranges of 0-25%, 25-50%, 50-75%, or 75-100%. While the completeness was occasionally impacted by the placement of later burials or more recent destructive activities (Schats, Hoogland, et al., 2017, p. 241), still 62.9% of individuals were found to be more than 50% complete.

The age-at-death distribution in the total population from St. Gertrude's infirmary can be divided in 78 adults (87.6%) and 11 non-adults (12.4%). Precise estimations of age-at-death categories could be given for 72 individuals (80.9%), with the remaining 17 individuals (19.1%) estimated to be of an adult age-at-death (Schats, Hoogland, et al., 2017, p. 237).

Biological sex was estimated by Schats, Hoogland, et al. (2017) for all adult individuals, which resulted in a distribution of 26 males (33.3%), 12 females (15.4%), 16 probable males (20.5%), 12 probable females (15.4%), and 12 individuals whose sex could not be determined (15.4%) (Schats, Hoogland, et al., 2017, p. 237). The methodology for these age-at-death and sex estimations is described below.

For this thesis, the entire assemblage of skeletal remains was re-examined on their presence of lesions possibly related to treponemal infections and a selection of individuals has been analysed on the presence of elemental mercury in their bone. The next chapter delves into the various methodologies that were performed.

5. Methods

This chapter discusses the various osteological, historical, and trace-elemental methods that were used for this research. It also describes the methods adopted by Schats, Hoogland, et al. (2017) in their physical anthropological report on the skeletal collection from Kampen, as their results form the foundation for the further osteological analysis in this thesis.

5.1 Osteoarchaeological analysis

5.1.1 Estimation of sex

The previous estimation of biological sex by Schats, Hoogland, et al. (2017) is necessary to gain a better understanding of syphilis and its treatment in relation to biological sex. This relation is especially interesting in light of an older study that suggests males with syphilis are more likely to develop skeletal lesions than females (Rosahn & Black-Schaffer, 1943, p. 596).

The estimation of sex in archaeology is based on skeletal elements that demonstrate the most sexual dimorphism, but it is important to note that this does not necessarily reflect an individual's gender (White & Folkens, 2005, pp. 385–386). During the initial osteological analysis by Schats, Hoogland, et al. (2017), sex estimations were established by following the recommendations by the Workshop of European Anthropologists (WEA) (1980), which requires examination and subsequent scoring of multiple morphological traits on the pelvis, cranium, and mandible. Given scores range from -2, (hyperfeminine), to +2, (hypermasculine), and some features, like the mastoid process, are given more weight than others (p. 518). Final scoring is attained by calculating the degree of sexualisation for the pelvis, cranium, and mandible by determining the average score for each element (Schats, Hoogland, et al., 2017, pp. 233–234). In addition, sex was estimated by analysing the shape of the ventral arc, ischiopubic ramus and subpubic concavity of the pubic bone, as outlined by Phenice (1969), and by examining the morphology of the sacrum, as described by Bass (1987). Besides this, osteometric analysis was conducted on various skeletal elements to support the final sex estimation. These included methods described by Bainbridge and Genovés (1956), McCormick et al. (1991), Steyn and Iscan (1999), and Stewart (1979) (for an in-depth overview, see Schats, Hoogland, et al. (2017, p. 234).

Sex estimation was only attempted for adult individuals (>18 years old), as current sex estimation methods for non-adult individuals (≤18 years old) are generally considered unreliable (Marino et al., 2021). The overall estimation of an adult individual's sex is comprised of a combination of the assessments described above, after which the final estimation was indicated as F (female), F? (probable female), I (indeterminate), M? (probable male), or M (male). However, to create the sample sizes that are appropriate for relevant statistical analyses, individuals with a probable female

estimation are included in the female category and probable males are grouped with the male category. As a result, the individuals discussed in this thesis can belong to one of three groups, namely female, indeterminate, or male.

5.1.2 Estimation of age-at-death

Estimation of age-at-death was also previously conducted by Schats, Hoogland, et al. (2017), and is of importance for this study to better understand the possible relation between age and syphilis and its treatment. Age-at-death estimation is based on the developmental or degenerative changes of numerous skeletal elements visible through multiple morphological formations, such as epiphyseal fusion. As the timing of these developmental or degenerative changes can also be dependent on individual variation, nutrition, workload and pathology, age-at-death is usually assigned by placing individuals in one of multiple sequential age categories (WEA, 1980, p. 533; White & Folkens, 2005, pp. 363-364). Both non-adults and adults can be analysed to study their age at death, with non-adult age categories being a bit more precise due to the greater degree of developmental growth and change in the non-adult skeleton (White & Folkens, 2005, p. 360).

The initial osteological analysis made use of four non-adult age-at-death categories and four adult age-at-death categories (Table 5.1). Non-adult age-at-death was estimated by observing teeth eruption (Ubelaker, 1978), formation of teeth and roots (Moorrees et al., 1963), ossification in the skull and spine, epiphyseal fusion of long bones (Schaefer et al., 2009), long bone length (Maresh, 1955), and clavicular length (Black & Scheuer, 1996). Adult age-at-death was estimated by observing ossification processes of the pubic symphysis (Brooks & Suchey, 1990; Todd, 1920), the auricular surface of the os

Table 5.1:

Non-adult and adult categories for age-at-death and the related chronological age.

Age Category	Chronological Age
Foetus	Unborn
Infant	0-3 years old
Child	4-12 years old
Adolescent	13-18 years old
Young adult	19-25 years old
Young middle adult	26-35 years old
Old middle adult	36-45 years old
Old/mature adult	>45 years old

coxa (Buckberry & Chamberlain, 2002; Lovejoy et al., 1985), and the sternal rib ends (İşcan et al., 1984, 1985). Lastly, the closure of cranial sutures (Meindl & Lovejoy, 1985), the closure of epiphyseal ends of long bones, and abrasion of the molars (WEA, 1980) were assessed. For a complete description of applied methodology, see Schats, Hoogland, et al. (2017). In archaeological remains, preservation or completeness do not always allow for a complete age-at-death estimation. In such cases, assessment of bone fusion and size could still provide whether the individual was considered to be adult (>18 years) at their time of death (Schats, Hoogland, et al., 2017, p. 235). This thesis adopts the age-at-death estimations by Schats, Hoogland, et al. (2017) for further analysis.

5.1.3 Other aspects of the biological profile

Besides sex and age-at-death, other aspects that make up the biological profile of individuals include measuring stature and indices (the shape of certain bones), evaluating dental status, and observing non-metric traits, which are morphogenetic, nonpathological features that cannot be purposefully measured (White & Folkens, 2005). These were all included in the initial osteological analysis (see Schats, Hoogland, et al., 2017), but will not be used further in this thesis, as they are unlikely to bear a meaningful relationship with syphilis and its treatment, and are under influence of many other factors, such as diet, genetics, activities and more, that are beyond the scope of this research.

Nonetheless, the initial pathological assessment by Schats, Hoogland, et al. (2017) provides an essential foundation for this thesis, as descriptions of lesions and differential diagnoses are crucial for reliable and accurate pathological analyses. Pathology was assessed on the basis of works from Aufderheide and Rodriguez (1998), Ortner (2003), Rogers and Waldron (1995), and Waldron (2009). The pathological analysis was broad and included joint disease, metabolic disease, and specific infectious diseases, but also trauma and dental pathology. The true prevalence was calculated for each pathology, meaning that the prevalence of a certain affliction can only be assessed for individuals whose skeletal remains allowed for proper diagnosis of said affliction. In simpler terms, this means that for example, only individuals whose skulls are present can be assessed on the presence of caries sicca.

5.1.4 Identifying treponemal disease

For this thesis, an osteological re-examination was conducted, with a more specific focus on identifying possible skeletal markers of treponemal disease. As the aim of this thesis is to gain insight into syphilis and its treatment at the St. Gertrude infirmary, it is essential to establish whether treponematosis can be identified through the human skeletal remains from that site. As discussed, it can be difficult to diagnose the infection in human remains, as its skeletal signatures, albeit numerous, can vary in severity and specificity.

The osteological analysis for this thesis adopted the scoring system devised by Harper et al. (2011), which allows for a standardized and objective approach. Based on criteria described by Hackett (1976) and Powell and Cook (2005), this recording system classifies lesion types as "consistent with", "suggestive of", or "specific to" treponemal disease. Taking into account the number of skeletal elements affected by these lesions, individuals can be given certain scores. Scoring for acquired treponemal disease range from 0 (non-treponemal) to 5 (specific to treponemal disease), while scoring for congenital syphilis ranges from 0 to 3 (Figure 5.1). It should be noted that this scoring does not reflect the intensity of infection, but merely ranks the potential of an accurate diagnosis. Importantly, Baker et al. (2020, p. 20) remark that Fournier's mulberry molars and especially flared scapulae, used for scoring congenital syphilis, should not be accredited with high diagnostic value, due to their low specificity. While this thesis follows these recommendations by not using these lesions in the scoring of congenital syphilis, their presence was still assessed in order to be as comprehensive as possible.

This scoring system also includes two histological microscopic lesions consistent with treponemal disease, polsters and grenzlinie. While some scholars consider these microscopic changes in bone structure to be tell-tale signs of treponemal infection (Schultz, 2001), their diagnostic value has been criticized. They are likely related to general chronic, inflammatory diseases, which indeed includes syphilis, but also many other infections, such as leprosy and osteomyelitis (von Hunnius et al., 2006; Weston, 2009). In addition, the required methodology entails destructive preparation and extensive analysis of thin-ground bone sections, which goes beyond the scope of this thesis. Because of this, polsters and grenzlinie were not considered during the osteological analysis. A similar problem occurs with the assessment of Wimberger's sign, which is localized bilateral erosion of the medial and proximal ends of the tibial metaphyses, often seen in early congenital syphilis. While generally considered to be pathognomonic of congenital syphilis, it can only be diagnosed radiologically (Baker et al., 2020, p. 22; Rasool & Govender, 1989, p. 753), which was not done for this study.

Diagnosis: Acquired treponemal disease	0	Lesions consistent with a nontreponemal process (e.g., taphonomic process, noninfectious etiology, etc.).
	1	Lesions consistent with treponemal disease on one or more skeletal elements (periostitis, tibial pseudo-bowing, polsters, grenzlinie).
	2	Lesions suggestive of treponemal disease on a single element [Hackett's (1976) *on trial* characteristics: Finely striated nodes and expansions; coarsely striated and pitted expansions; and rugose nodes and expansions on long bones]; or Stage 1–3 *caries sicca* lesions (clustered pits, confluent pits, focal superficial cavitation).
	3	Lesions suggestive of treponemal disease on multiple skeletal elements.
	4	Lesions specific to treponemal disease [Hackett's (1976) diagnostic criteria: Stage 4–6 *caries sicca* lesions (serpiginous cavitation, nodular cavitation, and *caries sicca*) or nodes/expansions with superficial cavitations on long bones] on a single skeletal element.
	5	Lesions specific to treponemal disease found on multiple skeletal elements or in the presence of lesions suggestive of treponemal disease on other skeletal elements
Diagnosis: Congenital syphilis	0	Lesions consistent with a nontreponemal process (e.g., taphonomic process, noninfectious etiology, etc.)
	1	Lesions consistent with congenital syphilis (periostitis, high palatal arch, disproportionate maxillae and mandible, true tibial bowing).
	2	Lesions suggestive of congenital syphilis (Parrot's/Higoumenakia sign, flared scapulae, Fournier's/ Mulberry molar).
	3	Lesions highly suggestive of congenital syphilis (Wimberger's sign, notched and tapering (Hutchinson's) incisors, Moon's molars).

Figure 5.1: Original scoring system for diagnosing acquired and congenital syphilis. (Harper et al., 2011, p. 119).

On another note, it appears that Harper et al. (2011) have combined Hackett's discrete and contiguous series of change into one sequence, as Hackett's caries sicca stages are numbered differently in this scoring system than in the original work (Hackett, 1976). Notably, Harper et al. (2011) name caries sicca stage 4-6 as serpiginous and nodular cavitation and caries sicca, and the authors remark that the former two are also known as circumvallate cavitation. However, Hackett originally identified these stages to be separate processes and numbered these stages as stage 6-8. For the sake of clarity and comparison, this thesis follows other studies (such as Baker et al., 2020) and will still make use of Hackett's original differentiation and ascribed diagnostic value as discussed in Chapter 2, section 2.3.2.

In addition to this scoring system, the presence of other lesions potentially indicative of syphilitic infection, but not mentioned by Harper et al. (2011), was also noted. These lesions include singular gummas on bones other than long bones (Aufderheide & Rodriguez-Martin, 1998, p. 160), Charcot's joints (Roberts & Buikstra, 2019, p. 391), aortic aneurysm (Castro et al., 2016), osteomyelitis (Baker et al., 2020, p. 22), dactylitis (Rasool & Govender, 1989), and, for congenital syphilis, osteochondritis (Waldron, 2009, p. 107). While these could also be brought forth by a variety of causes, they are also consistent with or even suggestive of treponemal disease (Baker et al., 2020, pp. 21–22). Due to this variable reliability and for the sake of comparability of this research with other studies following Harper et al. (2011), these additional lesions were not considered in assigning the final score. Table 5.2 shows the final scoring system that includes the aforementioned changes.

Microsoft Access 365 was used to record these lesions as present, absent, or unobservable for each individual. The recording form also included basic information (feature and find number, estimated sex, age-at-death, preservation, and completeness), space for descriptions, and the diagnostic score. In the case of lesions that can affect multiple bones, such as gummas, presence was recorded by specifying the affected bones. Additionally, periosteal new bone was assessed on whether it was active or healed.

While all 89 individuals from primary burials were re-analysed, the presence or absence of treponemal disease can only be ascertained if at least a number of relevant bones is available for observation. In order to better determine the true prevalence of treponemal infection, a subsample was selected by omitting individuals if they did not have either a cranium or one tibia and another long bone present (as suggested by Baker et al., 2020) and if their other available bones showed no relevant lesions. From the original assemblage of 89 individuals, the remains of ten individuals did not adhere to these requirements. This resulted in a pathological subsample of 79 individuals, of which 68 were adult and 11 were non-adult.

Table 5.2:

The adapted scoring system for diagnosing acquired and congenital treponemal disease used in this study. The recording is based on the original system by Harper et al. (2011), with the exclusion of grenzlinie, polsters, and Wimberger's sign, but with additional recommended lesions from various literary sources (see text above).

Score	Classification	Associated Lesions
	Acquired treponemal disease	
0	Lesions consistent with non-treponemal processes	Taphonomic processes, non-infectious aetiology etc.
1	Lesions consistent with treponemal disease on one or more elements	Periosteal new bone, tibial pseudo-bowing (sabre shin)
2	Lesions suggestive of treponemal disease on a single element	Hackett's (1976) *on trial* characteristics: Finely striated nodes and expansions, coarsely striated and pitted expansions, rugose nodes and expansions on long bones; Stage 1-3 caries sicca lesions: clustered pits, confluent pits, and focal superficial cavitation
3	Lesions suggestive of treponemal disease on multiple elements	Lesions described directly above on multiple elements
4	Lesions diagnostic of treponemal disease on a single element	Hackett's (1976) diagnostic criteria: Nodes/expansions with superficial cavitation (gummatous lesions) on long bones; Stage 4-8 caries sicca: circumvallate cavitation, radial scars, serpiginous cavitation, nodular cavitation, and true caries sicca
5	Lesions diagnostic of treponemal disease on multiple elements or in the presence of lesions suggestive of treponemal disease on other elements	Combination of suggestive and diagnostic lesions described above on multiple skeletal elements
N/A	Additionally recorded lesions	Charcot's joints, aortic aneurysm, osteomyelitis, and dactylitis
	Congenital syphilis	
0	Lesions consistent with non-treponemal processes	Taphonomic processes, non-infectious aetiology etc.
1	Lesions consistent with congenital syphilis	Periosteal new bone, high palatal arch, disproportionate maxillae and mandible, true tibial bowing
2	Lesions suggestive of congenital syphilis	Parrot's sign, Higoumenakis' sign, flared scapulae*, Fournier's/mulberry molar*
3	Lesions highly suggestive of congenital syphilis	Hutchinson's incisors, Moon's molars
N/A	Additionally recorded lesions	Osteochondritis

** The diagnostic value of flared scapulae and Fournier's or mulberry molars was not taken into consideration while determining scores for congenital syphilis, but their presence was noted, see discussion in text above.*

5.1.5 *Analytical methodology*

Following this paleopathological analysis, its findings were combined with the demographic analysis conducted by Schats, Hoogland, et al. (2017) in order to investigate the relation between the prevalence of skeletal treponemal infection and sex or age-at-death. Descriptive statistics were deployed to explore the possible correlations between these factors within the previously described subsample. Besides this, a number of case studies, selected on the presence of specific skeletal indicators of acquired treponemal disease (i.e. score 4 or 5), were described in full detail to provide an account of the application of the treponemal scoring system by Harper et al. (2011).

5.2 Archival records

As initial literature study for this thesis did not reveal much specific information on syphilis and it treatment in Kampen and the surrounding area, archival records from St. Gertrude's infirmary and other similar sites in Kampen were examined. Previous historic and archival research was conducted by Van Zanten (2017), and while this provided important knowledge on the infirmary's origin, spatial development, inhabitants, and personnel involved, it did not include much information about the specific ailments of the patients or the general care and medical treatment that was available to the infirmary's inhabitants.

Archival research was conducted at the municipal archives at *Stadsarchief Kampen* over a period of two full days in February and March of 2023. The archival records were selected through the online available archival database, but also on the basis of previous research by Van Zanten (2017). Additionally, some records, which were not found in the online database, were included in the study following recommendations from the local staff. The final selection included records from the inventories of *Oud Archief Kampen* (O.A.K.; entry code 00001), which includes the oldest records from the city archives, and *Sint Geertruids Gasthuis* (entry code 00151) and one record from the archive of *Schole Campensis Bibliotheca* (inventory no. L00185), both of which have not been digitally inventoried yet. A full list of records that were consulted for this study are available in Appendix 1.

As described by Van Zanten (2017), the majority of records describe financial or economic activities by the church warden, financial information from inhabitants, or new regulations and statutes. The aim of this archival research was to find records that describe disease and treatment, specifically syphilis and/or syphilis treatments with mercury or other substances, in Kampen during the active period of St. Gertrude's infirmary, in order to evaluate the presence of syphilis and treatment at the site from a historical perspective. While extensive efforts were made to decipher the older late medieval texts written in Middle Dutch with the help of the local staff, this was often difficult due to illegible writing and/or application of local dialects. In contrast, early modern texts were much more readable.

5.3 Portable X-Ray Fluorescence Spectrometry

Based on the osteological analysis described above, some individuals were identified to have treponemal lesions (see section 6.1). To investigate the use of mercury treatments at the site of St. Gertrude's infirmary, it is pertinent to understand which individuals may have been subjected to mercury treatment. To explore whether it is possible to identify mercury treatment, various trace element analytical techniques were conducted on the skeletal remains to assess the compositional levels of mercury (Hg) incorporated in the bone matrix.

Portable X-Ray Fluorescence Spectrometry (pXRF) is a non-destructive technique that does not require extensive sample pre-treatment and has the advantage of relatively rapid sample analysis, making the technique particularly useful for assessing qualitative and quantitative parameters of a large batch of samples (Shackley, 2010, pp. 8–9). It is a well-established method within archaeological disciplines like geoarchaeology or artefact studies to analyse the chemical composition of a material (Brent et al., 2017; Little et al., 2014, p. 19; Tykot, 2016). Despite its popularity, its application for analysing skeletal remains is limited, with only a handful of studies reporting such use (e.g. Bergmann, 2018; Gonzalez-Rodriguez & Fowler, 2013; Kilburn et al., 2021; Little et al., 2014; Zuckerman, 2016, 2017).

The chemical mechanism of this analytical method operates on the basis of known energy emissions, or fluorescent radiation, of certain elements in an excited and ionized state due to high-energy, short wavelength radiation, such as X-rays (Shackley, 2010, p. 16). In this case, the XRF instrument is able to generate and direct X-ray beams onto the sample, which in turn causes displacement and excitation of electrons within the atoms of a sample. The resulting instability of the atoms leads to secondary electron transitions within the atoms, which is responsible for the emission of element-specific fluorescent radiation that is registered by the instrument's detector. Quantification per element can be determined, either by the instrument itself or by additional software, by calculating the proportions in which the specific fluorescent radiations are detected (Bergmann, 2018, pp. 14–16; Bruker, n.d.). By counting the detected radiation pulses, digital spectra are generated, showcasing the relative energy for each element, as well as the background signal caused by the primary radiation from the instrument itself. Filters can be utilized to minimize the background signal and increase detection limits at certain energies of interest. After calibration with standards against the energy level and intensity of each reading, peaks and quantities of specific elements can be identified in the spectra. As different materials may complicate or facilitate the detection of emissions, calibration standards should be matrix-matched and of a similar composition (Drake & MacDonald, 2023, p. 20; Tykot, 2016, p. 43).

For this thesis, pXRF analysis was conducted for the large-scale examination of Hg levels in cortical bone of all adult individuals with relevant bones to study, but also to identify individuals whose bones may be of interest for further study by SEM-EDX and for absolute quantification by ICP-MS. This study

may account for treatments that involved applying mercury topically as ointment or inhaling mercuric fumes, which may have resulted in the systematic uptake of mercury and subsequent incorporation into the bone matrix. Two pXRF examinations were performed over the duration of the study. The first was conducted with a handheld Bruker Tracer III-SD and acted as a pilot study to gain insight into the skeletal collection and tracing abilities with pXRF. The second analysis made use of a newer and more advanced instrument that has a lower detection limit for mercury, a Bruker Tracer 5g which holds a graphene window and higher count rate detection capability. Settings on each of the instruments were optimised for the particular detection of mercury.

5.3.1 Sample selection and preparation

During the first pXRF pilot analysis, femora of all adult individuals with at least one relatively complete femur available were analysed. The choice for femora is based on the fact that these bones generally have the thickest cortical bone and largest flat surface area, which is helpful in placing measurements (Kilburn et al., 2021, p. 5). Following Zuckerman (2016; 2017), left femora were preferentially sampled. In addition, as one of the previously established syphilitic individual's skeletons did not include the lower extremities, a number of humeri were added to the selection to allow for some comparison and control samples for this individual. In addition to these long bones, ribs were also subjected to the pXRF analysis, due to their relatively higher trabecular composition, which has been found to yield higher mercury concentrations (Rasmussen et al., 2015, p. 366), and their more rapid bone turnover reflecting a period just prior to death (Fahy et al., 2017, p. 14). The main selection criterium was the rib's potential contact with the surface of the lungs, as Rasmussen et al. (2013) previously have found higher Hg concentrations in bones close to soft tissues (p. 10). To accommodate for this, ribs were selected to range from the second to sixth rib, with both left and right ribs selected when available.

In total, this resulted in a selection of 46 individuals, represented by 105 bones, comprised of 44 femora (43 left, one right), eight humeri (three left, five right), and 53 ribs (25 left, 28 right). In addition, three control samples from other sites were added to the analysis, to rule out possible regional elevated mercury levels at Kampen, which may occur as a result of environmental (Walser III et al., 2019, pp. 49–50), dietary (Sheehan et al., 2014), or activity-related influences (Katz & Krenkel, 1972). The control samples included left femora from three different Dutch collections: a medical collection dated to the early 20th century, the rural medieval collection of Blokhuizen, and the collection of Valkenburg, dated to the Roman period (R. Schats, personal communication, 2022).

As described in the results in section 6.3, the initial pXRF results were inconclusive. Therefore, the measurements were repeated on a subsample of femora, humeri, and ribs with a newly acquired and more sensitive instrument, the Bruker Tracer 5g. For this instrument, the limit of detection for Hg is

minimal 0.7-5.0 ppm for materials of high or medium density. Limits of detection are dependent on several factors, such as matrix interferences, overlapping elements and testing time. The subsample measured here was selected on the basis of the osteological analysis to include both treponemal bones and non-treponemal controls. Additionally, bones with lesions suggestive of or specific to treponemal infection were included to investigate the possibility of focal mercury treatment with skin ointments as opposed to systematic mercury uptake due to fumigation or ingestion. In total, this subsample was comprised of 20 individuals and contained 18 femora (17 left, one right), six humeri (one left, five right), 24 ribs (11 left, 13 right), ten tibiae (eight left, ten right), and one left fibula. Additionally, control samples consisted of two femora from the aforementioned medical and Blokhuizen collection, as well as one soil sample taken from a box with unwashed commingled bone material, that was found scattered throughout the excavation site. A complete list of measurements is available in Appendix 2.

Although the skeletal remains were washed following excavation in 2014, all bones used in this study received additional pre-treatment to remove soil and other debris from the bone's surface, to ensure minimal contamination and maximum pXRF analysis of the cortical bone. Sampling locations were cleaned with distilled water and, if needed, gently abraded with scrubbing sponges.

5.3.2 Analytical methodology

Each bone was analysed with the pXRF instrument on multiple locations (Figure 5.2), which were selected to account for different remodelling rates within bones, as acute and intensive mercury treatment at a later point in life could possibly result in varying levels of Hg at different bone locations (Rasmussen et al., 2013, p. 6). In addition, it is important to minimalize possible airspace between the sample and instrument window (Tykot, 2016, p. 43), and thus the selected sampling points were as flat and smooth as possible so that they could be positioned against the instrument window.

For femora, sampling locations were adopted from Zuckerman (2016; 2017), who performed a similar study into the presence of mercury, and consisted of five points: the anterior aspects of the head, proximal metaphysis, midshaft, and distal metaphysis, and the posterior aspect of the distal metaphysis. For humeri, similar sampling points included the head, the anterior aspects of the proximal metaphysis, midshaft diaphysis, and the distal metaphysis, as well as the posterior aspect of the distal metaphysis. Since the humerus is smaller and more variable in shape than the femur, the precise placement of the measurements differed slightly per individual, mostly in the measurement of the midshaft, which could be taken more medially or laterally depending on the flattest surface available. Ribs were, whenever skeletal preservation allowed for it, measured at two points, one at one-third along the shaft and the other at the sternal end of the shaft, both on the inner, visceral surface. The final pXRF analysis also measured pathological lesions on tibiae, a femur, and a fibula, as it has been

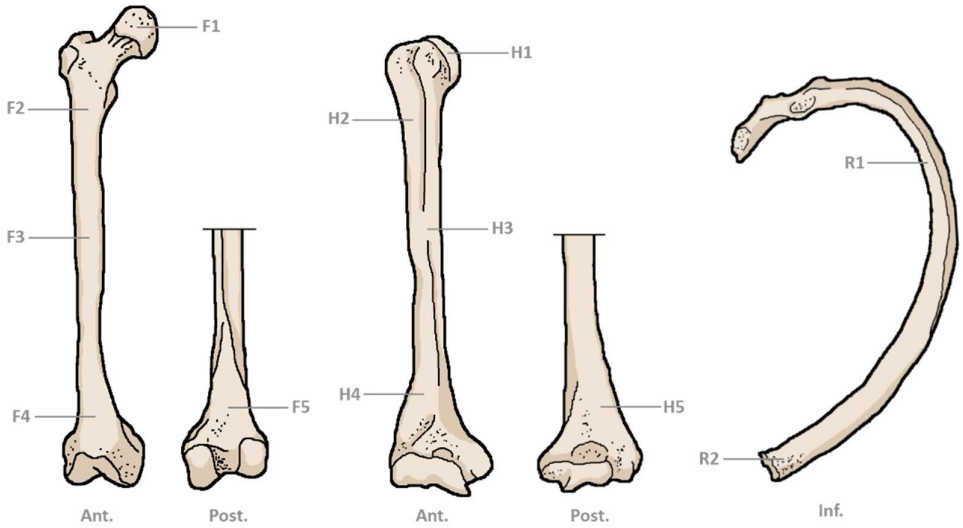

Figure 5.2: Sampling locations for the pXRF analyses. Left: sampling locations for the femur (F1-F4 on the anterior aspect, F5 on the posterior aspect). Middle: sampling locations for the humerus (H1-H4 anterior, H5 posterior). Right: sampling locations for ribs on the visceral surface (depicted from inferior perspective). Illustration by Boudewijn Sloff.

shown that treponemal lesions can demonstrate much higher Hg concentrations than non-lesion areas in the same individual (Rasmussen et al., 2015, p. 366). For these bones, measurements were conducted at specific lesions (Figure 5.3), such as periosteal new bone or lytic lesions, and, if available, an unaffected location as control sample.

Selected specimens were correctly positioned and held in place with the support of sand bags and Blu tack. The ground soil sample was measured in a standard sample cup with a Prolene thin film. Measurement settings for the pilot study with the Tracer III-SD initially followed recommendations by Speakman (n.d., p. 14) and Zuckerman (2016) by testing under 40kV and 4µA for 300 seconds with a 0.001" Cu, .001" Ti, .012 Al filter, with no-vacuum air atmosphere and a standard ca. 4.5mm spot size collimator. Following this, a selection of samples was retested with 40kV and 14µA for 100s to evaluate the effect of shorter reading time and higher current. Ribs were measured with 40kV and 14µA for 60s. Following this pilot study, it was decided that the final pXRF study with the Bruker Tracer 5g would measure for 30 seconds with 50kV and 11.9 µA to achieve optimum excitation of mercury (D.J.G. Braekmans, personal communication, 16-06-2023). In adherence to company recommendations (Bruker, 2020, p. 4), a 75µm Cu, 25µm Ti, 200µm Al filter and air atmosphere without vacuum was used, and the collimator was set to 8mm spot size. Additionally, the instrument was set to screen for heavy metals, which includes Hg, with the Restricted Material Calibration provided by Bruker. The soil sample was quantified an additional time by using the Mudrock Calibration provided by Bruker.

During the analysis, contextual information for each measurement (find and feature, type of bone, sampling location) was recorded in a Microsoft Excel file. X-ray counts from the second pXRF analysis were processed and analysed with the Bruker Artax 8 software. Within Artax, spectra were processed

Figure 5.3: pXRF analysis location on a gummatous lesion on the femur. This specific lesion is also depicted in Figure 2.4. Photo by Lotte Nagelhout.
Note: the instrument is lowered onto the bone as close as possible before conducting actual readings.

by conducting a Bayesian deconvolution to minimize background and inter-elemental effects, such as overlapping peaks for multiple elements. The results were exported to a Microsoft Excel file that reports the net count rates per element, after which the Hg intensities were normalized on the Compton Peak, or rhodium, which comes from the pXRF instrument itself. In doing so, the measurements are internally calibrated and quantified, which further reduces possible matrix effects (Shugar & Mass, 2013, p. 30). From these calibrated counts, the multiple measurements per bone were combined to generate aggregated mean values and standard deviations for each bone per individual. Due to differences in bone remodelling rates at specific sampling sites, this would reflect an average Hg concentration, for example the last ten years before death in the case of femora (Zuckerman, 2017, p. 244). It is important to note that these intensities are quantified emission values, but that they cannot be directly calibrated to absolute ppm or other concentration units, as there is currently no existing calibration standard for Hg in human cortical bone (Zuckerman, 2017, p. 245). Additionally, I have not found commercially or academically available reference material that provided low enough Hg concentrations to be of use in calibrating the emission values yielded from the XRF analysis.

These mean and standard deviation values were then subjected to descriptive statistics and statistical significance tests in SPSS IBM 29.0.1. Descriptive statistics were used to gain insight into mean Hg emission values in datasets with smaller sample sizes, for example when comparing between the soil samples and femoral mean Hg emission values of the Kampen site and the control samples or when comparing mean Hg emission values between treponemal lesions and control readings near these lesions. Statistical significance testing was conducted on the bone samples to explore the relationship in mean Hg levels between various groups. Prior to each statistical test, the dataset was tested for normality with a Shapiro-Wilks test and Levene's test for homogeneity when needed.

First, a Mann-Whitney U test was conducted to compare femoral mean Hg emission values between the Kampen and control samples. Following Zuckerman (2017, p. 236), Kampen's dataset was divided into non-pathological and pathological subgroups, in which pathological samples were defined as exhibiting at least one lesion suggestive of or specific to treponemal disease, corresponding to diagnostic scores 2-5. The mean Hg emission values for these groups were compared for femora by conducting an Independent Samples T-Test, and for ribs by conducting a Mann-Whitney U test. A One Way ANOVA and subsequent Tukey post hoc test were conducted to compare femoral mean Hg emission values between different treponemal scores attributed in the osteological analysis. To counteract the Multiple Comparison Problem, a Bonferroni correction was conducted before assessing statistical significance. By applying this correction, the significance threshold was set at $p<0.0125$.

5.4 Inductively Coupled Plasma-Mass Spectrometry

In order to further investigate the use of mercury treatments at the site of St. Gertrude's infirmary and quantify the concentration of mercury in various bone samples, a third trace element analytical technique was conducted, namely Inductively Coupled Plasma-Mass Spectrometry (ICP-MS).

ICP-MS is a high-precision type of mass spectrometry that is particularly useful in detecting metals and some non-metals in very low concentrations, dependent on the sample material. This low detection limit allows for accurate detection of elements and isotopes on a parts-per-billion (ppb) level, and in some cases even lower (Measurlabs, n.d.; Tucker, 2007, p. 221). ICP-MS is a widely-used analytical technique in fields such as geochemistry and pharmaceutical, ecological or environmental testing, among many others, as it is capable of multi-elemental analysis, providing concentrations for all detectable elements within a sample. This allows for time-efficient sampling with excellent precision and sensitivity throughout a wide measurement range (Kloprogge et al., 2020, pp. 42–43). Due to these advantages, it has been used successfully in other studies on heavy metal uptake, including mercury, in archaeological bone samples (see for example Biehler-Gomez et al., 2022; Rasmussen et al., 2017, 2020; Tucker, 2007; Walser III et al., 2019; Yamada et al., 1995). However, a major drawback of ICP-MS analysis is its destructive nature, as samples taken from dry bone require more extensive and irreversible preparation and analysis when compared to XRF or SEM-EDX techniques.

Analysis by ICP-MS is performed by a process that separates the sample's molecules into their respective atomic ions that undergo detection and quantification through mass spectrometry (Figure 5.4). The ionization process occurs after the sample, usually in solid or liquid form, is either dissolved or acid digested into a liquid solution and introduced as aerosol droplets into the heated plasma within the ICP-MS instrument, although there are various methods of sample introduction available (Agilent Technologies, n.d.; Kloprogge et al., 2020, pp. 43–44). With the help of the heated plasma, the sample's

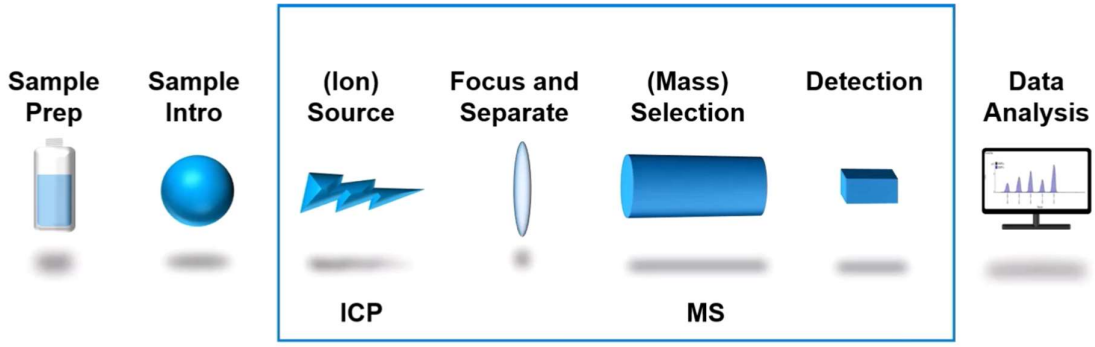

Figure 5.4: The fundamental components of ICP-MS analysis. From left to right the progress outside and inside the ICP-MS instrument (indicated by the blue square) is depicted. Adapted from Agilent Technologies (n.d.).

aerosol droplets are converted into individual atoms and ionized. Following this, positive ions can be separated from any other particles, which would create background noise, by passing through an ion lens, but again a multitude of techniques exist for this exact separation purpose. Interfering ions are removed with a collision or reactor cell to reduce interference of unwanted elements or isotopes on the spectrum and increase the visibility of ions of interest (Kloprogge et al., 2020, p. 44). The remaining ions are then filtered on the basis of their mass to charge ratio within the so-called quadrupole. At the end of this process, a detector identifies these ions and produce a mass spectrum that can be used to quantify the concentration of certain elements (Kloprogge et al., 2020, p. 43). For mercury specifically, the potential for ionization is low, and therefore the plasma temperature requires additional optimization to ensure a low detection limit and high sensitivity (Agilent Technologies, n.d.).

For this thesis, ICP-MS analysis was performed for the precise and accurate quantification of mercury concentrations in bone samples from both syphilitic and non-syphilitic individuals, as well as soil samples to approximate the natural background Hg levels in Kampen, the Netherlands. This analysis allows for additional assessment of mercury levels with a lower detection limit than XRF and SEM-EDX. The results obtained with ICP-MS would also be beneficial for the quantification and determination of detection limits of the conducted XRF analyses on archaeological bone samples.

Results from this ICP-MS study may reflect the administration of mercury as a treatment for syphilis, especially those that resulted in a systematic assimilation of mercury into the bone matrix of sampled individuals. However, gaining an understanding of which type of mercury treatment (e.g. fumigation, topical application, or ingestion) is reflected, depends on which skeletal elements and tissue show elevated mercury levels. In order to further investigate this, tandem ICP-MS analyses were performed with an Agilent 8800 ICP-MS/MS by Measurlabs in Finland. This instrument features a secondary quadrupole to provide an optimized removal of interfering ions and an increased sensitivity. This MS/MS mode permits the user to select only ions of a specific mass to charge ratio to enter for detection, allowing even more control over specificity (Balcaen et al., 2015).

5.4.1 Sample selection and preparation

As a limited number of samples could be selected for ICP-MS, due to the destructive nature of the analysis and limited funding, sample selection aimed to allow for later comparison between syphilitic and non-syphilitic individuals, as well as different skeletal tissues. The latter is important due to the differences in mercury absorption and remodelling rates between the outer layer of bone, or cortical bone, and the inner bone structure, or trabecular bone. Previous studies have established that cortical bone generally contains less mercury than trabecular bone (see for example Rasmussen et al., 2008, 2013, 2015), which could, among other reasons, be caused by administration of mercury-containing medicine closer to the time of death, resulting in the uptake in the tissues with quicker remodelling. Alternatively, higher levels of mercury in the trabecular bone could have occurred through post-mortem mercury absorption from the decaying soft tissues into the trabecular tissue, favoured by the large surface area of the trabecular structure (Rasmussen et al., 2017, p. 96). The latter hypothesis builds on the fact that Hg can initially accumulate in the kidneys and liver, before it is dispersed into the bloodstream, other organs, and the bone marrow (Rasmussen et al., 2020, pp. 2–3).

ICP-MS analyses were conducted on 19 samples in total, including two soil samples and 17 bone samples from 11 individuals (Table 5.3). These bone samples were taken from six individuals with one or more specific lesions (treponemal score = 4 or 5), three individuals with skeletal lesions suggestive of treponemal infection (score = 2 or 3), and two individuals that displayed limited lesions consistent with treponemal infection (score = 1). For three treponemal individuals in this subsample, multiple bones were subjected to sampling in order to permit comparison of Hg concentrations in the outer cortical versus the inner trabecular bone samples. From the individuals with diagnostic scores of two or lower, only one individual (S4019) was selected for both a cortical and trabecular sample in consideration of the relatively high destructive load of the cortical sampling. Cortical bone samples were taken from femora, scapulae and the skull, whereas ribs were selected to account for samples with a high proportion of trabecular bone.

For sampling, precise procedures differed per bone. For the two femora, the initial sampling procedure followed the protocol as described by Rasmussen et al. (2015, pp. 360–361), who removed the cortical tissue from the surface and sampled the underlying, uncontaminated cortical tissue using a mechanical drill. However, Rasmussen et al. (2015) only sampled 0.1 g of cortical tissue, whereas Measurlabs required a minimum sample weight of 1.0 g, demanding the sampling of a much larger area on the femur's exterior surface. After assessing the sampling of the first femur (S4019), it was decided to instead take cortical samples, including those from the skull and scapulae, from loose or almost loose fragments, to minimize the destructiveness of the method. Dirt and trabeculae attached to these samples were removed manually with the use of tweezers, a scalpel and a brush.

Table 5.3:

List of samples taken for ICP-MS analysis.

Feature and find no.	Treponemal score	Type of bone	Sample location	Sample weight (g)
S4011 V1012	1	Rib	Right rib 4, sternal end	1.43
S4019 V1018	1	Rib	Right rib 3, sternal end	1.21
S4019 V1018	1	Femur	Left femur, cortical sample just inferior to trochanter minor	1.05
S4040 V1041	2	Rib	Unidentified rib fragment	1.37
S4096 V1100	2	Rib	Left rib 6 or 7, sternal end	1.49
S4027 V1028	3	Rib	Right rib 6, sternal end	2.07
S4068 V1071	4	Rib	Right rib 8, sternal end	1.11
S4008 V1003	5	Rib	Right rib 5, sternal end	1.60
S4008 V1003	5	Femur	Left femur, posterior cortical fragment from distal diaphysis	1.34
S4008 V1003	5	Skull - parietal	Right parietal, approx. 3 cm above squamosal suture	1.83
S4013 V1008	5	Rib	Right rib 7, sternal end	1.09
S4033 V1032	5	Rib	Left rib 4 or 5, sternal end	1.34
S4033 V1032	5	Scapula	Left scapular body	0.75
S4045 V1049	5	Rib	Right rib 6, sternal end	1.20
S4084 V1086	5	Rib	Right rib 8, sternal end	1.69
S4084 V1086	5	Scapula	Right scapular body	1.22
S4084 V1086	5	Skull - parietal	Left parietal, fragment from temporal line	1.20
KM14 Soil 1	N/A	N/A	N/A	5.50
KM14 Soil 2	N/A	N/A	N/A	5.14

Sampling the ribs was performed by collecting all ribs for each individual and sorting them into anatomical positions. Rib fragments were selected on their incompleteness, identifiable rib of origin and relative cleanliness. Fragments were collected or removed from larger pieces of ribs. This was deemed to be minimally detrimental to the individual skeleton, as ribs are generally abundantly available and fragments are relatively dispensable and easily removed (Tucker, 2007, p. 221).

Even though all bones were washed and dried after excavation, heavy clay soil was often still present within the ribs. Depending on the visible soil contamination, a weight between 1.2 and 1.7 g was

collected from each fragment prior to cleaning. Samples were collected into plastic vials with MilliQ water and put into an ultrasonic bath for 30 minutes to remove heavy clay particles. After allowing the dirt particles to settle, the rib fragments were removed and dried within a laboratory fume hood for a week. Following this, all samples were mechanically pulverized with a SP Bel-Art Micro-Mill II Grinder for 1.5 to 3 min, dependent on the hardness of the sample, to retrieve a bone powder usable for ICP-MS analysis. Each sample was weighed to be between 1.00 to 2.00 g. The two different soil samples were retrieved from a box with unwashed commingled bones without treponemal lesions that were found scattered throughout the excavation site, as there are no remaining official soil samples from the excavation. The soil sample used during the pXRF analysis was also obtained from this box. These samples were weighed to contain between 5.0 and 5.5 g each and further pulverization was not necessary.

Between handling each sample between the preparation stages, all relevant tools were rinsed with MilliQ water and cleaned with ethanol, and if possible (in the case of tweezers and scalpel) heated with a flame to remove any remaining Hg. Samples were collected over sheets of aluminium and with gloves that were replaced after each sample to prevent contamination. All bones included in this analysis were sampled at the Faculty of Archaeology, Leiden University, and then transported to Measurlabs, Finland, where they received subsequent preparation and treatment before testing. Each sample received the same sample preparation and subsequent analysis by Measurlabs. Their sample preparation is further described in Appendix 3.

5.4.2 Analytical methodology

As described previously, ICP-MS/MS analyses were conducted through Measurlabs, and performed by an ISO/IEC 17025 accredited external service provider, funded through a SNMAP grant awarded to Lotte Nagelhout and thesis supervisors. Test results for a single elemental analysis (Hg) were reported in mg/kg by Measurlabs and subsequently explored using descriptive statistics in IBM SPSS 29.0.1. Statistical significance testing was not performed due to the highly selective nature of the samples in the ICP-MS dataset and the limited number of samples.

5.5 Scanning Electron Microscopy with Energy Dispersive X-rays Spectroscopy

To investigate the use of mercury treatments at the site of St. Gertrude's infirmary further, a second elemental analysis was conducted on various teeth to assess the presence of mercury. This study may reflect treatment methods that aimed to cure syphilis through ingestion of mercury-enriched foods and possibly fumigation, which may have resulted in the incorporation of Hg in dental calculus.

A number of teeth with dental calculus were analyzed using Scanning Electron Microscopy with Energy Dispersive X-rays Spectroscopy (SEM-EDX or SEM-EDS), performed together with dr. Ineke Joosten at

the Dutch Cultural Heritage Agency in Amsterdam, the Netherlands. SEM is a widely used non-destructive imaging technique that produces highly magnified images of a sample's surface. Combined with EDS, the technique is not only able to investigate the elemental composition on the material's surface, but can also map the location and distribution of these elements, making it a useful technique for examining samples with a high degree of compositional variability (Frahm, 2014, pp. 6487–6489).

Much like the name suggests, SEM uses electrons to capture the image of the sample. An electron beam is projected and run across the surface of the sample, producing numerous signals that can be used to construct a highly detailed image. This electron beam excites electrons within the sample's atoms and this process produces the emission of secondary X-rays within a small, localized area. Similar to the fundamental chemical mechanisms behind XRF analysis, the amount of energy from the emitted X-rays depends on the specific elements and can be identified with the EDX detector (Frahm, 2014, p. 6489). Such analyses result in an energy-dispersive X-ray spectrum that show the intensity (or counts) of certain elements by their respective energy emission, similar to the XRF spectra.

Its application in archaeology is broad, as it can be used to study a range of inorganic and organic materials, such as ceramics, glass, pollen, teeth, and bone (Frahm, 2014, pp. 6492–6494). For the examination of teeth, SEM-EDX is occasionally used to study the compositional make-up of dental calculus. As dental plaque calcifies into dental calculus during a person's lifetime, it acts as a bio-archaeological reservoir trapping a wide variety of foreign debris and bacteria that were adhered to the plaque's surface (Blatt et al., 2011, p. 669). This debris, that can consist of plant remains, parasites, bacteria, minerals, and other elements, has provided a detailed look into past human or hominin diet and activities as well as environmental conditions (Fialová et al., 2017, p. 1207; Hardy et al., 2012; Power et al., 2014; Vandermeersch et al., 1994). It can be very useful in providing knowledge on particles that were consumed or otherwise taken-up in a relatively short-term period, such as months to days, prior to death (Blatt et al., 2011, p. 676).

While the detection of mercury compounds with SEM-EDX has been studied previously, such studies were conducted from the perspective of mining and ore processing (Calvo et al., 1988), waste management (Rompalski et al., 2019), or environmental pollution (Nuić et al., 2022). As such, the SEM-EDX analysis conducted for this study is the first to examine mercury in human dental calculus. As mercury treatment for syphilis could have included the ingestion of mercury-enriched foods and potions, as well as the inhalation of mercuric vapours, it is hypothesized that elemental mercury may have become trapped in the dental calculus matrix.

5.5.1 Sample selection and preparation

SEM-EDX analyses were carried out on eight teeth that showed abundant calculus on the enamel surface, collected from six individuals excavated from St. Gertrude's infirmary. These individuals were selected on the presence or absence of possible syphilitic skeletal lesions, in order to create a representative subsample that contained individuals who were more likely to have received mercury treatment as well as those who were less likely to have come in contact with mercury. This resulted in a selection of four teeth from three syphilitic individuals, three teeth from two individuals with some suggestive lesions (treponemal score 2 and 3), and one tooth from an individual without syphilitic markers (Table 5.4). The tooth selection was based on the presence of abundant calculus on the enamel and their location was recorded in accordance with the *Federation Dentaire Internationale* (FDI) notation system. Additionally, for the examination to remain as non-destructive process as possible, only teeth that were easily removed or already loose from their sockets were sampled.

While some studies have included the removal of calculus from the enamel as well as sputter coating the surface with a layer of gold or chromium, this study opted for a less destructive approach without any surface modification, especially as elemental spectra with sputter coating have been shown to be comparable to those without sputter coating (Fialová et al., 2017, p. 1209).

Table 5.4:

All tooth samples taken for SEM-EDX analysis on dental calculus, including treponemal score.

Feature and find no.	Treponemal score	Tooth FDI code	Tooth
S4008 V1003	5	1.5	Upper right second premolar
S4033 V1032	5	3.1	Lower left first incisor
S4084 V1086	5	3.1	Lower left first incisor
		3.5	Lower left second premolar
S4027 V1028	3	4.1	Lower right first incisor
S4040 V1041	2	4.2	Lower right second incisor
		4.3	Lower right canine
S4032 V1031*	1*	3.2	Lower left second incisor

**Although this individual scored 1 due to periosteal new bone, it is believed that this was caused by trauma.*

5.5.2 Analytical methodology

For analysis, each tooth was mounted on a sampling tray and stabilized with conductive double-sided carbon tape and aluminium foil when necessary to produce a correct position that allowed for easy visibility and scanning of the calculus (Figure 5.5).

Each tooth was analysed with a Jeol JSM-IT700HR Scanning Electron Microscope with attached EDX detector. Images were produced with varying degrees of magnification, ranging from x40 to x9000 magnification, although the majority of the analyses were conducted at x300 to x1000 magnification. Compositional analyses were conducted at 20 or 25 kV and 30 Pa in low-vacuum mode and were taken both across wider areas and of specific spots of particles (Figure 5.6). Spot analysis was conducted for small particles that were optically identified through their brighter appearance on the SEM imaging, which indicates the presence of heavier materials like mercury (I. Joosten, personal communication, 07-10-2022). These area and spot readings were taken on multiple locations on each of the teeth, and included surfaces of the calculus as well as the calculus-free enamel surface of the crown and the cementum surface of the root. These analyses of the enamel and cementum were conducted to provide control samples to eliminate Hg contamination of the tooth surfaces in the event of transfer by non-archaeological processes, for example during earlier handling and preservation of the samples.

SEM images and energy-dispersive X-ray spectra for each analysis were collected and reported by dr. Ineke Joosten. Determination of the presence of Hg was done through visual analysis of the spectra. Chapter 6 provides an in-depth description for the spectra from two teeth, whereas a collection of selected images and spectra per teeth are available in Appendix 4. The raw data from this analysis is intended to be published in an open-access supplementary table that is currently under preparation.

Figure 5.5: Teeth samples mounted for SEM-EDX analysis. This image depicts a lower left incisor (3.1, shown left) and a lower left premolar (3.5, shown right) from a syphilitic individual (S4084 V1086) with extensive calculus. Photo by dr. Ineke Joosten.

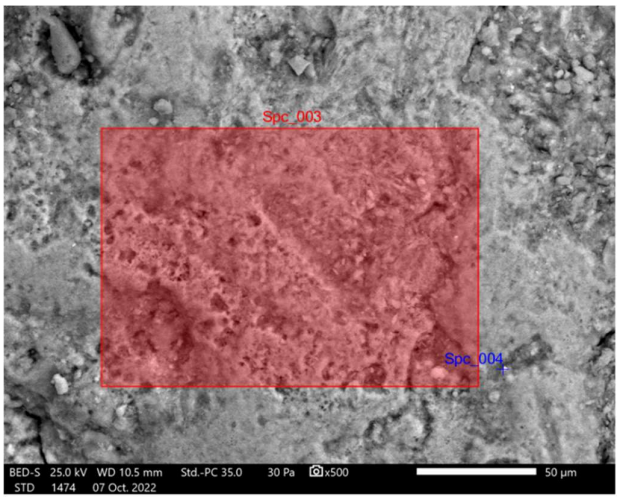

Figure 5.6: SEM image and EDX analysis of calculus. The red square (Spc_003) indicates analysis of a wider area, whereas the blue plus sign (Spc_004) indicates spot analysis of a bright particle. Imaging by dr. Ineke Joosten.

6. Results

This chapter will present the results of the various analyses conducted for this thesis. First, the osteoarchaeological research is discussed, comprising of an assessment of the demographic composition and presence of treponemal disease within the skeletal assemblage. A complete overview of the demographic information and treponemal score per individual can be found in Appendix 5.

Second, findings from the historic archival research at Stadsarchief Kampen are discussed. Third, the results and subsequent data analysis from the three trace element analyses will be discussed separately. Lastly, a short summary will be given to put the multidisciplinary data in a comparative context before proceeding to the in-depth discussion in Chapter 7.

6.1 Palaeopathological assessment

The osteoarchaeological research combines the previous analyses by Schats, Hoogland, et al. (2017) with the paleopathological re-examination of the remains from St. Gertrude's infirmary. This section starts with the assessment of the demographic composition, which comprises of the skeletal preservation and completeness and the distribution of biological sex and age-at-death, for the pathological subsample. For ten of the 89 individuals re-examined, the available bones did not adhere to the minimum requirements for treponemal scoring, meaning that they showed no relevant lesions and did not have either a cranium or tibiae and another long bone available for observation. In order to report the true prevalence of treponemal infection, these individuals were not included in subsequent analysis, which resulted in a subsample of 79 individuals.

While this assessment is partly derived from the aforementioned study, it has been updated to include recently revised sex determinations following aDNA findings. Following the demographic composition, the prevalence of treponemal disease is discussed on the basis of the treponemal scoring system. Pathological lesions consistent with or diagnostic of treponemal disease are further described in detail for the highest-scoring individuals.

6.1.1 Demographic composition

The pathological subsample contains relatively fewer individuals with poorly preserved remains or lacking skeletal elements than the total assemblage. In this subsample, only 1.3% of individuals showed poor preservation and 69.7% of individuals displayed more than 50% of the complete skeleton. See Table 6.1 and 6.2 for an overview of skeletal preservation and completeness in the pathological subsample, see Schats, Hoogland, et al. (2017).

Table 6.1:

Skeletal preservation in the pathological (N=79) sample from St. Gertrude's infirmary.

Preservation	*n* (*N*=79)	%
Good	47	59.5
Fair	31	39.2
Poor	1	1.3

Note: n = number of individuals, N = total sample population

Table 6.2:

Skeletal completeness in the pathological (N=79) sample from St. Gertrude's infirmary.

Completeness	*n* (*N*=79)	%
75-100%	45	57.0
50-75%	10	12.7
25-50%	21	26.6
0-25%	3	3.8

While the pathological subsample includes 68 adults, biological sex distribution accounts for a total of 69 individuals, as one adolescent individual (S4008V1003) was determined to be of male sex following recent aDNA research (Schats, Kootker, et al., 2017). As discussed in section 5.1.1., this thesis combines probable males and females with males and females with more convincing sex estimations to create sample sizes that are suitable for statistical comparison.

Following this, the subsample is comprised of 38 male individuals (55.1%), 23 female individuals (33.3%) and 8 individuals whose sex remains indeterminate (11.6%) (Figure 6.1). Generally, there appears to be an overrepresentation of males in this subsample, as the male to female ratio deviates strongly from the expected ratio of 1:1.

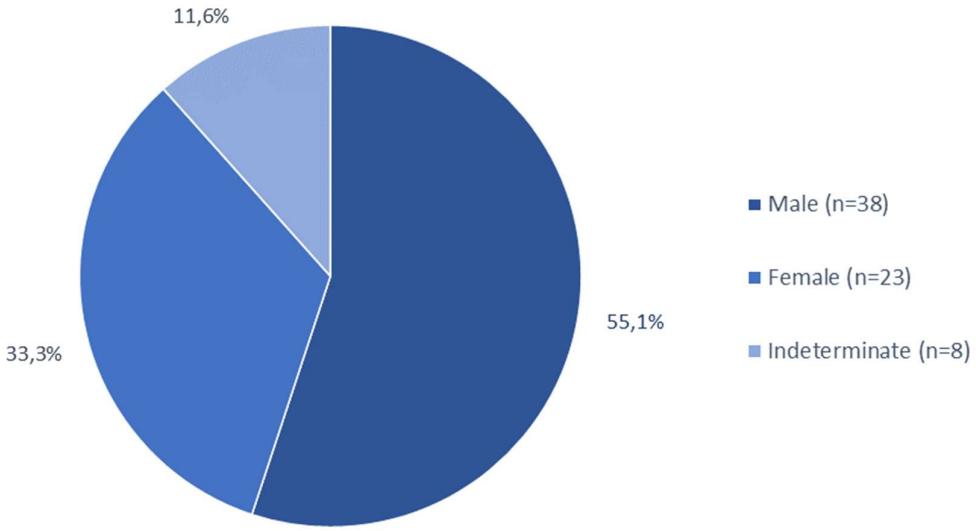

Figure 6.1: Distribution of estimated sex of individuals (n=69) in the subsample used for assessing the presence of treponemal disease at St. Gertrude's infirmary. Note that this includes an adolescent individual (S4008V1003), whose sex was determined through previous aDNA analysis.

The pathological subsample consists of 68 adults (86.1%) and 11 non-adults (13.9%). Of these, precise age-at-death estimates could be given for 66 individuals (83.5%), leaving 13 individuals (16.5%) to be of indeterminate age. All individuals of indeterminate age could still be considered to be of adult age-at-death due to the size, robusticity, and growth of their bones, which signified maturity (Schats, Hoogland, et al., 2017, p. 237).

Age-at-death distribution for the selected subsample is visually presented in Figure 6.2, which shows the high frequency of adult individuals when compared to non-adults. Notably, there were no individuals found to be below the age of 4. When looking at the adult age-at-death distribution, it is apparent that almost a quarter of all individuals died between the ages of 36 and 45 years, whereas older adults above the age of 45 are least present with occurrence rate of 12.7%.

Figure 6.3 shows the distribution of age-at-death when differentiated by biological sex. For males, the young and old middle adult categories have an equal distribution, showcasing that a vast majority died between the ages of 26 and 45 years old (64.6%). Notably, the category of 19-25 years has the lowest frequency, with only 12.9% of the male subsample represented in this group.

For females, the distribution is more variable, as a large proportion died between the ages of 36 and 45 years (35.0%) and between the ages of 19 and 25 years (30.0%). The older adult category (>46 years) is the least prevalent in the female subsample.

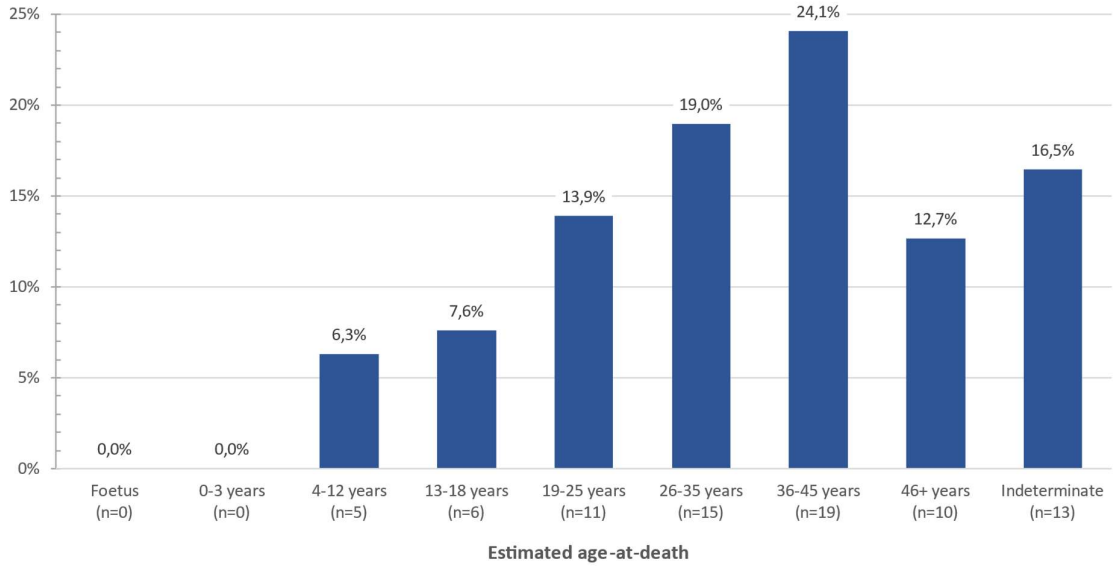

Figure 6.2: Age-at-death distribution. This graph includes all individuals in the pathological subsample (N=79). Note that all indeterminate individuals were concluded to be of adult age.

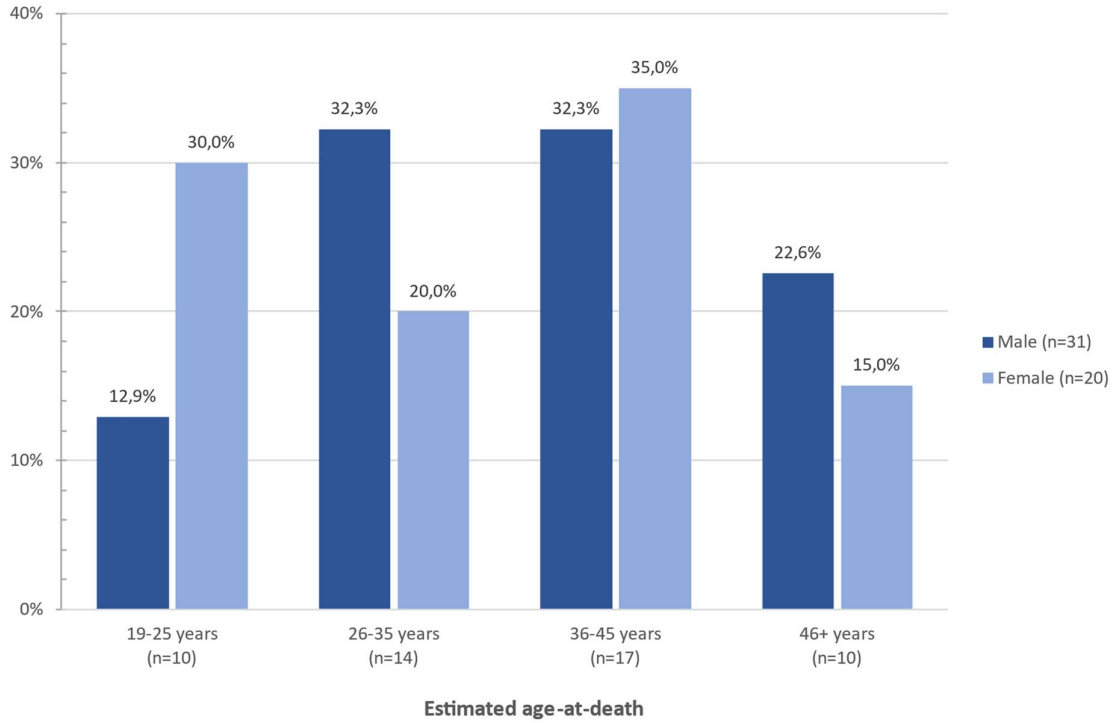

Figure 6.3: Adult age-at-death and estimated sex distribution. This graph includes all individuals in the pathological subsample that could be assessed for both age-at-death and biological sex (N=51).

6.1.2 Prevalence of treponemal disease

The previous osteological analysis and general paleopathological study by Schats et al. (2017) formed the basis of the treponemal-specific osteological analysis conducted for this study. They demonstrated the high prevalence of infectious markers, with 31 individuals (39.7%) affected by the formation of periosteal new bone (PNB). The majority of these affected individuals showed bilateral and diffuse periosteal new bone, which are consistent with systemic infectious diseases. Syphilis was the only specific infectious disease identified throughout the assemblage and was found in three individuals (3.4%). These three individuals, one male adolescent and a male and female adult, shows lesions characteristic of syphilis on their long bones and skull (Schats & Klomp, 2019, pp. 112–113). The remaining individuals who showed infectious markers could not be diagnosed for a specific infectious disease, but some could be further specified as having had non-specific lung infection (*n*=4), sinusitis (*n*=2), and osteomyelitis (*n*=1) (Schats et al., 2017, p. 240).

On the basis of the scoring system by Harper et al. (2011), this study found more evidence of possible treponematosis (see Table 6.3 for the occurrence and prevalence of each score for acquired treponemal disease). Multiple diagnostic treponemal lesions (score 5) were found in four (5.9%) of the examined adult skeletons and in one (9.1%) of the non-adult skeletons, which includes the three individuals identified in the previous osteological analysis. This results in a total true prevalence of

diagnostic treponemal infection of 6.3%. Only one adult individual (1.3%) showed a single specific lesion (score 4), but it should be noted that no cranium was available for inspection in this case. Score 3 was attributed in the case of two adults (2,9%) and one non-adult (1.9%). To summarize, a total of nine individuals (11.4%), comprised of seven adults (10.3%) and two non-adults (18.2%), displayed at least more than one suggestive lesion and/or one or more lesions specific to treponematosis. The two non-adults were both old adolescents (16-18 years) at their time of death, which is interesting due to the extensive amount and severity of third stage treponemal lesions.

Three adult individuals had suggestive lesions on a single skeletal element (score 2), one of which was subjected to additional X-ray analysis to determine whether a deformed, irregular, and thickened lesion along the shaft of the right fibula was caused by a fracture or a periosteal reaction. X-rays showed no evidence for a fracture, but confirmed cortical thickening (see Appendix 6), which follows Hackett's (1976) description of finely striate nodes and expansions, a lesion suggestive of treponemal disease. As expected on the basis of previously established high prevalence of periosteal new bone, a large number of individuals showed lesions consistent with syphilitic infection (score 1). This was the case for 37 adults (54.4%) and five non-adults (45.5%), which are both notably higher than the numbers of adults and non-adults showing no or non-treponemal lesions (score 0), which are 21 (30.9%) and 4 (36.4%) respectively.

Table 6.3:

Overview of the six treponemal scores and their occurrence and prevalence for adults and non-adults.

Acquired treponemal classification and score	Adult		Non-adult		Total	
	n	**%**	***n***	**%**	***n***	**%**
Non-treponemal (score=0)	21	30.9	4	36.4	25	31.6
Lesions consistent with (score=1)	37	54.4	5	45.5	42	53.2
Lesion suggestive of (score=2)	3	4.4	0	0	3	3.8
>1 lesions suggestive of (score=3)	2	2.9	1	9.1	3	3.8
Lesion specific to (score=4)	1	1.5	0	0	1	1.3
>1 lesions specific to (score=5)	4	5.9	1	9.1	5	6.3
Total	68	100	11	100	79	100

Table 6.4 shows the occurrence and frequency of each score for treponemal disease in males and females, which demonstrates that suggestive or diagnostic lesions (score >1) are relatively more prevalent in females (21.7%) when compared to males (15.8%). While this is especially notable for score 5, the prevalence rates are likely influenced by the small sample sizes, which is further apparent due to the minor differences in absolute numbers. A larger difference in prevalence rates is observed for score 1, with 63.2% of males affected by lesions consistent with treponemal disease in comparison to 39.1% of females. Almost all of the individuals within this scoring category were affected by PNB.

Table 6.5 shows the occurrence and prevalence of the various scores for acquired treponemal infection for each age category. For all categories, score 1 was most prevalent, followed by score 0. Unexpectedly, mature adults had a relatively low prevalence of more advanced, third stage treponemal lesions when compared to other age groups, whereas adolescents had the highest prevalence of suggestive or diagnostic lesions. However, the prevalence rates are subject to the small sample sizes for each age category, and the absolute numbers of occurrence do not differ drastically.

The re-examination of this skeletal assemblage did not result in the detection of lesions consistent with, suggestive of, or specific to congenital syphilis or in the detection of lesions known to be caused by mercury poisoning, such as mercurial teeth. Moreover, none of the additionally recorded lesions (e.g. Charcot's joints, aortic aneurysm, osteomyelitis, and dactylitis) that may be indicative of treponemal disease were observed.

Table 6.4:

Overview of the six treponemal scores and their occurrence and prevalence for males and females.

Acquired treponemal classification and score	Male		Female		Total	
	n	**%**	***n***	**%**	***n***	**%**
Non-treponemal (score=0)	8	21.1	9	39.1	17	27.9
Lesions consistent with (score=1)	24	63.2	9	39.1	33	54.1
Lesion suggestive of (score=2)	3	7.9	0	0	3	4.9
>1 lesions suggestive of (score=3)	1	2.6	1	4.3	2	3.3
Lesion specific to (score=4)	0	0	1	4.3	1	1.6
>1 lesions specific to (score=5)	2	5.3	3	13.0	5	8.2
Total	38	100	23	100	61	100

Table 6.5:

Overview of the six acquired treponemal scores and their occurrence and prevalence for each age category.

Acquired treponemal classification and score	Adolescents (13-18)		Young Adults (19-25)		Young Middle Adult (26-35)		Old Middle Adult (36-45)		Mature Adult (45+)	
	n	%	*n*	%	*n*	%	*n*	%	*n*	%
Non-treponemal (score=0)	1	16.7	2	18.2	5	33.3	5	26.3	2	20.0
Lesions consistent with (score=1)	3	50.0	7	63.6	8	53.3	10	52.6	6	60.0
Lesion suggestive of (score=2)	0	0	1	9.1	0	0	2	10.5	0	0
>1 lesions suggestive of (score=3)	1	16.7	0	0	0	0	0	0	2	20.0
Lesion specific to (score=4)	0	0	0	0	0	0	1	5.3	0	0
>1 lesions specific to (score=5)	1	16.7	1	9.1	2	13.3	1	5.3	0	0
Total	6	100	11	100	15	100	19	100	10	100

6.1.3 Treponemal disease - case studies

The following section will describe five case studies for which the highest treponemal score was ascertained (score 4 or 5).

S4008 V1003

This feature and find number relate to the skeletal remains of an older adolescent (16-18 years) individual, who, on the basis of aDNA research, was determined to be male (Schats, Kootker, et al., 2017). Although the skull was fragmented, it exhibited various lytic lesions on the frontal bone, both parietals, and both temporals. These lesions were representative for Hackett's (1976, p. 31) caries sicca sequence 2, 3, and 4 as the cranium showed confluent clustered pits, focal superficial cavitation, and circumvallate cavitation (Figure 6.4A). Differential diagnoses were considered for neoplasms and tuberculosis, which can also affect the skull in a similar manner as early syphilitic caries sicca. However, the changes in this individual were much more numerous and advanced on the outer surface of the cranial vault, characteristic for treponemal disease.

Post-cranial lesions supported the assumption of treponematosis. Gummatous lesions were found on numerous bones, with the most distinctive presentations on the right humerus (Figure 6.4B), both femora (Figure 6.4C), the right tibia (Figure 6.4D), and the right fibula (Figure 6.4E). These gummas were often surrounded by elevated rims of hypervascular and sclerotic new bone, precisely as

described by Aufderheide & Rodriguez-Martin (1998, p. 160) and representative of Hackett's (1976) diagnostic nodes/expansions with superficial cavitation (p. 93). Gummatous lesions lacking elevated rims and surrounding nodes/expansions were found on the mandible, the right humerus and ulna, the left scapula (Figure 6.4F) and radius, the sternum, and the left tibia. Smaller nodes and expansions, following Hackett's suggestive lesions, were found in the majority of these bones.

Additionally, bilateral and diffuse thickening is present along the entire shafts of the tibiae, with the left tibia showing more anterior thickening, a slight sabre-shin formation, and coarsely striated nodes, whereas the shaft of right tibia is more affected by smaller nodes of new bone formation and several deep gummatous lesions.

The skeleton also exhibits several non-gummatous changes, such as patches of striated new bone on the right humerus and radius, and bilaterally on the ulnae, femora, tibiae, and fibulae.

In short, the skeletal remains showed numerous diagnostic lesions, namely nodes/expansions with superficial cavitation/gummas, on multiple skeletal elements, and caries sicca stage 4, as well as many

Figure 6.4: Selection of lesions on the bones of individual S4008 V1003.
A: Caries sicca lesions in the form of confluent clustered pits, focal superficial cavitation, and circumvallate on the frontal bone and both parietals.
B: Anterior aspect of the right distal humerus shows two larger gummatous lesions superior to the coronoid fossa and a smaller lesion on the lateral supracondylar ridge.
C: Anterior aspect of the right distal femur shows cavitation on the anterior shaft and destruction of the anterior articular surface.
D: The right distal tibia, lateral aspect, features a pronounced node with gummatous cavitation that extends into the medullary cavity.
E: The right fibula is affected by expansions of new bone with several superficial cavitations, surrounded by elevated rims.
F: The left scapula, superior aspect, displays one focal destruction on the spine, and one lytic lesion on the posterior edge of the acromion.
Photos by Lotte Nagelhout and Nouschka Bosch.

suggestive lesions throughout the skeleton, including coarsely striated expansions, rugose nodes, and, caries sicca stage 2 and 3, and lesions consistent with treponemal disease, such as periosteal new bone and sabre-shin deformity. Taking this wide distribution and variety of lesions into account, the skeleton of S4008 V1003 was accredited a treponemal score of 5.

S4013 V1008

This feature and find number identify the skeletal remains of a young adult (19-25 years) female. Unfortunately, the remains are not complete, as the cranium and the majority of the right-sided extremities, save for the right fibula, were not retrieved during the excavation. While this impedes the observation and assessment of caries sicca or bilaterally present lesions, the skeleton shows numerous relevant lesions despite this.

Most significant is a lesion specific to treponemal infection on the left fibula, which exhibits a node of hypervascular, irregular new bone with superficial cavitation and irregular margins on the medial-posterior shaft (Figure 6.5A), although this cavitation is not as distinct as in the larger gummatous lesions of individual S4008 V1003. The cavitations form part of a larger rugose expansion of the entire proximal shaft, which striations and small pits on the surface. The right fibula also shows surface

Figure 6.5: Selection of lesions on the bones of individual S4013 V1008.
A: Treponemal-specific node with superficial cavitation accompanied by rugose expansion on the proximal shaft of the left fibula.
B: Suggestive lesion of rugose node with coarse striations on the distal shaft of the right fibula.
C: Lamellar periosteal new bone formation along the medial shaft of the left tibia, consistent with treponemal disease.
D: Lamellar periosteal new bone formation along the proximal shaft of the left femur (difficult to discern in image).
Photos by Rachel Schats.

changes, with a rugose node of dense new bone with some coarse striation on the posterior midshaft (Figure 6.5B) as well as several flatter patches of healing periosteal reactions along the shaft.

The left tibia exhibits a smooth and finely striated node on the posterior aspect of the distal shaft, with some plaque-like periosteal new bone formations on the medio-posterior aspect. Additionally, healed periosteal new bone formation is visible along the entire medial shaft as lamellar striations on the cortical surface, sometimes partially obscured by iron deposits on the bone surface (Figure 6.5C). The left femur shows similar lamellar PNB, most pronounced on the proximal medial shaft (Figure 6.5D).

Due to this combination of a specific lesion (node with superficial cavitation) on the left fibula, several suggestive lesions (rugose expansion, coarsely striated node and finely straited node) on the right fibula and left fibula and tibia, and multiple periosteal lesions consistent with treponemal disease on the left tibia and femur, S4013 V1008 was attributed a score of 5.

S4033 V1032

These skeletal remains belong to a young middle adult (26-35 years) male. Its completeness is relatively low (25-50%) due to the absence of the cranium, lower left arm, and lower extremities. This makes it impossible to assess caries sicca and lesions commonly found on the legs, such as sabre-shin deformities. Despite this, the skeleton exhibited a multitude of noteworthy pathologies in the remaining bones.

The distal left humerus exhibits a node with two superficial cavitations or gummas surrounded by a slightly elevated formation of irregular and sclerotic new bone on the posterior aspect (Figure 6.6A). One gumma, located more laterally, is larger and deeper, with overhanging margins, while the other, located medially next to the first, is shallower. Two other smaller pits are also starting to form, resulting in an irregular surface with coalescing focal destruction within the node, which is diagnostic for treponemal infection. On the anterior surface, this part of the distal humerus shows some irregular periosteal new bone formation.

The right radius shows lesions suggestive of treponemal disease. The distal shaft of the radius is affected by a rugose expansion, resulting in a thickened appearance and medio-lateral pseudo-bowing of the shaft. The ulna shows some finely striated PNB, which is consistent with treponematoses.

A multitude of gummatous lesions on the claviculae, scapulae, and two ribs support a possible treponemal origin, but as Hackett's (1976) original description of diagnostic lesions is only attributed to the cranium and long bones, these were not included in the scoring. However, they are still significant lesions to take into consideration.

The claviculae feature multiple pronounced gummatous lesions. The left clavicle shows four gummatous lesions on the superior surface: two on the shaft, one on the acromial end and one on the sternal end (Figure 6.6B). The right clavicle also shows three gummas, one on the inferior sternal end, one on the superior acromial end, and one on the superior shaft near the acromial end, which is surrounded by pitted new bone formation that slightly hangs over the cavity (Figure 6.6C).

Both scapulae are also heavily affected by generally smaller or less severe gummatous lesions. The left scapula features four gummas: two adjacent gummas on the scapular spine, one gumma on the inferior tip of the posterior body, and one gumma on a unidentified scapular fragment. Possibly more gummas are present on the scapular body, but these are difficult to differentiate from postmortem damage due to the fragmented state of the bone. The right scapula is more complete and exhibits two gummatous lesions on the scapular spine, positioned bilaterally with those found on the left scapular spine. The acromion features several shallow gumma on the superior surface. Interestingly, the medial edge of the scapular body has five notches that appear to be gummatous lesions, as the margins of each notch are slightly raised and dense, differentiating them from postmortem damage (Figure 6.6D).

Two left ribs also feature gummatous cavities, which is a rare occurrence in this specific assemblage, but has been reported as an occasional manifestation by clinical studies (Crissey & Denenholz, 1984,

Figure 6.6: Selection of lesions on the bones of individual S4033 V1032.
A: Treponemal-specific node with superficial cavitation on the posterior distal shaft of the left humerus.
B: Four distinct gummas on the superior aspect of the left clavicle, with the largest and deepest gumma on the midshaft surrounded by elevated new bone formation.
C: Two gummas on the superior aspect of the acromial end of the right clavicle, showing pitted new bone formation towards the shaft.
D: Five notches and cavities along the medial edge of the body on this right scapula are likely to have a gummatous origin.
Photos by Rachel Schats.

p. 114). The eighth rib has a gumma on the inferior, visceral surface of the rib angle. The ninth rib shows two gummas, one at the visceral midshaft, surrounded by irregular new bone, and one on the posterior surface of the angle, which has a more bored out appearance and lacks a rim of new bone.

In short, S4033 V1032 features a multitude of gummatous lesions, but only the gummas on the left humerus, present in a node of new bone, can be diagnostically ascribed as being specific for treponemal disease on the basis of Hackett's criteria. The rugose expansion of the right radius (a suggestive lesion) and the periosteal reactions on the right ulna (a consistent lesion) support the likelihood of a treponemal aetiology. As such, this individual scores a 5.

S4045 V1049

This feature and find number relate to the skeletal remains of a female between 36 and 45 years old at her time of death, with a high degree of skeletal completeness and good preservation. While the skull is available, cranial lesions related to treponemal disease could not be observed.

The postcranial skeleton shows one diagnostic lesion and numerous suggestive lesions, mostly on the tibiae (Figure 6.7A). The diagnostic lesion is a striated node with shallow superficial cavitation, found on the medial surface of the distal shaft of the left tibia (Figure 6.7B). Although the depth and extent of the cavitations is minimal when compared to some of the other nodes with superficial cavitations, its necrotic centre of concentrated pitting with irregular margins is believed to represent the initial stages of a progress of focal destruction, as seen in gummatous lesions.

As stated above, suggestive lesions are excessively presented throughout the lower extremities. Both tibiae show nodes and expansions along their entire shaft, with a varying thickness that results in a rugose silhouette of the entire bone (Figure 6.7A). Expansions take over the whole circumference of the distal halves of the tibiae, whereas the posterior surface of the proximal halves and the joints are free of lesions. The appearance of nodes and expansions ranges from finely striated in concentrated spots to rugose over larger areas. The fibulae are less drastically affected, but still exhibit suggestive lesions in the form of striated and sclerotic nodes around the midshafts (Figure 6.7C) and small and slight nodes with fine striations and micropitting on the distal shaft. Lesions consistent with treponemal infection are present in the form of periosteal reactions that striate longitudinally along the all sides of the fibular shafts. The femora are less heavily affected, with only the left femur exhibiting a node on its distal shaft. Situated posteriorly, the node covers a large portion of the popliteal surface and shows a few larger striations within a slightly rugose surface.

The distal shaft of the right radius appears to be thickened by a rugose expansion made up of dense, sclerotic bone (Figure 6.7D). It exhibits minimal striations and appears to be healing or healed due to the smoother appearance when compared with the nodes and expansions on the lower extremities.

In addition to these suggestive lesions, periosteal new bone formation consistent with treponemal infection was found in varying stages of healing and degrees of severity on the right humerus, ulna, and femur, and the left radius. Due to the combination of a diagnostic lesion and numerous lesions suggestive of and consistent with treponemal infection, individual S4045V1049 given a score of 5.

Figure 6.7: Selection of lesions on the bones of individual S4045 V1049.
A: The tibiae are affected by rugose nodes and expansions all along the shaft, most pronounced on the distal half.
B: A diagnostic node with shallow superficial cavitation on the medial surface of the left tibial shaft.
C: The left fibula is affected by a distinct node suggestive of treponemal infection at the midshaft, which also shows striations and sclerotic new bone.
D: The distal half of the shaft of the right radius is thickened by an irregular and rugose expansion new bone, a suggestive lesion.
Photos A, C, and D by Rachel Schats; photo B by Lotte Nagelhout.

S4068 V1071

These remains belong to a probable female of old middle adult age (36-45 years). While the cranium was absent, the postcranial skeleton was almost fully complete and in a state of good preservation. While the remains exhibit relatively few treponematosis-related pathological lesions when compared to the previously discussed individuals, some noteworthy lesions can be found on the lower legs.

Most significant is a node with superficial cavitation on the lateral aspect of the distal shaft of the left fibula (Figure 6.8A). The node consists of irregular new bone deposited on top of the undisturbed cortex, with fine and coarse striations throughout. A focal, lytic destruction through which the cortex is clearly visible, is situated in at the most elevated part of the node and surrounded by irregular, in some places slightly overhanging, margins (Figure 6.8B). This lesion perfectly aligns with Hackett's (1976) description of nodes with superficial cavitation and is therefore considered to be specific for treponemal infection (pp. 93-97).

In addition, both tibiae exhibited slight periosteal new bone formation, which was most pronounced on the left tibia along the antero-medial aspect of the shaft (Figure 6.8C). In addition, the medial aspect of the distal shaft features a distinct patch of periosteal new bone with deeper striations. However, this patch is not elevated, and thus more reminiscent of a plaque of new bone than a node. While the patch includes some cavities, these are likely to be the consequence of postmortem damage, as the margins of these cavities show fresh and lighter-coloured breaks. The anterior crest on the proximal end of the left tibia also features a lytic lesion small in size, but its appearance did not allow for the identification of its possible aetiology beyond a non-specific periosteal lesion (Figure 6.8D). The right tibia exhibited periosteal striations along the medial shaft, but as these were fully incorporated into the cortex, they are considered to be healed.

The individual was accredited with a treponemal score of 4, due to one diagnostic lesion on the left fibula. While no suggestive lesions were found, the left and right tibia featured lesions consistent with a treponemal diagnosis. However, this diagnosis should be met with reservations, as the individual was not affected by widespread and bilateral lesions that are suggestive of or specific to treponemal disease.

Figure 6.8: Selection of lesions on the bones of individual S4068 V1071.
A: Treponemal-specific node with superficial cavitation distal shaft of the left fibula.
B: Close-up of node with superficial cavitation on left fibula, showcasing the overhanging margins surrounding the cavity and the untouched cortex beneath.
C: Lamellar periosteal new bone formation along the medial shaft of the left tibia, consistent with treponemal disease, with a patch of more active periosteal new bone near the distal end of the shaft.
D: Lytic lesion with unknown aetiology on the anterior crest of the proximal shaft of the left tibia.
Photos A, C, and D by Rachel Schats; Photo B by Lotte Nagelhout

These well-preserved remains belong to a young middle adult (26-35 years), who was determined to be of female sex through aDNA analysis. The skeleton is mostly complete, lacking only the left scapula, clavicle and ulna. Almost all skeletal elements are affected by extensive and bilateral infectious lesions, except for the vertebral column and the ribs.

Caries sicca lesions cover the frontal bone and the right parietal and zygomatic bones, mostly consisting of focal superficial cavitation in the case of discrete lesions and serpiginous cavitation in the case of contiguous lesions, i.e. stage 3 and 6 (Figure 6.9A-B). All cavitations lack signs of nodulation or other healing, with the majority of these cavities marked by sharp and overhanging margins. The inner table of the cranium remains uninvolved with the pathological change, save for a patch of woven bone on the inner frontal bone. This observation supports the elimination of tuberculosis as a possible cause for the focal superficial cavitations (stage 3) (Hackett, 1976, p. 39). As such, these cranial lesions can be regarded as diagnostic for syphilis.

Other diagnostic lesions, in the form of nodes with superficial/gummatous cavitation, are found in the left femur, tibia, and fibula, and the right ulna, radius, tibia, and fibula. Due to the extensive distribution of the lesions, the following description will cover a limited number of lesions.

The distal shaft of the right radius is grossly expanded, featuring an overall rugose and complex surface pattern as well as extensive and confluent superficial cavitation within a granular surface on the posterior-lateral aspect (Figure 6.9C). The most distal aspects of this expansion display denser, sclerotic new bone. The right ulna also exhibits gross surface changes on both the proximal shaft and midshaft (Figure 6.9D). Proximally, the posterior surface is damaged by extensive lytic pitting that has altered the bone so that it seems covered by a thickened, granular, and gummatous surface. Around the midshaft, a similar phenomenon occurs, but features a deeper and wider cavitation within the granular bone matrix.

In the lower extremities, one of the most prominent diagnostic lesions is present on the distal anterior shaft of the left femur (Figure 2.4). The node is finely striate where it borders the untouched cortex, but becomes more irregular and dense near the centre, in which a deep cavity that extends into the cortical bone without penetrating into the medullary cavity.

The tibiae display several nodes and expansions of the bone in varying degrees of severity, but leaving the posterior surface mostly intact. The left tibia is most affected, with numerous overlapping nodes on the proximal shaft and major expansion of the distal shaft (Figure 6.9E). A total of eight nodes with superficial cavitation can be identified, although these occasionally interconnect to produce larger affected areas. Together, these cavitations and new bone formations form an irregular pattern of

nodes and depressions within a granular and highly porous surface. The right tibia is affected by an extensive formation of striate nodes, irregular nodes and superficial cavitation. Three nodes on the proximal metaphysis, proximal shaft, and distal shaft all include superficial cavitation that has coalesced to form an irregular and pitted pattern of depressions and margins. Cavities vary in depth, but none penetrate into the medullary cavity. The remaining area of the shafts of both tibiae do not feature nodes or superficial cavitation, but the majority of their surface is still covered by a pattern of fine striations.

Both fibulae are also deformed by several nodes of periosteal new bone, some with focal destruction that has amalgamated into larger depressions within nodes. The margins of these cavities are all sharp, irregular and overhanging, with limited signs of healing (Figure 6.9F).

Suggestive lesions were found on the left humerus, right humerus, right radius, and both femora. The appearance of these lesions range from rugose nodes or expansions in the humeri (Figure 6.9G) and radius to finely striate nodes on the femora.

Besides these long bones, the fourth metacarpal of the right hand (Figure 6.9H), the mandible, sternum, right clavicle (Figure 6.9I), and right scapula were also affected by gummatous or periosteal lesions, but as described above, these were not considered during the scoring process. The metacarpal lesion is notable, as similar lesions were not identified in any of the other individuals in this assemblage. Almost the entire bone has been altered by irregular new bone growth with extensive lytic lesions and destruction, with only the distal head intact. The other hand bones of this individual were not affected.

Taking this wide variety and bilateral distribution of lesions, which are both diagnostic and suggestive of treponemal disease, into consideration, this individual was attributed a treponemal score of 5.

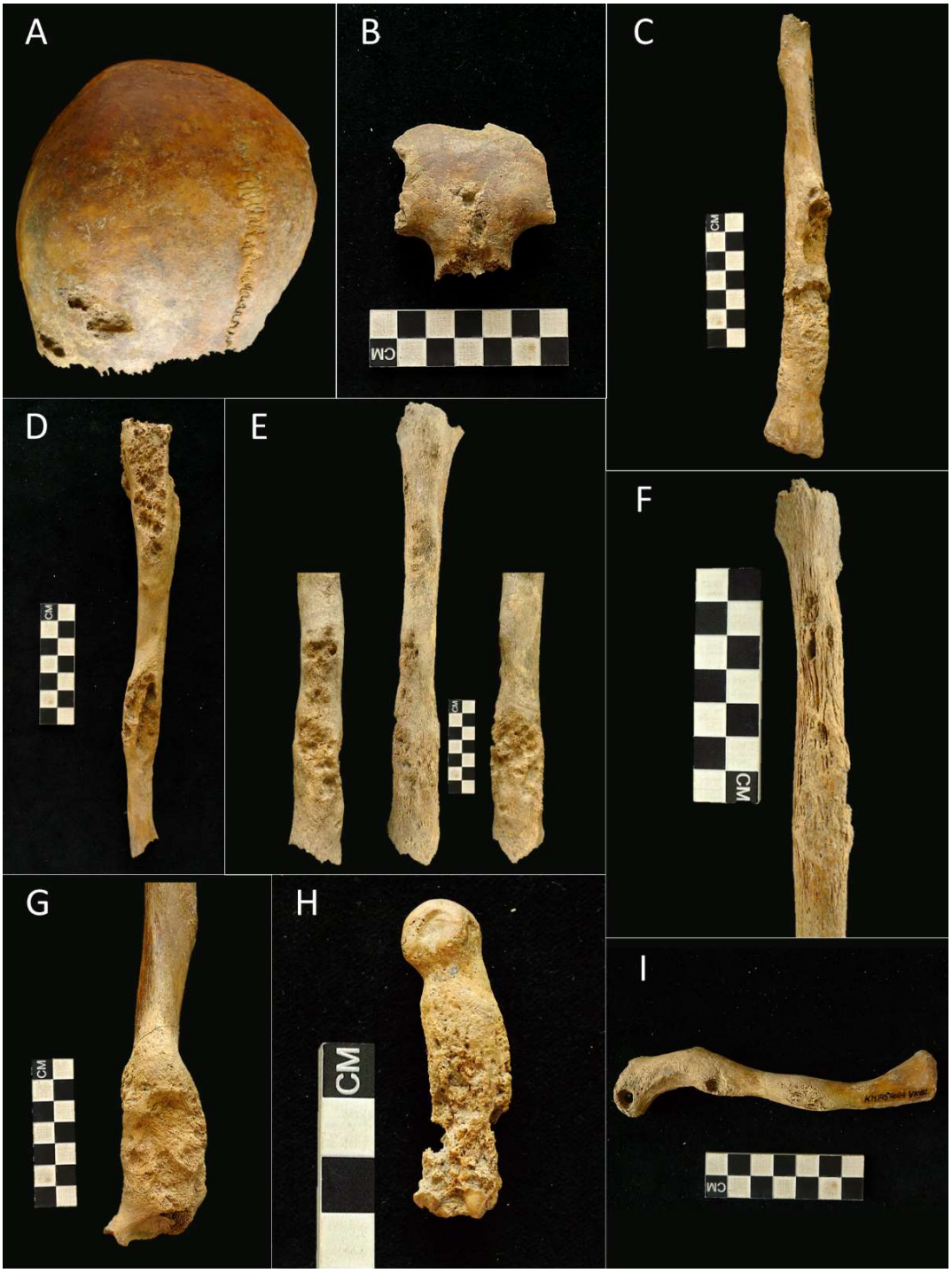

Figure 6.9: Selection of lesions on the bones of individual S4084 V1086.
A: Caries sicca lesions on the right parietal, displaying deep and confluent cavities with no nodular margins.
B: Caries sicca lesions on the frontal bone.
C: Posterior aspect of the right radius shows gross expansion of the distal shaft, with deeper cavitations around the midshaft.
D: Posterior aspect of the right ulna shows multiple areas of extensive new bone formation and gummatous lesions.
E: Medio-anterior (left), anterior (centre), and lateral (right) aspect of the left tibia, affected by expansions and gummas.
F: Lateral aspect of the proximal shaft of the right fibula displays a node with fine striations and superficial cavitation.
G: Medio-posterior aspect of the distal right humerus shows a suggestive lesion: rugose expansion.
H: Lateral aspect of the right fourth metacarpal exhibits extensive expansion and lytic destruction of all aspects.
I: Superior aspect of the right clavicle displays multiple gummatous lesions and finely striate nodes with superficial cavitation.
Photos by Rachel Schats.

6.2 Archival research

During the archival research, 22 records were studied, each containing one or multiple documents related to St. Gertrude's infirmary or the other healthcare institutions. The majority of these records came from *Oud Archief Kampen* (O.A.K.; entry code 00001), which includes many of the oldest archives of the city from the period between 1251 and 1813. Additionally, many of the consulted records are part of the archive of St. Gertrude's infirmary (*Sint Geertruids Gasthuis*; entry code 00151) and one record from the archive of *Schole Campensis Bibliotheca* (inventory no. L00185), which are both not yet digitally inventoried. A full list of the studied records, their inventory numbers, and a short description of their contents is available in Appendix 1.

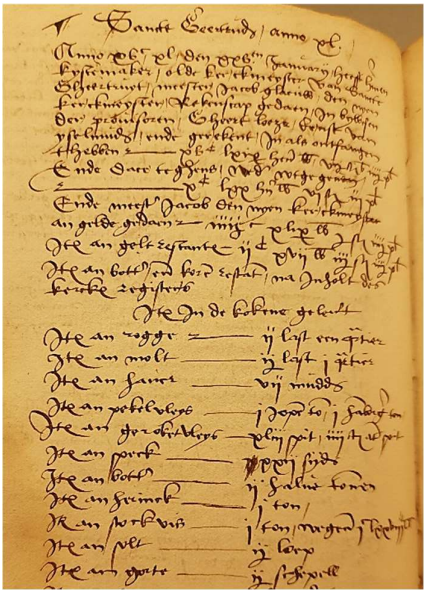

*Figure 6.10: O.A.K. 00001, inv. no. 1330, p. 123. Shows a list of ingredients used in the kitchen, including rye ('*rogge*'), butter ('*bott*r'), and barley ('*gorte*'), dated to 16th century. Photo by Lotte Nagelhout.*

Almost all records included extensive financial details from the church wardens about the infirmary and its *proveniers*, such as the services provided by tradesmen, the acquisition of foodstuffs (Figure 6.10), inventories of the infirmary's possessions, records of burials (Figure 6.11), and income from properties. While some records include occasional notations for the purchase of medicine from various people, the type and quantity of medicine is not specified further in these records (Figure 6.12).

Figure 6.11: O.A.K. 00001, inv. no. 1371. Record of the expenses for burials of seven individuals from St. Catharine and Gertrude's infirmary in 1729. Photo by Lotte Nagelhout.

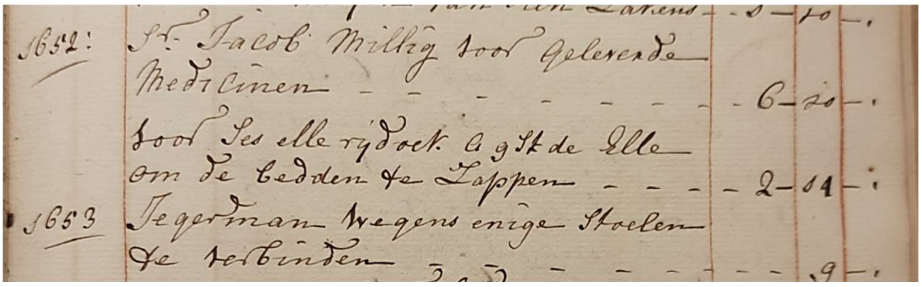

Figure 6.12: O.A.K. 00001, inv. no. 1345. Administrative and financial record dated to 1652 from the city hospital stating the price for medicine delivered by Jacob Millig (first sentence: "… geleverde Medicinen*"), as well as other expenses and services, such as the reparation of some chairs (last sentence: "…* enige stoelen te verbinden*"). Photo by Lotte Nagelhout.*

Although not directly linked to the infirmary, two records from a later period disclose more information on possible treatment methods. The first is a medical report addressed to the mayor and other stakeholders in Kampen regarding a wide-spread disease and its treatment, written by medical professor Matthias van Geuns on 17 September 1779 (O.A.K. 00001, inv. no. 2311). At the time, prof. dr. Van Geuns was a lecturer in medicine, obstetrics, chemistry, and botany at the provincial Academy in Harderwijk, although his ultimate influence would prove to shape the Dutch medical history much more than this specific report shows (Sypkens Smit, 1953). In the report, Van Geuns extensively describes a "*grasseerende ziekte",* or spreading disease, that is affecting the population of Kampen. He also comments on the widespread use of particularly harmful medicine, which are taken in heavy dosages and are even combined, which leaves the patient even more sick. He lists various laxatives, including mercury: "(…) *Resina Jalappa, jaa zelf Coloquint, Mercurius dulcis, xc.*" (Figure 6.13).

A second mention of mercury-containing medicine comes from another report by Van Geuns, this time dated to 19 September 1779. In the report, Van Geuns examines the practices of four pharmacies in Kampen and describes how one of these does not adhere to the regulations, commenting on their lack of quality medicine: "*Dan in de vierde (…) apotheek, waren de defecten zoo veele, en de qualiteit van 't gene voorhanden was (…) veelal zoo schraal of slegt, dat hier van geen goed getuigenis kan geeven."* (O.A.K. 00001, inv. no. 2311, pp. 1-2). He recommends that the pharmacies consult recently published

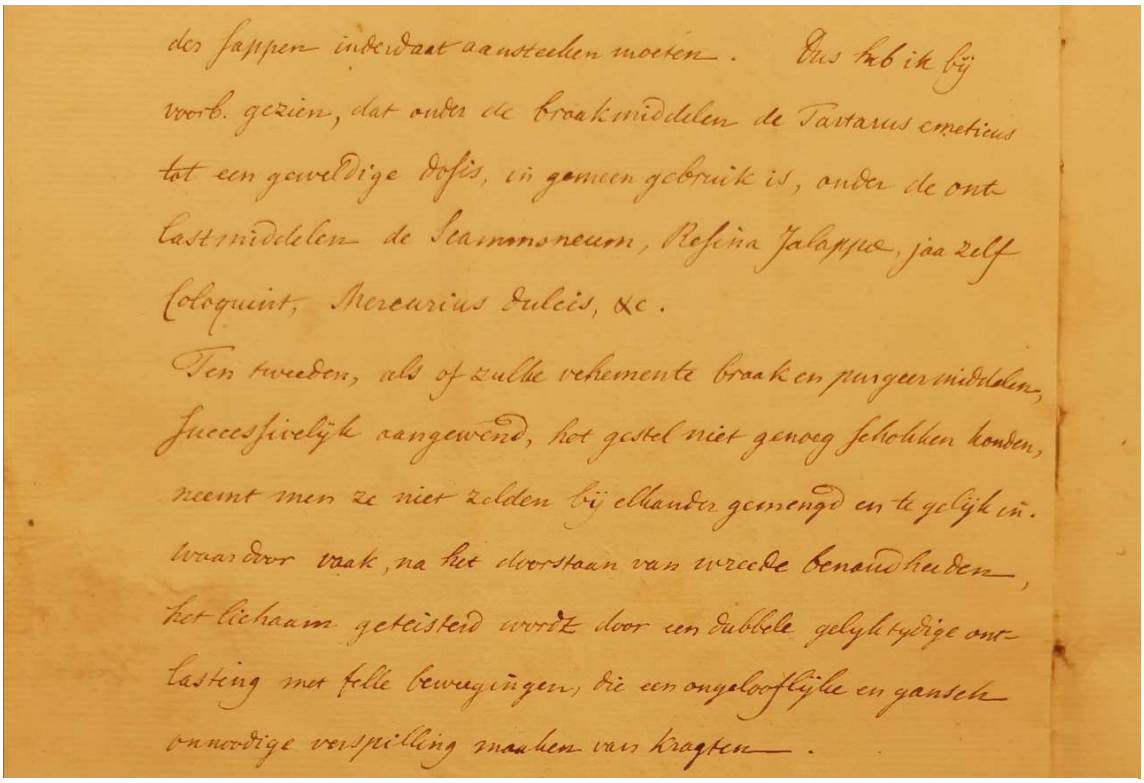

Figure 6.13: O.A.K. 00001, inv. no. 2311, folio 2, p. 16. Report by medical professor Van Geuns regarding the cause, spread, and treatment of an epidemic disease in the late summer of 1779, in which the use of Mercurius Dulcis is mentioned (line 5). Photo by Lotte Nagelhout.

pharmacological literature and that expert visitations should be scheduled regularly (pp. 2-3). On the final page, he argues whether the pharmacy without accreditation by a lawful medical practitioner should remain active, as the handling of dangerous medicine by ignorant apothecaries could have deadly consequences (Figure 6.14). Before advising that this necessitates stricter regulations, he names such dangerous medicine: "*Braakmiddelen en purgeermiddelen van de hevigste soort, slaapmiddelen, kwikmiddelen (…)".* The last one, "*kwikmiddelen*", refers to medicine containing mercury, known as *kwik* in Dutch.

On the basis of these two reports, it seems that mercury was readily available in at least one of Kampen's pharmacies during the late 18th century, and may have been used extensively, albeit not specifically in relation to syphilis, against the wishes of medical professors. However, in all of the consulted records, no mention of syphilis or other diseases was identified over the course of this study.

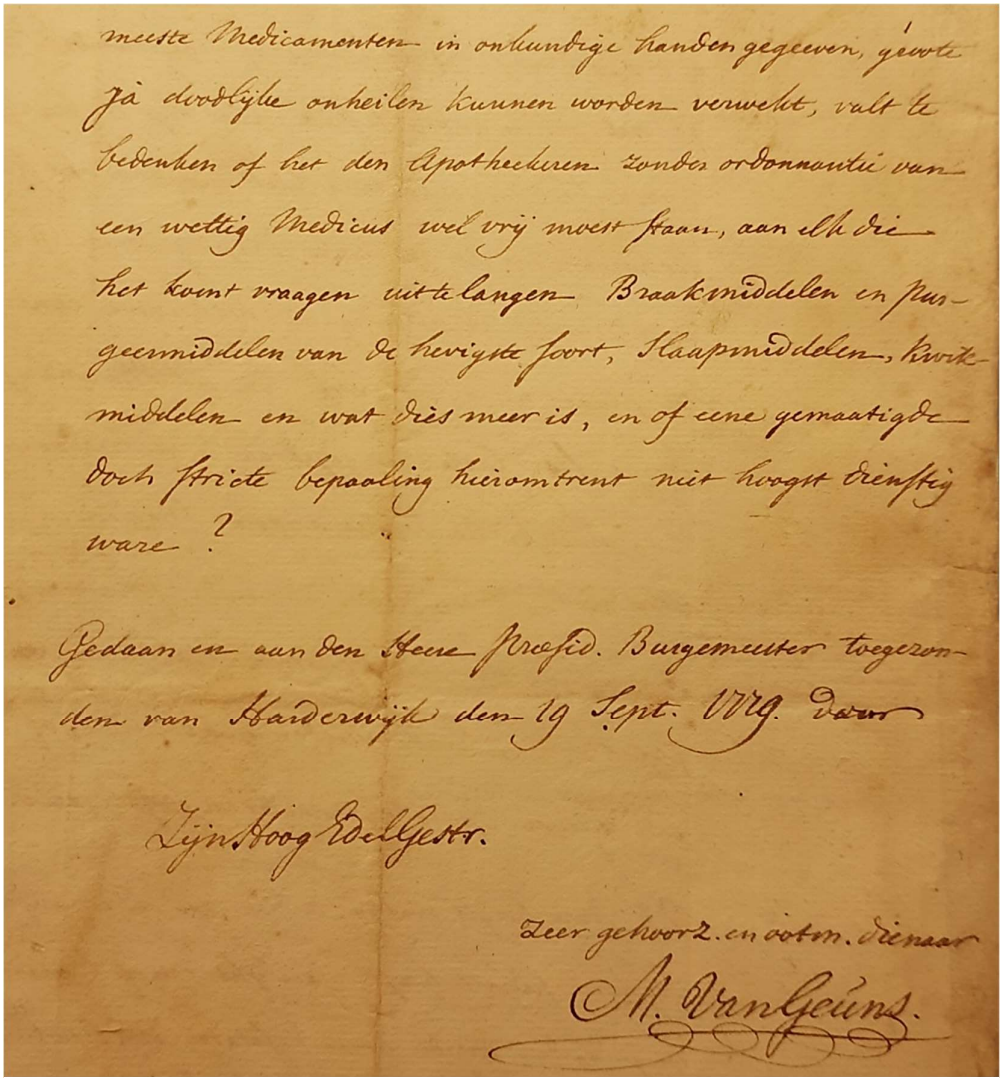

meeste Medicamenten in onkundige handen gegeeven, gewis
ja dood lijke onheilen kunnen worden verwekt, valt te
bedenken of het den Apotheekeren zonder ordonnantie van
een wettig Medicus wel vrij moest staan, aan elk die
het komt vraagen uit te langen Braakmiddelen en pur-
geermiddelen van de hevigste soort, Slaapmiddelen, kwik-
middelen en wat dies meer is, en of eene gemaatigde
doch stricte bepaaling hieromtrent niet hoogst dienstig
ware ?

Gedaan en aan den Heere Presid. Burgemeester toegezon-
den van Harderwijk den 19 Sept. 1779. Door

Zijn Hoog Edelgestr.

Zeer gehoorz. en ootm. dienaar

M. Van Geuns.

*Figure 6.14: O.A.K. 00001, inv. no. 2311, folio 1, p. 4. Report on Kampen's pharmacies from medical professor Van Geuns to the mayor of Kampen, in which he describes the unregulated use of medicine including "*kwikmiddelen*" (line 6-7), which contain mercury. Photo by Lotte Nagelhout.*

6.3 Portable X-Ray Fluorescence Spectrometry

As explained in Chapter 5, pXRF analysis was conducted in two batches, one pilot study and one definite study, to examine mercury levels on a larger-scale across the Kampen population. The pilot study was not able to detect meaningful, quantifiable mercury levels in any of the examined bones, as all readings yielded very low emission values, likely to be similar or below the detection limit of this pXRF instrument (Bruker Tracer III-SD) and by extent can be considered to be significantly below 5 ppm, up to 1 ppm.

Nonetheless, the pilot study provided a useful opportunity to gain more insight into the detection limits for Hg with this pXRF instrument as well as determining the effect of various settings and reading times on the output. In doing so, the pilot study could establish that an increased electric current and shorter reading time yielded higher emission peaks. Although this also resulted in a generally higher background signal that potentially obscures the Hg emissions, these settings do allow for quicker analysis, as such shorter reading time vastly increases the time efficiency of the analysis and thereby increases the number of possible measurements.

Since the Bruker Tracer 5g was expected to have a significantly lower detection limit and generally lower background interference, the approach from the pilot study was further applied to the final pXRF study. An overview of each analysed bone and their raw emission values from analysis with the Bruker Tracer 5g is available in Appendix 2. The following sections describe the statistical analyses that were performed with this dataset.

6.3.1 Results analysis Bruker Tracer 5g

Table 6.6 shows the aggregated mean and standard deviation in Hg emission values (after normalization to rhodium) of all measurements per bone for each analysed individual. It should be reiterated that these intensities are quantified emission values of Hg, which are comparative and proportional to other elemental emission values at the specific sampling location. As such, these emission values do not correspond with ppm or other absolute quantificational units.

These aggregated mean Hg emission values are compared in various groups to explore their relationship. To test statistical significance, each dataset was assessed on normality with a Shapiro-Wilks test or Levene's test for homogeneity when necessary. The statistical significance threshold was determined to be <0.0125 by conducting a Bonferroni correction.

Table 6.6:

Results from final pXRF analysis with Bruker Tracer 5g, showing the aggregate means and standard deviations in Hg emission values (normalized to Rh) per bone for each individual, as well as the soil samples.

Sample ID	Sex	Age	Trepo-nemal score	Femora		Ribs		Humeri	
				Mean (E^{-3})	SD (E^{-3})	Mean (E^{-3})	SD (E^{-3})	Mean (E^{-3})	SD (E^{-3})
S4000V1006	M	19-25	1			6.38	0	5.73	2.93
S4008V1003	F	16-18	5	6.53	3.50	3.39	2.69		
S4011V1012	F	36-45	1	6.77	5.36	5.73	0		
S4013V1008	F	19-25	5	5.44	3.40	3.46	0		
S4015V1019	F	> 45	3	5.17	2.90	7.63	0		
S4019V1018	M	26-35	1	6.89	5.52	6.64	5.68		
S4021V1021	M	36-45	1	5.49	5.40	10.66	0		
S4023V1025	M	19-25	2	7.10	3.04	4.48	0		
S4027V1028	N/A	12-18	3	4.87	3.00	1.86	0		
S4031V1030	M	> 45	0	6.32	6.14	16.49	0.34		
S4033V1032	M	26-35	5			5.35	3.27	4.07	1.99
S4040V1041	M	36-45	2	6.85	3.81	11.40	0		
S4045V1049	F	36-45	5	4.38	2.76	2.88	3.46	8.30	7.24
S4052V1052	M	> 45	3	6.84	3.58			4.40	5.68
S4053V1054	F	26-35	0	8.40	6.18	6.47	0		
S4063V1065	M	19-25	1	5.13	5.82	2.49	0		
S4068V1071	F	36-45	4	6.08	3.17	2.14	0		
S4074V1078	M	26-35	1	6.71	2.51	7.57	0		
S4084V1086	F	26-35	5	4.23	1.76	5.48	0	6.85	3.43
S4096V1100	M	36-45	2	5.68	3.69	1.95	0.19		
Control Bone Samples									
Medical Collection GPVI			0	1.89	3.08				
Blokhuizen 1983-1 64			0	7.32	2.16				
Control Soil Samples									
				Mean (E^{-3})	**SD (E^{-3})**				
Soil – Restricted Materials				9.20	5.44				
Soil – Mudrock Calibration				0.43	1.55				

Firstly, femoral mean Hg emission values from Kampen remains (abbreviated as KM14) are compared to the mean Hg emission values derived from the two bone controls as well as the soil samples (Figure 6.15). This boxplot shows that KM14's mean Hg emissions have a generally higher median and maximum value than the mean Hg emissions in the control group, whereas the soil sample has a much higher median and maximum value than both skeletal groups. This graph also displays the much wider spread of values within the control and soil group, which can be explained by the limited sample size and high variability in mean Hg values for both groups. A variance test to test the statistical significance of this difference in spread between the three groups was not conducted due to the low sample size. However, when compared to other elemental emission values (Appendix 2), the variability in Hg emission values seems to be quite low. Additionally, there are no discernible peaks in any of the Hg emission values, whereas other elements (e.g. Fe or Mn) demonstrated uniquely high peaks for certain measurements.

Secondly, this relationship between the mean Hg emissions from soil and bone is compared in more detail by comparing the mean Hg emissions separated by bone type, i.e. femora, humeri and ribs, with the soil samples (Figure 6.16). This graph shows that femora and humeri yield comparable Hg emissions, whereas these values are much more variable in ribs, with individuals having either much higher or much lower Hg emission values in their ribs than in their long bones. Additionally, one outlier (S4031 V1030) with a mean emission value of 16.49 E^{-3} was identified, which is the highest emission value for all measurements taken. Interestingly, no lesions consistent with, suggestive of, or specific to treponemal disease are present for this individual.

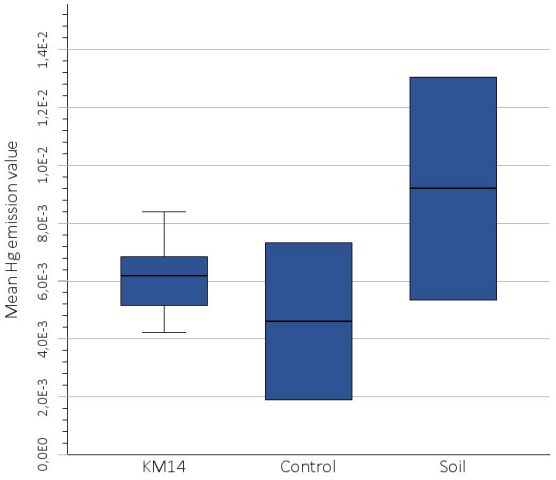

Figure 6.15: Mean Hg emission values for femora from KM14 (n=18) and the skeletal controls (n=2), as well the Hg emission values for the soil samples (n=2) (as analysed with Bruker's Restricted Materials calibration).

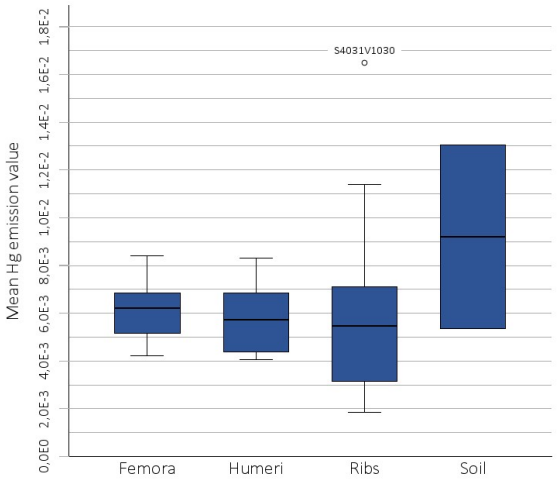

Figure 6.16: Mean Hg emission values for femora (n=18), humeri (n=5), and ribs (n=19) from KM14 and Hg emission values for soil samples (n=2) (as analysed with Bruker's Restricted Materials calibration).

Thirdly, femoral mean Hg emissions are compared between KM14 and control samples in Figure 6.17. This boxplot shows that the femora from Kampen have a higher median Hg emission than the two control samples, but this pattern is complicated by the high variability within the control group, with the sample from Blokhuizen yielding a higher emission value than the majority of KM14 femora. This dataset was subjected to statistical significance testing by performing a Mann Whitney U test to evaluate whether Hg emission values differed by skeletal assemblages from different periods and regions.

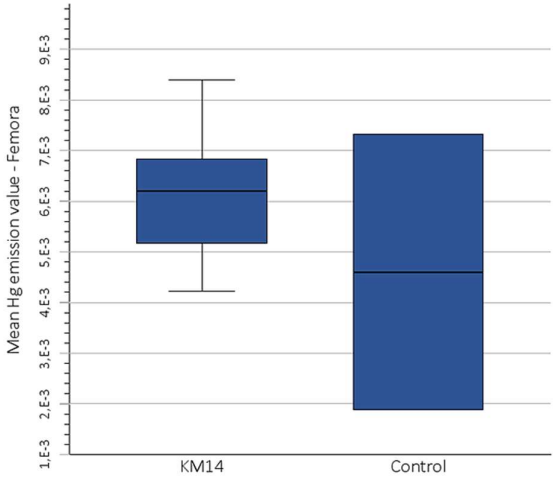

Figure 6.17: Mean femoral Hg emission values for samples from KM14 (n=18) and the skeletal control group (n=2).

The results indicated that there was no significant difference in the mean femoral Hg emission values between the KM14 sample (n = 18) and the control group (n = 2) (U = 17.00, z = -0.126, p = 0.947).

Next, several groups within the KM14 assemblage are compared to evaluate whether the mean Hg emission values co-vary with different factors. Firstly, non-pathological bones (treponemal score 1 or lower) are compared to pathological bones (treponemal score 2 or higher) for femora and ribs, to investigate the relation between infectious, possibly treponemal related, individuals and Hg emission values. Figure 6.18 shows this comparison for femora, and Figure 6.19 for ribs. As a result of the limited sample size for analysed humeri, only one non-pathological specimen could be compared to four pathological humeri, which did not yield any significant findings.

In the case of femora, the median for non-pathological is higher than for pathological bones, but this could be influenced by an outlier. Subsequent statistical analysis to investigate this relationship was performed by conducting an Independent Samples T-test, which showed there was not a significant difference in mean femoral Hg emission values between non-pathological and pathological bones (t(16) = 1.575, p = 0.135).

In the case of ribs, the median and interquartile range of the non-pathological group seem to be notably higher than that of the pathological group, but the non-pathological group also shows a wider distribution. However, a subsequent Mann-Whitney U test revealed that mean Hg emission values in ribs were not significantly higher in the non-pathological group (n = 8) compared to the pathological group (n = 11) (U = 19.00, z = -2.064, p = 0.041).

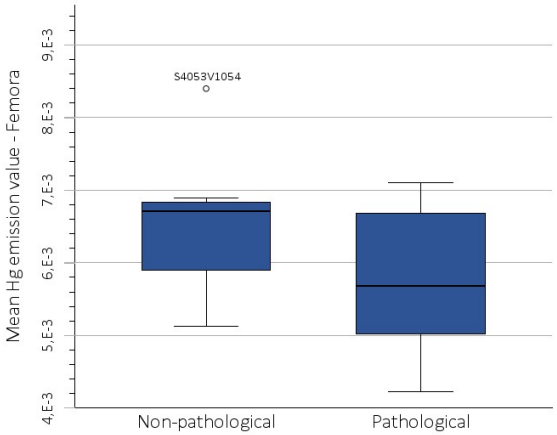

Figure 6.18: Mean Hg emission values for non-pathological (n=11) and pathological (n=7) femora from KM14.

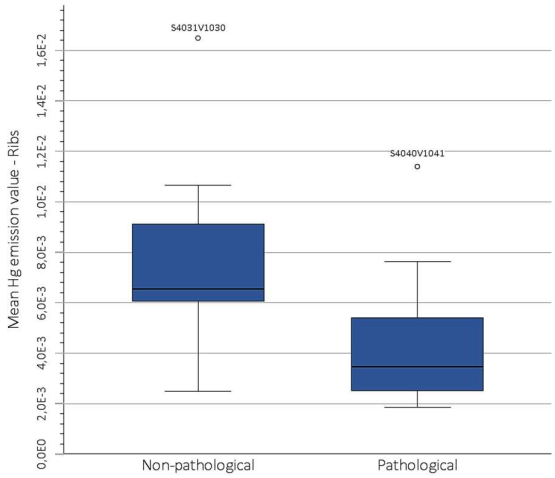

Figure 6.19: Mean Hg emission values for non-pathological (n=8) and pathological (n=11) ribs from KM14.

Additionally, the mean Hg emission values from femora in the non-pathological and pathological groups could be further analysed by differentiating between groups using the treponemal score acquired during the osteo-archaeological research (Figure 6.20). This dataset also includes the femora from the control group within the category score=0. The boxplot shows that the medians of the different groups seem relatively variable, but this could be explained by the low sample sizes for each of the category. Interestingly, the medians and interquartile ranges within the graph seem to suggest a trend of decreasing Hg values with increasing scores, as the categories that represent individuals with no to little lesions consistent with or suggestive of treponematosis (score 0-2) have generally higher Hg emissions than the categories that represent individuals with multiple suggestive and/or diagnostic lesions (score 3 and 5).

A one-way ANOVA test was conducted to evaluate this effect of the treponemal score on the mean Hg emission values. The test revealed that there is no statistically significant difference in Hg emissions between five groups, with the score=4 group omitted as a result of the sample size ($F(5, 14) = 0.351$, $p = 0.873$). A Tukey's HSD Test for Multiple Comparisons showed no statistical significance between any of the groups.

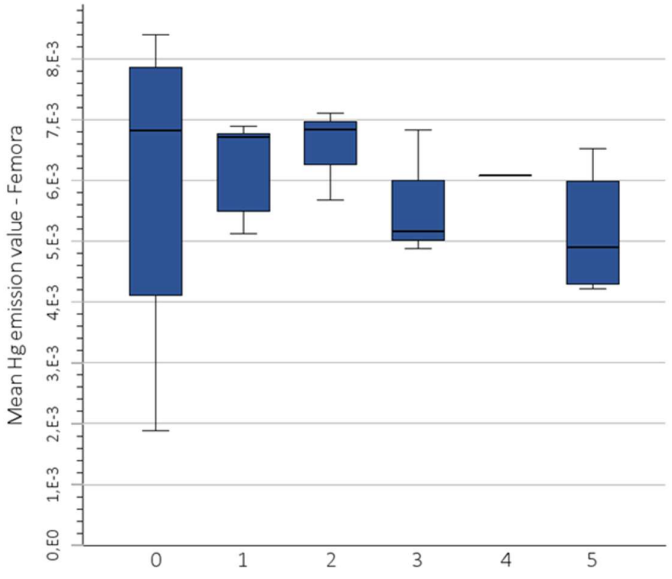

Figure 6.20: Mean femoral Hg emission values in the dataset for each treponemal score category: 0 (n=4), 1 (n=5), 2 (n=3), 3 (n=3), 4 (n=1), 5 (n=4).

Table 6.7 shows the descriptive statistics for the measurements of syphilitic lesions and control measurements taken at an unchanged location on the same bone. Conducting these control readings was not applicable for all lesion measurements, as extensive pathological expression on some of these bones that left no flat surface areas to conduct a proper pXRF reading. While the majority of the analysed lesions are located on tibiae, a few were measured on humeri, femora, and fibulae.

Two of these measurements (S4013 V1008 and S4033 V1032) are notably higher than the other measurements, reaching $10.4E^{-3}$ net count rates. In the case of S4013 V1008, the control measurement is significantly low, with $0.25E^{-3}$ net count rates. This may reflect topical mercury application and subsequent adsorption in two lesions on the left tibia and fibula. Other measurements on the femur and rib of this individual did not yield particularly high emission values (Table 6.6). However, as the absolute difference between the Hg values in lesions and controls cannot be quantified, this interpretation remains unsubstantiated.

Table 6.7:

Results from final pXRF analysis with Bruker Tracer 5g, showing the aggregate means and standard deviations in Hg counts (normalized to Rh) in measurements of syphilitic lesions on bone (most commonly the tibia) and control locations near these lesions.

Sample ID	Sex	Age	Treponemal score	On treponemal lesions		Control near lesions	
				Mean (E^{-3})	SD (E^{-3})	Mean (E^{-3})	SD (E^{-3})
S4008V1003	F	16-18	5	6.56	3.65		
S4013V1008	F	19-25	5	10.41	3.66	0.25	4.17
S4023V1025	M	19-25	2	3.21	0	1.36	0
S4027V1028	N/A	12-18	3	1.03	3.45		
S4033V1032	M	26-35	5	10.42	0		
S4045V1049	F	36-45	5	4.91	1.53	7.36	0
S4052V1052	M	> 45	3	4.17	0.38	3.62	0
S4063V1065	M	19-25	1	1.93	0	1.06	0
S4068V1071	F	36-45	4	3.96	0	4.78	0
S4074V1078	M	26-35	1	-1.30	0	5.16	0
S4084V1086	F	26-35	5	4.06	4.45	4.18	0

Note: control measurements for lesions could not be taken for of the sampled bones due to extensive pathology affecting the entirety of the bone and/or leaving no suitable bone surface to measure.

Figure 6.21 demonstrates that the median for these mean Hg emission values does not differ much between treponemal lesions and their respective control measurements. Despite this, the Hg emissions seem to be lower on average and display a more limited range for control measurements. This difference was not tested for statistical significance as the number of control measurements is limited and the sampling locations varied widely.

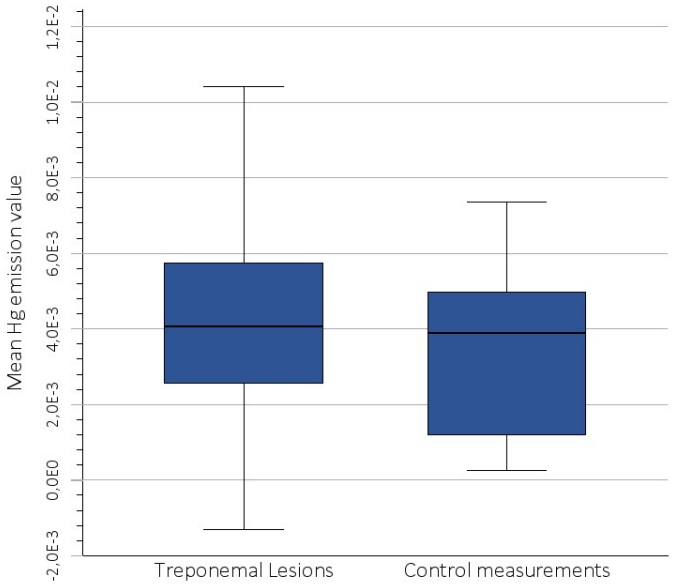

Figure 6.21: Mean Hg emission values for treponemal lesions (n=11) and control measurements (n=8).

Lastly, as Appendix 2 demonstrates, there does not seem to be a pattern in higher return rates for Hg emissions in specific sampling locations, as the values for each location are highly variable. While some individuals showed slightly higher Hg emission values in certain bones or certain lesions, the restriction in quantifying this data due to the values being below detection limit did not allow for extensive and relevant interpretation of these results.

6.3.2 Inter-elemental comparison

The reported Hg emission values are relatively low and have little variation when compared to other elemental emission values (Appendix 2). Notably, no measurement of the pXRF analysis shows uniquely high peaks in Hg emission values, whereas other elements, such as Fe or Mn, show discernible peaks of emission values for some measurements which can be more easily interpreted as elevated concentrations of that specific element. As such, it remains a possibility that the measured emission values for Hg represent background noise instead of antemortem uptake of medicinal mercury into the bone matrix of each analysed individual.

Still, on the basis of these emission values and the instrument's limit of detection, an absolute concentration of less than 5 ppm is expected. This analysis clearly showed that, even under circumstances that were likely to be rich in mercury, the uptake in human bone and subsequent successful detection by pXRF analysis is highly limited at best.

6.4 Inductively Coupled Plasma-Mass Spectrometry

The ICP-MS analysis was conducted by Measurlabs, Finland, of which the results are shown in Table 6.8. As descripted in section 5.4.1, these samples reflect bone samples with a relatively higher proportion of cortical bone (femora, scapulae, and cranial bones) as well as samples with a relatively higher proportion of trabecular bone (ribs). These results are further analysed by comparing various groups. The highly selective nature of the samples for this specific dataset restricted the use of statistical significance testing.

Table 6.8:

Results from ICP-MS analysis by Measurlabs, showing concentration of Hg in ppm for each sample.

Feature and find no.	Treponemal score	Type of bone	Sample location	Hg concentration in ppm
S4011 V1012	1	Trabecular	Right rib 4, sternal end	0.71
S4019 V1018	1	Trabecular	Right rib 3, sternal end	1.28
S4019 V1018	1	Cortical	Left femur, cortical sample just inferior to trochanter minor	0.06
S4040 V1041	2	Trabecular	Unidentified rib fragment	0.31
S4096 V1100	2	Trabecular	Left rib 6 or 7, sternal end	0.63
S4027 V1028	3	Trabecular	Right rib 6, sternal end	0.48
S4068 V1071	4	Trabecular	Right rib 8, sternal end	0.20
S4008 V1003	5	Trabecular	Right rib 5, sternal end	0.52
S4008 V1003	5	Cortical	Left femur, posterior cortical fragment from distal diaphysis	0.26
S4008 V1003	5	Cortical	Right parietal, approx. 3 cm above squamosal suture	0.18
S4013 V1008	5	Trabecular	Right rib 7, sternal end	0.64
S4033 V1032	5	Trabecular	Left rib 4 or 5, sternal end	0.26
S4033 V1032	5	Cortical	Left scapular body	0.53
S4045 V1049	5	Trabecular	Right rib 6, sternal end	0.54
S4084 V1086	5	Trabecular	Right rib 8, sternal end	0.33
S4084 V1086	5	Cortical	Right scapular body	0.51
S4084 V1086	5	Cortical	Left parietal, fragment from temporal line	0.17
KM14 Soil 1	N/A	N/A	N/A	0.52
KM14 Soil 2	N/A	N/A	N/A	0.51

Table 6.8 demonstrates that Hg concentrations in bone range from 0.06 to 1.28 ppm. These minimum and maximum values were found in two different bones from the same individual. Various groups of samples are compared by performing descriptive statistics to further understand their relationship. When cortical bone samples are compared to trabecular bone samples and soil samples (Figure 6.22), it appears that trabecular bone samples have a slightly higher Hg concentration than cortical bone tissues. The mean concentration for trabecular samples is 0.54 ppm, whereas the mean concentration for cortical samples is 0.29 ppm. However, this trend is not true for all individuals. For example, the two cortical samples from S4084V1086 show a difference in Hg concentrations: the scapular sample, taken from a similar area as the trabecular samples, has a concentration of 0.51 ppm, which is closer to the mean trabecular Hg concentration, whereas the parietal sample has a much lower concentration of Hg at 0.17 ppm. This is also the case for S4033V1032.

This graph also shows that the 1.28 ppm Hg measured in S4019V1018 is likely to be an outlier. If this reading is excluded, the Hg concentrations in bone range from 0.06 ppm to 0.71 ppm, a much smaller difference. However, as this outlier is still regarded as a legitimate measurement, it is included in further data analysis. In comparing the soil and bone samples, soils return similar Hg levels as the trabecular tissues and are consistent throughout the two different samples.

Figure 6.23 displays the Hg concentrations if trabecular bone samples are separated and compared in a non-pathological (treponemal score 0 or 1) and pathological (treponemal score 2 or higher) group. This demonstrates that higher concentrations of Hg were found in the individuals without suggestive or diagnostic treponemal lesions. However, it should be noted that due to the nature of the ICP-MS study, only two non-pathological individuals were sampled. A similar comparison for cortical samples is limited due to the small sample size, but the one non-pathological cortical sample does contain the lowest concentration of Hg in the entire batch.

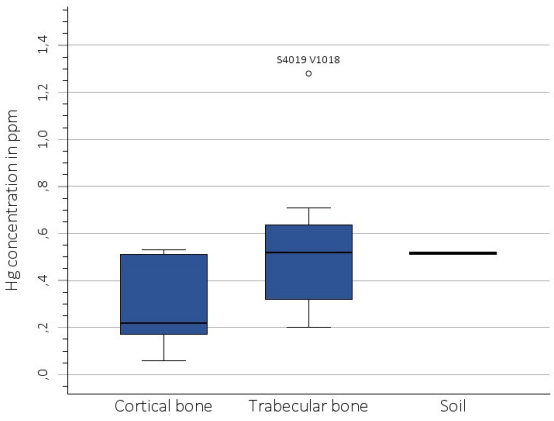

Figure 6.22: ICP-MS results. Hg concentrations in ppm in cortical bone samples, trabecular bone samples, and soil samples.

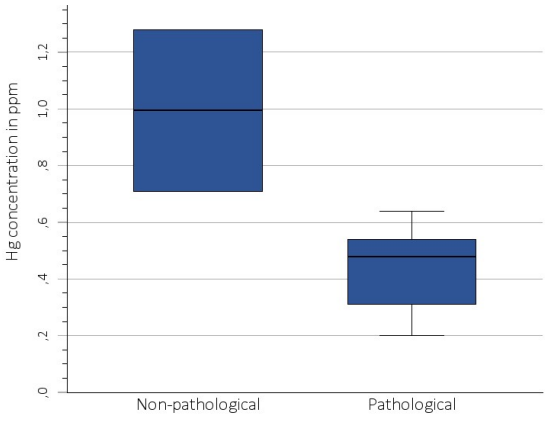

Figure 6.23: ICP-MS results. Hg concentrations in ppm in non-pathological (score <2) and pathological (score >1) trabecular bone samples.

Figure 6.24 displays Hg concentrations in trabecular bone samples for each treponemal scoring category. Although sample sizes are small and variable, this boxplot reinforces the trend of higher Hg concentrations in non-pathological samples displayed by Figure 6.23, as samples with treponemal score 2-5 show similar Hg concentrations that are all lower than those with score 1. However, this distribution is heavily influenced by the sampling strategy, and as such does not necessarily reflect the Hg concentration in the entire assemblage. The individual with score 4 has the lowest recorded Hg concentration for trabecular bone samples.

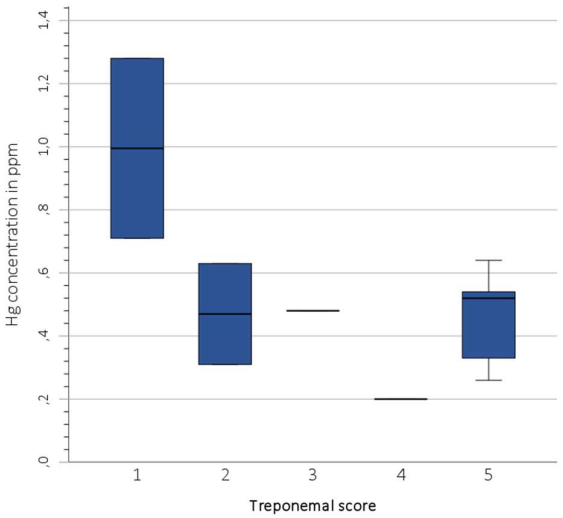

Figure 6.24: ICP-MS results. Hg concentrations in ppm in trabecular bone for each treponemal category.
Score 1: n=2, score 2: n=2, score 3: n=1, score 4: n=1, score 5: n=5.

6.5 Scanning Electron Microscopy with Energy Dispersive X-Ray

The SEM-EDX analyses were performed to investigate the possible incorporation of Hg in dental calculus as a result of ingestion of mercury-enriched foods or inhalation of mercuric vapour. Eight teeth were taken as samples, they are listed in Table 5.3.

In total, 101 measurements were taken, consisting of 70 measurements on calculus, 16 on cementum, and 15 on enamel. Figure 6.25 shows the locations and surfaces of these three areas in sample 4008-1-5. The cemental surface (C) has a cracked, but flat, appearance, whereas the enamel surface (E) is almost completely smooth in this magnification. The dental calculus (DC) forms a thick, complex matrix encrusted on top of the enamel. A selection of SEM images and EDX spectra for each sample is available in Appendix 4. The complete dataset from this analysis with all SEM images and EDX spectra will be published in an open-access supplementary table that is currently under preparation.

To gain more insight into this analysis, the results of two teeth samples from individuals S4008V1003 and S4084 V1086 are discussed in more detail below. The skeletal remains of both of these individuals are also discussed in section 6.1.3 as case studies for treponemal disease.

6.5.1 Sample 4008-1-5

This sample is the upper right second premolar from individual S4008 V1003 (Figure 6.25), an old adolescent with treponemal score 5 due to a variety of suggestive and specific skeletal lesions, including caries sicca and nodes with superficial cavitation on the long bones. Ten measurements were taken of this sample, which included six measurements of the dental calculus, two on the cemental

surface, and two on the enamel surface. Figure 6.26 shows the SEM imaging and energy dispersive X-ray spectra for four of these measurements, one on cementum, two on calculus, and one on enamel.

The analysis of the cemental surface (Figure 6.26-Spc_001) shows the high peaks for calcium (Ca), phosphorus (P), and oxygen (O), which corresponds with the natural inorganic composition of cementum, as it consists primarily of hydroxyapatite [$Ca_{10}(PO_4)_6(OH)_2$]. In addition, there are some traces of aluminium (Al) and silicon (Si), which could originate from natural soil materials such as quartz (SiO_2) or aluminosilicate minerals (Charlier et al., 2010, p. 170). Small peaks for carbon (C) and iron (Fe) can also be distinguished, of which the latter is likely to be the result of iron deposits from the soil in which the tooth was preserved prior to excavation.

The analysis for an area of dental calculus (Figure 6.26-Spc_005) also shows the presence of Ca, P, and O, but now with relatively more Al and Si. Small amounts of Fe and C are also still measured. In addition to this, smaller peaks for potassium (K) and magnesium (Mg) are now observed. Potassium frequently occurs naturally in silicate minerals (Kloprogge et al., 2020, pp. 255–256), whereas magnesium is a common trace element within tooth structures such as dentin and cementum, in addition to other elements like copper (Cu), zinc (Zn), and sodium (Na) (Tziafas, 2005, p. 183).

In addition to this surface area analysis, multiple measurements were taken of specific particles situated within the surface of the dental calculus. Figure 6.26-Spc_008 shows the imaging and spectra of such a particle, in which the compositional make-up appears very different from the previous two

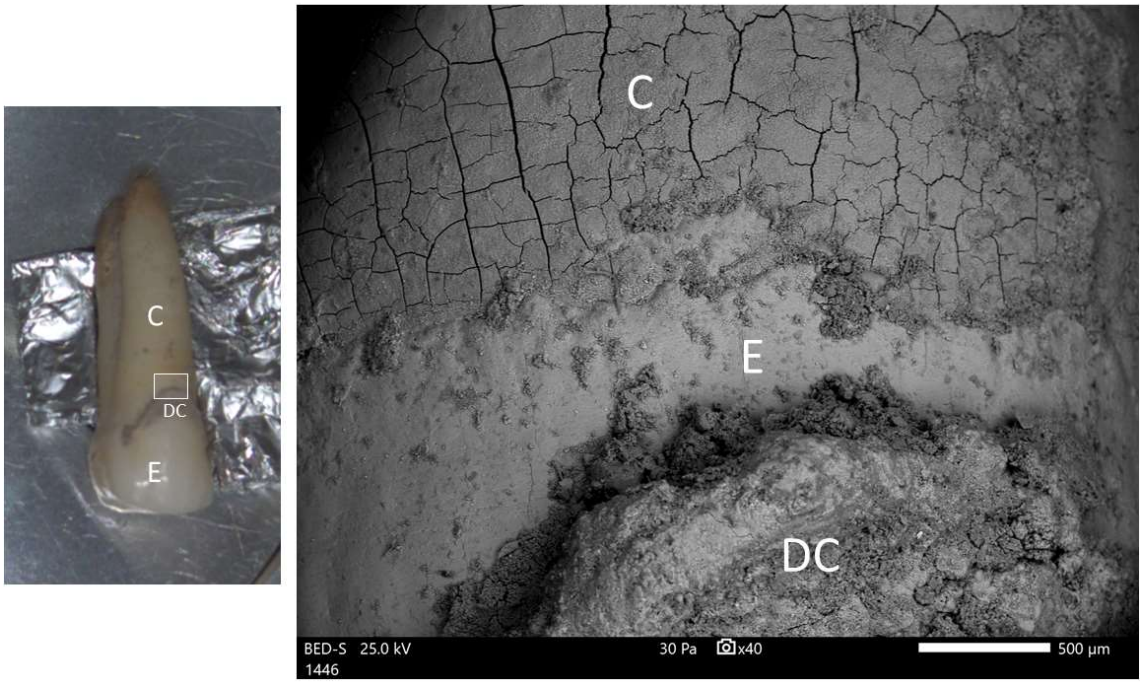

Figure 6.25: Sample 4008-1-5 and the locations of cementum (C), enamel (E), and dental calculus (DC). Left: sample 4008-1-5 positioned for SEM-EDX analysis. Right: close-up of cementoenamel junction and part of the dental calculus, located at the white outline in left image (SEM magnification = x40). Imaging by Ineke Joosten.

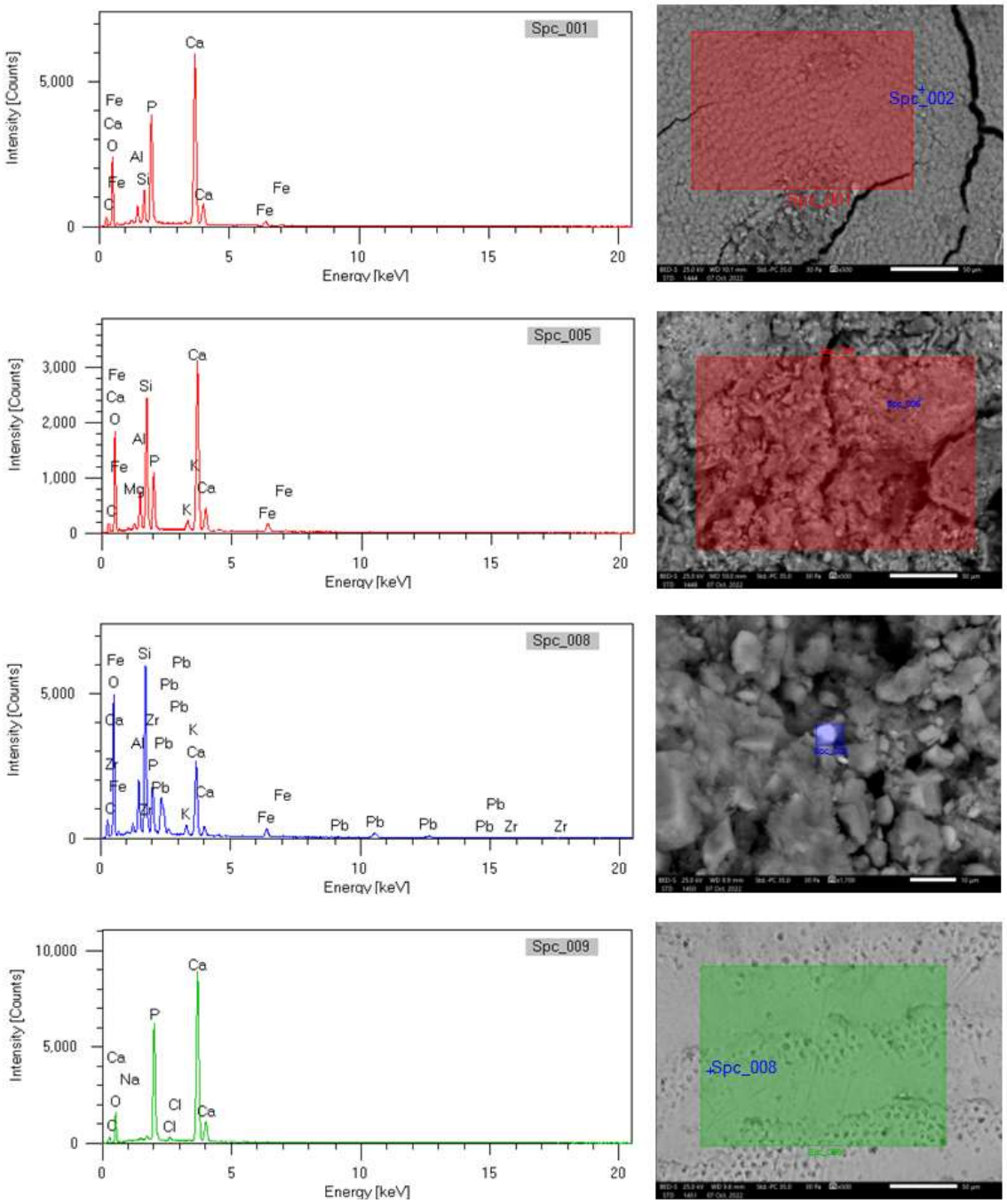

Figure 6.26: SEM-EDX images and spectra of four measurements of sample 4008-1-5.
Spc_001 (top): shows analysis of the cemental surface (magnification = x500);
Spc_005 and Spc_008 (second and third): show analyses of the calculus surface (magnification = x500) and a specific particle (magnification = x1700);
Spc_009 (bottom): shows the analysis of the enamel surface (magnification = x500).
Imaging and spectra provided by Ineke Joosten.

measurements. While Ca and P are still present, their intensity peaks are relatively small compared to the peaks of Si and O. Additionally, a variety of other elements is also observable, including Fe, K, Al, C, Pb (lead) and Zr (zirconium). As Pb does not naturally occur in calculus or other tooth structures, it

is likely that this particle is a lead compound that entered the dental calculus from an external source (I. Joosten, personal communication, 07-10-2022).

Figure 6.26-Spc_009 shows an area analysis for enamel, which has a relatively simple elemental output consisting of Ca, P, and O that match with hydroxyapatite, the main component of enamel. In addition, traces of carbon, sodium (Na) and chlorine (Cl) are notable by small intensity peaks. Na has previously been found to be present in enamel (Naujoks et al., 1967), but could also be the result of salt (NaCl) or sodium carbonate (NaC) intake, among many other explanations due to its high natural availability.

6.5.2 Sample 4084-3-5

This sample is the lower left second premolar from individual S4084 V1086 (see also Figure 5.5), a young middle adult female with a combination of suggestive and treponemal-specific lesions throughout the skeleton, which resulted in a score of 5. In total, eight measurements were taken, five on calculus, one on root cementum, and two on enamel. Figure 6.27 shows the SEM imaging and EDX spectra for four of these measurements, one on cementum, two on calculus, and one on enamel.

The analysis of the cemental surface (Figure 6.27; Spc_001) shows that high amounts of Ca, P, and O are present, which is consistent with the natural composition of cementum. Additionally, some traces of Fe, Mg, Al, Si, Na, and C can be discerned from the spectrum, suggesting a slightly more complex elemental composition than the cementum of sample 4008-1-5, as the instrument settings are identical for the two measurements.

The analyses of dental calculus were conducted of areas (e.g. Spc_002) and specific spots (e.g. Spc_005). Measurement Spc_002 shows a similar elemental make-up as the cementum, but with the inclusion of K and relatively higher levels of Al and Si. Measurement Spc_005 was taken of an optically lighter particle situated on the calculus' surface, and its spectrum is radically different from the usual matrix. It shows the expected presence of O, P, Si, Ca, and Al, but also lanthanum (La) and cerium (Ce), among traces of K, C, and Fe. The addition of La and Ce is likely to stem from naturally occurring minerals (Kloprogge et al., 2020, p. 652).

Spc_007 shows the analysis of the enamel surface, which elemental composition appears to be almost identical to that of the enamel surface from sample 4008-1-5.

In addition to these analyses, this sample was used to conduct a map analysis on an area of calculus, which is a type of measurement that creates unique images for each element identified in the sample and showcasing their distribution (Figure 6.28). This map analysis showed the presence of high quantities of Ca, O, and P, which is expected as different calcium phosphate crystals, such as hydroxyapatite, form the principal component of dental calculus (Aghanashini et al., 2016, p. 43).

Another prevalent element is silicon (Si), which could be the result of clay stuck to the calculus' surface. Furthermore, it shows the relatively wide-spread presence of aluminium (Al), zirconium (Zr), and kalium (K), as well as the more concentrated presence of iron (Fe), magnesium (Mg), and carbon (C), which is localized in one particle.

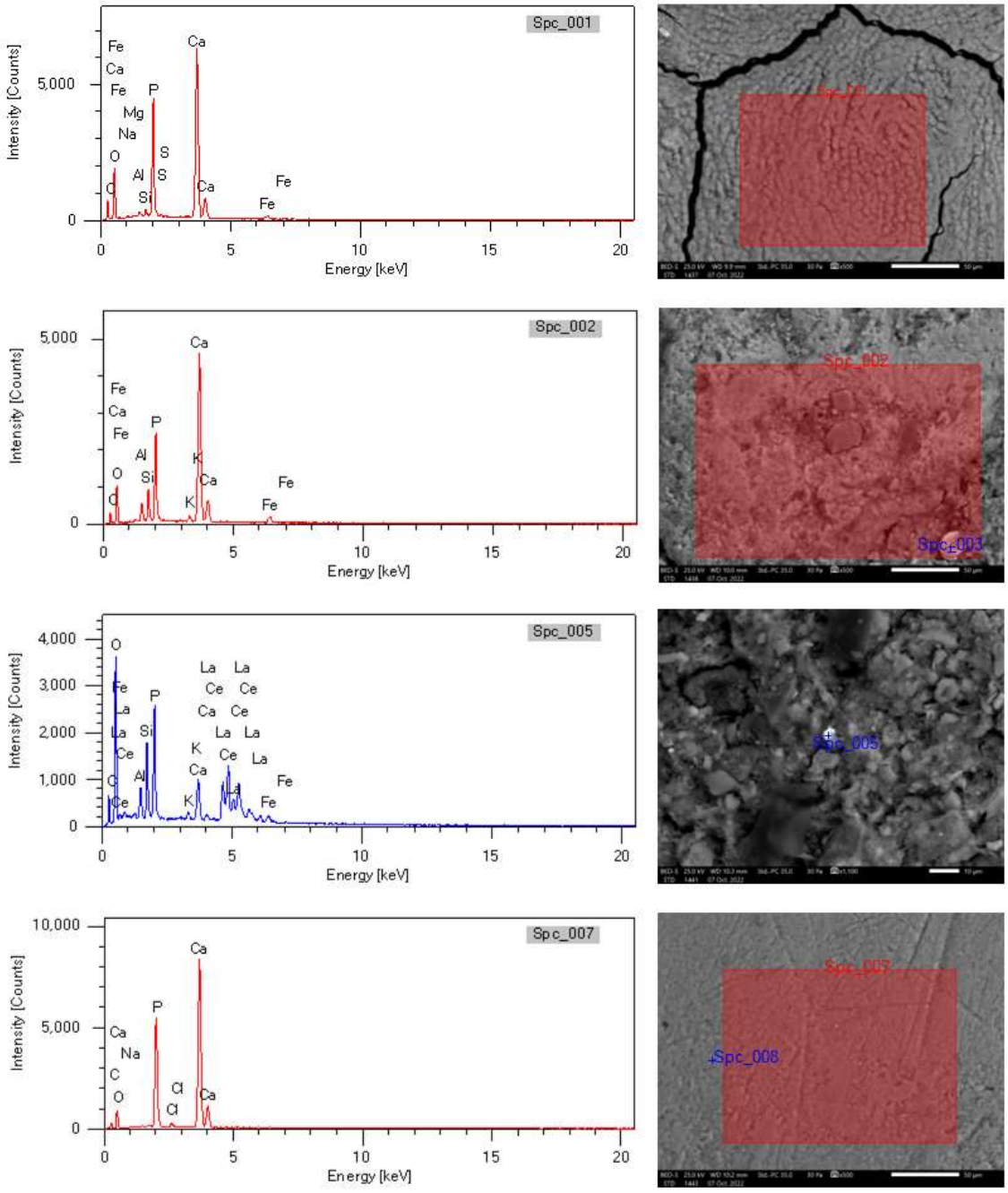

Figure 6.27: SEM-EDX images and spectra of four measurements of sample 4084-3-5.
Spc_001 (top) shows analysis of the cemental surface (magnification = x500);
Spc_002 and Spc_005 (second and third) show analyses of the calculus surface (magnification = x500) and a specific particle (magnification = x1100);
Spc_007 (bottom) shows the analysis of the enamel surface (magnification = x500).
Imaging and spectra provided by Ineke Joosten

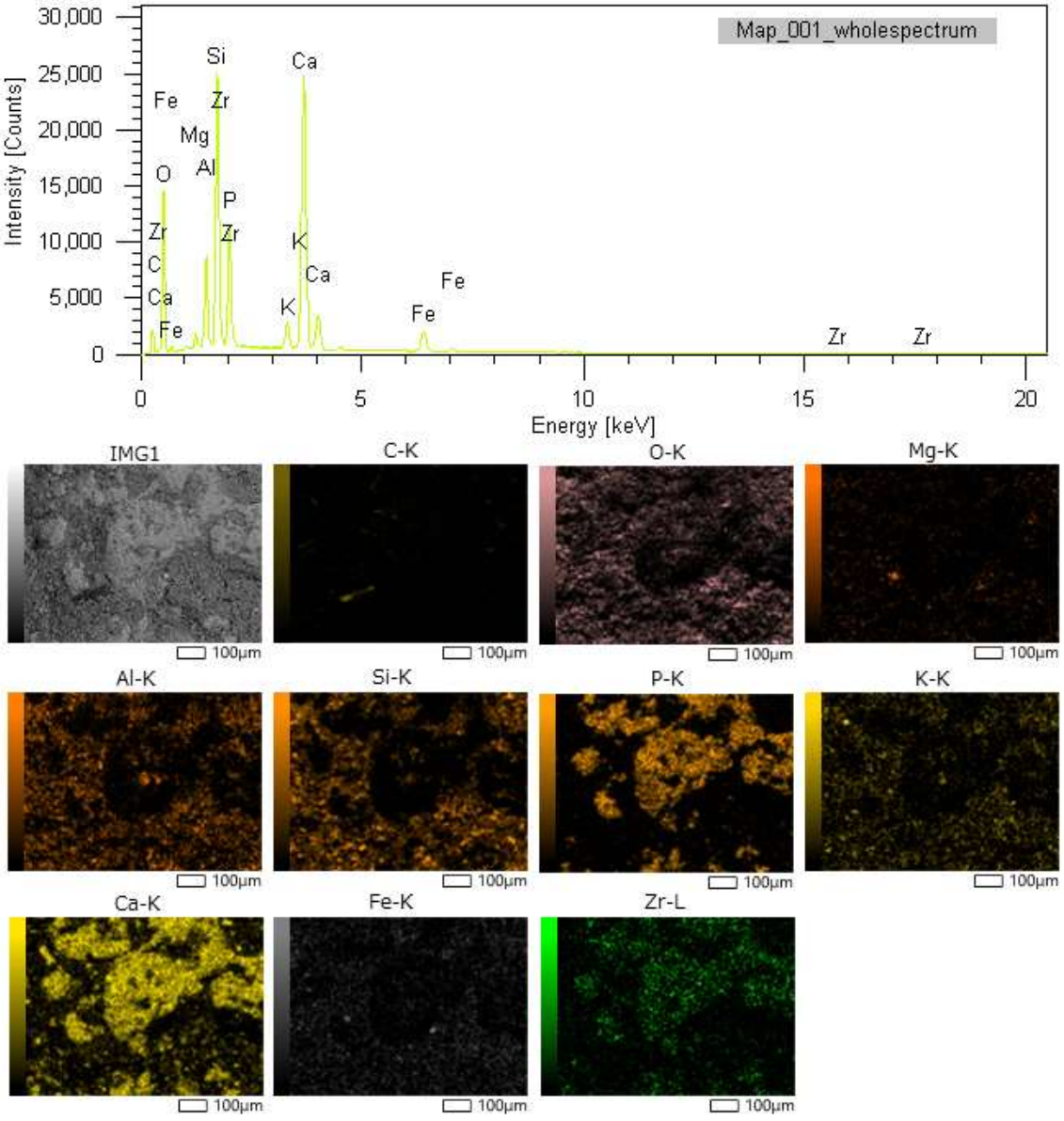

Figure 6.28: SEM-EDX map analysis of 4084-3-5 calculus. The spectrum (top left) and different maps show the distribution of different elements within the calculus matrix (original image top right). Imaging by Ineke Joosten.

6.6 Summary

The various methodologies paint a complex picture, so prior to discussing and contextualizing these results further, a small summary is necessary.

The osteoarchaeological analysis demonstrates that acquired treponemal disease, likely to have been venereal syphilis, is more prevalent in the assemblage of St. Gertrude's infirmary than previously thought, with a true prevalence of diagnostic treponemal infection of 6.3% and 11.4% for individuals with multiple suggestive and/or one or more diagnostic treponemal lesions. The majority of specific lesions are present in the form of nodes with superficial cavitations/gummatous lesions, whereas

diagnostic caries sicca is only observed in two cases. Most of these individuals are affected bilaterally and extensively throughout their skeleton. No signs of congenital syphilis or mercury poisoning were recorded.

The archival research was unsuccessful in gaining more insight into the precise healthcare provisions at St. Gertrude's infirmary, as most records re of a financial nature, but do not specify medicinal purchases. However, two medical reports from 1779 mention the use of mercurial medicine as a remedy against an ongoing disease outbreak and as an over the counter treatment in one of the city's pharmacies. While the author of the letters clearly disapproves of the heavy use of these medicine, it may signify a wider distribution and application of mercury in the city of Kampen during this time period. However, no direct evidence for mercury treatment at St. Gertrude's infirmary was indicated by these records.

In order to investigate whether the individuals from St. Gertrude's cemetery were subjected to mercurial treatments, three trace-element analytical techniques are deployed.

While the pilot pXRF study was useful for determining the most efficient settings with which the final pXRF study could be performed, this final analysis did not result in the identification of Hg values above the detection levels of the pXRF instrument, which therefore cannot be quantified into ppm units. While the Hg emission values are very low, some descriptive statistics and significance testing can still be performed. No statistically significant differences were found when comparing various groups, but there seems to be a tendency of higher mean Hg emissions in non-pathological bones when compared to pathological bones (treponemal score 2 or higher). This observation is most evident for ribs. Additionally, soil samples from the excavation site appear to return somewhat higher Hg emission values than bones.

Overall, the Hg emission values are relatively low and have little variation when compared to other elemental emission values. Notably, no measurement of the pXRF analysis shows uniquely high peaks in Hg emission values.

The ICP-MS analysis does report absolute quantification of Hg concentrations in bone, which ranges from 0.06 ppm to 1.28 ppm. In the comparison between cortical and trabecular bone samples, trabecular samples yield a slightly higher Hg concentration for most, but not all, individuals. Similar to the pXRF analysis, there seems to be higher levels of Hg in non-pathological bone in comparison to pathological bone. However, the selective sampling and small sample size does restrict statistical evaluation of this interpretation, and as such it cannot be further substantiated.

The SEM-IDX analysis shows no identification of mercury traces in the analysed dental calculus or other tooth structures. The various SEM-EDX analyses have resulted in the identification of compositional

elements that naturally occur in dental calculus, root cementum, and enamel. In addition, several elements have been identified within the dental calculus that are likely the result of uptake from external sources. Besides Pb, Zr, La, Ce and Fe in the previously described samples of 4008-1-5 and 4084-3-5, other measurements yielded identification of particles containing titanium (Ti), chromium (Cr), tin (Sn), barium (Ba), and sulphur (S) (see Appendix 4).

7. Discussion

The combination of osteoarchaeological and archival research, coupled with various trace elemental analyses, has produced a multidimensional view of syphilis and its possible treatment with mercury at the site of St. Gertrude's infirmary in Kampen. The primary objective of this discussion chapter is to interpret these various approaches and their findings within the broader context of bioarchaeological research into syphilis and its medieval treatment and to critically analyse their significance.

In order to do so, this chapter first describes the limitations of this study and the necessary considerations before delving into the interpretation of the data. This starts by synthesizing the osteoarchaeological and archival data, after which the various trace elemental analyses are integrated into a comparative analysis and contextualization with other research, to provide a comprehensive interpretation of syphilis and its treatment at St. Gertrude's infirmary during the late medieval and early modern period and help answer each of the research questions in the conclusion chapter. This chapter ends with a discussion of the limitations of this research and future research avenues.

7.1 Limitations and considerations

7.1.1 The osteological paradox

Before interpreting the results from the osteoarchaeological analysis on treponemal disease, the limitations of osteological study need to be laid out. This type of research analyses deceased individuals in order to infer palaeodemographic and palaeopathological data from a once-living population, but such reconstructions do not come without inherent problems. Wood et al. (1992) described three main considerations for osteological studies, together known as "the osteological paradox". The first concept is "demographic nonstationarity", which refers to the continuous change in the demographics of living populations, as influenced by mortality, fertility, and migration (Wood et al., 1992, p. 344). This is especially relevant for this thesis, considering the historical and societal setting of Kampen as an urban trading hub that likely experienced more migration than a regular contemporary Dutch town.

The second concept, known as "selective mortality", notes that the individuals under analysis are not representative of the whole original population, but instead only represent those that succumbed to selective pressures (Wood et al., 1992, p. 344). This is also relevant for St. Gertrude's skeletal assemblage, as the infirmary complex is likely to have housed and subsequently buried people from a very particular societal group: sick and older individuals.

The third concept, known as "hidden heterogeneity in risk", refers to individual variability in susceptibility to disease and death, and that the determining factors for this susceptibility are not

always observable (Wood et al., 1992, p. 344). Together with selective mortality, this entails that a high prevalence of skeletal lesions does not necessarily equate to an unhealthy population. Instead, high prevalence of lesions could demonstrate that the population had the health and means to survive disease for a longer period of time. This is especially relevant when studying treponemal disease, as the skeletal lesions may develop as late as four to five decades after initial infection (Singh & Romanowski, 1999, p. 194).

Taking these factors into consideration, it is unlikely that the skeletal assemblage excavated from St. Gertrude's infirmary is an accurate representation of the general population at Kampen during the late medieval and early modern period, which is further discussed below. As such, alternative interpretations for the prevalence of treponemal disease, accounting for the osteological paradox, should be considered.

7.1.2 Demographic composition

Although the skeletal remains are generally well-preserved and complete, a few notes on the demographic composition of St. Gertrude's infirmary's skeletal assemblage are necessary before proceeding with the interpretation of the prevalence of treponemal disease. As reported previously, this assemblage may not reflect the average late medieval population in Kampen. Schats et al. (2017, p. 242) found the overrepresentation of males in the skeletal assemblage to be statistically significant and, when compared to the infirmary sites in the cities Breda and Delft, it seems that this male overrepresentation was a common occurrence, especially in the case of Breda (Schats & Klomp, 2019, p. 110). It is hypothesized that the abundancy of males may be reflective of the Eighty Years War and the associated casualties among male soldiers, which would correlate with the notion that St. Gertrude's infirmary functioned as a shelter in times of need (van Zanten, 2017, p. 34), but definite conclusions cannot be drawn (Schats & Klomp, 2019, p. 110).

Individuals below the age of four were absent in the skeletal assemblage, and a relatively small number of individuals was below the age of 19. While child mortality was generally high during the medieval period, their absence in this and other archaeological collections is commonly attributed to the relative fragility and the small size of non-adult bones, as well as the possibility that children were laid to rest at different locations. Additionally, it could reflect the general absence of living children at the infirmary site in the past, as sick children may have been brought elsewhere or kept at home to receive care and treatment (Schats, Hoogland, et al., 2017, p. 242).

The wide range between the numbers of young adults and young middle adults in adult males is interesting, especially as a larger number of young adult males would be expected if the male overrepresentation is related to the housing of wounded soldiers (Schats & Klomp, 2019, p. 111).

However, this difference may also be influenced by the fact that the young adult age-at-death category spans fewer years (19-25) than the young middle adult category (26-35), and therefore represents a smaller percentage of the general male population.

For females, the varying frequencies of age-at-death categories are interesting. While childbirth complications offer a generally accepted explanation for higher mortality rates in younger females from regular burial grounds, this was likely to be a minor factor for infirmary sites such as St. Gertrude's (Schats & Klomp, 2019, p. 112). As of yet, no hypothesis except for coincidence has sufficiently explained this situation of female age-at-death distribution.

Lastly, it is important to keep in mind that the cemetery of St. Gertrude's infirmary may represent an estimated time period of roughly 230 years, but it is unknown when the individuals discussed in this thesis were alive and subsequently buried. As such, chronology may be a convoluting factor affecting the interpretation of St. Gertrude's demography, pathology, and treatment, that cannot be controlled for in the subsequent discussion. Additionally, it is likely that the 89 individuals identified through excavation are not representative of the entire cemetery population, as the original cemetery is believed to have covered a larger area prior to partial destruction due to construction in the 1970s (Schats & Klomp, 2019, p. 108).

7.1.3 Mercury in the skeleton: non-therapeutical exposure and diagenesis

When evaluating the possible evidence for the presence of mercury in skeletal samples, the origin of this mercury cannot be inferred from the data itself and should be considered with caution, especially as there is no direct historical evidence of the medicinal use of mercury at St. Gertrude's infirmary. While the focus of this thesis is on the therapeutical administration of mercury to syphilitic patients, other potential sources for mercury incorporation in teeth and bone will be considered here.

Mercury exposure can take place in various ways, such as inhaling mercury containing air, ingesting mercury containing food or water, and touching mercury. The way the body incorporates mercury depends on the specific mercuric forms (Pessanha et al., 2016, p. 27), but in most the cases the mercury is distributed to the central nervous system, kidneys, and brain through the blood circulation (Rasmussen et al., 2020, p. 3; Tchounwou et al., 2003, pp. 154–156). From there, it is distributed via blood cells to the liver, bone marrow, central nervous system, brain, and respiratory tract (Rasmussen et al., 2020, p. 3). During this processes, mercury-enriched blood can deposit the element into the bone structure during the natural remodelling processes of bone. However, it is known that soft tissues initially hold much higher concentrations of mercury compared to bone tissues, due to the slow absorption of Hg into bone. Consequently, high Hg levels in bone are likely to be representative of systematic exposure over a longer period (Emslie et al., 2019, p. 6).

Besides intentional therapeutic use for syphilis, these types of mercury can enter the human body from various sources, such as environmental contamination, occupational habits, and diet. Environmental contamination may occur in environments that are rich in volcanic activity (Walser III et al., 2019, p. 49), but also in environments with increased industrial activities or waste disposal (Tchounwou et al., 2003, p. 152). Since elevated atmospheric Hg levels have mostly been linked to heavily urbanized and industrialized areas (Davis et al., 1997, p. 558), systematic contamination through environmental levels is. unlikely for individuals living in late medieval Kampen, as the region does not contain volcanic activity and the period lacked intensive industrial activities.

Similarly, occupational exposure is heavily associated with increased industrialization, especially the felt industry (Aufderheide & Rodriguez-Martin, 1998, p. 320; Katz & Krenkel, 1972, p. 517), which was not present in Kampen during this time. Other occupational exposure may be linked to cinnabar, which produces the bright orange-red pigment known as vermillion, that was historically used in inks and paints (Carvalho et al., 2009, p. 435). While the coloured pigment was not found during the archival analysis for this thesis, it cannot be ruled out that a few individuals in Kampen occasionally came into contact with vermillion. However, systematic exposure to high doses of vermillion is deemed less likely.

The uptake of mercury through diet can occur through the consumption of seafoods contaminated with methylmercury (Sheehan et al., 2014). Seafood was a likely dietary component for Kampen citizens, which has been substantiated by previous stable isotope analysis (Schats, Kootker, et al., 2017). However, the reported mercury levels in marine and freshwater life mainly come from modern industrial contamination through waste disposal (Tchounwou et al., 2003, pp. 152–153) and given that St. Gertrude's infirmary is a preindustrial complex such external mercury exposure is unlikely.

Besides these potential sources, intentional exposure may have also occurred through mercury-based treatments for ailments other than treponemal infections, as it was used to treat various skin diseases and leprosy (Baker & Armelagos, 1988, p. 707; Demaitre, 2007, p. 264; Karamanou et al., 2013, p. 317). Skeletal signs of leprosy were not found in the assemblage, and its potential presence at St. Gertrude's infirmary is minimized further by the knowledge that Kampen had a specialized facility for the care of lepers: the *Melatengasthuis*. However, skin diseases are generally not recognizable in the skeleton and therefore mercury treatment for such ailments by non-syphilitic individuals cannot be ruled out.

Lastly, mercury in bone may be the result of postmortem exposure through diagenetic processes, during which elements in soil are degraded and diffused into buried skeletal remains. In this thesis, soil samples have been taken to establish an environmental baseline for the soil of the excavation grounds. However, multiple studies have demonstrated a lack of potential diagenetic transfer of Hg from soil to bone after deposition, and diagenesis is generally deemed to not be a factor in mercury incorporation

in bone (Emslie et al., 2019, p. 8; Rasmussen et al., 2015, p. 366; Yamada et al., 1995, p. 255; Zuckerman, 2017, p. 248). While the soil samples used in this thesis were retrieved from a box with commingled remains, these remains were found dispersed within the excavation area, and thus are likely to represent a more average environmental mercury content than soil taken near a specific individual or at a specific location.

7.2 Treponemal disease at St. Gertrude's infirmary

This thesis found osteoarchaeological evidence for treponemal infection, likely to be syphilis, in the skeletal remains from St. Gertrude's infirmary by deploying the scoring system devised by Harper et al. (2011). This part of the discussion aims to further interpret these results using the background knowledge gained in Chapters 2-4, but also to synthesize them with the archival data.

7.2.2 Osteoarchaeological evidence for treponemal disease

No signs of congenital syphilis were recorded during this study. This could be interpreted in relation to the lack of non-adults within the assemblage. As theorized previously, the underrepresentation of non-adults may be the result of preservation issues or lack of living children in St. Gertrude's infirmary. The latter notion is supported by the hypothesis that children were brought elsewhere to receive medicinal care. While the archival data and other sources from Kampen do not shine light on this specific theory, there is an example of such practices in relation to syphilis from late medieval Leiden, where a child born to a syphilitic mother in the *pokhuis* was transferred to the city's orphanage (Ladan, 2012, p. 54).

As for acquired treponemal disease, the true prevalence in the assemblage from St. Gertrude's infirmary cemetery is 6.3% for treponemal score 5. This prevalence is quite high, especially when compared to other sites in the late medieval and early modern Netherlands (Table 7.1). If individuals with multiple suggestive lesions are included, the prevalence would be increased to 11.4%. Taking into account that skeletal lesions only develop in 1-20% of individuals with tertiary stage syphilis (Roberts & Buikstra, 2019, pp. 381–382), the prevalence of the disease may have been much higher than what is reported here. This high prevalence in treponemal disease at the site in Kampen may be explained by several factors inherent to the city's urban setting and historical context. As a key trading hub, situated along various European trade routes, Kampen likely experienced a higher influx of people from diverse and international background, potentially facilitating the spread of infectious diseases. Syphilis specifically was renowned to prevail amongst international merchants and sailors, and was known to be a common occurrence in medieval port cities like Kampen (Koten, 2016, p. 3).

Besides merchants and sailors, military soldiers are accounted amongst frequent distributors of the bacteria (Koten, 2016, p. 3), and it is known that the city has taken in a number of soldiers on at least two occasions during 1588 and 1597 (van Zanten, 2017, p. 34).

Table 7.1:

Overview of the occurrence and prevalence of treponemal disease in various Dutch skeletal collections.

Location	Site	Time period	Treponemal disease		Literature
			n	%	
Kampen	St. Gertrude's infirmary	ca. 1382-1611	5	6.3	-
Haarlem	Botermarkt	15th century	2	4.3*	(Groot, 2013)
Den Haag	St. Jacob's Church	15th century-1681	2	4.0	(Pavlović et al., 2021, p. 186)
Hattem	Urban cemetery	17th-19th century	1	±1.1*	(Pavlović et al., 2021, p. 203)
Eindhoven	St. Catharine's Church	1650-1850	2	1.0	(Arts, 2019, p. 60)
Breda	Infirmary	13th-17th century	2	0.7	(de Jonge & Baetsen, 2013, p. 241)

**This prevalence rate is not reported in the literature, but has been calculated on the basis of the total number of individuals, thus may not reflect the true prevalence.*

Another factor could be the rapid population growth and subsequent overcrowding within Kampen during the 14th and 15th centuries. The city's population density is estimated to have been 173 to 240 citizens per hectare at the beginning of the 15th century. While this seems low for modern standards, the average population density for late medieval Dutch cities of a similar population size has been estimated to be 81 citizens per hectare (Kolman, 1990, p. 147).

Additionally, many agricultural spaces, such as stables and vegetable gardens, were situated within Kampen's city walls (Kolman, 1990, p. 150), which may have severely restricted the available living space for residents. These factors are likely to have contributed to small living spaces and an unhygienic environment that has a high potential to encourage the spread of disease (Roberts & Manchester, 2010, p. 173). This situation may have been exacerbated during times of military unrest, such as the two sieges of Kampen in 1572 and 1578 (Speet, 1986, p. 25).

The prevalence rates reported above do not reflect the large proportion of individuals from Kampen that express lesions consistent with treponemal disease, most notably periosteal new bone formation (PNB). Many individuals in this assemblage show PNB that takes on a diffuse and bilateral character, which could signify an underlying systemic infection or widespread inflammatory response (Rothschild, 2005, pp. 1454–1455; Schats & Klomp, 2019, p. 113). However, interpreting the potential aetiology of PNB remains an intricate matter, and, therefore, it is not feasible to definitively assert that these individuals suffered from chronic infection, much less treponemal disease specifically (Weston, 2011,

p. 507). Consequently, the remainder of this discussion will focus on those individuals with osseous lesions suggestive or diagnostic for treponematosis.

For the six individuals with one or more diagnostic lesions, caries sicca was present in only two. The relative rarity of diagnostic caries sicca is noteworthy, but may be explained by the absence of crania for some of these individuals. Nonetheless, it suggests that postcranial gummatous lesions were more common manifestations of syphilis in this population, as all individuals with score 4 or 5 displayed a node with superficial cavitation, or gummatous lesion, in one or more long bones. For those who were accredited with a score of 5, the widespread distribution and bilateral presentation of this type of lesion further established the treponemal diagnosis. Moreover, many others of St. Gertrude's skeletal remains exhibited various nodes and expansions of the bone as described by Hackett (1976) that supported a possible treponemal diagnosis in absence of diagnostic lesions. In a few of the analysed individuals, the extensive nature of the lesions must have had severe implications on their general health and wellbeing. Additionally, given that skeletal changes are not the only symptom of tertiary syphilis, the seriously debilitating symptoms stemming from other syphilitic syndromes, such as cardiovascular and neurosyphilis, must also have had a great effect on the wellbeing of these and possibly other individuals. These individuals may have been part of the inhabitants known as *proveniers*, and their stay at St. Gertrude's infirmary may have been a last resort where they received care until their death.

When examining the presentation of diagnostic and suggestive treponemal lesions between the sexes (Table 6.4), these lesions are more frequently found in females. As noted previously, the absolute numbers do not differ much, but still this trend could be interpreted as a result of a difference in the response of both sexes to the infection. In general, females are considered to have a more effective and robust immune response to many infectious diseases, whereas males are more often affected by skeletal diseases (Ortner, 1998). In the case of gummatous syphilis, which is responsible for skeletal changes, it has been reported that a higher proportion of the affected individuals are of female sex. The other third stage syphilitic syndromes, namely neurosyphilis and cardiovascular syphilis, occur in a higher proportion of males.

Additionally, syphilis' mortality is reportedly two times higher in males than females (Clark & Danbolt, 1955, p. 338; Singh & Romanowski, 1999, p. 191). The majority of syphilitic skeletal manifestations stem from a osteological response to soft tissue lesions or syndromes and therefore may take substantial time to develop or fail to develop at all. As a result, the higher prevalence of diagnostic and suggestive lesions in Kampen's females may reflect chronic skeletal change as a result of long-term survival of the treponemal infection (Roberts & Manchester, 2010, p. 173), whereas males may have succumbed to the infection before tertiary lesions had the time to properly develop in the skeleton.

However, considering the relatively small and selective sample size of St. Gertrude's assemblage, the small proportion of syphilitics actually experiencing osseous changes (1-20%) (Roberts & Buikstra, 2019, pp. 381–382), and the broad range of other extrinsic factors that could result in differences of bone involvement (Roberts & Manchester, 2010, p. 173), this observation cannot be positively confirmed with the available data.

When studying the distribution of treponemal infections among different age groups (Table 6.5), the proportion of mature adults with suggestive and/or diagnostic treponemal lesions is notably lower than any of the other age categories. This is interesting, as most skeletal changes due to syphilis only arise during the last stage of the infection, up to 46 years after secondary stage symptoms have been resolved. The retrospective autopsy research by Rosahn and Black-Schaffer (1943) has previously shown that 79% of those with syphilitic tissue lesions (both bone and soft tissue) are between 40 and 70 years of age at death, whereas those between 20 and 40 years of age constitute only 11.8% of individuals with syphilitic tissue changes (pp. 597-599). On this basis, one would expect that the mature adult age group would produce the highest proportion of skeletal changes, and the young adult age group would produce the lowest proportion of treponemal lesions, as these individuals would likely still experience the primary or secondary stage symptoms if indeed infected.

In order to compare the observations by Rosahn and Black-Schaffer (1943) and understand whether this hypothesis is corroborated by St. Gertrude's assemblage, the data from Table 6.5 needs to assessed per age category, instead of per treponemal score, which is shown in Table 7.2. Sorting the proportion of treponemal scores for each age group demonstrates that in case of the multiple suggestive lesions (score 3) the highest prevalence is attributable to mature adults. However, in the case of score 4 and 5, the highest prevalence is attributable to the younger and older middle adults.

Table 7.2:

Overview of the occurrence and prevalence of treponemal scores per age-at-death category.

Age-At-Death	Score 0		Score 1		Score 2		Score 3		Score 4		Score 5	
	n	**%**	***n***	**%**	***n***	**%**	***n***	**%**	***n***	**%**	***n***	**%**
13-18 years	1	6.7	3	8.8	0	0	1	33.3	0	0	1	20.0
19-25 years	2	13.3	7	20.6	1	33.3	0	0	0	0	1	20.0
26-35 years	5	33.3	8	23.5	0	0	0	0	0	0	2	40.0
36-45 years	5	33.3	10	29.4	2	66.7	0	0	1	100	1	20.0
45+ years	2	13.3	6	17.6	0	0	2	66.7	0	0	0	0
Total	15	100	34	100	3	100	3	100	1	100	5	100

Interestingly, two older adolescents also exhibit multiple suggestive and/or diagnostic skeletal lesions. While the development of tertiary lesions before adulthood is rare, their presence may be explained by the fact that these lesions can develop already one year after the secondary stage is resolved.

Taking these different perspectives into consideration, this complex pattern of age-at-death and treponemal lesions may be explained by the small sample groups, resulting in large prevalence differences due to a small difference in absolute numbers affected.

7.2.3 Archival evidence for syphilis

Besides osteoarchaeological study into treponemal disease at St. Gertrude's infirmary, archival research was performed to investigate the historical references of syphilis and/or its treatment in late medieval and early modern Kampen. While the osteoarchaeological research convincingly indicates the presence of syphilis in multiple individuals, the disease was not mentioned in the analysed records, illustrating the importance of a disease's osteoarchaeological visibility for identification and recognition in a historical context. The absence of corresponding historical documentation may be explained in various ways. Firstly, it may simply be the case that medical recordkeeping was limited or deemed unimportant by recordkeepers in Kampen. The prioritization of other matters such as financial records may have overshadowed the upkeep of detailed medical accounts (Mitchell, 2017, p. 90). This hypothesis is supported by the general lack of explicitly named diseases, except for a singular reference to the "*grasseerende ziekte*" in Dr. Van Geuns' medical letter dated 1779.

This letter is illustrative for an academic report on the origins, symptoms, and treatments of a specific disease and showcases Van Geuns' contemporary scholarly reasoning. It shows a standard practice in which such medical reports were primarily generated by qualified medical practitioners, such as the *pokmeesters* or *doctor medicinae*, at the behest of local authorities, in this case the mayor (McVaugh, 2006, p. 17, as cited in Mitchell, 2017, p.89). This practice could have limited other types of comprehensive medical documentation, such as routine recordkeeping at sick wards. In the case of St. Gertrude's infirmary, it is unknown whether a *doctor medicinae* or other academically trained medical staff was employed, although the lack of medical recordkeeping seems to suggest this.

Alternatively, the lack of references to syphilis could be attributed to the stigma and societal taboo associated with venereal infections (Tampa et al., 2014, p. 4), as recordkeepers may have purposefully omitted mentions of the ailment to protect individuals' privacy and avoid social shame. As syphilis was considered a "divine punishment" (Plagens-Rotman et al., 2021, p. 552), the religious ties of medieval infirmaries (Ladan, 2012, p. 72) like St. Gertrude's may have prevented the recording of these diseases.

Moreover, historic medical terminology may have obscured references to syphilis. As mentioned in section 3.1, syphilis was known by various names, and while the archival research was performed with a plethora of alternative names for syphilis and mercury kept in mind, the disease may have been documented under regionally-specific nicknames (Mitchell, 2017, p. 89).

Alternatively, recording disease in the medieval period may have been hindered by a lack of accurate recognition and diagnosis. However, since the records from St. Gertrude's infirmary seem to be lacking explicit reference to any one disease, these two explanations appear less supported within this particular context. Lastly, to follow the well-known idiom "absence of evidence is not evidence of absence", it remains plausible that the medical records of St. Gertrude's infirmary have been lost or degraded throughout time.

7.3 The use of mercury

The presence of treponemal disease, likely attributable to venereal syphilis, has now been established for the skeletal collection excavated from St. Gertrude's infirmary in Kampen. As described in Chapter 3, mercury was a commonly used anti-syphilitic agent in late medieval and early modern Europe. Archival research provided a few insights into possible medical practices involving mercury in the city of Kampen during the second half of the 18th century. Mercurial medicine was documented to be used as a remedy during a disease outbreak in 1779 and was noted to be an over-the-counter treatment in one of Kampen's pharmacies. Especially the report on Kampen's pharmacies (Figure 6.14) indicates that mercury was a relatively common or easily attainable substance, potentially implying that mercury was an already established remedy. Interestingly, both documentations do not relate mercury to syphilis or any other specific disease, which may indicate that the substance was used for various health issues and as a general purgative instead of a syphilis-specific treatment. However, it should be noted that both mentions are brief and do not provide any context of the application of these remedies.

Another important note is the timespan of these historical references to mercury and the burial ground at St. Gertrude's infirmary. The historical context of the two reports raises the possibility that mercury may already have been used as a medical treatment during earlier periods, such as the 1400-1600s during which the individuals buried in St. Gertrude's cemetery are believed to have lived. However, there is a notable gap of at least 168 years between the writing of these records and the likely closure of the cemetery. Consequently, while interesting, this archival research cannot confidently corroborate the use of mercury at St. Gertrude's infirmary. Instead, direct evidence for mercury uptake by individuals is required to investigate the potential use of mercury at the infirmary during the late medieval and early modern period.

7.3.1 Portable X-Ray Fluorescence Spectrometry

To further investigate mercury treatment, three types of trace elemental analyses were deployed to analyse the presence of mercury within the osteoarchaeological remains. The pXRF analysis aimed to detect and quantify mercury levels in the skeletal remains. The data was internally calibrated by normalization on rhodium, or the Compton Peak, which reduces matrix effects and can illuminate data in the lower ppm ranges (Shugar & Mass, 2013, p. 30). Despite this, the results indicate very low emission values that were near or below the instrument's detection limit, which restricts the quantification of absolute mercury concentration in the bone on a ppm level. As such, subsequent observation requires a balanced interpretation of the reliability of the data, as emission values close to the detection limit can be influenced by various sources of background scatter, making it challenging to distinguish between true mercury signals and background noise.

In comparison with the other elemental emission values generated by the pXRF study, one notable trend is the generally low and consistent Hg emission values observed across all analysed bones. Other elemental emission values returned uniquely high peaks of counts, whereas this cannot be said for Hg, indicating that mercury uptake may have been minimal for each sampled individual, regardless of their health status, sex, age, or period of living. If this hypothesis is explored in more depth, the absence of clear peaks in Hg emission values compared to other elements raises questions about the meaningfulness of the measured values. It may signify that all of the measured counts for Hg actually represent background scatter and not actual mercury contents within the bone. Unfortunately, this hypothesis cannot be disproven with the data gathered in this study, nor can other studies shed a light on this. Zuckerman (2016; 2017) has performed two similar experiments that have resulted in quantified, but not absolute, emission values of Hg, but these cannot be linearly compared to the data in this thesis due to inter-instrumental and inter-laboratory variability (Drake et al., 2023, p. 83). However, it is likely that the results reported by Zuckerman (2016; 2017) also represent compositions that are on the very edge of quantifiable data, i.e. less than or between 1 to 5 ppm.

Keeping this in mind, some patterns and tendencies can still be observed in the data. When comparing emission values between different bones, femora and humeri express similar emission patterns, whereas ribs show higher variability and maximum Hg values. This could indicate possible antemortem uptake of mercury in the ribs of certain Kampen individuals. Given that ribs have a higher proportion of trabecular bone, this trend may reflect higher Hg concentrations in trabecular tissues. This hypothesis is supported by trends found in other studies (Rasmussen et al., 2008, 2013, 2015, 2017) and could be interpreted in two ways. Firstly, considering that mercury is mostly stored in soft tissues during life, the presence of Hg in trabecular tissue may be the result of postmortem decay of the soft tissue. The Hg content of soft tissues may be subsequently deposited onto the trabecular tissue instead

of the cortical tissue, as trabecular bone incorporates more soft tissue (e.g. blood vessels and bone marrow) and has a greater surface area due to its structure (Rasmussen et al., 2013, pp. 9–10).

Alternatively, higher levels of Hg in the trabecular tissue of the ribs than cortical tissue of the long bones could resemble antemortem Hg uptake close to the time of death (Rasmussen et al., 2013, p. 10). This is related to the overall difference in bone remodelling rates of trabecular and cortical bone, with trabecular bone generally having faster turnover (Lee & Einhorn, 2001, as cited in Ruimerman, 2005, p. 3). As a result of this higher turnover rate, trabecular bone is quicker in incorporating elements present in the soft tissue, whereas cortical bone will be slower to incorporate these elements, acting as a longer-term reserve instead (Zuckerman, 2017, p. 249). Therefore, individuals with higher Hg emission values in ribs may have been exposed to mercury close to their time of death. This interpretation will be explored further when incorporating treponemal scores in the discussion.

While the median of the Hg emission values in ribs does not differ much from those for femora and humeri and consequently does not seem to corroborate these explanations, it should be noted that not all sampled individuals may have had increased mercury levels.

In addition to these hypotheses, I would like to propose an additional interpretation for the seemingly increased values in some rib samples that concerns the practical application of pXRF. In an ideal setting, XRF samples are infinitely thick to X-rays and of a homogenous make-up, but this is not possible for many archaeological materials (Shugar & Mass, 2013, p. 28). For this thesis, there is a definite difference between ribs and long bones in bone matrix and depth of the cortical layer. Others have estimated that the pXRF reaches the upper 5 mm of cortical tissue (Zuckerman, 2017, p. 245). While the first rib sampling location (Figure 5.2) has an average of 0.9 and 2.6 mm cortical thickness, this drastically decreases to a thickness as low as 0.1 mm at the sternal end (Holcombe et al., 2019). As a result, the XRF measurements of ribs are likely to include trabecular tissue, which is also noted above. However, trabecular bone has an irregular surface, porosity, and probable contamination of soil, which all can influence the analytical performance (Byrnes & Bush, 2016, p. 1042). As such, the variability of Hg emission values observed in ribs may just be influenced by the variability of the cortical thickness between samples and sample locations, or the variability in density of the trabecular bone tissue.

Another trend emerges from the comparison between the Kampen femoral samples and control samples, with slightly higher median emission values in the former, but this difference is clouded by the high variability within the control group and is found not to be statistically significant.

The examination of the relation between Hg emission values and osteoarchaeological treponemal scores also shows an interesting trend. Non-pathological (score 0-1) samples were compared with pathological samples (score 2-5) for femora and ribs. Interestingly, both bones showed a tendency of

higher median Hg emission values in the non-pathological group compared to the pathological group, while neither of these relationships are deemed statistically significant. When dividing the femoral measurements into each treponemal score, this trend of decreasing Hg values with increasing disease score seems to be supported, although yet again no statistical significance was determined.

These observations can be interpreted in many ways. Firstly, higher Hg values in the non-pathological group may be the result of unintentional mercury intake unrelated to treponemal infection, such as environmental, occupational, or dietary exposure as described in section 7.1.3. A second interpretation could be the intentional uptake of mercury by the non-pathological group, for example to treat skin diseases. Thirdly, keeping the osteological paradox in mind, hidden heterogeneity in risk may be at play, as the individuals without lesions may have succumbed earlier and thus had no time to develop the skeletal lesions. Considering that syphilis is not often fatal (Tucker, 2007, p. 223) the intake of toxic mercury could be one of the reasons that they died earlier than their peers who received no treatment during any phase of their disease trajectory. This phenomenon of higher Hg in non-pathological individuals was also observed in the ICP-MS data, and as this can be more accurately compared to other studies, a more in-depth interpretation and contextualization will be provided later.

Lastly, the comparison of mean Hg counts between treponemal lesions and control locations indicates subtle differences for a few individuals. Most notably, S4013 V1008, which was given a treponemal score of 5, showed higher Hg counts in the measurements of treponemal lesions compared to controls. The lesion measurements were taken on the left tibia and left fibula, with the tibial Hg emission values being particularly high at $12.99E^{-3}$. This measurement was taken on a patch of striated new bone, located on the posterior aspect of the distal shaft. The control location on the same bone measured $3.20E^{-3}$, which may reflect the topical application of mercury on the lesion and subsequent local uptake through the lesion. This hypothesis is supported by previous findings in a Danish individual, who showed elevated mercury levels on treponemal lesions (Rasmussen et al., 2015, p. 366). However, the type of lesion challenges this interpretation, as a patch of striated new bone does not necessarily correlate to gummatous lesions in the soft tissue, on which mercury ointments were usually applied.

In conclusion, while this data provides valuable insights into potential mercury exposure in Kampen, the interpretation is riddled with complexities. The limitations of detection sensitivity, instrument noise, and small sample sizes hinder the ability to draw definitive conclusions about mercury presence and its significance. Considering the small absolute difference between Hg emission values and the lack of statistical significance, the observed trends are more likely to be caused by chance variations and may not be representative of an actual difference in antemortem mercury exposure. The limited sample size and lack of variability in emission values when compared to other elements complicate definitive conclusions, and the observed trends may not hold true in a larger, more diverse dataset.

7.3.2 Inductively Coupled Plasma-Mass Spectrometry

The third trace elemental analysis conducted for this study is that of ICP-MS. The aim of this study was to establish absolute and precise concentrations of Hg in various bone samples, to see whether elevated mercury levels in certain individuals or certain bone types can be distinguished.

While no statistical testing was conducted on the samples, several trends are notable. Firstly, the majority of trabecular bone samples have a slightly higher Hg concentration than cortical bone samples. A similar trend was observed in the data from the pXRF study, in which ribs showed slightly higher Hg emission values than femora and humeri, and in various other studies (Rasmussen et al., 2008, 2013, 2015, 2017). Since the trabecular samples for ICP-MS were also selected from ribs, a similar interpretation arises: either a trace amount of Hg was present in the soft tissues and deposited onto the trabecular bone postmortem, or Hg is the result of antemortem exposure close to the time of death, through for example mercury treatment (Rasmussen et al., 2017, p. 96).

Two individuals (S4033V1032 and S4084V1086) form an exception to this trend, and demonstrated higher Hg levels in cortical than trabecular bone. Such a distribution may have resulted from exposure to Hg earlier in life, as cortical bone preserves the element for longer periods than soft or trabecular tissues (Zuckerman, 2017, p. 249) due to the slower bone remodelling rates of cortical bone (Rasmussen et al., 2015, p. 365). Considering that these individuals both showed extensive skeletal lesions suggestive and diagnostic of tertiary stage treponemal disease, they may have been treated with mercury during the first or second stage of the disease, but refused or sought out other treatment methods during the latest stage of the disease. This is supported by the hypothesis that mercury treatments were most frequently used to treat the dermatological lesions of the first and secondary stages of the infection (Zuckerman, 2017, p. 250). This is also consistent with other studies which have found that younger adults (<36 years) to generally yield higher Hg concentrations in bone than older adults (>35 years) (Walser III et al., 2019, pp. 52–55; Zuckerman, 2016, p. 51).

Additionally, the ICP-MS results demonstrate that non-pathological samples (score 1) have much higher Hg concentrations in bone than those with extensive pathological lesions (score 2-5), a trend that is also observed in the pXRF data. Interestingly, studies on Hg levels in other skeletal collections have reported similar findings. Tucker (2007) conducted ICP-MS analysis on various skeletal remains from post-medieval London, and detected a number of individuals with highly elevated mercury levels ranging from 14.87 to 17.24 ppm. However, their skeletal remains did not show extensive and severe skeletal changes, and the author suggests that the mercury may indeed have resulted in reducing bone involvement (p. 223). Walser II et al. (2019) found another individual with treponemal lesions but an extremely low mercury concentration of 0.069 ppm (p. 56). They add to Tucker's (2007) original hypothesis that the individual may have rejected mercury treatment, died before treatment could be

administered, or died during treatment from complications or another unknown condition (Walser II et al., 2019, p. 56). Alternatively, the non-pathological group may include individuals that were exposed to mercury through the preparation and administration of the treatment to syphilitic patients (Rasmussen et al., 2020, p. 3), although they would only make up a small part of the assemblage.

Contrary to the pXRF and SEM-EDX results, the Hg concentrations gleaned from the ICP-MS analyses can be evaluated on whether they represent elevated, abnormally high concentrations or whether they constitute background levels. Rasmussen et al. (2015, pp. 365-366) estimated thresholds of background levels of Hg in archaeological femora from Denmark and Northern Germany, with the threshold being 0.3 ppm for trabecular and 0.08 ppm for cortical tissues. Following this study, other studies have taken these values as established background levels (Biehler-Gomez et al., 2022, p. 507; Forbes et al., 2022; Rasmussen et al., 2020, p. 3), or have adapted them to be more considerate of local environmental conditions (Walser III et al., 2019, p. 51). If we apply these background levels to the analysed samples, only three samples would fall below these thresholds, with the remaining samples showing elevated mercury levels (Table 7.3). This would suggest that external mercury exposure would have been a regular occurrence at St. Gertrude's infirmary during the late medieval and early modern period, either through mercury treatments or through non-therapeutical factors.

For two of the three individuals with Hg concentrations that fall below the elevation threshold, other locations did yield elevated Hg concentrations. The cortical Hg levels for S4019V1018 were the lowest concentration of the whole study, but the trabecular tissue showed elevated Hg levels, possibly caused by mercury intake weeks to years prior to the individuals death (Walser III et al., 2019, p. 58). In the case of S4033V1032, the opposite is true, as cortical Hg levels were well above the elevation threshold of 0.08 ppm, whereas the trabecular levels were within background range. As discussed above, this may indicate that the individual was exposed to mercury earlier in life rather than the last few years, as the Hg was largely removed from the trabecular tissue, yet still preserved in the cortical tissue.

For the third individual (S4068V1071), only a trabecular sample was taken, which resulted in the lowest Hg concentration of trabecular tissues in this analysis. This individual retrieved treponemal score 4 and exhibited one diagnostic gummatous lesion on the left fibula, in combination with striated periosteal new bone on both tibiae. The individual was an old middle adult female, which could support the hypothesis that if she received mercury treatment, it may have been much earlier in her life. In this case, the Hg may still be present in the cortical tissues, but has been completely removed from the trabecular tissues through normal bone turnover. However, it is also very likely that this individual was not exposed to any mercury at all, and on the basis of this data a definite conclusion cannot be drawn.

Table 7.3:

Overview of ICP-MS results, with concentrations deemed to be elevated according to estimations by Rasmussen et al. (2015) marked in red. Elevation threshold is set at 0.3 ppm for trabecular and 0.08 ppm for cortical bone.

Feature and find no.	Treponemal score	Type of bone	Sample location	Hg concentration in ppm
S4011 V1012	1	Trabecular	Right rib 4, sternal end	0.71
S4019 V1018	1	Trabecular	Right rib 3, sternal end	1.28
S4019 V1018	1	Cortical	Left femur, cortical sample just inferior to trochanter minor	0.06
S4040 V1041	2	Trabecular	Unidentified rib fragment	0.31
S4096 V1100	2	Trabecular	Left rib 6 or 7, sternal end	0.63
S4027 V1028	3	Trabecular	Right rib 6, sternal end	0.48
S4068 V1071	4	Trabecular	Right rib 8, sternal end	0.20
S4008 V1003	5	Trabecular	Right rib 5, sternal end	0.52
S4008 V1003	5	Cortical	Left femur, posterior cortical fragment from distal diaphysis	0.26
S4008 V1003	5	Cortical	Right parietal, approx. 3 cm above squamosal suture	0.18
S4013 V1008	5	Trabecular	Right rib 7, sternal end	0.64
S4033 V1032	5	Trabecular	Left rib 4 or 5, sternal end	0.26
S4033 V1032	5	Cortical	Left scapular body	0.53
S4045 V1049	5	Trabecular	Right rib 6, sternal end	0.54
S4084 V1086	5	Trabecular	Right rib 8, sternal end	0.33
S4084 V1086	5	Cortical	Right scapular body	0.51
S4084 V1086	5	Cortical	Left parietal, fragment from temporal line	0.17
KM14 Soil 1	N/A	N/A	N/A	0.52
KM14 Soil 2	N/A	N/A	N/A	0.51

However, before concluding that the majority of these samples show elevated mercury, the applicability of the elevation threshold for this skeletal assemblage must be critically evaluated, even though it has been applied as a firmly established threshold by other studies. Rasmussen et al. (2015) originally established the thresholds by selecting rural and relatively isolated populations and determining that 95% of the individuals in these populations were unlikely to have been exposed to abnormal Hg levels in any way at any time (pp. 365-366). In doing so, they generated a population- and

criterion-specific elevation threshold, which has now been applied to other skeletal assemblages from various other geographical areas and historical periods (Biehler-Gomez et al., 2022; Forbes et al., 2022; Rasmussen et al., 2020; Walser III et al., 2019). However, to accurately apply such elevation standards to other skeletal remains, one would need to reproduce a similar population-, period-, and location-specific threshold. Considering the selective nature and small sample size of this ICP-MS analysis, establishing a population-specific threshold is not reproducible for this thesis. Even then, the elevation threshold would be created by drawing an arbitrary boundary that is not based on actual local and time-specific background levels of Hg.

Additionally, the application of these thresholds in this thesis is complicated even more by the results of the soil sample analyses, which both indicate that the local environmental Hg concentrations are above the elevation thresholds established by Rasmussen et al. (2015). Taking this into consideration, it should be concluded that while the ICP-MS data for this thesis is particularly useful for gaining more insight into the possible exposure to mercury at St. Gertrude's infirmary, it cannot be used to establish which individuals have abnormal, above background, levels.

7.3.3 Scanning Electron Microscopy with Energy Dispersive X-Ray

The second trace elemental analysis performed to detect mercury in skeletal remains is SEM-EDX. The aim of this study is to analyse the presence of Hg in dental calculus on teeth, to see whether individuals ingested mercury-enriched foods or inhaled mercury vapour that resulted in the incorporation of mercury into the dental calculus. Unfortunately, particles or areas containing mercury were not detected during any of the analyses of these teeth samples.

Instead, the various SEM-EDX analyses resulted in the identification of compositional elements of calcium (Ca), phosphorus (P), and oxygen (O), which form the natural make-up of dental calculus, root cementum, and dental enamel. The analyses on enamel reported only a minimal number and concentration of other elements, mostly Na and Cl. This is to be expected as dental enamel does not take up or hold external materials after its formation, unlike dental calculus, and its formation is completed once the tooth is protruded from the jaw (Scott et al., 2020, p. 110).

Additionally, root cementum and dental calculus demonstrated the inclusion of other elements, such as aluminium (Al), silicon (Si), potassium (K), magnesium (Mg), lead (Pb), zirconium (Zr), iron (Fe), titanium (Ti), copper (Cu), tin (Sn), barium (Ba), sulphur (S), lanthanum (La), cerium (Ce), and chromium (Cr). These are likely to be the result of external uptake, as these elements all have a relatively common natural occurrence. Some of the elements, such as Al, Si, and Fe, are likely to have been incorporated or deposited on top of the dental calculus and root cementum postmortem through diagenetic processes (Rasmussen et al., 2017, p. 95, 2020, p. 17), as they are naturally found in a wide variety of

soils and minerals like quartz (Al and Si) and are common occurrences in dental calculus (Charlier et al., 2010, p. 170). The presence of other trace elements, such as Pb, Ba, and Cu, could be explained by antemortem exposure and deposition through ingestion and subsequent absorption from the gastrointestinal tract (Rasmussen et al., 2020, pp. 2–4).

However, most relevant for this specific thesis is the absence of Hg in all 101 measurements of the six samples, both in wider surface areas and specific heavy particles. As other elements, specifically other toxic heavy metals, have been positively identified during this analysis, the lack of mercury in the data suggests that the individuals represented by these tooth samples were not significantly exposed to mercury-containing substances, such as mercury treatments. If true, this would account for the latest stages of dental calculus formation, as the analyses were taken on the upper surface of the dental calculus and singular particles embedded therein. For individuals with thick encrustations of dental calculus deposits, the earlier stages of calculus formation cannot be examined without a destructive sampling process. Due to the non-destructive sampling methodology adopted for this thesis, mercury ingestion or inhalation earlier in life cannot be ruled out on the basis of the obtained data.

8. Conclusion

The primary objective of this thesis is to enhance our understanding of syphilis and its medicinal treatment during the late medieval and early modern period in the Netherlands. This investigation involved a detailed analysis of the skeletal collection from St. Gertrude's infirmary (1382 - ca. 1611) in Kampen, by employing a multidisciplinary approach to determine the extent of treponemal disease presence and to explore potential usage of mercury-based treatments. The methodology encompassed an osteoarchaeological and paleopathological re-examination with a specific focus on treponemal lesions. This analysis, based on the foundational scoring system by Harper et al. (2011), was expanded by conducting three trace elemental analyses (pXRF, ICP-MS, and SEM-EDX) on samples from both bones and teeth. Additionally, archival research was undertaken to gain insights into the presence of disease at the infirmary as well as the treatments that may have been available to patients and inhabitants. This comprehensive approach was designed to address the central research question:

To what extent can the presence of syphilis and its treatment with mercury be identified in the human skeletal remains from the late medieval and early modern St. Gertrude's infirmary in Kampen, the Netherlands?

This question is separated in five sub-questions that are answered separately in this chapter. From these, the main research question is answered. The chapter ends with suggestions for future research.

8.1 Treponemal disease at St. Gertrude's infirmary

How can treponemal disease be best identified in skeletal remains and what is the prevalence of treponemal disease in the skeletal remains from the late medieval and early modern St. Gertrude's infirmary in Kampen?

Treponemal disease was successfully identified in the osteoarchaeological record from St. Gertrude's infirmary by employing the scoring system designed by Harper et al. (2011). By using a slightly revised scoring system that was suitable for this skeletal collection and the scope of this thesis, skeletal remains were assessed on the basis of lesions they exhibited and the associated diagnostic value. This made it possible to gain more insight into the presence of individuals highly likely to be affected by treponemal disease at St. Gertrude's infirmary, while also being able to ascertain whether individuals had lesions suggestive of or consistent with treponemal disease. Such a standardized approach is highly favorable for comparing the presence and prevalence of treponemal disease between archaeological sites, as the basis for treponemal diagnosis is not always clear in academic literature.

This prevalence of acquired treponemal disease among St. Gertrude's infirmary remains is 6.3%, which is significantly higher than other sites from similar time periods in the Netherlands. This demonstrates

that citizens in Kampen may have been exceptionally affected by treponemal infections. Kampen's role as an international trading hub and its periods of significant overcrowding likely contributed to the elevated prevalence of this infectious disease. If individuals with multiple lesions suggestive of treponemal disease are also accounted for, the prevalence rate is raised to 12.4%, possibly reflecting the disease's broader impact on the skeletal assemblage. Considering the extensive impact of diffuse and bilateral periosteal new bone formation in the assemblage that may resemble systematic infection, and the invisibility of cardiovascular and neurosyphilis in the skeleton, the true presence of treponemal disease at St. Gertrude's infirmary could still be underestimated.

Although *caries sicca* lesions were only encountered in two individuals, the severe and extensive presentation of the postcranial pathological lesions in a number of individuals from this archaeological site sheds a light on the debilitating nature and drastic effects of this disease in a pre-antibiotic era.

When looking at the distribution of treponemal skeletal lesions between biological sex groups, the prevalence observed in females raises intriguing questions on the influence of variability in immune responses. A similar complex picture appears when examining lesions between various age-at-death groups, which shows that all adult age groups are affected, although to varying degrees. The absence of congenital syphilis may be attributed to limited non-adult representation. The findings highlight the complex interplay of factors influencing the prevalence of treponemal disease, but possible limitations posed by sample size and the variability of skeletal manifestation of the infection muddy the waters.

No indications of skeletal changes as a result of mercury treatment were found, and as such, the trace elemental analyses are needed to gain more insight into possible mercury-based treatment at the site.

8.2 Syphilis and mercury: archival research

Can evidence of syphilis infections and treatment with mercury be found in archival records from late medieval and early modern Kampen?

The archival records of St. Gertrude's infirmary did not reveal a reference to syphilis or any other specific disease, and also remained ambiguous on medicinal treatment. While the presence of treponemal disease has been established through osteoarchaeological research, and the trace elemental analysis highlighted the potential use of mercury by these individuals, this is not reported in the archival records. Mercury is named in two letters from 1779, which could be indicative of its widespread use as a remedy. Ultimately, the identification of references to syphilis and mercury may be severely limited by the sociocultural stigma of the disease, other priorities in recordkeeping, and different practices in naming or diagnosing the disease or by historical doctors. This lack of conclusive historical evidence again emphasizes the need for trace elemental analyses to investigate mercury intake by the individuals laid to rest at St. Gertrude's infirmary.

8.3 Mercury in bone: pXRF

Can elemental mercury be detected in human skeletal remains from late medieval and early modern Kampen through portable X-Ray Fluorescence Spectrometry (pXRF) and what does this say about the use of mercury treatments at St. Gertrude's infirmary?

Through the pXRF analysis it was found that mercury emissions were notably low and consistent across all analyzed bones, possibly indicating minimal mercury uptake across the sample. The Hg are emission values close to or below the instrument's detection limit, hampering precise quantification of absolute mercury concentrations in the bone samples. This limitation necessitates cautious interpretation due to potential background scatter influence on emission values near the detection limit.

Despite this, a few trends could be discerned from the available data. Firstly, femora and humeri exhibited similar emission patterns, while ribs displayed higher variability and potentially higher mercury levels. Due to the difference in average bone remodeling rates, this pattern could be indicative of mercury exposure closer to the time of death. This trend aligns with findings in other studies, but the interpretation is constrained by a lack of statistical significance. Additionally, these observations may be explained by an inherent difference in the practical application of pXRF analysis on rib versus long bone samples, possibly stemming from a difference in cortical thickness and the proportion of trabecular bone between long bones and ribs.

Secondly, mercury emission values were compared on the basis of osteoarchaeologically assigned treponemal scores, which demonstrated the potentially higher mercury concentration in individuals that showed no suggestive or diagnostic signs of treponemal infection. This could suggest potential unintentional mercury exposure, but also may be exemplary of the complex interactions between disease, historical treatment methods, and the remaining archaeological record.

Overall, the application of pXRF analysis did raise intriguing trends in potential mercury exposure and difference in mercury uptake for different bones. It was useful in gaining a sense of the distribution of mercury between various groups and bones for a larger number of individuals. Yet, the complexity of the findings, combined with the detection limits of the instrument and sample size constraints, emphasizes the need for cautious interpretation. Consequently, the applicability of pXRF analysis may not be suitable for datasets that require the precise and accurate concentration of Hg in bone.

8.4 Mercury in bone: ICP-MS

Can elemental mercury be detected in human skeletal remains from late medieval and early modern Kampen through Inductively Coupled Plasma Mass Spectrometry (ICP-MS) and what does this say about the use of mercury treatments at St. Gertrude's infirmary?

The ICP-MS analysis was conducted on a selection of bone samples from syphilitic and control individuals as well as soil samples to determine their precise mercury levels. This resulted in the successful detection and quantification of Hg concentrations for 17 samples from 11 individuals, as well as two soil samples, with concentrations ranging from 0.06 ppm to 1.28 ppm.

Although statistical significance could not be tested for, the data revealed trabecular bone generally exhibited slightly higher Hg concentrations than cortical bone and that non-pathological individuals had generally higher Hg concentrations than pathological individuals, both aligning with the pXRF data. However, it is challenging, if not impossible, to ascertain whether these higher levels are the result of intentional therapeutical mercury exposure, possibly to treat the early stages of syphilis, or if they are the result of unintentional uptake through environmental, dietary, or occupational exposure. Yet, the data can aid in interpreting the potential period of life in which mercury exposure has taken place, as two individuals indicated potential variations in the timing of mercury intake. Additionally, it shows that mercury exposure was potentially a common occurrence at St. Gertrude's infirmary, although limitations in establishing background versus elevated mercury levels complicate the matter.

Ultimately, while the method is destructive, it showed the best results in detecting quantified mercury concentrations in human skeletal remains. This makes it possible to conduct comparisons with other sites, and may more accurately reflect therapeutical mercury uptake in certain individuals.

8.5 Mercury in bone: SEM-EDX

Can elemental mercury be detected in human dental calculus from late medieval and early modern Kampen through Scanning Electron Microscopy with Energy Dispersive X-rays Spectroscopy (SEM-EDX) and what does this say about the use of mercury treatments at St. Gertrude's infirmary?

The SEM-EDX analysis aimed to ascertain the presence of elemental mercury in eight teeth from St. Gertrude's infirmary, focusing on whether individuals ingested mercury-rich substances or were exposed to mercury vapour, resulting in its incorporation into dental calculus. Unfortunately, the SEM-EDX analysis did not detect any particles or areas containing mercury in the examined teeth samples. While traces of other substances, including toxic heavy metals such as lead, were identified, the lack of mercury suggests that the represented individuals were not significantly exposed to mercury-containing substances or vapours. This insight particularly pertains to the later stages of dental calculus formation, as analyses were conducted on the upper surface of the dental calculus and embedded particles. However, the inability to examine earlier stages of calculus formation without destructive sampling precludes ruling out mercury exposure earlier in life. Consequently, this research question remains partially unanswered, as the successful identification of other toxic heavy metals suggests that mercury could potentially be detected if it was present.

8.6 Final conclusion of this thesis

To what extent can the presence of syphilis and its treatment with mercury be identified in the human skeletal remains from the late medieval and early modern St. Gertrude's infirmary in Kampen, the Netherlands?

The presence of acquired treponemal disease was successfully identified through the application of the scoring system based on Harper et al. (2011). While osteoarchaeological study cannot confidently distinguish between venereal syphilis and the other treponematoses, the location, time period and historical context from which the skeletal assemblage originates increase the likelihood of venereal syphilis as the instigator of the lesions encountered. The extent of the lesions indicates the severity of the disease for those who were affected in pre-antibiotic times. Yet, taking into account the large number of individuals with lesions suggestive of or consistent with treponemal disease and the invisibility of cardiovascular and neurosyphilis in the archaeological record, the prevalence rate of 6.3% reported here may still represent only a fraction of those who were affected by the disease in late medieval and early modern Kampen.

Whether mercury was offered as a potential remedy for syphilis by those working at St. Gertrude's infirmary remains a more intricate matter. While non-destructive trace elemental analytical methods like pXRF and SEM-EDX would be preferred, they failed in detecting quantified and comparable mercury concentrations in bone, due to the absolute quantities that are below or near the limit of detection of the instrumentation. While general trends can be discerned, the true significance of the low emission values from the pXRF analysis cannot be identified due to the lack of available calibration methods for Hg in bone. A custom bone and mercury specific calibration would thus be needed to push the limit of detection boundaries enough to detect Hg through pXRF.

The ICP-MS analysis demonstrated that the Hg quantities are indeed of low ppm values, and, although destructive, it remains the only technique used here that was able to generate absolute and quantified Hg concentrations. It showed that mercury was potentially used to treat syphilis at St. Gertrude infirmary, although the precise source of higher mercury levels could not be confidently identified.

8.7 Suggestions for future research

The site of St. Gertrude's infirmary has proven to be an interesting case study on syphilis and mercury treatment in the late medieval Netherlands. Employing a systematic scoring mechanism for identifying potential treponemal diseases yielded successful results. Thus, it is advisable for forthcoming paleopathological investigations to embrace a comparable and standardized methodology, as it would enhance the precise diagnosis of treponematosis in diverse contexts, facilitating the creation of a consistent and replicable dataset. This, in turn, would enable a more accurate assessment of syphilis'

impact across historical Europe. In conjunction with the integration of ancient DNA research focused on *Treponema pallidum*, such standardized approaches hold promise for a more comprehensive and nuanced strategy in addressing the longstanding discourse surrounding the disease's origins.

Investigating the impact of the disease on historical communities may be done by further unravelling the use of mercury treatments. However, the analytical limitations of detecting trace elements in bone restrict the calibration and comparability between datasets. A prospective avenue of research involves conducting further experimental inquiries to establish a standardized, minimally invasive methodology that yields precise and reliable mercury concentrations on a large scale. Yet, the success of such techniques hinges upon the ability to distinguish between normal and elevated mercury levels within archaeological contexts. The incorporation of pXRF calibration standards pertaining to mercury in trabecular and cortical bone would greatly facilitate population-wide investigations of mercury concentrations, which, in turn, would help establish contextual-specific baseline levels across a broader range of historical and geographical settings. Furthermore, the ongoing research into the biological aspects underlying the incorporation and distribution of mercury within the skeleton is essential to further interpret this type of archaeological data. To further test the accuracy of various methods, skeletal assemblages that are known to have been subjected to mercury treatment should form an integral part of future studies. For the Netherlands, it seems that the assemblages excavated from the *Oude en Nieuwe Gasthuis* in Delft are particularly interesting, as historical records have indicated the substantial use of toxic mercurial treatments during the early modern period.

Other avenues for studying the treatment of syphilis may include trace elemental analyses focused on arsenic, which was used as a remedy during the postmedieval period, or residue-analyses in ceramics from infirmary sites focused on guaiacum and sarsaparilla.

Lastly, while many regions in Europe have received plenty of scholarly attention regarding the history of syphilis, large parts of Africa, Asia, and other regions have gone largely unnoticed in the syphilis debate, even though they are known to have been severely affected by yaws, bejel, and pinta, as well as venereal syphilis. As such, possible research avenues on the treponematoses, their impact, and history in these regions form a vast and relatively unexplored data field, which may just reveal previously hidden elucidations that could help unravel the history of one of the world’s most infamous diseases.

Abstract

During the early modern period (1500-1800 CE), Europe was plagued by syphilis, a venereal infection caused by the bacteria *Treponema pallidum,* resulting in chronic and debilitating symptoms. Desperate to resolve the infection, patients were often subjected to prolonged and extensive treatments with toxic mercury. Unfortunately, osteoarchaeological study of syphilis is challenging due to the limited skeletal visibility of the infection. Moreover, historical evidence is sparse and often influenced by sociocultural stigma attributed to the venereal nature of the disease. This scarcity of data on syphilis in the early modern period has limited more holistic research into the disease and its treatment.

Therefore, this study adopted a multidisciplinary approach to investigate syphilis and its treatment at St. Gertrude's infirmary (1382 - ca. 1611) in Kampen, the Netherlands, where presence of the disease has been previously reported. Human skeletal remains (n=79) were re-examined with a focus on treponemal disease, following the scoring system laid out by Harper et al. (2011). The potential therapeutical use of mercury was investigated by conducting archival research and multiple trace elemental analyses. Using portable X-Ray Fluorescence Spectrometry (pXRF) and Inductively Coupled Plasma-Mass Spectrometry (ICP-MS), subsamples of the skeletal assemblage were assessed on the presence of mercury in human bone. Scanning Electron Microscopy with Energy Dispersive X-Ray (SEM-EDX) was conducted to assess the potential uptake of mercury in dental calculus on the teeth.

Osteoarchaeological study identified several diagnostic cases of treponemal infection at the site (n=5 or 6.33%), as well as a number of cases with lesions suggestive of treponemal disease. This finding demonstrates the influence of treponemal disease, likely attributable to venereal syphilis, at St. Gertrude's infirmary in Kampen, especially when compared to the prevalence of the disease in human skeletal assemblages from similar Dutch sites.

Research into historical archives indicated that mercury was indeed used therapeutically in Kampen during the 18th century. However, it showed no direct evidence for syphilis or mercury treatment at St. Gertrude's infirmary in the period of interest (1382 – ca. 1611).

Unfortunately, elemental analyses revealed no substantial evidence for significantly elevated mercury concentrations, although interesting trends were found. In particular, both pXRF and SEM-EDX analyses did not result in absolute and quantifiable mercury concentrations. While ICP-MS analysis showed absolute concentrations of mercury in a subsample of bone material, interpreting and contextualising these results remains challenging. These observations may be explained by a lack of available mercury treatment in Kampen or a preference for other treatment methods. Nonetheless, this study helps to understand syphilis and its treatment in the early modern Netherlands and provides an evaluation of chemical analyses to detect mercury in archaeological bone.

Reference list

Aghanashini, S., Puvvalla, B., Mundinamane, D. B., Apoorva, S., Bhat, D., & Lalwani, M. (2016). A comprehensive review on dental calculus. *Journal of Health Sciences & Research*, *7*(2), 42–50. https://doi.org/10.5005/jp-journals-10042-1034

Agilent Technologies. (n.d.). *An introduction to the fundamentals of Inductively Coupled Plasma – Mass Spectrometry (ICP-MS)*. Retrieved 20 June 2023, from https://www.agilent.com/en/product/atomic-spectroscopy/inductively-coupled-plasma-mass-spectrometry-icp-ms/what-is-icp-ms-icp-ms-faqs

Anastasiou, E., & Mitchell, P. D. (2013). Palaeopathology and genes: Investigating the genetics of infectious diseases in excavated human skeletal remains and mummies from past populations. *Gene*, *528*(1), 33–40. https://doi.org/10.1016/j.gene.2013.06.017

Armelagos, G. J., Zuckerman, M. K., & Harper, K. N. (2012). The science behind pre-Columbian evidence of syphilis in Europe: Research by documentary. *Evolutionary Anthropology: Issues, News, and Reviews*, *21*(2), 50–57. https://doi.org/10.1002/evan.20340

Arora, N., Schuenemann, V. J., Jäger, G., Peltzer, A., Seitz, A., Herbig, A., Strouhal, M., Grillová, L., Sánchez-Busó, L., Kühnert, D., Bos, K. I., Davis, L. R., Mikalová, L., Bruisten, S., Komericki, P., French, P., Grant, P. R., Pando, M. A., Vaulet, L. G., … Bagheri, H. C. (2016). Origin of modern syphilis and emergence of a pandemic Treponema pallidum cluster. *Nature Microbiology*, *2*(1), 1–6. https://doi.org/10.1038/nmicrobiol.2016.245

Arts, N. (2019). Digging up the dead in Eindhoven: The choir and churchyard of St. Catharine's, 1200-1850. In R. van Oosten, R. Schats, & K. Fast (Eds.), *Osteoarchaeology in historical context: Cemetery research from the Low Countries* (pp. 37–68). Sidestone Press.

Aufderheide, A. C., & Rodriguez-Martin, C. (1998). *The Cambridge encyclopedia of human paleopathology*. Cambridge University Press.

Bainbridge, D., & Tarazaga, S. G. (1956). A study of sex differences in the scapula. *The Journal of the Royal Anthropological Institute of Great Britain and Ireland*, *86*(2), 109–134. https://doi.org/10.2307/2843994

Baker, B. J., & Armelagos, G. J. (1988). The origin and antiquity of syphilis: Paleopathological diagnosis and interpretation [and comments and reply]. *Current Anthropology*, *29*(5), 703–737. https://doi.org/10.1086/203691

Baker, B. J., Crane-Kramer, G., Dee, M. W., Gregoricka, L. A., Henneberg, M., Lee, C., Lukehart, S. A., Mabey, D. C., Roberts, C. A., Stodder, A. L. W., Stone, A. C., & Winingear, S. (2020). Advancing the understanding of treponemal disease in the past and present. *American Journal of Physical Anthropology*, *171*(S70), 5–41. https://doi.org/10.1002/ajpa.23988

Balcaen, L., Bolea-Fernandez, E., Resano, M., & Vanhaecke, F. (2015). Inductively coupled plasma – Tandem mass spectrometry (ICP-MS/MS): A powerful and universal tool for the interference-free determination of (ultra)trace elements – A tutorial review. *Analytica Chimica Acta*, *894*, 7–19. https://doi.org/10.1016/j.aca.2015.08.053

Bass, W. M. (1987). *Human osteology: A laboratory and field manual*. Missouri Archaeological Society.

Bergmann, C. L. (2018). *Elemental analyses of archaeological bone using PXRF, ICP-MS, and a newly developed calibration to assess Andean paleodiets* [Unpublished M.A. Thesis, University of Sout Florida]. https://digitalcommons.usf.edu/etd/7264

Biehler-Gomez, L., Mattia, M., Sala, C., Giordano, G., Di Candia, D., Messina, C., Sconfienza, L. M., Franchini, A. F., Porro, A., Galimberti, P. M., Slavazzi, F., & Cattaneo, C. (2022). Mercury poisoning in two patients with tertiary syphilis from the Ca' Granda hospital (17th-century Milan). *Archaeometry*, *64*(2), 500–510. https://doi.org/10.1111/arcm.12721

Black, S., & Scheuer, L. (1996). Age changes in the clavicle: From the early neonatal period to skeletal maturity. *International Journal of Osteoarchaeology*, *6*(5), 425–434.

Blankaart, S. (1696). *Venus belegert en ontset: Zynde een verhandelinge van de pokken, en des selfs toevallen, van druipers, chankers, klap-ooren, Spaanse kragen, sand-klooten, cordeé uitwasschen, enz. met een zekere en grondige genezinge steunende op de Cartesiaanse philosophie, en het sondigende suur en sout*. Timotheus ten Hoorn. http://archive.org/details/gri_33125010841472

Blatt, S. H., Redmond, B. G., Cassman, V., & Sciulli, P. W. (2011). Dirty teeth and ancient trade: Evidence of cotton fibres in human dental calculus from Late Woodland, Ohio. *International Journal of Osteoarchaeology*, *21*(6), 669–678. https://doi.org/10.1002/oa.1173

Bouwman, A. S., & Brown, T. A. (2005). The limits of biomolecular palaeopathology: Ancient DNA cannot be used to study venereal syphilis. *Journal of Archaeological Science*, *32*(5), 703–713. https://doi.org/10.1016/j.jas.2004.11.014

Brent, R. N., Wines, H., Luther, J., Irving, N., Collins, J., & Drake, B. L. (2017). Validation of handheld X-ray fluorescence for in situ measurement of mercury in soils. *Journal of Environmental Chemical Engineering*, *5*(1), 768.

Brooks, S., & Suchey, J. M. (1990). Skeletal age determination based on the os pubis: A comparison of the Acsádi-Nemeskéri and Suchey-Brooks methods. *Human Evolution*, *5*(3), 227–238. https://doi.org/10.1007/BF02437238

Bruker. (n.d.). *Handheld XRF: How it works*. Retrieved 13 June 2023, from https://www.bruker.com/en/products-and-solutions/elemental-analyzers/handheld-xrf-spectrometers/how-xrf-works.html

Bruker. (2020). *Application Note # 2001: TRACER 5 Spectrometer Mode*. https://www.bruker.com/en/products-and-solutions/elemental-analyzers/handheld-xrf-spectrometers/TRACER-5.html

Buckberry, J. L., & Chamberlain, A. T. (2002). Age estimation from the auricular surface of the ilium: A revised method. *American Journal of Physical Anthropology*, *119*(3), 231–239. https://doi.org/10.1002/ajpa.10130

Byrnes, J. F., & Bush, P. J. (2016). Practical Considerations in Trace Element Analysis of Bone by Portable X-ray Fluorescence. *Journal of Forensic Sciences*, *61*(4), 1041–1045. https://doi.org/10.1111/1556-4029.13103

Calvo, F. A., Guilemany, J. M., De Salazar, J. M. G., & Urena, A. (1988). Study by SEM-EDS of the in situ dynamic leaching of mercury ores. *Metallurgical Transactions B*, *19*(2), 165–170. https://doi.org/10.1007/BF02654200

Carvalho, M.-L., Manso, M., Pessanha, S., Guilherme, A., & Ferreira, F. R. (2009). Quantification of mercury in XVIII century books by Energy Dispersive X-Ray Fluorescence (EDXRF). *Journal of Cultural Heritage*, *10*(3), 435–438. https://doi.org/10.1016/j.culher.2008.11.003

Castro, M. M., Benavente, M. A., Ortega, J., Acuña, R., Montero, C., Thomas, C., & Castro, N. (2016). Thoracic aortic aneurysm in a pre-Columbian (210 BC) inhabitant of Northern Chile: Implications for the origins of syphilis. *International Journal of Paleopathology*, *13*, 20–26. https://doi.org/10.1016/j.ijpp.2016.01.002

Chapel, T. A. (1980). The signs and symptoms of secondary syphilis. *Sexually Transmitted Diseases*, *7*(4), 161–164. https://doi.org/10.1097/00007435-198010000-00002

Charlier, P., Huynh-Charlier, I., Munoz, O., Billard, M., Brun, L., & Grandmaison, G. (2010). The microscopic (optical and SEM) examination of dental calculus deposits (DCD). Potential interest in forensic anthropology of a bio-archaeological method. *Legal Medicine (Tokyo, Japan)*, *12*, 163–171. https://doi.org/10.1016/j.legalmed.2010.03.003

Clark, E. G., & Danbolt, N. (1955). The Oslo study of the natural history of untreated syphilis. *Journal of Chronic Diseases*, *2*(3), 311–344. https://doi.org/10.1016/0021-9681(55)90139-9

Coronel, S., Sr. (1880). Staatkunde en geschiedenis; Volksgezondheid en volksbeschaving; Na de Hervorming. *De Tijdspiegel*, *37*(2), 374–396. https://www.dbnl.org/tekst/_tij008188001_01/_tij008188001_01_0067.php

Cremers, W. (2018). *The niche that is timber: Late-Medieval timber and timber-framed buildings in Kampen* [Unpublished Master Thesis, Leiden University]. https://hdl.handle.net/1887/61105

Crissey, J. T., & Denenholz, D. A. (1984). Benign tertiary syphilis. *Clinics in Dermatology*, *2*(1), 107–116. https://doi.org/10.1016/0738-081X(84)90015-4

Crosby, A. W. (1969). The early history of syphilis: A reappraisal. *American Anthropologist*, *71*(2), 218–227. https://doi.org/10.1525/aa.1969.71.2.02a00020

Daey Ouwens, I. M. (2019). *Neurosyphilis in the Netherlands: Then and now*. Erasmus Universiteit Rotterdam (EUR). hdl.handle.net/1765/120021

Davis, A., Bloom, N. S., & Que Hee, S. S. (1997). The environmental geochemistry and bioaccessibility of mercury in soils and sediments: A review. *Risk Analysis*, *17*(5), 557–569. https://doi.org/10.1111/j.1539-6924.1997.tb00897.x

Dawes, J. D., & Magilton, J. R. (1980). *The cemetery of St Helen-on-the-walls, Aldwark*. Council for British archaeology.

de Jonge, L., & Baetsen, S. (2013). Fysische antropologie van de begraven individuen. In J. Hendriks, H. De Kievith, & E. Peters (Eds.), *'Tot behoef van de siecken ende armen'. Archeologisch onderzoek naar het Bredase Gasthuis, 1958-2006* (pp. 199–276). Gemeente Breda. https://doi.org/10.17026/dans-278-x3bg

de Melo, F. L., de Mello, J. C. M., Fraga, A. M., Nunes, K., & Eggers, S. (2010). Syphilis at the crossroad of phylogenetics and paleopathology. *PLoS Neglected Tropical Diseases*, *4*(1), 1–11. https://doi.org/10.1371/journal.pntd.0000575

de Ruiter, H. (2021, December 17). *Notities over Mercurius*. Antroposana. https://www.antroposana.nl/2021-3-notities-over-mercurius-298

Demaitre, L. E. (2007). *Leprosy in premodern medicine: A malady of the whole body*. Johns Hopkins University Press.

Dennie, C. C. (1962). *A history of syphilis*. Charles C Thomas.

Dobson, M. (2015). *Murderous contagion: A human history of disease*. Quercus.

Don, J. (1966). *Gedeponeerde archieven: Kerken en kloosters; Memoriën, vergaderingen, armenkamer; Gasthuizen; Pesthuis, later stadsziekenhuis; Weeshuizen.* (Vol. 2). Gemeente Kampen.

Drake, B. L., & MacDonald, B. L. (Eds.). (2023). *Advances in portable x-ray fluorescence spectrometry: Instrumentation, application and interpretation*. Royal Society of Chemistry.

Drake, B. L., Taylor, B., & Hamilton, M. (2023). Quantitative analysis. In B. L. Drake & B. L. MacDonald (Eds.), *Advances in Portable X-ray Fluorescence Spectrometry: Instrumentation, Application and Interpretation* (pp. 81–107). Royal Society of Chemistry.

Dutour, O., Palfi, G., Berato, J., & Brun, J.-P. (Eds.). (1994). *L'origine de la syphilis en Europe: Avant ou après 1493?* Centre archéologique du Var ; Editions Errance.

Edmondson, D. G., Hu, B., & Norris, S. J. (2018). Long-term *in vitro* culture of the syphilis spirochete *Treponema pallidum* subsp. *Pallidum*. *mBio*, *9*(3), e01153-18. https://doi.org/10.1128/mBio.01153-18

Edmondson, D. G., & Norris, S. J. (2021). In vitro cultivation of the syphilis spirochete Treponema pallidum. *Current Protocols*, *1*(2), 1–20. https://doi.org/10.1002/cpz1.44

Emslie, S. D., Alderman, A., McKenzie, A., Brasso, R., Taylor, A. R., Molina Moreno, M., Cambra-Moo, O., González Martín, A., Silva, A. M., Valera, A., García Sanjuán, L., & Vijande Vila, E. (2019). Mercury in archaeological human bone: Biogenic or diagenetic? *Journal of Archaeological Science*, *108*, 104969. https://doi.org/10.1016/j.jas.2019.05.005

Fahy, G. E., Deter, C., Pitfield, R., Miszkiewicz, J. J., & Mahoney, P. (2017). Bone deep: Variation in stable isotope ratios and histomorphometric measurements of bone remodelling within adult humans. *Journal of Archaeological Science*, *87*, 10–16. https://doi.org/10.1016/j.jas.2017.09.009

Fialová, D., Skoupý, R., Drozdová, E., Paták, A., Piňos, J., Šín, L., Beňuš, R., & Klíma, B. (2017). The Application of Scanning Electron Microscopy with Energy-Dispersive X-Ray Spectroscopy (SEM-EDX) in Ancient Dental Calculus for the Reconstruction of Human Habits. *Microscopy and Microanalysis*, *23*(6), 1207–1213. https://doi.org/10.1017/S1431927617012661

Fokker, A. A. (1860). Geschiedenis der syphilis in de Nederlanden. *Nederlands Tijdschrift Voor Geneeskunde*, *4*, 419–446.

Fokker, A. A. (1861). De syphilis in de Nederlanden. *Nederlands Tijdschrift Voor Geneeskunde*, *5*, 451–472.

Forbes, M. N. S., Scott, A. B., & Rasmussen, K. L. (2022). *Getting freaky at the Fortress? An examination of venereal syphilis and medicinal mercury treatments at the 18th century Fortress of Louisburg, Nova Scotia, Canada.* [Poster]. Canadian Association for Biological Anthropology Annual Meeting, Winnipeg.

Forrai, J. (2011). History of different therapeutics of venereal disease before the discovery of penicillin. In N. S. Sato (Ed.), *Syphilis—Recognition, Description and Diagnosis*. IntechOpen. https://doi.org/10.5772/24205

Frahm, E. (2014). Scanning Electron Microscopy (SEM): Applications in Archaeology. In C. Smith (Ed.), *Encyclopedia of Global Archaeology* (pp. 6487–6495). Springer New York. https://doi.org/10.1007/978-1-4419-0465-2_341

Frangos, C. C., Lavranos, G. M., & Frangos, C. C. (2011). Higoumenakis' sign in the diagnosis of congenital syphilis in anthropological specimens. *Medical Hypotheses*, *77*(1), 128–131. https://doi.org/10.1016/j.mehy.2011.03.044

Frith, J. (2012). Syphilis: Its early history and treatment until penicillin and the debate on its origins. *Journal of Military and Veterans' Health*, *20*(4). https://jmvh.org/article/syphilis-its-early-history-and-treatment-until-penicillin-and-the-debate-on-its-origins/

Giacani, L., & Lukehart, S. A. (2014). The endemic treponematoses. *Clinical Microbiology Reviews*, *27*(1), 89–115. https://doi.org/10.1128/CMR.00070-13

Gladykowska-Rzeczycka, J. (1994). Syphilis in ancient and medieval Poland? In O. Dutour, G. Palfi, J. Berato, & J.-P. Brun (Eds.), *L'origine de la syphilis en Europe: Avant ou après 1493?* (pp. 116–118). Centre Archeologique du Var ; Editions Errance. https://dro.dur.ac.uk/7303/

Gladykowska-Rzeczycka, J., Kwiatkowska, B., Nowakowski, D., & Trnka, J. (2003). Treponematosis in a 14th century skeleton from Wroclaw, Poland. *Journal of Paleopathology*, *15*, 187–193.

Gonzalez-Rodriguez, J., & Fowler, G. (2013). A study on the discrimination of human skeletons using X-ray fluorescence and chemometric tools in chemical anthropology. *Forensic Science International*, *231*(1–3), 407.e1-407.e6. https://doi.org/10.1016/j.forsciint.2013.04.035

Groot, R. de. (2013). *Begravingen en muren uit de 15e eeuw: Graven naar het Gangolf-gasthuis Een archeologische opgraving van (een deel van) de begraafplaats van het Gangolf-gasthuis aan de Botermarkt in Haarlem* (Rapport 2509). RAAP Archeologisch Adviesbureau B.V. https://www.academia.edu/8732785/Begravingen_en_muren_uit_de_15e_eeuw_graven_naar_het_Gangolf_gasthuis_Een_archeologische_opgraving_van_een_deel_van_de_begraafplaats_van_het_Gangolf_gasthuis_aan_de_Botermarkt_in_Haarlem

Hackett, C. J. (1963). On the origin of the human treponematoses (pinta, yaws, endemic syphilis and venereal syphilis). *Bulletin of the World Health Organization*, *29*(1), 7–41.

Hackett, C. J. (1975). An introduction to diagnostic criteria of syphilis, treponarid and yaws (treponematoses) in dry bones, and some implications. *Virchows Archiv A, Pathological Anatomy and Histology*, *368*(3), 229–241. https://doi.org/10.1007/BF00432525

Hackett, C. J. (1976). *Diagnostic criteria of syphilis, yaws and treponarid (treponematoses) and of some other diseases in dry bones*. Springer. https://doi.org/10.1007/978-3-662-06583-9

Hallema, A. (1957). Uit de geschiedenis van het St. Catharinen-gasthuis, Pesthuis en Stadsziekenhuis. Hoe Kampen zijn Engelenberg-Stichting kreeg. *Kamper Almanak*, 193–237.

Hardy, K., Buckley, S., Collins, M. J., Estalrrich, A., Brothwell, D., Copeland, L., García-Tabernero, A., García-Vargas, S., de la Rasilla, M., Lalueza-Fox, C., Huguet, R., Bastir, M., Santamaría, D., Madella, M., Wilson, J., Cortés, Á. F., & Rosas, A. (2012). Neanderthal medics? Evidence for food, cooking, and medicinal plants entrapped in dental calculus. *Die Naturwissenschaften*, *99*(8), 617–626. https://doi.org/10.1007/s00114-012-0942-0

Harper, K. N., Zuckerman, M. K., Harper, M. L., Kingston, J. D., & Armelagos, G. J. (2011). The origin and antiquity of syphilis revisited: An Appraisal of Old World pre-Columbian evidence for treponemal infection. *American Journal of Physical Anthropology*, *146*(S53), 99–133. https://doi.org/10.1002/ajpa.21613

Hays, J. N. (2009). *The burdens of disease: Epidemics and human response in Western history* (Rev. ed). Rutgers University Press.

Heinsius, N. (1704). *Genees- en natuur-kundige verhandeling van het kwik-zilver.* Engelbrecht Boucquet.

Heinsius, N. (1705). *De kwijnende Venus, ofte Naukeurige verhandeling van de venus-ziekte.* Jan ten Hoorn.

Henneberg, M., & Henneberg, R. J. (1994). Treponematosis in an ancient Greek colony of Metaponto, southern Italy, 580–250 BCE. In O. Dutour, G. Palfi, J. Berato, & J.-P. Brun (Eds.), *L'origine de la syphilis en Europe: Avant ou après 1493?* (pp. 92–98). Centre Archeologique du Var ; Editions Errance.

Hillson, S., Grigson, C., & Bond, S. (1998). Dental defects of congenital syphilis. *American Journal of Physical Anthropology*, *107*(1), 25–40.

Holcomb, R. C. (1937). *Who gave the world syphilis? The Haitian myth*. Froben Press.

Holcomb, R. C. (1934). Christopher Columbus and the American origin of syphilis. *United States Naval Medical Bulletin*, *32*(4), 401–432.

Holcombe, S. A., Kang, Y., Derstine, B. A., Wang, S. C., & Agnew, A. M. (2019). Regional maps of rib cortical bone thickness and cross-sectional geometry. *Journal of Anatomy*, *235*(5), 883–891. https://doi.org/10.1111/joa.13045

Hudson, E. H. (1958). The treponematoses—Or treponematosis? *British Journal of Venereal Diseases*, *34*(1), 22–23.

Hudson, E. H. (1963). Treponematosis and anthropology. *Annals of Internal Medicine*, *58*(6), 1037. https://doi.org/10.7326/0003-4819-58-6-1037

Hudson, E. H. (1965). Treponematosis and man's social evolution. *American Anthropologist*, *67*(4), 885–901. https://doi.org/10.1525/aa.1965.67.4.02a00020

Ioannou, S., & Henneberg, M. (2017). Dental signs attributed to congenital syphilis and its treatments in the Hamann-Todd Skeletal Collection. *Anthropological Review*, *80*(4), 449–465. https://doi.org/10.1515/anre-2017-0032

Ioannou, S., Sassani, S., Henneberg, M., & Henneberg, R. J. (2016). Diagnosing congenital syphilis using Hutchinson's method: Differentiating between syphilitic, mercurial, and syphilitic-mercurial dental defects. *American Journal of Physical Anthropology*, *159*(4), 617–629. https://doi.org/10.1002/ajpa.22924

İşcan, M. Y., Loth, S. R., & Wright, R. K. (1984). Metamorphosis at the sternal rib end: A new method to estimate age at death in white males. *American Journal of Physical Anthropology*, *65*(2), 147–156. https://doi.org/10.1002/ajpa.1330650206

İşcan, M. Y., Loth, S. R., & Wright, R. K. (1985). Age estimation from the rib by phase analysis: White females. *Journal of Forensic Sciences*, *30*(3), 853–863. https://doi.org/10.1520/JFS11018J

Jager, A. (2015). *Middeleeuws Kampen: De ruimtelijke en economische structuur van de stad aan de hand van archeologische, bouwhistorische, numismatische en historische bronnen.* SPA Uitgevers.

Karamanou, M., Kyriakis, K., Tsoucalas, G., & Androutsos, G. (2013). Hallmarks in history of syphilis therapeutics. *Le Infezioni in Medicina : Rivista Periodica Di Eziologia, Epidemiologia, Diagnostica, Clinica e Terapia Delle Patologie Infettive*, *21*, 317–319.

Katz, A., & Krenkel, P. A. (1972). Mercury pollution: The making of an environmental crisis. *CRC Critical Reviews in Environmental Control*, *2*(1–4), 517–534. https://doi.org/10.1080/10643387209381589

Kawahata, T., Kojima, Y., Furubayashi, K., Shinohara, K., Shimizu, T., Komano, J., Mori, H., & Motomura, K. (2019). Bejel, a nonvenereal treponematosis, among men who have sex with men, Japan. *Emerging Infectious Diseases*, *25*(8), 1581–1583. https://doi.org/10.3201/eid2508.181690

Kent, M. E., & Romanelli, F. (2008). Reexamining syphilis: An update on epidemiology, clinical manifestations, and management. *The Annals of Pharmacotherapy*, *42*(2), 226–236. https://doi.org/10.1345/aph.1K086

Kilburn, N. N., Gowland, R. L., Halldórsdóttir, H. H., Williams, R., & Thompson, T. J. U. (2021). Assessing pathological conditions in archaeological bone using portable X-ray fluorescence (pXRF). *Journal of Archaeological Science: Reports*, *37*, 102980. https://doi.org/10.1016/j.jasrep.2021.102980

Klomp, M. (2017a). Het Sint Geertruidengasthuis. In M. Klomp (Ed.), *Myosotis, in de schaduw van het Sint Geertruidengasthuis: Archeologisch onderzoek tussen Boven Nieuwstraat en Burgwal.* (pp. 95–102). Gemeente Zwolle.

Klomp, M. (2017b). *Myosotis, in de schaduw van het Sint Geertruidengasthuis: Archeologisch onderzoek tussen Boven Nieuwstraat en Burgwal.* (4; Archeologische Rapporten Kampen, pp. 1–334). Gemeente Zwolle.

Kloprogge, J. T., Ponce, C. P., & Loomis, T. A. (2020). *The periodic table: Nature's building blocks. An introduction to the naturally occurring elements, their origins and their uses*. Elsevier.

Kolman, C. J. (1990). De verstedelijking van Kampen in de Late Middeleeuwen. *Kamper Almanak*, 145–177.

Kossmann-Putto, J. A., & Kossmann, F. J. (1989). Het ontstaan van Kampen. *Tijdschrift Voor Historische Geografie*, *7*(1), 1–9.

Koten, J. W. (2016). Syfilis, een geschiedenis. *Genealogisch Erfgoed Magazine*, *24*(4), 2–8.

Kreek, J. C. G. (2020). Ontstaan en vroege ontwikkeling van Kampen: De topografie van de binnenstad opnieuw bekeken. *Tijdschrift voor Historische Geografie*, *5*(2), 66–87. https://doi.org/10.5117/THG2020.2.001.KREE

Ladan, R. (2012). *De gezondheidszorg van Leiden in de late middeleeuwen.* [PhD Dissertation, Leiden University]. https://hdl.handle.net/1887/20284

Little, N. C., Florey, V., Molina, I., Owsley, D. W., & Speakman, R. J. (2014). Measuring heavy metal content in bone using portable X-ray fluorescence. *Open Journal of Archaeometry*, *2*(1), 19–21. https://doi.org/10.4081/arc.2014.5257

Livingstone, F. B. (1991). On the origin of syphilis: An alternative hypothesis. *Current Anthropology*, *32*(5), 587–590.

Lopez, B., Lopez-Garcia, J. M., Costilla, S., Garcia-Vazquez, E., Dopico, E., & Pardiñas, A. F. (2017). Treponemal disease in the Old World? Integrated palaeopathological assessment of a 9th–11th century skeleton from north-central Spain. *Anthropological Science*, *125*(2), 101–114. https://doi.org/10.1537/ase.170515

Lovejoy, C. O., Meindl, R. S., Pryzbeck, T. R., & Mensforth, R. P. (1985). Chronological metamorphosis of the auricular surface of the ilium: A new method for the determination of adult skeletal age at death. *American Journal of Physical Anthropology*, *68*(1), 15–28. https://doi.org/10.1002/ajpa.1330680103

Lukehart, S. A. (2008). Biology of Treponemes. In K. K. Holmes, P. F. Sparling, W. E. Stamm, P. Piot, J. N. Wasserheit, L. Corey, M. S. Cohen, & D. H. Watts (Eds.), *Sexually transmitted diseases* (4th ed, pp. 647–659). McGraw-Hill Medical.

Majander, K., Pfrengle, S., Kocher, A., Neukamm, J., du Plessis, L., Pla-Díaz, M., Arora, N., Akgül, G., Salo, K., Schats, R., Inskip, S., Oinonen, M., Valk, H., Malve, M., Kriiska, A., Onkamo, P., González-Candelas, F., Kühnert, D., Krause, J., & Schuenemann, V. J. (2020). Ancient bacterial genomes reveal a high diversity of Treponema pallidum strains in Early Modern Europe. *Current Biology*, *30*(19), 3788-3803. https://doi.org/10.1016/j.cub.2020.07.058

Maresh, M. M. (1955). Linear growth of long bones of extremities from infancy through adolescence; Continuing studies. *American Journal of Diseases of Children*, *89*(6), 725. https://doi.org/10.1001/archpedi.1955.02050110865010

Marino, R., Tanganelli, V., Pietrobelli, A., & Belcastro, M. G. (2021). Evaluation of the auricular surface method for subadult sex estimation on Italian modern (19th to 20th century) identified skeletal collections. *American Journal of Physical Anthropology*, *174*(4), 792–803. https://doi.org/10.1002/ajpa.24146

Mays, S., Crane-Kramer, G., & Bayliss, A. (2003). Two probable cases of treponemal disease of Medieval date from England. *American Journal of Physical Anthropology*, *120*(2), 133–143. https://doi.org/10.1002/ajpa.10132

Mays, S., Vincent, S., & Meadows, J. (2012). A possible case of treponemal disease from England dating to the 11th–12th century AD. *International Journal of Osteoarchaeology*, *22*(3), 366–372. https://doi.org/10.1002/oa.1210

McCormick, W. F., Stewart, J. H., & Greene, H. (1991). Sexing of human clavicles using length and circumference measurements. *The American Journal of Forensic Medicine and Pathology*, *12*(2), 175–181. https://doi.org/10.1097/00000433-199106000-00017

McGough, L. J. (2005). Syphilis in history: A response to 2 articles. *Clinical Infectious Diseases*, *41*(4), 573–575. https://doi.org/10.1086/432127

Measurlabs. (n.d.). *ICP-MS Analysis*. Retrieved 20 June 2023, from https://measurlabs.com/methods/inductively-coupled-plasma-mass-spectrometry-icp-ms/

Meindl, R. S., & Lovejoy, C. O. (1985). Ectocranial suture closure: A revised method for the determination of skeletal age at death based on the lateral-anterior sutures. *American Journal of Physical Anthropology*, *68*(1), 57–66. https://doi.org/10.1002/ajpa.1330680106

Meyer, C., Jung, C., Kohl, T., Poenicke, A., Poppe, A., & Alt, K. W. (2002). Syphilis 2001—A palaeopathological reappraisal. *HOMO*, *53*(1), 39–58. https://doi.org/10.1078/0018-442X-00037

Mikalová, L., Strouhal, M., Oppelt, J., Grange, P. A., Janier, M., Benhaddou, N., Dupin, N., & Šmajs, D. (2017). Human Treponema pallidum 11q/j isolate belongs to subsp. Endemicum but contains two loci with a sequence in TP0548 and TP0488 similar to subsp. Pertenue and subsp. Pallidum, respectively. *PLOS Neglected Tropical Diseases*, *11*(3), e0005434. https://doi.org/10.1371/journal.pntd.0005434

Mitchell, P. D. (2017). Improving the use of historical written sources in paleopathology. *International Journal of Paleopathology*, *19*, 88–95. https://doi.org/10.1016/j.ijpp.2016.02.005

Moorrees, C. F. A., Fanning, E. A., & Hunt, E. E. (1963). Age variation of formation stages for ten permanent teeth. *Journal of Dental Research*, *42*(6), 1490–1502. https://doi.org/10.1177/00220345630420062701

Naujoks, R., Schade, H., & Zelinka, F. (1967). Chemical composition of different areas of the enamel of deciduous and permanent teeth (The content of Ca, P, CO2, Na and N2). *Caries Research*, *1*(2), 137–143. https://doi.org/10.1159/000259508

Nissanka-Jayasuriya, E. H., Odell, E. W., & Phillips, C. (2016). Dental Stigmata of Congenital Syphilis: A Historic Review With Present Day Relevance. *Head and Neck Pathology*, *10*(3), 327–331. https://doi.org/10.1007/s12105-016-0703-z

Norris, S. J., Cox, D. L., & Weinstock, G. M. (2001). Biology of Treponema pallidum: Correlation of functional activities with genome sequence data. *Journal of Molecular Microbiology and Biotechnology*, *3*(1), 37–62.

Nuić, I., Gosar, M., Ugrina, M., & Trgo, M. (2022). Assessment of natural zeolite clinoptilolite for remediation of mercury-contaminated environment. *Processes*, *10*(4), 639. https://doi.org/10.3390/pr10040639

Onisto, N., Maat, G. J. R., & Bult, E. J. (1998). *Human remains from the infirmary 'Oude en Nieuwe Gasthuis' of the city of Delft in the Netherlands; 1265—1652 AD*. Barge's Anthropologica 2. https://doi.org/10.17026/dans-xps-3bgv

Ortner, D. J. (1998). Male – female immune reactivity and its implications for interpreting evidence in human skeletal paleopathology. In A. L. Grauer & P. Stuart-Macadam (Eds.), *Sex and gender in paleopathological perspective* (pp. 79–82). Cambridge University Press.

Ortner, D. J. (2003). *Identification of pathological conditions in human skeletal remains* (2nd ed). Academic Press.

O'Shea, J. G. (1990). 'Two minutes with Venus, two years with Mercury': Mercury as an antisyphilitic chemotherapeutic agent. *Journal of the Royal Society of Medicine*, *83*(6), 392–395. https://doi.org/10.1177/014107689008300619

Pavlović, A., van Veen, M. M. A., Veselka, B., Kersing, V. L. C., Vermeeren, C., Comis, S. Y., & Nieweg, D. C. (2021). *Het kerkhof rond de Grote- of St. Jacobskerk in Den Haag: Archeologisch onderzoek in het kader van de herinrichting van het Kerkplein en het gebied rond de kerk* (22; Haagse Oudheidkundige Publicaties, pp. 1–390). Afdeling Archeologie & Natuur- en Milieueducatie Gemeente Den Haag. https://archeologie.denhaag.nl/wp-content/uploads/2022/02/HOP22_Het-kerkhof-rond-de-Grote-of-St.-Jacobskerk-in-Den-Haag-web.pdf

Peeling, R. W., & Hook, E. W. (2006). The pathogenesis of syphilis: The Great Mimicker, revisited. *The Journal of Pathology*, *208*(2), 224–232. https://doi.org/10.1002/path.1903

Pessanha, S., Carvalho, M., Carvalho, M. L., & Dias, A. (2016). Quantitative analysis of human remains from 18th–19th centuries using X-ray fluorescence techniques: The mysterious high content of mercury in hair. *Journal of Trace Elements in Medicine and Biology*, *33*, 26–30. https://doi.org/10.1016/j.jtemb.2015.08.004

Phenice, T. W. (1969). A newly developed visual method of sexing the os pubis. *American Journal of Physical Anthropology*, *30*(2), 297–301. https://doi.org/10.1002/ajpa.1330300214

Plagens-Rotman, K., Jarząbek-Bielecka, G., Merks, P., Kêdzia, W., & Czarnecka-Operacz, M. (2021). Syphilis: Then and now. *Postepy Dermatologii I Alergologii*, *38*(4), 550–554. https://doi.org/10.5114/ada.2021.108930

Powell, M. L., & Cook, D. C. (Eds.). (2005). *The myth of syphilis: The natural history of treponematosis in North America*. University Press of Florida.

Power, R. C., Salazar-García, D. C., Wittig, R. M., & Henry, A. G. (2014). Assessing use and suitability of scanning electron microscopy in the analysis of micro remains in dental calculus. *Journal of Archaeological Science*, *49*, 160–169. https://doi.org/10.1016/j.jas.2014.04.016

Radolf, J. D. (1996). Treponema. In S. Baron (Ed.), *Medical Microbiology* (4th ed.). University of Texas Medical Branch. http://www.ncbi.nlm.nih.gov/books/NBK7716/

Rasmussen, K. L., Boldsen, J. L., Kristensen, H. K., Skytte, L., Hansen, K. L., Mølholm, L., Grootes, P. M., Nadeau, M.-J., & Flöche Eriksen, K. M. (2008). Mercury levels in Danish Medieval human bones. *Journal of Archaeological Science*, *35*(8), 2295–2306. https://doi.org/10.1016/j.jas.2008.03.003

Rasmussen, K. L., Delbey, T., d'Imporzano, P., Skytte, L., Schiavone, S., Torino, M., Tarp, P., & Thomsen, P. O. (2020). Comparison of trace element chemistry in human bones interred in two private chapels attached to Franciscan friaries in Italy and Denmark: An investigation of social stratification in two medieval and post-medieval societies. *Heritage Science*, *8*(65), 1–21. https://doi.org/10.1186/s40494-020-00407-x

Rasmussen, K. L., Skytte, L., D'imporzano, P., Orla Thomsen, P., Søvsø, M., & Lier Boldsen, J. (2017). On the distribution of trace element concentrations in multiple bone elements in 10 Danish medieval and post-medieval individuals. *American Journal of Physical Anthropology*, *162*(1), 90–102. https://doi.org/10.1002/ajpa.23099

Rasmussen, K. L., Skytte, L., Jensen, A. J., & Boldsen, J. L. (2015). Comparison of mercury and lead levels in the bones of rural and urban populations in Southern Denmark and Northern Germany during the Middle Ages. *Journal of Archaeological Science: Reports*, *3*, 358–370. https://doi.org/10.1016/j.jasrep.2015.06.021

Rasmussen, K. L., Skytte, L., Pilekær, C., Lauritsen, A., Boldsen, J. L., Leth, P. M., & Thomsen, P. O. (2013). The distribution of mercury and other trace elements in the bones of two human individuals from medieval Denmark—The chemical life history hypothesis. *Heritage Science*, *1*(10), 1–13. https://doi.org/10.1186/2050-7445-1-10

Rasool, M. N., & Govender, S. (1989). The skeletal manifestations of congenital syphilis: A review of 197 cases. *Journal of Bone and Joint Surgery*, *71*(5), 752–755. https://www.doi.org/10.1302/0301-620X.71B5.2584243

Rehm, J. (2018). Syphilis cases in US newborns spike to 20-year high. *Nature*. https://doi.org/10.1038/d41586-018-06910-3

Roberts, C. A. (1994). Treponematosis in Gloucester, England: A theoretical and practical approach to the pre-Columbian theory. In O. Dutour, G. Palfi, J. Berato, & J.-P. Brun (Eds.), *L'origine de la syphilis en Europe: Avant ou après 1493?* (pp. 101–108). Centre Archeologique du Var ; Editions Errance. https://dro.dur.ac.uk/7303/

Roberts, C. A. (2019). Infectious disease: Introduction, periostosis, periostitis, osteomyelitis, and septic arthritis. In J. E. Buikstra (Ed.), *Ortner's identification of pathological conditions in human skeletal remains* (3rd ed., pp. 285–319). Academic Press. https://doi.org/10.1016/B978-0-12-809738-0.00011-9

Roberts, C. A., & Buikstra, J. E. (2019). Bacterial infections. In J. E. Buikstra (Ed.), *Ortner's identification of pathological conditions in human skeletal remains* (3rd ed., pp. 321–439). Academic Press. https://doi.org/10.1016/B978-0-12-809738-0.00011-9

Roberts, C. A., & Manchester, K. (2010). *The archaeology of disease* (3rd ed). The History Press.

Rogers, J., & Waldron, T. (1995). *A field guide to joint disease in archaeology*. John Wiley & Sons, Ltd.

Romeis, E., Tantalo, L., Lieberman, N., Phung, Q., Greninger, A., & Giacani, L. (2021). Genetic engineering of Treponema pallidum subsp. Pallidum, the Syphilis Spirochete. *PLoS Pathogens*, *17*(7), e1009612–e1009612. https://doi.org/10.1371/journal.ppat.1009612

Rompalski, P., Smoliński, A., Krztoń, H., Gazdowicz, J., Howaniec, N., & Róg, L. (2019). Determination of mercury content in hard coal and fly ash using X-ray diffraction and scanning electron microscopy coupled with chemical analysis. *Arabian Journal of Chemistry*, *12*(8), 3927–3942. https://doi.org/10.1016/j.arabjc.2016.02.016

Rosahn, P. D., & Black-Schaffer, B. (1943). Studies in syphilis: III. Mortality and morbidity findings in the Yale autopsy series. *The Yale Journal of Biology and Medicine*, *15*(4), 587–602.

Rothschild, B. M. (2005). History of syphilis. *Clinical Infectious Diseases*, *40*(10), 1454–1463. https://doi.org/10.1086/429626

Rothschild, B. M., & Rothschild, C. (1995). Treponemal disease revisited: Skeletal discriminators for yaws, bejel, and venereal syphilis. *Clinical Infectious Diseases*, *20*(5), 1402–1408. https://doi.org/10.1093/clinids/20.5.1402

Ruimerman, R. (Ronald). (2005). *Modeling and remodeling in bone tissue* [PhD Dissertation, Technische Universiteit Eindhoven]. https://doi.org/10.6100/IR583545

Russo, P. E., & Shryock, L. F. (1945). Bone lesions of congenital syphilis in infants and adolescents: Report of 46 cases. *Radiology*, *44*(5), 477–484. https://doi.org/10.1148/44.5.477

Schaefer, M., Scheuer, L., & Black, S. M. (2009). *Juvenile osteology: A laboratory and field manual*. Elsevier Academic Press.

Schats, R., Hoogland, M., & Waters-Rist, A. (2017). Fysisch antropologisch rapport Margaretha terrein Kampen. In M. Klomp (Ed.), *Myosotis, in de schaduw van het Sint Geertruidengasthuis: Archeologisch onderzoek tussen Boven Nieuwstraat en Burgwal.* (pp. 233–255). Gemeente Zwolle.

Schats, R., & Klomp, M. (2019). In sickness and in health: An archaeological and osteoarchaeological analysis of St. Gertrude's infirmary in Kampen (1382-c. 1611). In R. van Oosten, R. Schats, & K. Fast (Eds.), *Osteoarchaeology in historical context: Cemetery research from the Low Countries*. Sidestone Press.

Schats, R., Kootker, L., & Hoogland, M. (2017, September 9). *Syphilis in the Netherlands. Dating and provenance of three syphilitic individuals from Kampen* [Conference Presentation]. BABAO 2017 Conference, Liverpool, United Kingdom.

Schreiber, B. E., Twigg, S., Marais, J., & Keat, A. C. (2014). Saddle-nose deformities in the rheumatology clinic. *Ear, Nose, & Throat Journal*, *93*(4–5), 45–47.

Schuenemann, V. J., Kumar Lankapalli, A., Barquera, R., Nelson, E. A., Iraíz Hernández, D., Acuña Alonzo, V., Bos, K. I., Márquez Morfín, L., Herbig, A., & Krause, J. (2018). Historic Treponema pallidum genomes from Colonial Mexico retrieved from archaeological remains. *PLoS Neglected Tropical Diseases*, *12*(6), e0006447–e0006447. https://doi.org/10.1371/journal.pntd.0006447

Schultz, M. (2001). Paleohistopathology of bone: A new approach to the study of ancient diseases. *American Journal of Physical Anthropology*, *116*(S33), 106–147. https://doi.org/10.1002/ajpa.10024

Scott, S. R., Shafer, M. M., Smith, K. E., Overdier, J. T., Cunliffe, B., Stafford Jr, T. W., & Farrell, P. M. (2020). Elevated lead exposure in Roman occupants of Londinium: New evidence from the archaeological record. *Archaeometry*, *62*(1), 109–129. https://doi.org/10.1111/arcm.12513

Sefton, A. M. (2001). The Great Pox that was…syphilis. *Journal of Applied Microbiology*, *91*(4), 592–596. https://doi.org/10.1046/j.1365-2672.2001.01494.x

Shackley, M. S. (2010). An Introduction to X-Ray Fluorescence (XRF) Analysis in Archaeology. In *X-Ray Fluorescence Spectrometry (XRF) in Geoarchaeology* (pp. 7–44). Springer. https://doi.org/10.1007/978-1-4419-6886-9_2

Sheehan, M. C., Burke, T. A., Navas-Acien, A., Breysse, P. N., McGready, J., & Fox, M. A. (2014). Global methylmercury exposure from seafood consumption and risk of developmental neurotoxicity: A systematic review. *Bulletin of the World Health Organization*, *92*(4), 254-269F. https://doi.org/10.2471/BLT.12.116152

Shugar, A. N., & Mass, J. L. (Eds.). (2013). *Handheld XRF for Art and Archaeology*. Leuven University Press. https://doi.org/10.2307/j.ctt9qdzfs

Singh, A. E., & Romanowski, B. (1999). Syphilis: Review with emphasis on clinical, epidemiologic, and some biologic features. *Clinical Microbiology Reviews*, *12*(2), 187–209. https://doi.org/10.1128/CMR.12.2.187

Sparling, P. F., Swartz, M. N., Musher, D. M., & Healy, B. P. (2008). Clinical manifestations of syphilis. In K. K. Holmes, P. F. Sparling, W. E. Stamm, P. Piot, J. N. Wasserheit, L. Corey, M. S. Cohen, & D. H. Watts (Eds.), *Sexually transmitted diseases* (4th ed, pp. 661–684). McGraw-Hill Medical.

Spates, W. H. (2011). Mythopoeia and medicine: Decoding Fracastoro's *Syphilis sive Morbus Gallicus* . In V. Tinkler-Villani & C. C. Barfoot (Eds.), *Restoring the mystery of the rainbow* (Vol. 1, pp. 225–247). Brill. https://doi.org/10.1163/9789401200011_014

Speakman, S. A. (n.d.). *Using the Bruker Tracer III-SD Handheld X-Ray Fluorescence Spectrometer using PC software for data collection*. Retrieved 14 June 2023, from http://prism.mit.edu/xray/oldsite/Bruker%20XRF%20SOP.pdf

Speet, B. J. M. (1986). Kampen. In G. Van Herwijnen, C. Van de Kieft, J. C. Visser, & J. G. Wegner, (Eds.), *Historische Stedenatlas van Nederland, Aflevering 4.* Delftse Universitaire Pers. http://resolver.tudelft.nl/uuid:4c4a1bfb-42f4-45e6-837f-38fde534fcdf

Stewart, T. D. (1979). *Essentials of forensic anthropology*. Charles C. Thomas.

Steyn, M., & İşcan, M. Y. (1999). Osteometric variation in the humerus: Sexual dimorphism in South Africans. *Forensic Science International*, *106*(2), 77–85. https://doi.org/10.1016/S0379-0738(99)00141-3

Stirland, A. (1991). Pre-Columbian treponematosis in medieval Britain. *International Journal of Osteoarchaeology*, *1*(1), 39–47. https://doi.org/10.1002/oa.1390010106

Stirland, A. (2009). *Criminals and paupers: The graveyard of St. Margaret Fyebriggate in combusto, Norwich*. Norfolk Museums and Archaeology Service.

Swiderski, R. M. (2008). *Quicksilver: A history of the use, lore and effects of mercury*. McFarland & Co.

Sypkens Smit, J. H. (1953). *Leven en werken van Matthias van Geuns M.D., 1735-1817*. Koninklijke Van Gorcum.

Tampa, M., Sarbu, I., Matei, C., Benea, V., & Georgescu, S. R. (2014). Brief history of syphilis. *Journal of Medicine and Life*, *7*(1), 4–10.

Tchounwou, P. B., Ayensu, W. K., Ninashvili, N., & Sutton, D. (2003). Review: Environmental exposure to mercury and its toxicopathologic implications for public health. *Environmental Toxicology*, *18*(3), 149–175. https://doi.org/10.1002/tox.10116

Todd, T. W. (1920). Age changes in the pubic bone: I. The male white pubis. *American Journal of Physical Anthropology*, *3*(3), 285–334. https://doi.org/10.1002/ajpa.1330030301

Tucker, F. (2007). Kill or cure? The osteological evidence of the mercury treatment of syphilis in 17th- to 19th-century London. *London Archaeologist*, *11*, 220–224. https://doi.org/10.5284/1071108

Turk, J. L. (1995). Syphilitic caries of the skull—The changing face of medicine. *Journal of the Royal Society of Medicine*, *88*(3), 146–148.

Tykot, R. H. (2016). Using nondestructive portable X-ray Fluorescence Spectrometers on stone, ceramics, metals, and other materials in museums: Advantages and limitations. *Applied Spectroscopy*, *70*(1), 42–56. https://doi.org/10.1177/0003702815616745

Tziafas, D. (2005). Composition and structure of cementum: Strategies for bonding. In G. Eliades, D. Watts, & T. Eliades (Eds.), *Dental Hard Tissues and Bonding: Interfacial Phenomena and Related Properties* (pp. 177–193). Springer. https://doi.org/10.1007/3-540-28559-8_8

Ubelaker, D. H. (1978). *Human skeletal remains: Excavation, analysis, interpretation*. Taraxacum.

Urdang, G. (1948). The early chemical and pharmaceutical history of calomel. *Chymia*, *1*, 93–108. https://doi.org/10.2307/27757117

van der Sligte-de Jong, W. H. (1993). *Het gasthuis, een 'weldadige' oudedagsvoorziening?* [Unpublished Master Thesis, Open Universiteit]. https://www.dboverijssel.nl/archieven/5321

van Vliet, L. (2013). Het St. Geertruiden en St. Catharinagasthuis in 1613. *Kamper Almanak*, 135–154.

Van Voorst Vader, P. C. (2016). Bijdrage tot de kennis van de geschiedenis der syfilis in ons land, J.W. van der Valk, 1910. *Nederlands Tijdschrift Voor Dermatologie En Venereologie*, *26*(1), 23–25.

van Zanten, S. (2017). Op ziekenbezoek. Een kijkje in het dagelijks leven van het Sint Geertruidengasthuis. In M. Klomp (Ed.), *Myosotis, in de schaduw van het Sint Geertruidengasthuis: Archeologisch onderzoek tussen Boven Nieuwstraat en Burgwal.* (pp. 27–38). Gemeente Zwolle.

Vandermeersch, B., Arensburg, B., Tillier, A., Rak, Y., Weiner, S., Spiers, M., & Aspillaga, E. (1994). Middle Palaeolithic dental bacteria from Kebara, Israël. *Comptes Rendus De L Academie Des Sciences Serie Ii*, *319*(6), 727–731.

Vargová, L., Vymazalová, K., & Horáčková, L. (2019). A brief history of syphilis in the Czech Lands. *Archaeological and Anthropological Sciences*, *11*(2), 521–530. https://doi.org/10.1007/s12520-017-0558-6

von Hunnius, T. E., Roberts, C. A., Boylston, A., & Saunders, S. R. (2006). Histological identification of syphilis in pre-Columbian England. *American Journal of Physical Anthropology*, *129*(4), 559–566. https://doi.org/10.1002/ajpa.20335

von Hunnius, T. E., Yang, D., Eng, B., Waye, J. S., & Saunders, S. R. (2007). Digging deeper into the limits of ancient DNA research on syphilis. *Journal of Archaeological Science*, *34*(12), 2091–2100. https://doi.org/10.1016/j.jas.2007.02.007

Waldron, T. (2009). *Palaeopathology*. Cambridge University Press.

Walser III, J. W., Kristjánsdóttir, S., Gowland, R., & Desnica, N. (2019). Volcanoes, medicine, and monasticism: Investigating mercury exposure in medieval Iceland. *International Journal of Osteoarchaeology*, *29*(1), 48–61. https://doi.org/10.1002/oa.2712

Weston, D. A. (2008). Investigating the specificity of periosteal reactions in pathology museum specimens. *American Journal of Physical Anthropology*, *137*(1), 48–59. https://doi.org/10.1002/ajpa.20839

Weston, D. A. (2009). Paleohistopathological analysis of pathology museum specimens: Can periosteal reaction microstructure explain lesion etiology? *American Journal of Physical Anthropology*, *140*(1), 186–193. https://doi.org/10.1002/ajpa.21081

Weston, D. A. (2011). Nonspecific infection in paleopathology: Interpreting periosteal reactions. In *A Companion to Paleopathology* (pp. 492–512). John Wiley & Sons, Ltd. https://doi.org/10.1002/9781444345940.ch27

White, T. D., & Folkens, P. A. (2005). *The human bone manual*. Elsevier Academic.

Wicher, V., & Wicher, K. (2001). Pathogenesis of Maternal-Fetal Syphilis Revisited. *Clinical Infectious Diseases*, *33*(3), 354–363. https://doi.org/10.1086/321904

Wood, J. W., Milner, G. R., Harpending, H. C., Weiss, K. M., Cohen, M. N., Eisenberg, L. E., Hutchinson, D. L., Jankauskas, R., Cesnys, G., Katzenberg, M. A., Lukacs, J. R., McGrath, J. W., Roth, E. A., Ubelaker, D. H., & Wilkinson, R. G. (1992). The Osteological Paradox: Problems of Inferring Prehistoric Health from Skeletal Samples [and Comments and Reply]. *Current Anthropology*, *33*(4), 343–370. https://doi.org/10.1086/204084

Workshop of European Anthropologists. (1980). Recommendations for age and sex diagnoses of skeletons. *Journal of Human Evolution*, *9*(7), 517–549. https://doi.org/10.1016/0047-2484(80)90061-5

Yamada, M., Tohno, S., Tohno, Y., Minami, T., Ichii, M., & Okazaki, Y. (1995). Accumulation of mercury in excavated bones of two natives in Japan. *The Science of the Total Environment*, *162*(2–3), 253–256. https://doi.org/10.1016/0048-9697(95)04435-4

Zuckerman, M. K. (2016). More harm than healing? Investigating the iatrogenic effects of mercury treatment on acquired syphilis in Post-Medieval London. *Open Archaeology*, *2*(1). https://doi.org/10.1515/opar-2016-0003

Zuckerman, M. K. (2017). Mercury in the midst of Mars and Venus: Reconstructing gender and socioeconomic status in the context of mercury treatments for acquired syphilis in 17th to 19th century England. In S. C. Agarwal & J. K. Wesp (Eds.), *Exploring sex and gender in bioarchaeology* (pp. 223–261). University of New Mexico Press.

Appendix 1: List of consulted records for archival research

Archive	Inventory numbers	Recorded date (AD)	Description of contents
Oud Archief Kampen (O.A.K., entry code 00001)	1330	1452-1564	Various financial records of Kampen's infirmaries and religious institutions, with records from St. Gertrude's dated 1497-1564
	1344	1564-1658	Various financial records of Kampen's infirmaries and religious institutions
	1345	1641-1796	Financial records of the city hospital
	1371	1729-1742	Financial records by the church wardens of the St. Catharine and Gertrude infirmary
	1372	1743-1756	Financial records by the church wardens of the St. Catharine and Gertrude infirmary
	1373	1757-1768	Financial records by the church wardens of the St. Catharine and Gertrude infirmary
	1374	1769-1780	Financial records by the church wardens of the St. Catharine and Gertrude infirmary
	1375	1781-1793	Financial records by the church wardens of the St. Catharine and Gertrude infirmary
	1376	1794-1807	Financial records by the church wardens of the St. Catharine and Gertrude infirmary
	1377	1808-1811	Financial records by the church wardens of the St. Catharine and Gertrude infirmary
	2311	1603-1796	Various records and letters about general healthcare regulations
	2319	22-01-1799	Letter from the city doctor tot the municipality regarding public health and healthcare regulations
	2328	1475	Draft of new statutes for St. Gertrude's infirmary
Sint Geertruids Gasthuis (entry code 00151)	177	16th century*	Financial and proveniers' registration records of the infirmary
	178	16th-17th century*	Financial and proveniers' registration records of the infirmary
	179	16th-17th century*	Financial and proveniers' registration records of the infirmary
	180	16th-17th century*	Financial and proveniers' registration records of the infirmary
	181	16th-17th century*	Financial and proveniers' registration records of the infirmary
	182	15th-16th century*	Financial records of the infirmary, including more information on owned properties and income
	183	14th century*	Older records, about finances, properties, and the earlier Melijs infirmary
	184	?*	Financial records
Scholae Campensis Bibliotheca	L00185	1710	Catalogue of the library of the Latin school, indicating the available medical literature

*As this archive collection has not yet been digitally inventoried, the exact dating is based on readable date notations and additional notes by Van Zanten (2017).

Appendix 2: List of pXRF samples and raw counts from final analysis with Bruker Tracer 5g

Part 1: elements As to P

Identification	Location	Hg:Rh	As K12	As L1	Ba K12	Ba L1	Ca K12	Cr K12	Cu K12	Fe K12	Hg L1	Hg M1	K K12	La K12	La L1	Mn K12	Nd K12	Nd L1	P K12
S4000V1006	HumR_1	0,005732	1	0	418	29	19791	16	229	5800	15	31	28	22	3	621	4	1	435
S4000V1006	HumR_2	0,003072	1	19	376	0	17750	11	348	5799	9	32	7	370	28	663	1	-5	324
S4000V1006	HumR_3	0,004536	1	73	521	49	17198	1	356	5994	13	21	1	54	16	572	49	1	261
S4000V1006	HumR_4	0,004599	35	0	306	19	20106	14	337	4150	14	22	44	208	34	694	40	11	321
S4000V1006	HumR_5	0,010687	1	26	396	48	20719	5	380	3628	35	42	16	263	12	572	68	-1	405
S4000V1006	RibR_1	0,006382	1	0	168	57	18881	18	425	8740	13	8	73	146	1	978	1	4	317
S4008V1003	RibR_1	0,004933	2	70	241	37	17386	8	217	4307	11	13	10	137	0	510	1	26	353
S4008V1003	RibL_2	0,000733	1	42	439	51	18222	25	269	4128	2	16	64	306	28	563	1	11	298
S4008V1003	RibL_2	0,007928	14	11	347	52	17669	1	188	3929	21	17	38	154	10	468	1	3	285
S4008V1003	RibL_2	0,001063	8	92	283	35	17953	3	197	3917	3	21	11	34	6	505	81	0	256
S4008V1003	RibL_2	0,003157	1	66	350	-1	16927	9	170	3696	8	42	4	155	1	472	11	7	325
S4008V1003	RibL_2	0,002540	1	49	337	17	16682	1	182	3500	6	30	1	116	36	407	87	-1	336
S4008V1003	FemL_1	0,005807	1	32	429	68	20216	34	357	9367	15	7	54	92	5	1274	59	13	268
S4008V1003	FemL_2	0,012195	1	11	592	0	18427	14	268	2247	32	19	36	267	9	176	1	13	317
S4008V1003	FemL_3	0,002554	1	23	270	50	17359	13	393	4149	7	34	6	73	37	214	33	22	363
S4008V1003	FemL_4	0,005726	1	29	401	1	20175	1	411	6472	17	43	43	58	9	387	40	31	357
S4008V1003	FemL_5	0,006344	87	34	441	-29	16508	1	359	10246	19	20	30	232	1	1058	147	3	264
S4008V1003	TibL_l	0,004881	1	-9	642	99	12662	10	546	10126	16	43	190	316	15	610	1	1	173
S4008V1003	TibL_l	0,012420	1	32	368	10	15225	30	333	5290	31	33	52	162	14	618	54	5	168
S4008V1003	TibR_l	0,002628	1	48	497	4	14513	23	375	6250	7	25	97	93	10	749	39	4	279
S4008V1003	TibR_l	0,006950	1	17	281	27	16681	29	479	4996	17	12	96	41	13	693	65	14	294
S4008V1003	FemR_l	0,005934	44	48	748	42	12664	31	312	8742	15	23	165	131	8	551	7	0	194
S4011V1012	RibL_1	0,005730	1	-2	387	14	21041	6	298	2542	17	34	24	131	1	506	67	10	470
S4011V1012	FemL_1	0,007023	1	22	324	1	22579	2	204	4177	18	1	36	85	11	766	70	27	342
S4011V1012	FemL_2	0,000361	1	53	111	8	17888	1	305	5170	1	6	17	243	12	1153	41	36	348
S4011V1012	FemL_3	0,012298	1	13	243	16	21334	27	378	3611	38	0	1	109	15	646	48	19	508
S4011V1012	FemL_4	0,002464	2	6	327	1	16314	49	410	6291	6	22	28	105	0	1464	32	10	263

Identification	Location	Hg:Rh	As K12	As L1	Ba K12	Ba L1	Ca K12	Cr K12	Cu K12	Fe K12	Hg L1	Hg M1	K K12	La K12	La L1	Mn K12	Nd K12	Nd L1	P K12
S4011V1012	FemL_5	0,011720	1	41	369	33	19700	4	347	9698	31	16	87	96	27	1087	65	1	355
S4013V1008	FemL_1	0,001280	1	48	473	114	21473	8	486	13759	4	30	37	167	-2	755	94	1	555
S4013V1008	FemL_2	0,005525	1	10	253	122	12868	16	242	22984	14	17	115	114	60	818	1	28	221
S4013V1008	FemL_3	0,005670	1	12	518	59	17872	40	236	15990	17	13	1	114	30	1064	222	1	326
S4013V1008	FemL_4	0,010635	16	26	702	135	16767	25	218	26204	31	22	47	290	30	1877	15	0	353
S4013V1008	FemL_5	0,004100	1	-1	288	17	21277	17	252	6143	13	26	1	147	1	675	99	35	473
S4013V1008	TibL_c	0,003204	1	27	329	20	21321	43	341	4205	11	47	57	246	-7	487	49	0	271
S4013V1008	TibL_l	0,012997	1	7	361	46	14483	20	444	8960	33	12	68	155	15	1369	14	0	251
S4013V1008	FibL_l	0,007825	1	26	385	2	15161	56	445	5249	19	23	112	138	2	891	139	12	246
S4013V1008	FibL_c	-0,002699	1	29	334	1	14930	16	352	6442	-7	23	130	273	4	672	111	3	213
S4013V1008	RibR_1	0,003465	1	19	600	36	15273	1	174	8773	8	32	1	209	9	990	61	14	315
S4015V1019	RibR_2	0,007630	1	47	282	7	19319	14	201	2042	17	16	1	19	15	143	1	10	336
S4015V1019	FemL_1	0,008808	1	16	334	12	17158	17	214	6794	26	12	250	145	1	318	48	2	271
S4015V1019	FemL_2	0,004203	1	57	144	42	18046	9	175	2949	10	33	18	144	0	187	75	8	350
S4015V1019	FemL_3	0,001531	1	4	482	62	17139	2	181	6926	4	54	8	93	33	269	73	4	291
S4015V1019	FemL_4	0,007340	1	21	243	36	16423	23	124	1390	17	15	9	42	33	156	2	1	291
S4015V1019	FemL_5	0,003956	1	16	482	0	20138	17	143	1250	12	17	1	168	54	138	30	11	436
S4019V1018	FemL_1	-0,000364	1	14	99	35	21568	32	216	4226	-1	30	61	58	35	333	89	0	419
S4019V1018	FemL_2	0,012681	1	29	179	3	18838	29	222	1754	35	22	14	155	11	230	51	12	386
S4019V1018	FemL_3	0,004912	1	13	121	69	19802	10	323	3126	15	22	1	90	32	283	1	1	395
S4019V1018	FemL_4	0,005017	1	9	105	24	21946	49	500	6402	16	7	41	80	11	1438	1	23	384
S4019V1018	FemL_5	0,012218	39	0	330	-1	19962	13	266	12675	33	37	44	157	1	1171	1	3	456
S4019V1018	RibL_2	0,003686	47	0	450	7	20816	30	228	4298	9	14	9	120	0	697	1	29	447
S4019V1018	RibL_1	0,002621	2	5	313	56	20025	4	505	8073	7	42	38	145	13	1212	1	0	319
S4021V1021	RibL_2	0,010655	50	46	249	-27	19819	4	228	2019	27	16	1	171	38	212	62	1	326
S4021V1021	FemL_1	0,000941	1	43	470	30	19387	1	347	8574	3	19	63	154	9	347	1	1	346
S4021V1021	FemL_2	0,005183	1	19	209	11	18979	1	283	3344	15	30	24	81	6	184	1	9	434
S4021V1021	FemL_3	0,012442	1	59	189	14	20086	1	305	2605	40	18	48	201	2	158	25	19	341
S4021V1021	FemL_4	0,009190	1	29	134	12	18948	11	437	2519	27	46	113	162	18	235	25	-1	275
S4021V1021	FemL_5	-0,000315	64	20	235	41	20678	28	368	9321	-1	36	4	196	19	679	42	5	383
S4023V1025	FemL_1	0,002538	1	54	622	48	20950	44	230	6483	7	47	30	134	31	567	38	6	398

Identification	Location	Hg:Rh	As K12	As L1	Ba K12	Ba L1	Ca K12	Cr K12	Cu K12	Fe K12	Hg L1	Hg M1	K K12	La K12	La L1	Mn K12	Nd K12	Nd L1	P K12
S4023V1025	FemL_2	0,006100	8	10	304	90	16496	30	524	11367	16	15	48	172	275	1366	131	1	287
S4023V1025	FemL_3	0,009705	1	15	480	16	18701	12	498	13508	26	56	1	110	0	1074	167	5	373
S4023V1025	FemL_4	0,007164	1	18	565	20	17609	32	540	10585	19	57	22	96	47	1078	1	1	277
S4023V1025	FemL_5	0,010007	54	55	286	38	19660	43	737	9275	27	35	16	8	28	906	78	-1	386
S4023V1025	TibL_c	0,001360	43	28	686	26	16048	1	385	21481	4	12	81	98	1	1437	81	7	298
S4023V1025	TibL_l	0,003212	1	20	493	19	19610	33	576	10573	10	13	76	194	34	1706	1	11	401
S4023V1025	RibL_2	0,004475	1	42	580	1	20032	7	285	3772	11	32	1	97	19	550	131	13	337
S4027V1028	RibR_2	0,001857	1	46	441	65	17316	14	421	8868	5	24	89	111	22	965	1	1	283
S4027V1028	FemL_1	0,006870	1	13	630	93	17431	9	335	5837	20	10	42	204	2	624	1	9	322
S4027V1028	FemL_2	0,001747	42	55	82	32	18508	26	157	3351	5	23	4	126	17	122	1	14	427
S4027V1028	FemL_3	0,007886	1	67	355	68	20961	23	376	3463	25	9	1	168	64	142	208	11	394
S4027V1028	FemL_4	0,001538	1	28	277	3	20190	45	307	2813	5	30	21	306	12	214	1	8	353
S4027V1028	FemL_5	0,006331	1	26	404	89	18618	0	299	7175	18	31	1	263	22	789	1	8	302
S4027V1028	TibL_l	0,001229	1	54	459	35	18564	21	403	6110	4	20	87	126	45	595	102	6	258
S4027V1028	TibL_l	-0,002526	1	27	487	16	18639	1	441	2954	-8	30	1	246	11	125	45	10	331
S4027V1028	TibL_l	0,004372	10	45	331	28	15350	1	332	5379	11	18	72	63	1	313	96	13	285
S4031V1030	RibR_1	0,016730	1	0	517	13	19228	10	407	6050	44	5	37	455	1	232	1	7	360
S4031V1030	RibR_2	0,016249	1	-1	378	-1	12315	1	224	5991	24	37	20	1	16	268	19	0	263
S4031V1030	FemL_1	0,003227	1	76	546	25	20470	14	341	8355	11	12	73	38	18	879	1	1	440
S4031V1030	FemL_2	0,003945	1	54	416	43	20259	16	336	6824	12	38	1	209	4	336	1	-1	415
S4031V1030	FemL_3	0,017014	1	32	-30	16	11507	13	251	3665	31	41	1	78	4	178	1	12	280
S4031V1030	FemL_4	0,001736	1	42	181	79	18368	26	452	8689	5	32	129	41	-2	655	75	1	428
S4031V1030	FemL_5	0,005678	1	31	419	5	19677	9	453	7768	16	24	1	41	0	689	39	3	382
S4033V1032	HumR_1	0,005876	1	32	163	9	17682	19	282	7787	17	8	96	274	-1	589	46	-2	294
S4033V1032	HumR_2	0,001899	1	13	318	26	21439	11	415	3375	6	20	3	242	13	219	60	2	495
S4033V1032	HumR_3	0,003530	1	67	469	32	20373	1	448	2579	11	17	1	230	27	272	55	0	403
S4033V1032	HumR_4	0,001685	38	0	478	28	14607	1	331	3383	4	26	25	208	5	369	12	0	244
S4033V1032	HumR_5	0,006207	1	62	406	57	14386	8	325	14114	17	44	97	92	14	1472	71	0	183
S4033V1032	HumL_3	0,005215	1	10	247	56	20205	10	337	3654	17	23	95	148	26	158	38	4	379
S4033V1032	HumL_l	0,010417	1	-2	424	1	12158	30	508	8717	28	9	169	250	4	1081	167	19	175
S4033V1032	RibR_2	0,007661	1	14	404	59	19048	5	253	2973	17	38	1	93	41	892	1	1	344

Identification	Location	Hg:Rh	As K12	As L1	Ba K12	Ba L1	Ca K12	Cr K12	Cu K12	Fe K12	Hg L1	Hg M1	K K12	La K12	La L1	Mn K12	Nd K12	Nd L1	P K12
S4033V1032	RibL_2	0,003034	55	57	506	-7	19469	1	302	2960	8	19	11	104	0	1938	61	46	370
S4040V1041	FemR_1	0,000687	53	20	405	1	22477	129	194	6516	2	8	57	233	7	1078	82	8	364
S4040V1041	FemR_2	0,009272	28	42	279	41	18861	20	161	5383	26	35	24	100	14	697	1	17	356
S4040V1041	FemR_3	0,005597	1	21	100	43	19900	12	221	6075	18	27	61	196	7	751	8	2	363
S4040V1041	FemR_4	0,009581	1	30	183	60	17108	1	298	11816	27	8	71	0	18	948	118	-1	261
S4040V1041	FemR_5	0,009095	15	13	224	58	16825	14	249	13015	22	26	52	348	2	947	1	-1	390
S4040V1041	RibL_1	0,011397	30	1	504	5	19227	5	233	7554	31	28	1	83	30	747	1	0	276
S4045V1049	FemL_l	0,007184	1	61	186	1	20432	20	283	3435	21	21	13	62	5	442	1	35	363
S4045V1049	FemL_2	0,003180	1	23	238	36	17130	21	273	4281	9	23	65	128	33	640	1	1	194
S4045V1049	FemL_3	0,000649	1	28	58	86	19457	1	304	5134	2	59	1	152	2	934	1	0	498
S4045V1049	FemL_4	0,007034	39	6	131	74	17795	46	276	7265	17	23	1	98	9	1184	136	0	279
S4045V1049	FemL_5	0,003833	3	22	451	1	14881	3	317	4140	9	4	61	392	-6	686	51	18	259
S4045V1049	TibL_c	0,007361	1	35	304	10	16442	1	325	7574	19	31	82	142	29	1163	50	11	285
S4045V1049	TibL_l	0,003283	1	17	166	51	16284	32	477	8717	9	34	60	45	13	771	1	4	251
S4045V1049	TibL_l	0,006317	1	28	325	11	13150	8	412	8093	17	30	171	170	-1	835	26	2	257
S4045V1049	TibL_l	0,005123	29	14	492	51	17564	11	338	7950	14	36	129	135	20	956	47	1	218
S4045V1049	HumR_1	0,005800	1	49	585	28	19320	1	741	7688	17	11	52	59	1	598	63	3	312
S4045V1049	HumR_2	0,006892	1	26	292	1	19704	28	552	5062	20	8	55	125	-15	483	19	17	327
S4045V1049	HumR_3	-0,001587	1	-2	270	20	20544	21	721	4688	-5	37	65	248	7	424	89	-4	264
S4045V1049	HumR_4	0,013187	1	38	378	73	13615	1	467	3226	24	17	54	52	4	292	1	0	231
S4045V1049	HumR_5	0,017221	1	5	178	18	12032	19	438	2189	29	6	1	185	0	210	36	9	267
S4045V1049	RibL_2	0,005328	19	13	339	17	16748	13	484	4371	10	34	32	194	24	479	1	0	304
S4045V1049	RibR_2	0,000441	1	0	262	26	19609	3	350	2389	1	33	28	104	1	373	1	1	361
S4052V1052	HumR_1	0,004235	18	19	395	2	20169	31	228	4692	15	24	1	122	7	537	2	6	237
S4052V1052	HumR_2	0,001041	1	37	114	0	13712	1	217	2471	2	11	1	128	5	374	56	30	319
S4052V1052	HumR_3	0,000423	1	0	163	2	17872	5	172	2511	1	5	36	107	20	371	1	2	332
S4052V1052	HumR_4	0,014223	1	18	615	32	15917	4	340	11136	39	35	31	205	6	1348	75	10	268
S4052V1052	HumR_5	0,002058	1	0	206	61	19848	17	379	7888	6	54	1	123	-5	704	1	24	400
S4052V1052	FemL_1	0,004227	1	31	392	53	21426	3	325	3402	15	21	38	162	40	583	131	12	448
S4052V1052	FemL_2	0,003928	1	-5	363	17	18837	53	305	8897	10	22	1	148	20	1975	1	5	298
S4052V1052	FemL_3	0,005333	1	52	180	16	19396	11	292	8049	16	16	22	69	42	1585	1	1	277

Identification	Location	Hg:Rh	As K12	As L1	Ba K12	Ba L1	Ca K12	Cr K12	Cu K12	Fe K12	Hg L1	Hg M1	K K12	La K12	La L1	Mn K12	Nd K12	Nd L1	P K12
S4052V1052	FemL_4	0,008214	1	-22	229	49	21130	14	388	7314	24	10	34	104	12	1555	166	24	320
S4052V1052	FemL_5	0,012476	40	33	296	61	17217	103	542	6520	33	78	3	189	6	1176	184	1	331
S4052V1052	TibL_c	0,003622	1	40	309	37	17386	21	391	10121	9	45	69	43	0	1299	1	12	219
S4052V1052	TibL_l	0,004431	44	37	460	0	16948	24	340	13329	13	36	88	-1	22	1312	174	5	378
S4052V1052	TibL_l	0,003900	1	-2	297	47	19315	0	313	12253	13	13	1	120	13	1323	23	6	301
S4053V1054	FemL_1	0,018631	15	22	765	15	20493	6	495	11055	49	23	46	146	0	1573	26	1	408
S4053V1054	FemL_2	0,006366	1	18	394	58	15178	1	447	9185	12	14	21	20	24	980	38	0	367
S4053V1054	FemL_3	0,005247	1	28	617	59	21736	1	353	9916	15	53	1	139	13	1181	1	11	400
S4053V1054	FemL_4	0,009150	79	0	799	38	21689	1	464	10634	31	12	13	294	18	1174	13	1	423
S4053V1054	FemL_5	0,002606	1	23	443	78	20261	7	241	4951	8	20	1	203	3	604	81	6	321
S4053V1054	RibL_2	0,006474	1	52	671	31	19388	23	310	5777	17	7	2	184	28	604	1	14	424
S4063V1065	FemL_1	0,008037	1	-1	788	22	20221	1	313	7878	21	11	30	139	1	693	19	5	362
S4063V1065	FemL_2	0,000423	1	71	230	50	17525	1	493	2329	1	9	3	79	40	360	137	0	417
S4063V1065	FemL_3	0,009844	1	0	446	5	21487	21	333	7784	31	22	24	-15	2	1081	78	0	375
S4063V1065	FemL_4	-0,002602	1	0	374	54	21338	6	444	4111	-8	16	1	337	34	446	91	14	352
S4063V1065	FemL_5	0,009936	1	29	494	64	20107	1	226	5323	28	6	21	88	4	520	41	4	302
S4063V1065	TibR_c	0,001059	1	-39	243	-1	17920	12	327	3261	3	18	102	268	0	339	93	-2	244
S4063V1065	TibR_l	0,001927	1	24	664	52	17388	6	700	9042	6	16	107	166	0	1053	1	1	337
S4063V1065	RibL_2	0,002491	1	0	598	36	18518	14	263	6859	6	30	5	250	4	765	38	16	337
S4068V1071	RibR_2	0,002137	108	19	854	78	20581	16	507	5320	7	23	22	375	23	864	129	16	353
S4068V1071	FemL_1	0,000672	1	50	382	46	20208	9	599	3205	2	19	38	248	2	185	40	0	290
S4068V1071	FemL_2	0,007143	17	43	106	15	14395	2	191	3700	15	18	43	152	6	295	110	3	197
S4068V1071	FemL_3	0,009063	1	51	339	24	18900	33	318	2615	27	19	61	145	55	275	18	-1	325
S4068V1071	FemL_4	0,006674	1	33	310	18	18371	1	371	5362	19	17	99	17	14	409	88	21	284
S4068V1071	FemL_5	0,006844	1	16	368	0	17863	15	266	4700	17	21	58	200	5	537	30	7	372
S4068V1071	TibL_c	0,004779	1	25	339	35	15285	34	368	5672	12	7	70	287	2	667	1	5	293
S4068V1071	TibL_l	0,003956	1	42	134	12	13345	30	404	5282	9	25	108	142	6	391	58	28	141
S4074V1078	RibR_2	0,007573	21	51	495	37	17866	16	174	4675	18	17	23	292	-1	639	3	-12	325
S4074V1078	FemL_1	0,009240	120	47	1161	57	18420	1	213	22788	26	22	86	1	0	1513	17	0	369
S4074V1078	FemL_2	0,005376	1	0	182	0	18992	1	309	5390	16	29	69	118	0	1005	1	1	437
S4074V1078	FemL_3	0,009635	1	31	186	17	17845	12	324	9612	29	5	58	155	-1	1428	39	4	324

Identification	Location	Hg:Rh	As K12	As L1	Ba K12	Ba L1	Ca K12	Cr K12	Cu K12	Fe K12	Hg L1	Hg M1	K K12	La K12	La L1	Mn K12	Nd K12	Nd L1	P K12
S4074V1078	FemL_5	0,004765	1	30	239	38	17828	20	307	13842	14	37	146	128	1	1935	142	4	338
S4074V1078	FemL_4	0,004538	1	22	247	8	20916	61	390	6199	14	8	5	220	20	802	159	37	396
S4074V1078	HumR_c	0,005165	18	-15	189	1	21010	1	450	8648	16	38	3	0	7	1220	1	5	436
S4074V1078	HumR_l	-0,001296	1	31	1035	53	13438	3	365	17396	-3	54	204	78	1	1178	54	4	228
S4084V1086	RibR_2	0,005478	8	34	332	14	19661	31	268	10033	16	12	74	44	10	606	66	1	352
S4084V1086	FemL_1	0,005837	1	21	343	19	19771	28	232	4642	16	14	153	113	12	414	88	0	287
S4084V1086	FemL_2	0,004498	1	0	293	43	18465	31	592	7262	13	17	20	120	34	688	96	5	298
S4084V1086	FemL_3	0,002786	1	19	431	23	19949	1	621	7323	9	44	70	196	-6	1038	1	2	361
S4084V1086	FemL_4	0,002065	1	28	175	30	20757	22	359	12018	6	16	101	139	13	1124	30	8	477
S4084V1086	FemL_5	0,005950	1	-7	444	16	13923	5	168	4772	13	11	31	352	6	504	4	1	231
S4084V1086	FemL_l	0,010181	1	0	884	74	13539	5	365	17091	27	47	224	-6	0	1136	33	1	187
S4084V1086	TibL_c	0,004181	1	42	266	16	17139	12	352	5202	13	3	227	119	6	1043	74	1	270
S4084V1086	TibL_l	0,002561	1	53	631	9	12592	48	275	11409	6	14	126	27	-1	1809	70	5	200
S4084V1086	TibL_l	0,000400	1	38	558	3	13654	3	275	10872	1	22	142	191	12	1576	111	1	226
S4084V1086	TibL_l	0,007145	1	-5	519	27	12336	26	281	13933	20	19	186	336	13	927	1	-3	193
S4084V1086	HumL_1	0,002471	1	47	249	46	17673	12	346	5245	6	34	15	127	5	604	1	5	344
S4084V1086	HumL_2	0,011617	1	32	219	35	18633	1	200	1773	36	25	2	19	16	256	49	3	325
S4084V1086	HumL_3	0,008544	1	22	91	57	17495	15	400	4140	22	39	36	1	1	519	10	10	247
S4084V1086	HumL_4	0,005546	1	57	374	40	19771	3	341	5858	17	8	12	132	10	756	147	19	363
S4084V1086	HumL_5	0,006054	1	47	216	70	15333	15	365	7822	16	33	23	62	0	809	6	4	270
S4084V1086	HumL_l	0,000000	1	12	1543	93	13410	44	374	17946	0	15	276	43	5	1250	51	8	195
S4096V1100	RibR_2	0,002084	15	35	220	46	18475	4	241	5600	5	13	38	4	2	841	48	-1	317
S4096V1100	RibL_2	0,001820	114	44	263	1	20337	1	414	5082	5	26	40	38	2	751	1	2	417
S4096V1100	FemL_1	0,008568	21	60	724	35	23001	56	473	7591	28	3	24	51	7	1424	1	0	467
S4096V1100	FemL_2	0,005252	1	30	259	72	21758	0	374	7860	15	28	14	172	16	1615	45	9	427
S4096V1100	FemL_3	0,009911	1	16	273	46	20549	1	321	7525	29	6	1	121	31	1474	56	26	407
S4096V1100	FemL_4	0,004037	1	0	208	68	17502	10	342	13688	11	27	1	142	3	1849	112	14	307
S4096V1100	FemL_5	0,000645	94	11	372	11	21248	1	328	12598	2	20	9	223	1	1587	49	2	504
Medische collectie GPVI	FemL_1	-0,000692	1	41	59	0	19290	3	178	855	-2	19	82	1	1	71	65	2	273
Medische collectie GPVI	FemL_2	0,006603	1	-1	207	25	16791	14	220	717	18	53	204	42	9	31	54	1	259
Medische collectie GPVI	FemL_3	0,002088	1	45	81	88	16774	14	163	1259	6	41	227	150	4	66	1	16	291

Identification	Location	Hg:Rh	As K12	As L1	Ba K12	Ba L1	Ca K12	Cr K12	Cu K12	Fe K12	Hg L1	Hg M1	K K12	La K12	La L1	Mn K12	Nd K12	Nd L1	P K12
Medische collectie GPVI	FemL_4	-0,001057	1	18	147	30	15966	1	154	845	-3	28	135	104	15	43	48	7	209
Medische collectie GPVI	FemL_5	0,002509	1	50	288	48	17853	19	129	1129	8	34	144	206	0	54	67	-2	283
Blokhuizen 1983-1 64	FemL_1	0,005089	1	100	436	0	18734	1	95	5606	18	15	148	150	50	86	31	9	254
Blokhuizen 1983-1 65	FemL_2	0,009123	16	0	276	41	14533	38	99	2085	18	10	83	122	11	113	42	9	267
Blokhuizen 1983-1 66	FemL_3	0,007711	280	11	232	30	18002	86	105	29053	22	18	1	311	93	848	40	13	317
Blokhuizen 1983-1 67	FemL_4	0,005061	74	40	348	15	12820	1	90	6263	10	15	163	281	10	139	109	15	159
Blokhuizen 1983-1 68	FemL_5	0,009597	176	87	428	96	16722	1	112	23528	30	14	142	68	49	7285	3	10	236
Soil - Restricted materials	N/A	0,013048	1	40	540	1	2765	5	217	10730	28	30	375	39	-1	175	14	0	1
Soil - Restricted materials	N/A	0,005348	1	55	629	13	2723	34	253	11541	11	14	373	-10	-4	193	83	16	66
Soil - Mudrock Air	N/A	0,001534	1	81	938	88	25434	210	1667	104052	34	27	3407	291	1	1493	1	20	99
Soil - Mudrock Air	N/A	-0,000665	1	93	720	85	26330	85	1841	106537	-15	48	3669	259	1	1513	108	15	32

Appendix 2: List of pXRF samples and raw counts from final analysis with Bruker Tracer 5g
Part 2: elements Pb to Zn

Identification	Location	Pb L1	Pb M1	Pd K12	Pd L1	Rb K12	Rb L1	Rh K12	Rh L1	Sn K12	Sn L1	Sr K12	Sr L1	Ti K12	U L1	U M1	Y K12	Y L1	Zn K12
S4000V1006	HumR_1	431	6	1590	-1	123	20	2617	1	1288	-1	6949	1	46	52	0	86	1	962
S4000V1006	HumR_2	390	0	1845	1	1	12	2930	6	1548	23	7099	29	39	15	1	114	1	767
S4000V1006	HumR_3	326	0	2156	35	5	20	2866	1	1834	10	6759	18	1	48	4	76	44	1063
S4000V1006	HumR_4	464	11	2326	36	3	23	3044	0	1766	4	6077	0	34	0	0	72	128	1171
S4000V1006	HumR_5	392	0	2359	0	16	63	3275	13	1741	2	5454	1	3	8	0	53	1	741
S4000V1006	RibR_1	438	0	1547	20	10	35	2037	9	1605	34	7506	13	41	14	1	122	25	1408
S4008V1003	RibR_1	242	25	1747	0	27	4	2230	23	1385	15	6327	19	21	16	0	24	1	851
S4008V1003	RibL_2	470	10	2034	14	28	27	2728	1	1602	3	4871	17	8	1	4	6	1	641
S4008V1003	RibL_2	415	25	1918	1	35	12	2649	13	1660	0	4650	0	1	16	6	-1	62	623
S4008V1003	RibL_2	436	29	2097	0	7	86	2823	36	1741	2	4557	4	17	18	0	32	102	643
S4008V1003	RibL_2	373	13	2055	0	12	18	2534	27	1656	9	4567	40	49	17	16	43	1	594
S4008V1003	RibL_2	419	15	1971	2	25	0	2362	53	1537	8	4468	-1	7	9	1	17	86	526
S4008V1003	FemL_1	577	4	1387	41	45	26	2583	14	1190	35	9232	9	23	23	0	98	79	908

Identification	Location	Pb L1	Pb M1	Pd K12	Pd L1	Rb K12	Rb L1	Rh K12	Rh L1	Sn K12	Sn L1	Sr K12	Sr L1	Ti K12	U L1	U M1	Y K12	Y L1	Zn K12
S4008V1003	FemL_2	294	7	2115	2	27	18	2624	10	1388	2	3606	0	38	7	0	40	46	780
S4008V1003	FemL_3	313	26	2170	-2	31	8	2741	1	1462	3	3595	35	15	24	0	34	1	1340
S4008V1003	FemL_4	443	0	2348	0	7	50	2969	47	1695	0	6750	28	50	-9	0	31	10	889
S4008V1003	FemL_5	267	0	2126	0	45	23	2995	41	1491	1	4879	14	102	16	6	18	13	483
S4008V1003	TibL_l	514	0	2234	36	565	64	3278	1	1767	0	6714	0	139	69	0	250	38	652
S4008V1003	TibL_l	432	4	1874	1	20	39	2496	22	1501	7	7191	36	58	30	0	55	67	428
S4008V1003	TibR_l	463	12	1929	0	229	44	2664	1	1395	0	7429	29	77	29	1	125	1	626
S4008V1003	TibR_l	500	0	1939	58	168	21	2446	1	1580	0	7166	7	29	13	30	140	1	654
S4008V1003	FemR_l	395	0	1772	0	171	-1	2528	31	1484	3	8100	40	55	25	0	93	52	706
S4011V1012	RibL_1	272	16	2304	1	115	26	2967	10	1903	0	5615	41	-1	27	0	147	11	852
S4011V1012	FemL_1	667	0	1713	24	45	28	2563	0	1188	2	6160	12	89	9	25	68	79	1210
S4011V1012	FemL_2	665	20	2093	2	21	3	2768	0	1405	0	5506	52	31	9	7	141	1	1148
S4011V1012	FemL_3	517	16	2371	27	5	24	3090	-9	1768	1	4945	0	108	29	0	90	1	927
S4011V1012	FemL_4	540	5	1793	1	1	7	2435	29	1477	8	6306	26	115	9	2	70	2	881
S4011V1012	FemL_5	466	9	2093	0	4	48	2645	65	1760	30	5241	0	91	11	4	64	73	1137
S4013V1008	FemL_1	750	1	1927	45	104	31	3125	4	1356	-1	7649	33	1	18	-1	103	1	1555
S4013V1008	FemL_2	418	1	1984	2	57	42	2534	0	1697	0	5718	0	41	11	14	68	39	1000
S4013V1008	FemL_3	219	16	2213	27	18	-3	2998	37	1485	0	5827	-8	1	29	44	1	109	818
S4013V1008	FemL_4	595	1	2059	1	8	6	2915	46	1439	0	7163	24	38	35	-1	36	42	976
S4013V1008	FemL_5	392	28	2266	1	4	44	3171	29	1630	7	5073	20	52	26	0	33	1	764
S4013V1008	TibL_c	440	4	2258	13	38	23	3433	22	1765	16	4241	0	35	8	0	37	131	891
S4013V1008	TibL_l	441	0	1858	27	106	9	2539	1	1687	9	5714	0	64	27	0	58	50	1102
S4013V1008	FibL_l	508	1	1757	1	102	3	2428	1	1457	1	6100	48	165	37	6	87	46	1054
S4013V1008	FibL_c	388	4	1991	50	1	59	2594	8	1597	0	5228	10	110	22	-2	104	18	936
S4013V1008	RibR_1	242	0	1973	3	42	71	2309	39	1557	0	5525	13	9	35	1	14	52	868
S4015V1019	RibR_2	408	24	2031	0	268	1	2228	1	1629	26	5168	2	47	18	0	155	1	667
S4015V1019	FemL_1	1604	34	1860	0	177	28	2952	17	1339	0	4846	40	73	9	0	166	14	950
S4015V1019	FemL_2	582	13	2009	0	1	10	2379	13	1273	27	3959	9	15	-6	0	74	36	1268
S4015V1019	FemL_3	902	1	2033	0	5	9	2613	107	1503	0	3976	14	12	24	49	19	15	841
S4015V1019	FemL_4	566	1	1677	21	53	-1	2316	11	1214	19	2823	47	17	20	0	45	8	571

Identification	Location	Pb L1	Pb M1	Pd K12	Pd L1	Rb K12	Rb L1	Rh K12	Rh L1	Sn K12	Sn L1	Sr K12	Sr L1	Ti K12	U L1	U M1	Y K12	Y L1	Zn K12
S4015V1019	FemL_5	410	20	2219	8	1	3	3033	1	1716	11	3535	49	24	2	0	0	56	421
S4019V1018	FemL_1	421	0	1888	1	86	24	2747	26	1311	6	5395	1	1	3	-1	7	1	870
S4019V1018	FemL_2	344	7	2247	0	8	-10	2760	17	1587	23	3236	27	41	-1	6	18	1	714
S4019V1018	FemL_3	594	1	2378	8	1	39	3054	26	1663	1	3595	0	45	-3	0	49	42	1292
S4019V1018	FemL_4	948	37	2246	32	12	13	3189	1	1532	4	5259	34	111	-9	0	77	23	1623
S4019V1018	FemL_5	393	30	2103	15	45	3	2701	22	1801	0	4342	21	63	13	9	10	1	874
S4019V1018	RibL_2	353	2	1557	3	61	36	2442	10	1566	17	7057	43	32	49	0	57	41	1106
S4019V1018	RibL_1	625	0	2098	0	34	17	2671	34	1741	9	6908	0	3	20	0	72	62	1612
S4021V1021	RibL_2	236	11	2249	11	121	2	2534	0	1517	4	3831	62	13	31	1	47	41	531
S4021V1021	FemL_1	779	15	2064	42	223	29	3189	0	1608	0	6214	19	32	31	0	112	23	731
S4021V1021	FemL_2	410	23	2404	13	3	50	2894	14	1585	11	2411	32	1	-7	0	-1	32	598
S4021V1021	FemL_3	395	32	2583	44	23	0	3215	28	1960	0	2206	27	87	-3	7	0	19	744
S4021V1021	FemL_4	387	0	2144	8	32	5	2938	38	1493	11	3285	2	21	4	17	35	72	547
S4021V1021	FemL_5	557	17	2166	26	10	30	3172	1	1848	0	3818	1	5	-2	9	37	33	940
S4023V1025	FemL_1	340	11	1484	0	47	49	2758	46	1343	-1	8055	7	1	16	0	73	1	751
S4023V1025	FemL_2	368	8	2101	0	10	53	2623	20	1508	-2	9927	21	1	21	0	87	49	1329
S4023V1025	FemL_3	430	0	2293	8	1	8	2679	18	1588	0	9896	0	23	18	-1	39	55	1194
S4023V1025	FemL_4	402	22	1866	1	27	61	2652	102	1337	9	10072	2	39	9	0	-3	114	872
S4023V1025	FemL_5	425	3	2195	4	1	21	2698	23	1657	20	9218	9	1	-1	21	55	1	1855
S4023V1025	TibL_c	719	22	1839	1	30	27	2941	7	1470	7	12215	1	105	-1	0	103	98	1251
S4023V1025	TibL_l	606	28	2213	0	9	-1	3113	2	1861	0	11656	28	75	60	0	101	1	984
S4023V1025	RibL_2	406	9	1678	1	14	1	2458	27	1289	10	7060	26	27	22	1	60	39	731
S4027V1028	RibR_2	429	0	1939	0	63	38	2692	37	1433	0	7391	20	40	35	1	58	1	1398
S4027V1028	FemL_1	343	0	2065	8	307	14	2911	1	1440	0	6927	40	1	33	1	161	1	559
S4027V1028	FemL_2	254	4	1913	9	26	64	2862	1	1560	40	3530	0	1	12	0	0	1	1180
S4027V1028	FemL_3	529	9	2550	17	10	2	3170	16	1883	1	5718	15	1	15	-1	68	67	1210
S4027V1028	FemL_4	279	1	2168	0	1	1	3250	30	1643	24	5496	37	0	17	23	24	82	542
S4027V1028	FemL_5	288	0	2210	9	19	7	2843	53	1575	44	5359	2	14	-5	11	-1	7	683
S4027V1028	TibL_l	551	4	2000	1	76	47	3254	36	1530	0	10036	34	93	28	0	16	47	922
S4027V1028	TibL_l	423	4	2135	30	57	66	3167	39	1644	0	8001	27	15	12	36	39	12	888

Identification	Location	Pb L1	Pb M1	Pd K12	Pd L1	Rb K12	Rb L1	Rh K12	Rh L1	Sn K12	Sn L1	Sr K12	Sr L1	Ti K12	U L1	U M1	Y K12	Y L1	Zn K12
S4027V1028	TibL_l	465	11	1974	0	75	25	2516	35	1435	9	7233	27	93	12	0	19	31	758
S4031V1030	RibR_1	814	45	1898	35	95	31	2630	0	1492	2	6034	63	47	24	0	37	2	1161
S4031V1030	RibR_2	295	13	1383	10	47	2	1477	0	1285	9	4489	0	1	7	2	12	1	513
S4031V1030	FemL_1	533	6	2192	23	58	90	3409	2	1690	1	6768	1	7	4	1	-1	1	1188
S4031V1030	FemL_2	480	1	2292	66	-7	32	3042	2	1610	10	3615	33	15	0	7	-2	61	1188
S4031V1030	FemL_3	273	12	1537	1	12	19	1822	37	1220	0	2347	24	18	20	2	30	23	915
S4031V1030	FemL_4	869	16	2008	0	41	26	2881	-2	1448	0	5687	22	1	7	0	91	1	1103
S4031V1030	FemL_5	642	0	1920	1	11	8	2818	10	1397	23	4676	26	12	8	-29	14	61	1140
S4033V1032	HumR_1	420	38	1839	0	164	31	2893	13	1559	-87	5719	35	75	23	0	67	1	796
S4033V1032	HumR_2	384	1	2076	-2	17	36	3160	1	1599	1	5454	12	39	23	25	61	9	1741
S4033V1032	HumR_3	374	-1	2298	1	7	38	3116	15	1637	25	4813	31	1	20	2	0	1	1649
S4033V1032	HumR_4	490	3	1841	0	46	0	2374	43	1528	5	5442	6	15	-3	0	25	30	1615
S4033V1032	HumR_5	637	3	2088	14	50	38	2739	26	1559	0	6816	1	69	13	16	0	46	1904
S4033V1032	HumL_3	271	7	2137	26	10	22	3260	-30	1696	15	4567	66	3	2	0	-1	1	868
S4033V1032	HumL_l	449	1	2153	0	374	60	2688	-5	1683	0	5515	3	193	61	0	134	64	1302
S4033V1032	RibR_2	279	2	1700	1	242	0	2219	35	1653	13	5119	25	1	29	0	72	23	1122
S4033V1032	RibL_2	188	9	2186	0	76	8	2637	1	1536	2	6350	15	0	16	2	31	19	875
S4040V1041	FemR_1	412	0	1814	1	51	17	2910	22	1356	0	8024	7	61	4	1	46	68	1536
S4040V1041	FemR_2	188	28	2243	1	2	41	2804	56	1556	3	3807	19	1	-8	0	28	73	1014
S4040V1041	FemR_3	269	1	2462	1	17	26	3216	63	1622	13	3334	38	60	4	-4	17	11	732
S4040V1041	FemR_4	518	4	2036	0	107	17	2818	26	1565	25	5600	42	75	12	0	85	47	949
S4040V1041	FemR_5	240	26	2102	0	48	12	2419	23	1694	7	5061	31	3	22	1	72	1	910
S4040V1041	RibL_1	242	29	2391	3	108	2	2720	4	1638	1	6852	0	64	21	0	67	134	627
S4045V1049	FemL_l	602	13	1851	1	41	32	2923	21	1293	10	5173	4	79	31	0	26	33	1085
S4045V1049	FemL_2	400	10	1983	7	24	24	2830	3	1520	2	3446	16	17	24	23	39	29	1135
S4045V1049	FemL_3	320	0	2403	0	1	66	3083	36	1681	11	4410	61	1	6	-1	9	1	787
S4045V1049	FemL_4	454	11	2021	0	37	12	2417	16	1217	0	5194	1	1	5	-1	29	50	668
S4045V1049	FemL_5	277	8	1828	22	15	25	2348	14	1753	1	5876	1	44	5	11	44	1	536
S4045V1049	TibL_c	558	0	2151	27	15	-1	2581	1	1512	0	5359	54	66	28	1	31	1	943
S4045V1049	TibL_l	439	0	2006	19	95	24	2741	1	1404	1	7413	1	53	32	0	106	7	577

Identification	Location	Pb L1	Pb M1	Pd K12	Pd L1	Rb K12	Rb L1	Rh K12	Rh L1	Sn K12	Sn L1	Sr K12	Sr L1	Ti K12	U L1	U M1	Y K12	Y L1	Zn K12
S4045V1049	TibL_l	543	12	2050	2	136	87	2691	40	1790	0	7811	8	180	38	0	124	1	589
S4045V1049	TibL_l	372	7	1973	0	68	53	2733	3	1466	0	8191	2	80	15	5	33	76	659
S4045V1049	HumR_1	816	1	1866	1	163	1	2931	1	1284	0	6890	41	1	25	0	0	1	1738
S4045V1049	HumR_2	514	1	2090	0	13	20	2902	49	1635	0	4192	11	68	30	1	36	1	663
S4045V1049	HumR_3	561	15	2458	0	2	22	3151	-1	1631	0	3917	0	44	30	1	87	106	2251
S4045V1049	HumR_4	369	28	1637	18	31	61	1820	3	1153	0	3465	0	46	-1	5	54	27	515
S4045V1049	HumR_5	324	11	1680	15	1	1	1684	2	1391	9	2785	7	1	13	2	72	1	446
S4045V1049	RibL_2	301	13	1985	0	6	7	1877	83	1453	0	4611	0	24	33	4	28	60	775
S4045V1049	RibR_2	257	16	1939	16	24	20	2267	44	1312	0	5382	33	0	18	0	25	60	760
S4052V1052	HumR_1	731	26	2118	0	16	36	3542	1	1511	38	5719	1	63	1	0	43	123	707
S4052V1052	HumR_2	226	11	1766	42	1	10	1921	1	1355	-1	2574	0	11	13	0	37	1	514
S4052V1052	HumR_3	325	12	1988	41	35	40	2364	50	1428	24	2627	6	46	14	16	43	59	527
S4052V1052	HumR_4	506	2	1929	1	38	48	2742	1	1571	8	6762	0	40	4	15	-1	74	1121
S4052V1052	HumR_5	571	9	2169	2	40	82	2916	47	1864	14	4960	16	19	18	0	90	86	1345
S4052V1052	FemL_1	715	1	1921	0	33	10	3549	1	1703	0	6676	23	1	13	43	50	14	659
S4052V1052	FemL_2	879	11	1907	1	1	15	2546	17	1492	7	6648	24	38	2	7	59	58	1060
S4052V1052	FemL_3	498	0	2199	0	14	7	3000	4	1833	2	6174	24	3	4	1	-1	83	1211
S4052V1052	FemL_4	478	9	1927	1	1	30	2922	25	1523	13	7887	4	1	28	0	75	64	1248
S4052V1052	FemL_5	624	-1	2224	0	22	62	2645	1	1630	10	5609	37	84	1	6	33	12	992
S4052V1052	TibL_c	668	1	1870	1	25	15	2485	81	1366	0	7008	10	70	20	0	108	117	1417
S4052V1052	TibL_l	531	18	2013	0	37	41	2934	19	1491	1	9140	1	158	27	2	85	32	2801
S4052V1052	TibL_l	393	29	2185	0	24	13	3333	16	1548	12	7530	24	60	16	0	65	69	1976
S4053V1054	FemL_1	481	14	1662	1	110	31	2630	35	1116	9	10260	0	44	53	0	86	1	720
S4053V1054	FemL_2	797	44	1749	45	22	1	1885	27	1289	7	4925	21	28	21	0	69	1	675
S4053V1054	FemL_3	339	0	2401	1	5	8	2859	25	2102	0	5481	29	1	4	24	56	40	1092
S4053V1054	FemL_4	286	-1	1953	44	5	0	3388	12	1487	9	6070	0	18	-2	2	234	13	992
S4053V1054	FemL_5	232	12	2298	0	12	10	3070	1	1521	36	2834	0	1	18	0	14	128	377
S4053V1054	RibL_2	396	1	2292	0	141	-111	2626	1	2146	16	5554	46	8	20	0	59	1	553
S4063V1065	FemL_1	994	2	1834	1	148	6	2613	28	1469	20	7684	1	70	24	0	125	49	927
S4063V1065	FemL_2	448	1	1867	17	24	1	2363	3	1571	7	3443	6	1	-4	16	20	6	844

Identification	Location	Pb L1	Pb M1	Pd K12	Pd L1	Rb K12	Rb L1	Rh K12	Rh L1	Sn K12	Sn L1	Sr K12	Sr L1	Ti K12	U L1	U M1	Y K12	Y L1	Zn K12
S4063V1065	FemL_3	675	10	1898	28	10	35	3149	9	1805	6	9290	0	1	25	5	52	26	1301
S4063V1065	FemL_4	621	10	2116	4	11	74	3075	26	1888	-1	4178	20	1	-9	-1	47	113	792
S4063V1065	FemL_5	378	17	2057	1	8	10	2818	42	1441	0	3994	43	1	22	8	49	62	822
S4063V1065	TibR_c	480	19	2147	3	1	57	2834	1	1611	0	2692	1	88	20	3	50	33	946
S4063V1065	TibR_l	1055	30	2259	48	93	59	3113	1	1860	6	9687	0	78	19	0	79	0	1515
S4063V1065	RibL_2	415	19	1718	0	65	21	2409	50	1620	18	7447	23	43	18	2	31	15	1243
S4068V1071	RibR_2	633	23	2158	0	91	20	3275	15	1590	1	6183	39	1	13	0	128	16	743
S4068V1071	FemL_1	1030	53	1965	26	205	13	2977	29	1645	7	4773	32	1	21	0	137	12	795
S4068V1071	FemL_2	399	4	1919	0	28	41	2100	13	1472	9	3108	1	0	9	0	35	43	623
S4068V1071	FemL_3	906	35	2180	43	0	4	2979	38	1907	0	3452	17	27	-6	0	40	120	817
S4068V1071	FemL_4	670	0	1970	0	103	35	2847	24	1461	1	5443	27	94	12	0	77	30	614
S4068V1071	FemL_5	651	20	2068	0	1	1	2484	24	1863	5	4336	38	7	0	-2	37	13	792
S4068V1071	TibL_c	683	9	1992	34	29	32	2511	31	1709	19	4666	0	8	17	0	64	2	717
S4068V1071	TibL_l	544	6	1921	1	175	53	2275	27	1274	6	4266	15	70	14	0	116	89	503
S4074V1078	RibR_2	178	5	2158	0	1	4	2377	37	1556	6	5340	28	5	36	0	7	1	491
S4074V1078	FemL_1	526	9	1636	13	134	54	2814	7	1374	1	10171	62	37	28	0	113	1	718
S4074V1078	FemL_2	518	3	2166	12	1	29	2976	10	1516	20	4219	8	49	1	4	14	1	1162
S4074V1078	FemL_3	556	0	2351	1	19	29	3010	5	1611	0	4148	29	40	16	2	0	37	981
S4074V1078	FemL_5	252	4	2276	30	39	27	2938	36	1806	0	5956	4	127	39	0	39	21	1282
S4074V1078	FemL_4	897	23	2277	1	10	-2	3085	18	1570	6	5273	5	58	1	3	56	77	974
S4074V1078	HumR_c	521	0	2268	0	5	58	3098	37	1855	0	5329	0	41	12	1	100	41	1370
S4074V1078	HumR_l	464	4	1436	20	168	70	2314	5	1564	8	9279	61	106	35	0	239	1	1088
S4084V1086	RibR_2	434	0	1756	9	52	33	2921	15	1354	8	6389	1	21	2	0	52	56	668
S4084V1086	FemL_1	596	-3	1824	37	135	9	2741	1	1444	0	7109	23	43	26	18	78	15	683
S4084V1086	FemL_2	523	1	2266	0	9	8	2890	39	1538	-1	4777	0	1	22	29	68	130	653
S4084V1086	FemL_3	707	7	2303	1	29	25	3231	27	1713	0	5557	4	24	9	18	80	94	791
S4084V1086	FemL_4	1242	9	2056	8	8	22	2905	1	1480	14	7540	1	42	4	0	85	1	647
S4084V1086	FemL_5	316	15	2005	33	25	23	2185	20	1371	19	2825	0	19	11	8	43	72	425
S4084V1086	FemL_l	772	0	1812	0	396	29	2652	1	1641	0	9960	21	128	42	7	224	57	770
S4084V1086	TibL_c	810	20	2182	0	59	24	3109	33	1958	16	5430	0	124	13	0	92	44	550

Identification	Location	Pb L1	Pb M1	Pd K12	Pd L1	Rb K12	Rb L1	Rh K12	Rh L1	Sn K12	Sn L1	Sr K12	Sr L1	Ti K12	U L1	U M1	Y K12	Y L1	Zn K12
S4084V1086	TibL_l	490	14	1652	0	119	24	2343	4	1384	1	8479	15	109	46	5	57	31	449
S4084V1086	TibL_l	487	9	1932	0	164	66	2503	14	1893	1	7227	0	159	21	12	70	12	560
S4084V1086	TibL_l	560	9	2076	1	218	78	2799	20	1667	0	7217	17	128	24	0	98	11	654
S4084V1086	HumL_1	593	14	1564	1	1	20	2428	11	1074	2	6702	43	19	4	0	31	19	591
S4084V1086	HumL_2	230	14	2392	0	14	22	3099	4	1501	27	2265	19	1	10	2	26	35	380
S4084V1086	HumL_3	665	7	2013	6	26	24	2575	1	1582	13	3797	0	19	11	0	52	62	584
S4084V1086	HumL_4	696	38	2326	-1	1	33	3065	1	1471	24	5442	0	48	10	12	68	75	817
S4084V1086	HumL_5	2281	31	2326	0	1	17	2643	46	1532	4	4515	43	38	4	0	76	26	1333
S4084V1086	HumL_l	816	-1	1636	1	177	24	2678	1	1557	20	10485	16	153	46	-1	240	27	1266
S4096V1100	RibR_2	374	1	1910	0	18	0	2399	16	1412	0	5465	53	7	18	1	94	12	508
S4096V1100	RibL_2	308	1	1938	24	22	22	2748	3	1452	0	4856	39	103	16	-1	95	8	518
S4096V1100	FemL_1	999	45	2026	52	1	21	3268	0	1519	1	8737	9	1	6	0	134	2	1060
S4096V1100	FemL_2	984	14	2378	0	1	-1	2856	14	1585	1	6274	25	1	23	0	148	20	1142
S4096V1100	FemL_3	1065	56	2212	19	16	2	2926	0	1642	3	5236	21	28	19	-1	119	1	852
S4096V1100	FemL_4	550	23	1966	2	10	11	2725	2	1314	2	5552	34	42	6	17	71	68	765
S4096V1100	FemL_5	488	5	2120	0	13	23	3102	7	1592	2	6975	1	11	28	1	58	1	952
Medische collectie GPVI	FemL_1	2005	143	1933	1	20	-3	2891	1	1536	0	1129	9	11	-2	0	0	42	2426
Medische collectie GPVI	FemL_2	1016	1	2076	1	14	20	2726	1	1593	0	1007	15	1	14	0	19	1	1524
Medische collectie GPVI	FemL_3	1486	88	2321	0	7	28	2873	1	1887	17	1253	5	22	-1	0	37	1	3215
Medische collectie GPVI	FemL_4	855	40	2110	4	34	14	2839	0	1510	1	1136	10	2	-3	2	24	28	1088
Medische collectie GPVI	FemL_5	1192	81	2402	-1	29	43	3189	1	1746	0	1316	0	10	12	0	0	97	2061
Blokhuizen 1983-1 64	FemL_1	118	29	2046	44	580	81	3537	1	1698	1	6275	7	63	34	0	327	60	885
Blokhuizen 1983-1 65	FemL_2	144	10	1527	26	112	4	1973	32	1404	7	5998	14	27	29	0	304	25	718
Blokhuizen 1983-1 66	FemL_3	135	16	1864	1	139	72	2853	1	1673	1	8064	27	24	18	0	196	3	888
Blokhuizen 1983-1 67	FemL_4	157	0	1619	0	137	32	1976	32	1083	3	6599	8	15	17	0	342	32	685
Blokhuizen 1983-1 68	FemL_5	113	11	2280	0	32	1	3126	33	1608	0	6474	30	63	18	0	165	30	733
Soil - Restricted materials	N/A	300	0	2162	0	889	79	2146	45	1587	1	2537	40	273	86	58	250	42	239
Soil - Restricted materials	N/A	306	22	1993	0	852	53	2057	14	1653	0	2610	68	269	74	0	236	1	242
Soil - Mudrock Air	N/A	2118	-1	12147	114	5464	823	22169	2	3560	0	15253	120	2649	466	0	1277	1	1712
Soil - Mudrock Air	N/A	2123	0	12050	0	5703	851	22546	40	2774	0	15249	114	2653	298	0	1086	1	1777

Appendix 3: ICP-MS/MS sample preparation, courtesy of Measurlabs

We weighed 0.5 g of sample (accurate to 0.0001 g) into pressure-resistant quartz tubes, then 5.0 ml of concentrated nitric acid and 2.0 ml of 30% hydrogen peroxide were pipetted onto the sample. The quartz tubes were sealed with Teflon caps, placed in the microwave fracturer, and the excavation was carried out using the appropriate operating program.

The operating program used:

Steps	Time (min)	Temperature (°C)
1. step	10	110
2. step	15	180
3. step	10	230
4. step	5	230
5. step	cooling	

After the microwave destruction, the contents of the quartz tubes were filtered into a 25 ml volumetric flask. We washed the quartz tubes with a few ml of high-purity deionized water, then after adding an internal standard solution containing Sc, Rh, Lu (25 µl with a concentration of 50 mg/l), we filled the measuring flask up to the mark with high-purity water.

Appendix 4: Collection of images and spectra from SEM-EDX analysis

See supplementary .pdf file.

Appendix 5: Osteological database with demographic information and treponemal score

Feature no.	Find no.	Estimated sex	Age category	Treponemal score	Completeness	Caries sicca	Nodes/ expansion with superficial cavitation	Short description
4000	1006	Male?	Young Adult	1	25-50%	Absent	Absent	Score 1 because of PNB on one or more skeletal elements.
4001	1005	Male?	Mature Adult	0	25-50%	Unobserv.	Absent	Minimal observation not possible, so no score accredited.
4002	1002	Female?	Young Middle Adult	0	0-25%	Unobserv.	Absent	N/A
4003	1013	Male?	Old Middle Adult	1	50-75%	Absent	Absent	Score 1 due to slight PNB, but healed.
4004	1010	Male	Old Middle Adult	1	75-100%	Absent	Absent	Score 1 due to PNB.
4006	1004	Female	Young Adult	1	50-75%	Unobserv.	Absent	Score 1 due to various slight and healed periosteal reactions in legs and metatarsal.
4007	1011	Male?	Old Middle Adult	0	25-50%	Absent	Absent	N/A.
4008	1003	Male	Old Adolescent	5	75-100%	Frontal bone; Parietal bones; Temporal bones	Femur_L; Femur_R; Fibula_L; Fibula_R; Humerus_L; Humerus_R; Radius_L; Tibia_R; Ulna_R	Score of 5 due to nodes/expansions with superficial cavitation on multiple bones and caries sicca stage 4.
4009	1009	Male	Mature Adult	1	75-100%	Unobserv.	Absent	Score 1 due to pnb on multiple skeletal elements.
4010	1015	Male	Old Middle Adult	1	75-100%	Absent	Absent	Score 1 due to periosteal reactions.
4011	1012	Female	Old Middle Adult	1	75-100%	Absent	Absent	Score 1 due to periosteal reaction on multiple skeletal elements, but all (almost) healed.
4012	1007	N/A	Old Adolescent	1	50-75%	Unobserv.	Absent	Score 1 due to pnb on multiple skeletal elements.
4013	1008	Female	Young Adult	5	75-100%	Absent	Fibula_L	Score 5 due to a node with superfic. cavitation in combination with suggestive lesions multiple skeletal elements.

Feature no.	Find no.	Estimated sex	Age category	Treponemal score	Completeness	Caries sicca	Nodes/ expansion with superficial cavitation	Short description
4014	1024	Indeterminate	Old Middle Adult	0	25-50%	Absent	Absent	N/A
4015	1019	Female	Mature Adult	3	75-100%	Absent	Absent	Nodes do have a slightly rugose pattern, but are very small in diameter (Hackett, 1976, p. 420). Due to this, Score of 3, but it is likely more related to possible Paget's disease, which can also produce slight nodes.
4016	1017	Female	Mature Adult	1	75-100%	Absent	Absent	Score 1 due to periosteal reactions on several bones.
4017	1014	Male?	Adult	0	25-50%	Unobserv.	Absent	Score of 0 due to lack of treponemal lesions.
4018	1016	Male	Young Adult	1	50-75%	Unobserv.	Absent	Score 1 due to periosteal reactions on multiple skeletal elements.
4019	1018	Male	Young Middle Adult	1	75-100%	Unobserv.	Absent	Score 1 due to some periosteal reactions.
4020	1020	Male	Mature Adult	1	75-100%	Absent	Absent	Score of 1 due to periosteal reactions on various bones.
4021	1021	Male	Old Middle Adult	1	75-100%	Absent	Absent	Score of 1 due to active periosteal reactions on multiple skeletal elements.
4022	1022	N/A	Non-Adult	1	50-75%	Absent	Absent	Score of 1 due to periosteal reaction on femur_L, but healed.
4023	1025	Male	Young Adult	2	75-100%	Absent	Absent	Score of 2 due to periosteal reactions with finely striated nodes.
4024	1023	Male	Young Middle Adult	0	0-25%	Unobserv.	Unobserv.	Minimal observation not possible, so no score accredited.
4025	1026	Female?	Adult	1	75-100%	Unobserv.	Absent	Score of 1 due to periosteal reactions, but healed.
4026	1027	Male?	Mature Adult	1	75-100%	Absent	Absent	Score 1 due to PNB.
4027	1028	N/A	Old Adolescent	3	75-100%	Absent	Absent	Due to suggestive lesions on multiple skeletal elements, and very much bilaterally present, Score of 3.
4030	1029	N/A	Old Adolescent	0	25-50%	Absent	Absent	N/A
4031	1030	Male	Mature Adult	0	75-100%	Absent	Absent	N/A
4032	1031	Male	Young Middle Adult	1	75-100%	Absent	Absent	Score 1 due to (mostly healed) periosteal reactions.

Feature no.	Find no.	Estimated sex	Age category	Treponemal score	Completeness	Caries sicca	Nodes/ expansion with superficial cavitation	Short description
4033	1032	Male	Young Middle Adult	5	25-50%	Unobserv.	Humerus_L	Score of 5 due to one node with superficial cavitation (although small) on the distal Humerus_L, with other suggestive lesions on multiple bones.
4034	1033	Indeterminate	Adult	0	75-100%	Absent	Absent	N/A
4036	1035	Female?	Young Middle Adult	0	25-50%	Absent	Absent	N/A
4037	1036	Indeterminate	Young Adult	0	0-25%	Unobserv.	Absent	Minimal observation not possible, so no score accredited.
4038	1038	Male?	Adult	1	0-25%	Unobserv.	Absent	Score 1 due periosteal reactions, but slight and healed.
4039	1043	Female	Young Adult	0	75-100%	Unobserv.	Absent	N/A
4040	1041	Male	Old Middle Adult	2	75-100%	Absent	Absent	Score is 2 due to a suggestive lesion on one skeletal element. But supported by extensive periosteal new bone on other leg bones.
4041	1042	Female?	Adult	0	50-75%	Absent	Absent	N/A
4042	1045	Indeterminate	Old Middle Adult	0	25-50%	Unobserv.	Absent	N/A
4045	1049	Female	Old Middle Adult	5	75-100%	Absent	Tibia_L	Score of 5 due to node with superficial cavitation and many suggestive lesions on other skeletal elements.
4049	1050	Indeterminate	Adult	1	25-50%	Unobserv.	Absent	Score 1 due to small patch of healed periosteal reaction on tibia_L.
4051	1051	Indeterminate	Adult	0	25-50%	Unobserv.	Unobserv.	Minimal observation not possible, so no score accredited.
4052	1052	Male	Mature Adult	3	75-100%	Unobserv.	Absent	Lower legs resemble osteo-myelitis, but no sequestrum or cloacae are present. Therefore suggestive lesions lead to score 3.
4053	1054	Female?	Young Middle Adult	0	75-100%	Absent	Absent	N/A
4054	1055	Male	Young Middle Adult	1	50-75%	Unobserv.	Absent	Score 1 due to some periosteal reactions.
4055	1056	Indeterminate	Adult	0	50-75%	Unobserv.	Absent	N/A
4058	1058	N/A	Old Child	0	75-100%	Absent	Absent	N/A
4059	1059	N/A	Old Child	1	25-50%	Unobserv.	Absent	Score 1 due to periosteal reaction on tibiae.

Feature no.	Find no.	Estimated sex	Age category	Treponemal score	Completeness	Caries sicca	Nodes/ expansion with superficial cavitation	Short description
4060	1062	Male?	Adult	1	0-25%	Unobserv.	Absent	Score 1 due to periosteal reactions on tibiae.
4061	1063	Female	Young Adult	0	50-75%	Unobserv.	Absent	N/A
4062	1064	Male	Young Adult	0	25-50%	Unobserv.	Absent	Minimal observation not possible, so no score accredited.
4063	1065	Male	Young Adult	1	75-100%	Absent	Absent	Although periosteal reactions are more extensive, no finely striated nodes or rugose expansions or other suggestive lesions. Therefore, score 1.
4064	1066	Indeterminate	Adult	1	25-50%	Unobserv.	Absent	Score 1 due to periosteal reactions.
4065	1067	N/A	Young Child	0	75-100%	Absent	Absent	N/A
4066	1068	Male?	Young Middle Adult	1	75-100%	Unobserv.	Absent	Score 1 due to periosteal reactions on multiple skeletal elements.
4067	1070	Female?	Old Middle Adult	1	75-100%	Absent	Absent	Score 1 due to periosteal reactions on tibiae.
4068	1071	Female?	Old Middle Adult	4	75-100%	Unobserv.	Fibula_L	Score 4 due to diagnostic lesion on one single skeletal element.
4069	1072	Indeterminate	Young Adult	0	0-25%	Unobserv.	Absent	Minimal observation not possible, so no score accredited.
4070	1073	Female	Old Middle Adult	0	25-50%	Absent	Absent	N/A
4071	1074	Indeterminate	Young Middle Adult	1	75-100%	Absent	Absent	Score 1 due to periosteal reactions on multiple skeletal elements, although legs are very slight.
4072	1076	Male?	Adult	0	25-50%	Absent	Absent	N/A
4073	1075	Male	Young Middle Adult	0	25-50%	Absent	Absent	N/A
4074	1078	Male	Young Middle Adult	1	75-100%	Absent	Absent	Score 1 due to periosteal reactions, but a score of 4 could be debated. Humerus_R has a lesion that resembles a node with superficial cavitation. However, the margins of the cavities are rounded and smooth, and the node is irregular and not striated. Therefore, it does not fully correspond with the description by Hackett 1976. Inside of cavity also does not seem necrotic in nature.

Feature no.	Find no.	Estimated sex	Age category	Treponemal score	Completeness	Caries sicca	Nodes/ expansion with superficial cavitation	Short description
4075	1079	Male	Mature Adult	1	75-100%	Unobserv.	Absent	Score 1 due to periosteal reactions.
4076	1080	Male	Young Middle Adult	1	75-100%	Unobserv.	Absent	Score 1 due to periosteal reactions.
4077	1087	Male	Old Middle Adult	1	75-100%	Absent	Absent	Score 1 due to periosteal reactions (that are quite extensive, but not typical of treponemal).
4078	1088	Male	Old Middle Adult	1	75-100%	Absent	Absent	Score 1 due to periosteal reactions.
4079	1081	Male?	Adult	0	0-25%	Unobserv.	Absent	Minimal observation not possible, so no score accredited.
4080	1082	Female	Adult	0	25-50%	Absent	Absent	N/A
4081	1083	Indeterminate	Young Adult	1	25-50%	Unobserv.	Absent	Score 1 due to very localized patch of periosteal woven bone on femur.
4082	1084	N/A	Old Child	0	75-100%	Unobserv.	Absent	N/A
4083	1085	Female	Young Adult	1	25-50%	Unobserv.	Absent	Score 1 due to periosteal reactions, but no legs or cranium present.
4084	1086	Female	Young Middle Adult	5	75-100%	Frontal bone; Parietal bones; Zygomatic bones.	Femur_L; Fibula_L; Fibula_R; Radius_R; Tibia_L; Tibia_R; Ulna_R	Score 5 due to suggestive and diagnostic lesions throughout the skeleton.
4085	1090	Female?	Mature Adult	0	75-100%	Unobserv.	Absent	N/A
4088	1091	Indeterminate	Adult	0	0-25%	Unobserv.	Unobserv.	Minimal observation not possible, so no score accredited.
4089	1092	N/A	Old Child	1	75-100%	Absent	Absent	Score 1 due to periosteal reactions on tibiae, but very slight and totally healed.
4090	1093	Male	Young Middle Adult	0	25-50%	Absent	Absent	N/A
4091	1094	Female?	Adult	0	0-25%	Unobserv.	Absent	Minimal observation not possible, so no score accredited.
4093	1096	Male?	Mature Adult	1	50-75%	Absent	Absent	Score 1 due to periosteal reactions on tibiae.
4094	1097	N/A	Old Adolescent	1	25-50%	Absent	Absent	Score 1 due to periosteal reaction on tibia, but some bones missing.
4095	1099	Male	Young Middle Adult	1	75-100%	Absent	Absent	Score 1 due to slight periosteal reactions on legs.

Feature no.	Find no.	Estimated sex	Age category	Treponemal score	Completeness	Caries sicca	Nodes/ expansion with superficial cavitation	Short description
4096	1100	Male	Old Middle Adult	2	75-100%	Absent	Absent	Score 2 due to finely striate node and expansion on fibula_R (confirmed by X-ray).
4097	1101	Female?	Old Middle Adult	1	75-100%	Absent	Absent	Score 1 due to one periosteal reaction.
4098	1106	Female?	Young Adult	0	50-75%	Unobserv.	Absent	Minimal observation not possible, so no score accredited.
4101	1105	Male?	Old Middle Adult	0	25-50%	Absent	Absent	N/A
4102	1108	Male?	Adult	1	25-50%	Unobserv.	Absent	Score of 1 due to periosteal reactions on tibiae.
4103	1110	Male?	Adult	0	75-100%	Unobserv.	Absent	N/A
4104	1111	Female?	Young Adult	1	75-100%	Absent	Absent	Score 1 due to periosteal reactions.
4105	1112	Female	Old Middle Adult	1	75-100%	Absent	Absent	Score 1 due to periosteal reactions on lower legs (bilateral). Although diffuse, they all appear healed.

Appendix 6: X-Ray imaging of the right fibula from S4096V1100

This individual shows various degrees of periosteal reactions along the shafts of all leg bones. Most notable is a deformation that thickened the right fibula along the entire shaft. The medial surface s least affected, whereas the lateral/posterior aspect shows node/expansion with dense and smooth new bone, with pitting. Extending from the midshaft, there is more striation, with some very deep and sharp striations. However, there are also more irregular and "bulbous" surface patterns present. Due to irregular formation, X-ray imaging was performed to see whether these changes were the result of a fracture or other trauma, or if they were the result of actual cortical thickening. The images are shown below.

The anterior aspect shows no changes in the medullary cavity or original cortex of the bone, with notable depositions of new bone formation, especially visible in the lateral view. The distal aspect shows more variable changes, with the anterior view showing a narrowed medullary cavity and thickened cortex. These are characteristics of extensive finely striate nodes and expansions as described by Hackett (1967, p. 81), and are thus lesions suggestive of treponemal infection.

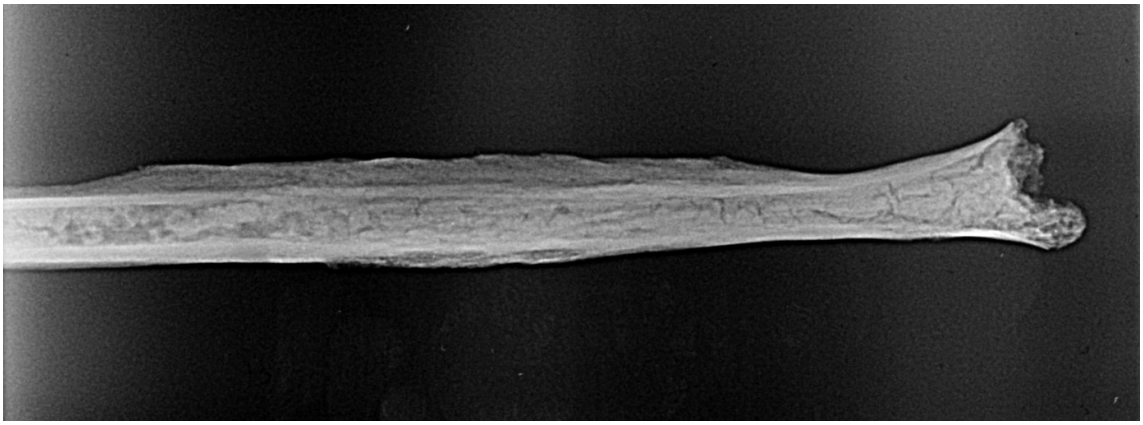

Proximal aspect of the right fibula, lateral view. Imaging by Marijke Langevoort.

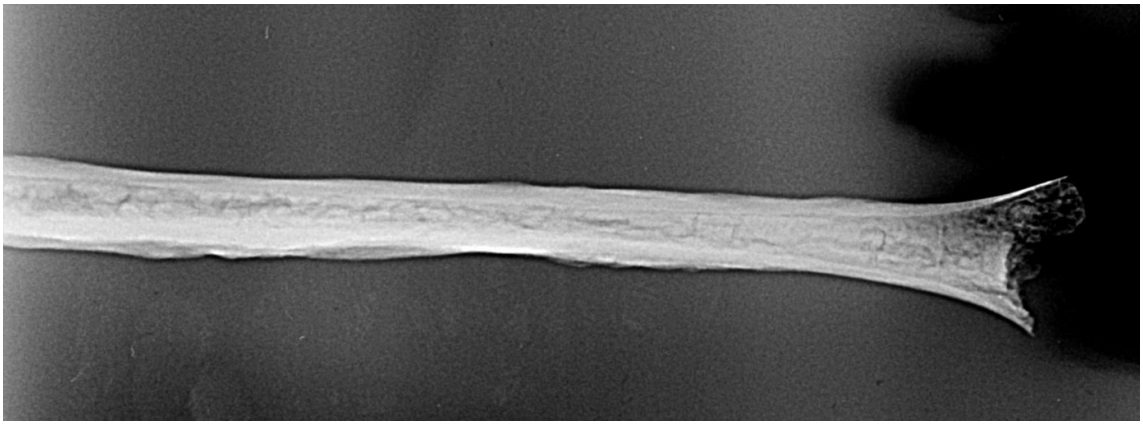

Proximal aspect of the right fibula, anterior view. Imaging by Marijke Langevoort.

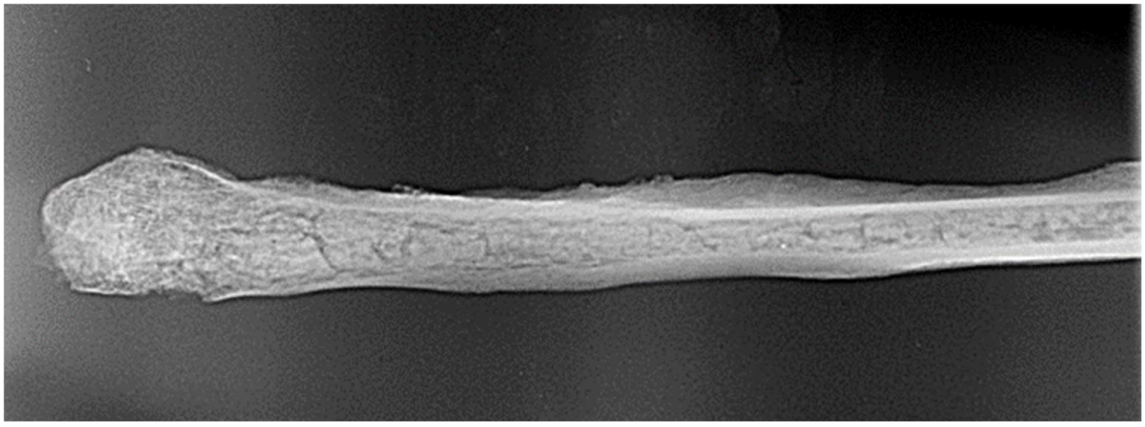

Distal aspect of the right fibula, lateral view. Imaging by Marijke Langevoort.

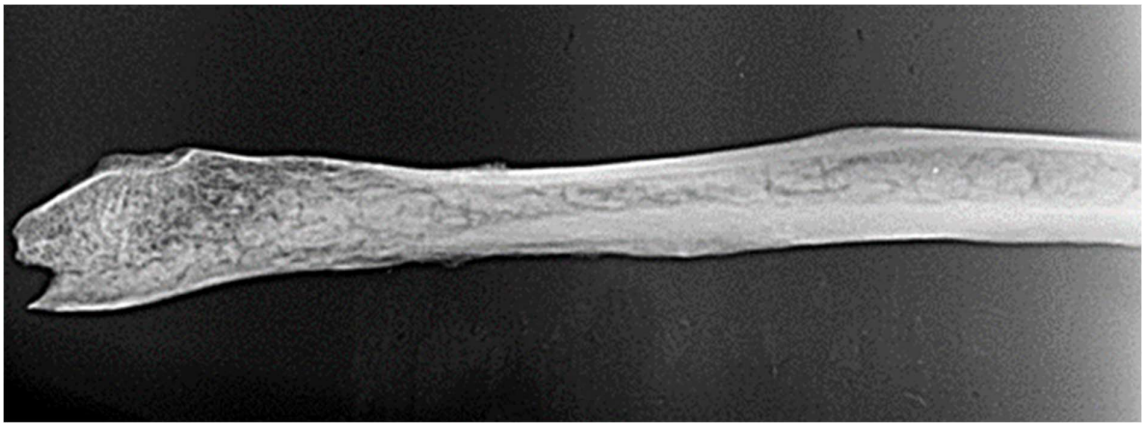

Distal aspect of the right fibula, anterior view. Imaging by Marijke Langevoort.